







Program Book

32nd National and 10th International Iranian Conference on

Biomedical Engineering

Science & Technology

Tabriz University of Technology (Sahand), Tabriz, Iran

19-20 November 2025



All rights reserved.

No part of this publication may be reproduced, stored in a retrieval system, or transmitted in any form or by any means, electronic, mechanical, photocopying, recording, or otherwise, without prior permission of the copyright owner.

Published by:

Biomedical Engineering Department, Tabriz University of Technology (Sahand) Tabriz, Iran

Editors:

Prof. Farzan Ghalichi

Prof. Hanieh Niroomand-Oscuii

Dr. Iman Zoljanahi Oskui

Dr. Faezeh Yaghoubian

Mr. Danial Sedighpour

Mr. Navid Moshtaghi Kashanian

Ms. Arefeh Yaghoubi

Ms. Mohadeseh Nazouri

Ms. Shaghayegh Hassanzadeh

Ms. Fatemeh Shalchizadeh

Designer:

Ms. Elmira Baghaeifar



Preface:

It is with great pleasure that we welcome all distinguished researchers, students, and industry professionals to the 32nd National and 10th International Iranian Conference on Biomedical Engineering (ICBME 2025), jointly organized by Tabriz University of Technology, the Iranian Society of Biomedical Engineering, and Tabriz University of Medical Sciences. This enduring conference series has long served as a leading platform for scientific dialogue, technological advancement, and academic collaboration in the field of biomedical engineering.

This year's conference continues that tradition, hosting a vibrant exchange of ideas across the full spectrum of biomedical engineering disciplines. With 465 papers submitted from universities, research institutes, and industries in Iran and abroad, ICBME 2025 reflects both the depth and diversity of research being conducted in this rapidly evolving field. All accepted papers written in English may, at the authors' request, be indexed in the IEEE Xplore digital library, ensuring international visibility and dissemination of their work.

The program features plenary lectures by world-renowned experts, keynote and invited presentations, and a balanced mix of oral and poster sessions showcasing innovative work from across the biomedical engineering community. In addition, several specialized workshops are being held, providing participants with valuable opportunities for hands-on learning and professional development in emerging areas of research and technology.

The Organizing Committee extends its sincere gratitude to all reviewers, session chairs, and contributors for their dedication to maintaining the high academic standards of ICBME. We also express our appreciation to our partner institutions, the Iranian Society of Biomedical Engineering, and Tabriz University of Medical Sciences, for their invaluable support and collaboration in making this event possible.

We hope that ICBME 2025 will not only highlight cutting-edge research but also inspire new collaborations and foster a spirit of innovation that strengthens the biomedical engineering community in Iran and worldwide. On behalf of the Organizing Committee, we welcome you all to Tabriz, a city rich in history, culture, and scientific achievement.











About ICBME 2025:

The 32nd National and 10th International Iranian Conference on Biomedical Engineering (ICBME 2025) attracted 465 paper submissions, of which 331 were accepted following a rigorous peer-review process—an acceptance rate of approximately 71%. Among the accepted papers, 264 (around 80%) were written in English and 67 (around 20%) in Persian. In total, 198 papers (about 60%) were presented orally, while 133 (around 40%) were presented in poster format.

The top three institutions with the highest number of submissions were Tabriz University of Technology, the University of Technology. Additional charts present the distribution of papers by research area. Together, these data reflect the strong national collaboration and broad scientific scope of ICBME 2025.



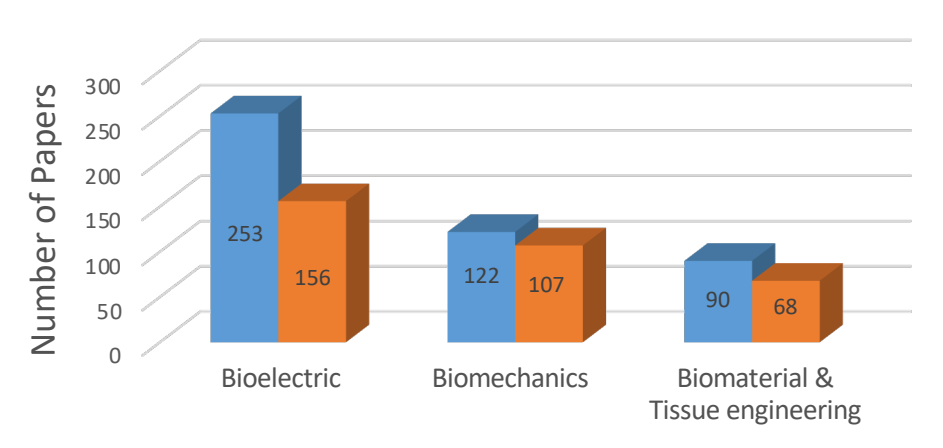




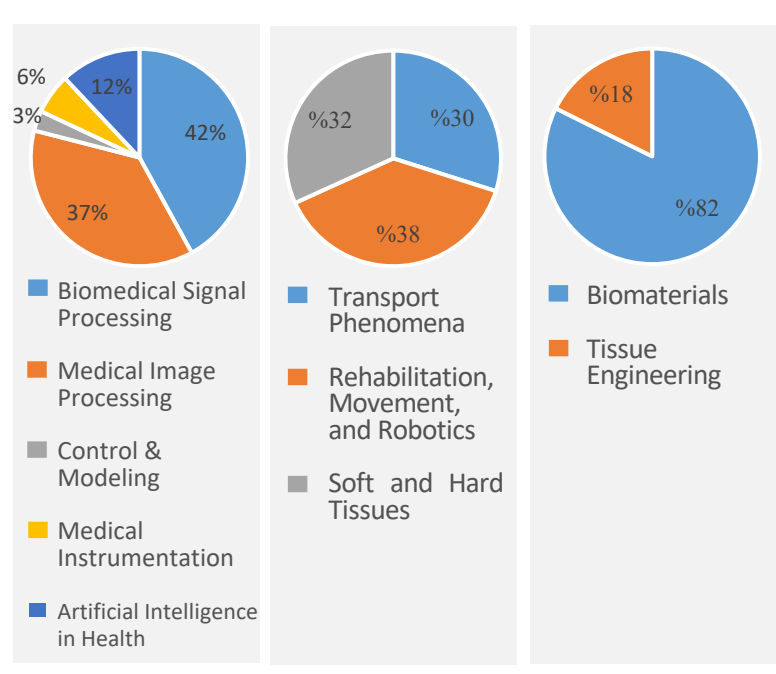




Number of Paper by Research Area

















Executive Committees

Prof. Esmaeil Fatehifar Prof. Farzad Towhidkhah

Prof. Farzan Ghalichi

Prof. Hanieh Niroomand-Oscuii

Dr. Peyvand Ghaderyan

Dr. Iman Zoljanahi Oskui

Dr. Seyed Esmaeel Hashemi Aghdam

Dr. Hadi Taghizadeh

Dr. Alireza Hashemi Oskouei

Dr. Zahra Sadat Hosseini

Dr. Asghar Zarei

Dr. Hamed Danandeh

Mr. Hamed Asadpour

Dr. Faezeh Yaghoubian

Mr. Mohammad Kiumarsi

Dr. Seyedeh Fatemeh Molaeezadeh

Dr. Mahdi Yousefi Azar Khanian

Mr. Mohammad Shakouri

Ms. Elmira Baghaeifar

Ms. Shaghayegh Hassanzadeh

Mr. Navid Moshtaghi Kashanian

Ms. Mohadeseh Nazouri

Ms. Fatemeh Shalchizadeh

Mr. Danial Sedighpour

Ms. Arefeh Yaghoubi











Scientific Committees

Prof. Farhang Abbasi

Prof. Hamid Abrishami Moghadam

Prof. Aydin Akan

Prof. Ali Baradar Khoshfetrat

Dr. Mahmood Reza Azghani

Prof. Habib Badri Ghavifekr

Dr. Fariba Bahrami Boodelalou

Dr. Hamid Behnam

Prof. Reza Boostani

Dr. Mostafa Charmi

Dr. Ayoub Daliri

Prof. Mohammad Reza Daliri

Dr. Hamed Danandeh

Prof. Afshin Ebrahimi

Dr. Mohammad Reza Etminanfar

Prof. Farzam Farahmand

Dr. Emad Fatemizadeh

Dr. Nasser Faturaee

Dr. Mohammad Firouzmand

Dr. Peyvand Ghaderyan

Prof. Farzan Ghalichi

Dr. Amir Ghiamirad

Prof. Robert Guidoin

Dr. Alireza Hashemi Oskouei

Dr. Mehran Jahed

Dr. Akbar Karkhaneh

Prof. Jafar Khalil-Allafi

Dr. Mahshid Kharaziha

Dr. Mahsa Kharazi

Dr. Amir Kiumarsi

Dr. Zahra Mohamadi

Prof. Babak Mohammadzadeh Asl

Dr. Afsaneh Mojra

Prof. Ali Motie-Nasrabadi

Dr. Vahid Reza Nafisi

Prof. Esmaeil Najafiaghdam

Prof. Mahdi Navidbakhsh

Prof. Hanieh Niroomand-Oscuii

Dr. Fariborz Rahimi

Prof. Mostafa Rezaei

Prof. Hossein Roghani-Mamaqani

Dr. Saeed Sadigh-Eteghad

Prof. Mehdi Salami-Kalajahi

Prof. Seyed Kamaledin Setarehdan

Dr. Seyed Mohammad-Reza Seyed Noorani

Dr. Sina Shamekhi

Prof. Moosa Shamsi

Prof. Mohammad Bagher Shamsollahi

Dr. Atefeh Solouk

Prof. Hamid Soltanian Zadeh

Dr. Hadi Taghizadeh

Dr. Saeed Tiari

Prof. Farzad Towhidkhah

Dr. Bahman Vahidi

Dr. Mohammad Zabetian Targhi

Dr. Iman Zoljanahi Oskui











Student Executive Committees

Amir Alaei Mohammad Parsa Asadi

Behnam Asadi Mahya Banapour Mehdi Bashiri Danyial Karimi

Mohammad Hassan Ferdousi Sara Heyat Hosseinian

Armin Ghasimi Sara Pourlafteh

Amirhossein Abbasi Arvan Karimkhani Javad Abdi Mohammad Kiumarsi

Zahra Akhari Maryam Kouhpeyma

Naser Alizadeh Maryam Maniei Amirhesam Amanpour Farzaneh Manzari Zahra Amini Nader Mazraeshadi

Fatemeh Meshkani Majid Bagheri

Fatemeh Bahmani Aslan Modir Kousar Mohammadi

Pourya Dorostkar

Faezeh Gharadaghi Tina Mokhtari Zahra Ghazi Fereshteh Mousavi

Aref Oranghi Nazila Hamidi Amin Partovi Fard

Elham Hazrati Pouria Rezazadeh

Kiana Heidari Reza Sahebi Kuzehkanan

Tina Heidarvand Fatemeh Shahmari

Ali Jafari Asal Yousefi

Amirhossein Zarezadeh Mahdi Jafari Asl

Behrouz Jafarzadeh

Ilia Haeri











Review Committee

Dr. Farhang Abbasi

Dr. Karim Abbasian

Dr. Seyyed Behnam Abdollahi Boraei

Dr. Seyed Sadjad Abedi-Shahri

Dr. Roozbeh Abedini-Nassab

Dr. Nabiollah Abolfathi

Dr. Vahid Abootalebi Dr. Ali Abouei Mehrizi

Dr. Reza Afrouzian

Dr. Hamed Aghapanah Roudsari

Dr. Mohammad Mehdi Ahmadi

Dr. Ahmad Akbari

Dr. Babak Akbari Dr. Mahsa Akhbari

Dr. Mina Alafzadeh

Dr. Mina Alizadeh

Dr. Akbar Allahverdizadeh

Dr. Mohamad Javad Amooshahy

Dr. Mehrdad Anbarian

Dr. Zohreh Ansari

Dr. Vahid Arbabi

Dr. Mohammad Ali Asadollahi

Dr. Azadeh Asefneiad

Dr. Hamed Azarnoush

Dr. Masoumeh Azghani

Dr. Mahmood Reza Azghani

Dr. Fatemeh Badie

Dr. Majid Badieirostami

Dr. Golnaz Baghdadi

Dr. Zahra Bahmani

Dr. Ali Bahrami

Dr. Fariba Bahrami Boodelalou

Dr. Farid Bahrpeyma

Dr. Mohamad Amin Bakhshali

Dr. Ali Baradar Khoshfetrat

Dr. Hamid Behnam

Dr. Borhan Beigzadeh

Dr. Reza Boostani

Dr. Mostafa Charmi

Dr. Farzam Dadgar-Rad

Dr. Mohammad Reza Daliri

Dr. Hamed Danandeh

Dr. Farideh Ebrahimi

Dr. Afshin Ebrahimi

Dr. Hosein Ebrahimnezhad

Dr. Elias Ebrahimzadeh

Dr. Mohammadjavad (Matin) Einafshar

Dr. Faezeh Eskandari

Dr. Mir Ali Eteraf Oskouei

Dr. Ali Fahmi Jafargholkhanloo

Dr. Farzam Farahmand

Dr. Mehdi Fardmanesh

Dr. Marvam Farokhi

Dr. Laleh Fatahi

Dr. Emad Fatemizadeh

Dr. Mohammadhossein Fathi

Dr. Nasser Faturaee

Dr. Bahar Firoozabadi

Dr. Amir Foruzan

Dr. Fariba Ganji

Dr. Peyvand Ghaderyan

Dr. Aboozar Ghaffari











Review Committee

Dr. Farzan Ghalichi

Dr. Zahra Ghanbari

Dr. Mahdieh Ghasemi

Dr. Farnaz Ghassemi

Dr. Maryam Ghorbani

Dr. Azadeh Ghouchani

Dr. Faegheh Golabi

Dr. Zahra Goli

Dr. Taha Goudarzi

Dr. Hasan Haj Ghasem Sabounpaz

Dr. Sepideh Hajipour Sardouie

Dr. Mohammad Ali Hajizadeh

Dr. Ataallah Hashemi

Dr. Alireza Hashemi Oskouei

Dr. Nahid Hassanzadeh Nemati

Dr. Gholam Ali Hossein-Zadeh

Dr. Zahra Sadat Hosseini

Dr. Rana Imani

Dr. Azadeh Jafari

Dr. Amir Homayoun Jafari

Dr. Arezoo Jahani

Dr. Mehran Jahed

Dr. Kivumars Jalili

Dr. Sina Jalili

Dr. Nima Jamshidi

Dr. Amin Janghorbani

Dr. Atefeh Jannathabaei

Dr. Ata Jodeiri

Dr. Hosein Jokar

Dr. Elaheh Jooybar

Dr. Morteza Kafaee Razavi

Dr. Sedigheh Kahrizi

Dr. Mohammad Reza Karami

Dr. Narges Karimzadeh Dehkordi

Dr. Hamid Reza Katoozian

Dr. Hamid Keshvari

Dr. Ali Khadem

Dr. Mahdieh Khalighfard

Dr. Jafar Khalil-Allafi

Dr. Mohammad Ali Khalilzadeh

Dr. Hamid Khaloozadeh

Dr. Mahshid Kharaziha

Dr. Mohammadbagher Khodabakhshi

Dr. Mohammad Taghi Khorasani

Dr. Sahar Khoubani

Dr. Behnam Kiani Kalejahi

Dr. Hamid reza Kobravi

Dr. Mehrdad Kokabi

Dr. Javad Koohsorkhi

Dr. Ali Lesani

Dr. Reza Lotfi Mayan Sofla

Dr. Soheil Mahdavi

Dr. Ali Maleki

Dr. Mahdi Marefat

Dr. Shohreh Mashayekhan

Dr. Nargess Meghdadi

Dr. Maryam Mehdizadeh

Dr. Alireza Mehridehnavi

Dr. Faramarz Mehrnejad

Dr. Seyedeh Naghmeh Miri Ashtiani

Dr. Ezeddin Mohajerani

Dr. Zahra Mohamadi











Review Committee

Dr. Javad Mohammadnejad

Dr. Babak Mohammadzadeh Asl

Dr. Sadaf Moharreri

Dr. Maryam Mohebbi

Dr. Afsaneh Mojra

Dr. Hussain Montazery Kordy

Dr. Mohammad Hassan Moradi

Dr. Nayyer Mostaghim

Dr. Ali Motie-Nasrabadi

Dr. Hamid Movahedian Attar

Dr. Malikeh Nabaei

Dr. Vahid Reza Nafisi

Dr. Esmaeil Najafiaghdam

Dr. Mohamad Najafiashtiani

Dr. Mahdi Navidbakhsh

Dr. Fateme Navvab

Dr. Mohammad Ali Nazari

Dr. Fahimeh Nazarimehr

Dr. Hanieh Niroomand-Oscuii

Dr. Ahmad Nooraeen

Dr. Amir Nourani

Dr. Mohammad Mahdi Ochi

Dr. Mansooreh Pakravan

Dr. Mohammad Pooyan

Dr. Hamoon Pourmirzaagha

Dr. Mohsen Rabbani

Dr. Sadra Rafatnia

Dr. Mohammad Rafienia

Dr. Mehdi Rahaie Jahromi

Dr. Javad Rahbar Shahrouzi

Dr. Fariborz Rahimi

Dr. Mohammad Rahimigorji

Dr. Sayed Reza Ramezani

Dr. Abbas Ramyar

Dr. Ehsan Rashedi

Dr. Aisa Rassoli

Dr. Fatemeh Rezaei

Dr. Mostafa Rezaei

Dr. Mandana Rezaei

Dr. Marzieh Rezazadeh

Dr. Hosein Roghani

Dr. Azin Rostami

Dr. Mostafa Rostami

Dr. Gholamreza Rouhi

Dr. Maryam Saadatmand

Dr. Saeed Sadigh-Eteghad

Dr. Hamid Safavi

Dr. Farzaneh Safshekan

Dr. Zahra Saghaei

Dr. Reza Sahebi-Kuzeh Kanan

Dr. Zahra Salahzadeh

Dr. Mehdi Salami-Kalajahi

Dr. Moloud Sadat Salehi

Dr. Sevedeh Sarah Salehi

Dr. Mohammad Hossein Salimi

Dr. Naser Samadzadehaghdam

Dr. Mohammad Ali Sanjari

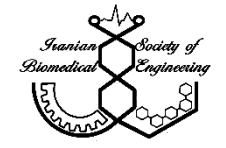
Dr. Amirmohammad Sattari

Dr. Ali Selk Ghafari

Dr. Seyed Mohammad-Reza Seyed Noorani

Dr. Hadi Seyedarabi

Dr. Sina Shamekhi











Review Committee

Dr. Moosa Shamsi

Dr. Elham Shamsi

Dr. Mohammad Bagher Shamsollahi

Dr. Mahkameh Sharbatdar

Dr. Farzaneh Shayegh

Dr. Sobhan Sheykhivand

Dr. Seyed Omid Reza Sheykholeslami

Dr. Meisam Soleimani

Dr. Atefeh Solouk

Dr. Mahdiyeh Soltanalipour

Dr. Hamid Soltanian Zadeh

Dr. Hadi Taghizadeh

Dr. Masoud Tahani

Dr. Mohammad Tahmasebipour

Dr. Farzad Towhidkhah

Dr. Bahman Vahidi

Dr. Mansour Vali

Dr. Ali Vazifedoost Saleh

Dr. Bijan Vosoughi Vahdat

Dr. Faezeh Yaghoubian

Dr. Mehran Yazdi

Dr. Fatemeh Yazdian

Dr. Hashem Yousefi

Dr. Mahdi Yousefi Azar Khanian

Dr. Mohammad Zabetian

Dr. Hesam Zandi

Dr. Hadi Zare-Zardini

Dr. Asghar Zarei

Dr. Seyed Mojtaba Zebarjad

Dr. Atefeh Ziaei

Dr. Iman Zoljanahi Oskui











Acknowledgment of Sponsors

We gratefully acknowledge the generous support of our sponsors, whose commitment and collaboration have made this conference possible. Their contributions reflect a shared dedication to advancing science, innovation, and education in the field of biomedical engineering. We extend our sincere appreciation to all organizations and partners for their invaluable role in fostering a vibrant exchange of ideas and supporting the next generation of researchers and innovators.













Keynote Speakers:



Professor **Gerhard A. Holzapfel** is Head of the Institute of Biomechanics at Graz University of Technology, Austria, and a globally recognized leader in biomechanics. He holds adjunct and visiting professorships at NTNU and the University of Glasgow, and previously served at KTH Stockholm. Following his PhD, he was a Visiting Scholar at Stanford University. He has received numerous prestigious honors, including the START-Award, Erwin Schrödinger Prize, William Prager Medal, Warner T. Koiter Medal, Huiskes Medal, EUROMECH Solid Mechanics Prize, and

election to the U.S. National Academy of Engineering. His pioneering research spans experimental and computational biomechanics, particularly cardiovascular mechanics, soft tissue modeling, and continuum mechanics. Author of the acclaimed textbook Nonlinear Solid Mechanics, over 300 journal papers, and co-founder of the journal Biomechanics and Modeling in Mechanobiology, Professor Holzapfel continues to shape the field through groundbreaking research and international collaboration.



Professor M. Reza Kaazempur-Mofrad is a distinguished interdisciplinary scientist in bioengineering and mechanical engineering, currently leading the Molecular Cell Biomechanics Laboratory at the University of California, Berkeley. With prior appointments at the Massachusetts Institute of Technology and the Charles Stark Draper Laboratory, he has made pioneering contributions to mechanotransduction, cellular biomechanics, and optical coherence tomography. His research Integrates molecular biophysics, computational biology, and deep learning to

unravel the mechanical behavior of cells and biomolecules, explore bacterial mechanotransduction and microbiome interactions, and advance AI-driven digital medicine for personalized diagnostics and therapies. With an h-index of 24 and over 40 peer-reviewed publications, Professor Kaazempur-Mofrad continues to bridge engineering innovation and biomedical discovery to transform modern healthcare.











Professor Ali Khaleghi is a Research Professor at the Department of Electronic Systems, Norwegian University of Science and Technology (NTNU), and at the Intervention Center, Oslo University Hospital. He earned his Ph.D. in Physics from the University of Paris XI and École Supérieure d'Électricité (Supélec) in 2006, followed by postdoctoral research at the Institute d'Électronique et de Télécommunications de Rennes (INSA Rennes) and Oslo University Hospital (2006–2010). From 2010 to 2015, he



served as an Assistant Professor in the Department of Electrical and Computer Engineering at K.N. Toosi University of Technology in Tehran. His research spans antennas and wave propagation, wireless communications, electromagnetic compatibility, measurement techniques, and bio-electromagnetics. He has led multiple industrial R&D projects and major initiatives funded by the Norwegian Research Council (such as WINNOW, CIRCLE, and CLIPEUS), and contributes as Co-PI to several EU H2020 projects, including FET Open programs GLADIATOR, 5G-HEART, and B-CRATOS. Author of over 120 peer-reviewed papers and holder of nine patents, he also serves as CTO of SalveoSolutions AS, advancing cutting-edge battery-free implant technology.





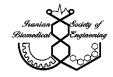






Invited Speakers	ICBME2025
	Dr. Wentao Sheng Jiangsu University of Technology, Zhenjiang, China
	Titel: How exoskeleton assist lower limbs?
	Prof. Reza Boostani CSE & IT Department at Shiraz University, Shiraz, Iran
	Titel: Artificial intelligence in medicine
	Dr. Sandipan Roy SRM Institute of Science and Technology Chennai, Namil Nadu, India
	Titel: Design and Development of Dental Implant Materials to Enhance Osseointegration
	Dr. Maryam Parviz SDIP Innovations, New South Wales, Australia
	Titel: Bone Alternative Development - The JAZBI™ Pathway
	Dr. Mohammad Hossein Salimi Assistant Professor at University of Tehran
	Title: Advanced Tissue Engineering and Biomaterials Enhanced by Artificial Intelligence

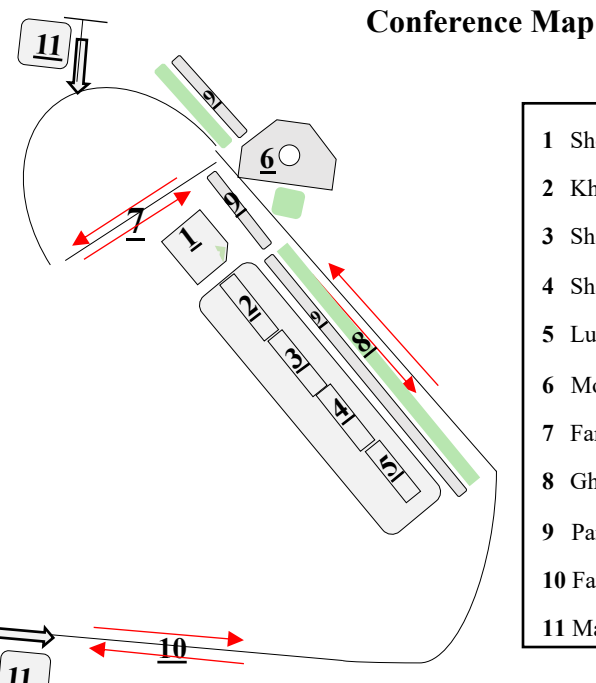












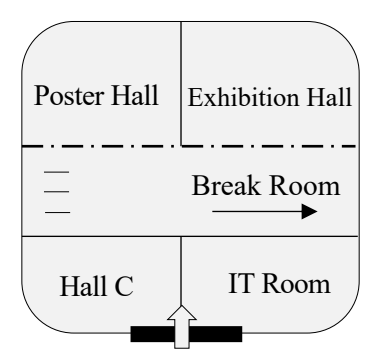
- - 2 Khajeh Nasir Building

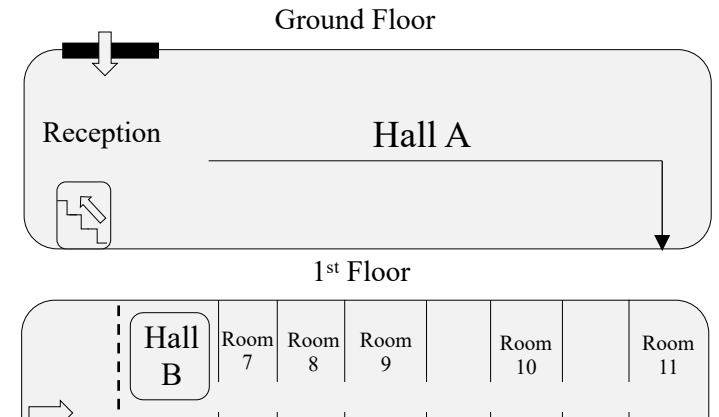
1 Shohada Khedmat Building

- 3 Shahid Soleimani Auditorium (Hall A)
- 4 Shahid Motahari Building
- 5 Lunch Venue
- 6 Mosque
- 7 Fanavari Street
- 8 Ghazi Tabatabaei Street
- 9 Parking Lot
- 10 Farzanegan Street
- 11 Main Entrance

Khajeh Nasir Building

Shohada Khedmat Building





Room

3



Room Room



Room

Room



Room





Program Agenda:



Wednesday, 19 November

07:00-8:30	Ground Floor, Khajeh Nasir Building
	Reception

08:30-9:30	Hall A
.	Opening Ceremony

09:30-10:15	Hall A
<u>\$</u>	Keynote Speech: Prof. Holzapfel

10:15-10:30	Break Room
	Coffee Break

10:15-11:00	Poster Hall
İ	Poster Evaluation 1

10:15-11:00	Exhibition Hall
₽'n	Exhibition Opening Ceremony











11:00-12:30	Hall B & Rooms 2 - 9
À	Paper Presentation Session 1

12:30-14:00	Mosque & Lunch Venue
91 €	Prayer & Lunch

14:00-15:30	Hall B & Rooms 1 - 9
4	Paper Presentation Session 2

15:30-16:00	Break Room & Poster Hall
	Coffee Break & Poster Evaluation 2

16:00-17:30	Hall B & Rooms 1 - 9
À	Paper Presentation Session 3

17:30-18:00	Poster Hall
	Poster Evaluation 3

17:30-18:00	Hall B
i ,*** ,i	General Meeting of the Biomedical Engineering Association













Thursday, 20 November

07:00-9:00	Ground Floor, Khajeh Nasir Building
	Reception

09:00-09:45	Hall A
<u>*</u>	Keynote Speech: Prof. Kazempour Mofrad

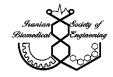
09:45-10:30	Hall A
<u>\$</u>	Keynote Speech: Prof. Khaleghi

10:30-11:00	Break Room & Poster Hall
	Coffee Break & Poster Evaluation 4

11:00-12:30	Rooms 1 - 8
À	Paper Presentation Session 4

12:30-14:00	Mosque & Lunch Venue
91 £	Prayer & Lunch











14:00-15:30	Rooms 1 - 8
	Paper Presentation Session 5

15:30-16:00	Break Room & Poster Hall
	Coffee Break & Poster Evaluation 5

16:00-17:30	Hall A
	Closing Ceremony











ORAL SESSION SCHEDULE: Biomaterial

Wednesday, 19 November

VENUE: Hall B TIME: 11:00 – 12:15		
SESSION CHAIRS: Dr. Mohamadi and Dr. Salami-Kalajahi		
SESSION SUBJECT: Bone Replacement Materials and Strategies		
11:00 – 11:30	Keynote: Dr. Maryam Parviz	
11:30 – 11:45	ICBME-1036: Injectability enhancement and optimization of a biphasic calcium phosphate bone cement	
11:45 – 12:00	ICBME-1065: Engineering injectable gelatin-tyramine/alginate-tyramine hydrogels for bone tissue engineering: A ratio-dependent study of structure, mechanics, and biocompatibility	
12:00 – 12:15	ICBME-1415: ساخت داربست پلییورتان گرمانرم-هیدروکسی آپاتیت-اکسید گرافن احیا شده و بررسی رفتار زیستتخریبپذیری و زیستسازگاری آن	

VENUE: Room 1 TIME: 14:00 – 15:15		
	SESSION CHAIRS: Dr. Mahdavi and Dr. Rezvani Moghaddam	
SESSION	SESSION SUBJECT: Bio-Coatings and Surface Engineering for Medical Applications	
14:00 – 14:15	ICBME-1289: Plasma electrolytic oxidation-derived HAp–Ta ₂ O ₅ Coatings on Ti6Al4V for biomedical applications	
14:15 – 14:30	ICBME-1149: توسعه پوشش چند جزئی بر پایه لیگنین و نانوذرات اکسید سریم بر سطح آلیاژ AZ91 برای استفاده در ایمپلنتهای فلزی	
14:30 – 14:45	ICBME-1435: Antimicrobial and bioactivity evaluation of laser-modified biodegradable magnesium alloy coated with chitosan—graphene oxide	
14:45 – 15:00	ICBME-1386: Multifunctional coatings for biomedical alloys: Biocompatibility and antibacterial activity of hydroxyapatite with YSZ and silver on nitinol	
15:00 – 15:15	ICBME-1413: Gravity-directed Growth of ZnO nanorods: Morphological control via chemical bath deposition	











VENUE: Room 1 TIME: 16:00 – 17:15		
	SESSION CHAIRS: Dr. Rezaei and Dr. Baradar Khoshfetrat	
	SESSION SUBJECT: Smart Hydrogels for Regenerative Medicine	
16:16:30	Keynote: Dr. Mohammad Hossein Salimi	
16:00 – 16:15	ICBME-1464: Proposed amniotic membrane/alginate dialdehyde based injecta hydrogel as a biofunctional scaffold for soft tissue engineering	ble
16:15 – 16:30	ICBME-1]: ساخت و مشخصهیابی چسب زیستالهام برپایه ژلاتین با اتصالات دوگانه آرژنین و اسید یک برای هموستاز سریع	
16:30 – 16:45	ICBME-1022: Innovative biomimetic skin repair strategies utilizing bari titanate	um
16:45 – 17:00	ICBME-1205: Preparation of a plant-based multifunctional nanocomposity hydrogel with conductivity and self-healing property for health monitoring	site
17:00 – 17:15	ICBME-1385: Synthesis and characterization of an injectable magnetic scaff based on alginate/chitosan and zero-valent iron for hyperthermia	old











ORAL SESSION SCHEDULE: Biomaterial

Thursday, 20 November

VENUI	E: Room 1 TIME: 11:00 – 12:15	
	SESSION CHAIRS: Dr. Davaran and Dr. Salami-Kalajahi	
SESS	SESSION SUBJECT: Nanocarriers and Controlled Drug Release for Cancer	
11:00 – 11:15	ICBME-1097: Photoresponsive zwitterionic block copolymer nanoparticles prepared by a one-step nanoprecipitation–photocrosslinking strategy for precision cancer chemotherapy	
11:15 – 11:30	ICBME-1350: Development of folic acid-conjugated iron oxide nanoparticles loaded with doxorubicin via arc discharge: A novel approach for synergistic photothermal-chemotherapy of cancer using bacterial cellulose-polyvinyl alcohol hydrogel	
11:30-11:45	ICBME-1145: بررسی رهایش هوشمند داروی زولدرنیک اسید از نانوذره پلی دوپامین	
11:45 – 12:00	ICBME-1009: بررسی اثر ضد سرطانی لیپوزوم پگیله حاوی ترکیب جنسینوساید Rh2 بر سرطان روده بزرگ در مدل آزمایشگاهی و حیوانی	
12:00 – 12:15	ICBME-1294: توسعه سامانه میکرونیدلهای هیدروژلی زیستسازگار فیبروئین ابریشم-صمغ عربی با پایداری و کارایی بهبودیافته در دارورسانی	

VENUE: Room 1 TIME: 14:00 – 15:15		
	SESSION CHAIRS: Dr. Mohammadi and Dr. Goli	
SESSION S	SESSION SUBJECT: Biomaterials for Soft Tissue, Biological diagnostics and discoveries	
14:00 – 14:15	ICBME-1426: Chondrocyte-imprinted substrates: Promoting MSC chondrogenesis and regulating inflammatory gene expression	
14:15 – 14:30	ICBME-1359: Dual pH-and glucose-responsive terpolymer based on phenylboronic acid	
14:30 – 14:45	ICBME-1076: In-silico Molecular Investigation of Caulobacter crescentus Bioadhesive Proteins	
14:45–15:00	ICBME-1061: Microfluidic generation of core-shell breast tumor spheroids for evaluating dose-dependent responses to quercetin	
15:00 – 15:15	ICBME-1190: Application of nanomaterials in biomaterials for the regeneration of bone and cartilage tissues	











ORAL SESSION SCHEDULE: Biomechanics

Wednesday, 19 November

VENUE: Room 3 TIME: 11:00 - 12:15		
	SESSION CHAIRS: Dr. Rahimi and Dr. Selk Ghafari	
SES	SESSION SUBJECT: Gait Analysis, Motor Control, and Postural Stability	
11:00 – 11:15	ICBME-1134: Kinematic Synergy Reconstruction Analysis for Assessing Gait Complexity and Adaptability in Children With Cerebral Palsy	
11:15 – 11:30	ICBME-1195: Optimal Control and Emergence of Kinematic Synergies in Underactuated Biped Locomotion	
11:30 – 11:45	ICBME-1287: Excessive and Variable Center of Mass Motion Characterizes Gait Instability in Elderly Women with Obese Knee Osteoarthritis	
11:45 – 12:00	ICBME-1437: Backward Walking Under Dual-Task Conditions Among Young Adults: A Potential Tool for Early Detection of Gait Instability and Fall Risk	
12:00 – 12:15	ICBME-1178: Corrective Insoles Enhance Center of Mass Stability During Stair Descent in Individuals with Leg Length Discrepancy	

VENUE: Room 2 TIME: 11:00 - 12:15		
	SESSION CHAIRS: Dr. Hashemi and Dr. Rassoli	
	SESSION SUBJECT: Advanced Modeling Methods	
11:00 –11:15	ICBME-1308: Implementation of Anisotropic Hyperelastic Materials in NL-SBFEM Framework: The HGO Model	
11:15 –11:30	ICBME-1442: طراحی بهینهی پلاکهای ارتوپدی برای ترمیم شکستگی ساب تروکانتریک استخوان ران بر پایهی مدلسازی آماری و روشهای یادگیری ماشین	
11:30–11:45	ICBME-1417: Ensemble Learning-Based Surrogate Models for Non-Invasive Estimation of Corneal Mechanical Properties	
11:45 –12:00	ICBME-1377: Optimization of the Mechanical Properties of PVA/Gelatin Hydrogel Reinforced with Polycaprolactone Nanofibers Using the Finite Element Method	
12:00 –12:15	ICBME-1306: Cancer-Associated Actin Mutations Enhance Cofilin Binding Affinity: Insights from Steered Molecular Dynamics Simulations	











VENUE: Room 5 TIME: 11:00 - 12:15		
	SESSION CHAIRS: Dr. Ghalichi and Dr. Vahidi	
	SESSION SUBJECT: Multiphysics Modeling in Biological Systems	
11:00 - 11:15	ICBME-1275: Anastomosis Angle Effects in Beatin Grafts: A Fluid–Structure Interaction Study	ng-Heart Coronary Bypass
11:15 - 11:30	ی انقباض بطن راست قلب جنین انسان به روش تعامل سیال و جامد	ICBME-1095 : شبیه سازی عدد
11:30 - 11:45	ICBME-1371: Physics-Informed Neural Networks for 2D Simplified Human Right Ventricular Geometry	Cardiac Flow Estimation in
11:45 - 12:00	ICBME-1156: FSI Modeling of Osteocyte Mechanotra Loading	ansduction Under Dynamic
12:00 - 12:15	ICBME-1283: In silico Evaluation of a High-Porosi Bioreactor for Bone Tissue Engineering Applications:	

VENUE: Hall B TIME: 14:00 - 15:15		
	SESSION CHAIRS: Dr. Farahmand and Dr. Azghani	
	SESSION SUBJECT : Exoskeleton, Robotics and Rehabilitation	
14:00 – 14:30	Keynote: Dr. Wentao Sheng	
14:30 – 14:45	ICBME-1309: Phase-Specific Analysis of Arm-Leg Load Sharing in Exoskeleton-Assisted Gait Using Biomechanical Indices	
14:45 – 15:00	ICBME-1135: Inverse Dynamics Analysis of the Crutch-Assisted Gait with a Lower-Limb Robotic Exoskeleton	
15:00 – 15:15	ICBME-1315: Robotic-Assisted Early Rehabilitation Post Total Knee Arthroplasty: An Experimental Investigation	











VENUE: Room 2 TIME: 14:00 - 15:15		
	SESSION CHAIRS: Dr. Rassoli and Dr. Abedi-Shahri	
SESSIO	SESSION SUBJECT: Design, Optimization and Analysis of Orthopedic Implants	
14:00 –14:15	ICBME-1441: طراحی و تحلیل المان محدود ایمپلنت ماژولار شخصیسازیشده مفصل ران مبتنی بر تصاویر CT: تمرکز بر عملکرد اتصال مخروطی تحت بارهای عملکردی	
14:15 –14:30	ICBME-1081: Finite Element Analysis of Mechanical Stability in Hip Joint Implants: A Comparative Study of Ti-6Al-4V and Ti-13Nb-13Zr Alloys	
14:30 –14:45	ICBME-1151: برنامه ریزی قبل از عمل شلف استابولوپلاستی، با هدف ایجاد یک مفصل کانگروئنت و بررسی ارتباط کانگروئیتی و جذب آلوگرافت	
14:45 –15:00	ICBME-1169: Finite Element Analysis of Spine ProDisc-L Using Titanium, CFR-PEEK and CoCr Endplates with UHMWPE-GUR1020 75kGy RM Core	
15:00 –15:15	ICBME-1132: The Influence of Insertion-Induced Prestress and Viscoelastic Properties in Fixational Stability of Pedicle Screws in UHWMPE block: A Finite Element Study	

VENUE:Room 5 TIME: 14:00 - 15:15	
SESSION CHAIRS: Dr. Faturaee, Dr. Shafiei	
SESSION SUBJECT: Microfluidics: Separation and Manipulation of Particles	
14:00 - 14:15	ICBME-1427: Comparative Numerical Analysis of Spiral Geometries for Passive Particle Separation in Microfluidic Devices
14:15 – 14:30	ICBME-1050: Parametric study on the separation of extracellular vesicles in a sheathless spiral microfluidic device
14:30 - 14:45	ICBME-1316: Acoustofluidic Separation of Circulating Tumor Cells from Semen via Induced Microvortices
14:45 - 15:00	ICBME-1457: Development of a spiral microfluidic platform for predicting reduced mechanical damage in oocyte denudation
15:00 – 15:15	ICBME-1393: Investigation of microbubble motion in a microvessel with various obstructions filled with viscous fluid: A finite element modeling study











VENUE: Room 3 TIME: 16:00 - 17:15		
	SESSION CHAIRS: Dr. Seyed Noorani and Dr. Rezaei	
SE	SSION SUBJECT: Neurological Diseases, Assessment and Retraining	
16:00 –16:15	ICBME-1221: Effects of Levodopa and Visual Condition on the Complexity of Postural Control in Parkinson's Disease Patients With and Without Freezing of Gait Through a Multiscale Entropy Approach	
16:15 –16:30	ICBME-1170: تجزیه و تحلیل رفتار بیماران پارکینسون با استفاده از نیروسنج صفحهای مبتنی بر هوش مصنوعی	
16:30 –16:45	ICBME-1406: Gait Retraining of Musculoskeletal Patients Using Deep Learning Techniques	
16:45 –17:00	ICBME-1239: Recovery of Hand Motor Function in Children with Hemiparetic Cerebral Palsy using an Interactive Computer Game Combined with Mechanoreceptor Stimulation: A Pilot Study	
17:00 -17:15	ICBME-1106: طراحی ربات نرم پوشیدنی مچ پا با کنترل پیشبین مدل برای توانبخشی پس از سکته	

VENUE: Room 2 TIME: 16:00 - 17:15		
	SESSION CHAIRS: Dr. Hashemi and Dr. Abedi-Shahri	
SESSION SU	SESSION SUBJECT: Mechanics of Biological Tissues: From the Cellular Level to Medical	
	Implants	
16:00 –16:15	ICBME-1390: Biomechanical Contrast Between Native and Decellularized Triple-Negative Breast Tumors in Mice	
16:15 –16:30	ICBME-1460: تحليل اثر انشعاب فيبر بر خواص مكانيكي تاندون در محل اتصال به استخوان	
16:30 –16:45	ICBME-1408: تحليل المان محدود تنشهاي وارده به بافتهاي نرم مفصل زانو در درجات مختلف فلكشن	
16:45 –17:00	ICBME-1422: ارزیابی بیومکانیکی آسیبپذیری پلاک آترواسکلروتیک و تأثیر مورفولوژی و خواص مکانیکی با استفاده از روش اجزای محدود	
17:00 –17:15	ICBME-1472: Finite Element Analysis of Polyoxymethylene Hemostatic Clips: Stress Distribution and Hinge Geometry Optimization	











VENUE: Room 5 TIME: 16:00 - 17:15		
SESSION CHAIRS: Dr. Vahidi and Dr. Rassoli		
S	SESSION SUBJECT : Hemodynamics, Valves and Cardiac Implants	
16:00 - 16:15	ICBME-1107: How Geometric Asymmetry Impacts Aortic Valve Bioprosthesis Performance – A Finite Element Analysis	
16:15 - 16:30	ICBME-1126: Novel SMA-Integrated Bileaflet Mechanical Heart Valve: Two-Way FSI Simulation with Dynamic Mesh and Hemodynamic Validation	
16:30 - 16:45	ICBME-1420: Comparative Hemodynamic Analysis of Bicuspid and Tricuspid Aortic Valves Through CFD Simulation	
16:45 – 17:00	ICBME-1475: Impact of Impeller Blade Number on the Hemodynamic Performance of Specially Designed Mini VAD	
17:00 – 17:15	ICBME-1382: بررسی عددی اثر همزمانی آریتمی قلبی و کلسترول بالا بر تشکیل و رشد پلاگ چربی در آئورت انسان	











ORAL SESSION SCHEDULE: Biomechanics

Thursday, 20 November

VENUE: Room 3 TIME: 11:00 - 12:30		
	SESSION CHAIRS: Dr. Farahmand and Dr. Rahimi	
SE	SESSION SUBJECT: Modeling, Optimization, and Machine Learning	
11:00 –11:15	ICBME-1211: OpenSim Musculoskeletal Modeling Framework for sEMG-Based Knee Torque Estimation	
11:15 –11:30	ICBME-1235: Optimization Dynamic Stability and Energy Efficiency in Human- Like Bipedal Robot Over a Full Gait Cycle	
11:30 –11:45	ICBME-1375: Automated Kinematic Analysis of Barbell Curl Using Custom IMU and Deep Learning Techniques	
11:45 –12:00	ICBME-1339: Investigating the Impact of Arm Swing on Lower Limb Forces Using Machine Learning Techniques	
12:00 –12:15	ICBME-1314: Dynamic Modeling of a Cable-Driven Series Elastic Upper Extremity Exoskeleton for Post-Stroke Rehabilitation	
12:15 –12:30	ICBME-1194: Effects of laminectomy on active-passive spine loads: a musculoskeletal finite element modeling investigation	

VENUE: Hall B TIME: 11:00 - 12:30		
	SESSION CHAIRS: Dr. Hashemi and Dr. Taghizadeh	
SESSIO:	N SUBJECT: Biomechanics of the Mouth, Jaw, Face and Dental Implants	
11:00 – 11:30	Keynote: Dr. Sandipan Roy	
11:30–11:45	ICBME-1181: شبیهسازی المان محدود رفتار ناهمسانگرد لیگامان پریودنتال بر اساس توزیع سهبعدی فیبرهای کلاژن	
11:45 – 12:00	ICBME-1228: Patient-Specific TMJ Implants: A Finite Element Study on Placement and Material Effects	
12:00 – 12:15	ICBME-1212: Role of Protective Pads in Mandibular Biomechanics During Frontal Impact	
12:15 – 12:30	ICBME-1379: Evaluation of Primary Stability of Dental Implants in Synthetic and Natural Bone: A Comparative Study	











VENUE: Room 5 TIME: 11:00 - 12:15		
	SESSION CHAIRS: Dr. Faturaee and Dr. Vahidi	
SESSION	SESSION SUBJECT : Microfluidics and the Applications of Simulation in Medicine	
11:00 – 11:15	ICBME-1148: High-throughput microfluidic electroporation system using 3D-hydrodynamic focusing	
11:15-11:30	ICBME-1082 : ساخت و انتقال ريزقطرات مغناطيسي در تراشه ميكروفلويديك	
11:30 – 11:45	ICBME-1428: Programmable Flow Control in Rotating Microfludic Systems using elastic patch valves	
11:45 – 12:00	ICBME-1206: Finite Element Modeling of Bare-Tip and Cylindrical Diffusing Optical Fibers for Prostate Cancer Focal Laser Ablation	
12:00 – 12:15	ICBME-1159: Simulation of Mechanical Property Changes in Biodegradable Scaffolds under Various Loading Conditions	

VENUE: Room 3 TIME: 14:00 - 15:15		
	SESSION CHAIRS: Dr. Hashemi Oskouei and Dr. Salahzadeh	
	SESSION SUBJECT: Sports, Anthropometry and Orthopedics	
14:00 –14:15	ICBME-1312 : Impact of Dynamic and Static Sports on Growth and Anthropometric Characteristics (Height, Weight, BMI) in Children and Adolescents	
14:15 –14:30	ICBME-1313: Effects of Athletic Status on Plantar Pressure Distribution and Biomechanical Foot Health in Children and Adolescents	
14:30 –14:45	ICBME-1154 : Alterations in Muscle Coordination During Different Gait Phases Following Knee Injury	
14:45 –15:00	ICBME-1058 : محاسبه نیروی عضلانی اندام تحتانی و نیروی تماسی مفصل زانو در بیماران مبتلا به ستئوآرتریت زانو	
15:00 –15:15	ICBME-1090 : تحلیل بیومکانیکی موقعیت بهینه زاویه چرخش استابولوم پس از جراحی پریاستابولار ستئوتومی گنز با مدلسازی سهبعدی و تحلیل المان محدود	











VENUE: Room 2 TIME: 14:00 - 15:15		
	SESSION CHAIRS: Dr. Taghizadeh and Dr. Abedi Shahri	
	SESSION SUBJECT: Fracture Repair and Fixation	
14:00 – 14:15	ICBME-1187: Screws That Hold: Stability Analysis of Distal Tibial Fractures Using FEA and a Novel Fixation Index	
14:15 – 14:30	ICBME-1362: Topology Optimization for Optimal Design of Human Tibial Fixation Plates toward Improving Biomechanical Compatibility	
14:30 – 14:45	ICBME-1120: Design and Biomechanical Comparison of a Patient-Specific Anatomical Plate Versus Conventional Plate for Distal Humerus Fractures: A Finite Element Analysis	
14:45 – 15:00	ICBME-1355: Ultimate Failure Load of Plate-Based Fixation and a Suture Anchor for Rotator Cuff Repair Across Polyurethane Bone Densities	
15:00 – 15:15	ICBME-1096: تحلیل پارامترهای کلیدی مؤثر در شکست پچ چسبنده ترمیمی تاندون روتاتورکاف با مدل سازی اجزای محدود	











ORAL SESSION SCHEDULE: Bioelectrics

Wednesday, 19 November

V	VENUE: Room 8 TIME: 11:00 - 12:00	
	SESSION CHAIRS: Dr. Shamsi and Dr. Fahmi Jafargholkhanloo	
Sl	SESSION SUBJECT: Oncological Imaging and Tumor Segmentation	
11:00 – 11:15	ICBME-1243: A survey over deep learning methods for early detection mammogram images	in
11:15 – 11:30	ICBME-1046: An Attention-Guided Convolutional Neural Network for Predicti Neoadjuvant Chemotherapy Response in Breast Cancer Patients	ing
11:30 – 11:45	ICBME-1226: Benchmarking nnU-Net vs. Custom 3D U-Net for Kidney Tun Segmentation: A Controlled Study on KiTS19 Dataset	nor
11:45 – 12:00	ICBME-1196: Lightweight 3D U-Net for Robust Liver Segmentation in Mul Institutional CT Datasets	lti-

VENUE: Room 9 TIME: 11:00 - 12:00		
	SESSION CHAIRS: Dr. Ebrahimnezhad and Dr. Danandeh	
SES	SESSION SUBJECT: Computer Vision and Multimodal AI Applications	
11:00 – 11:15	ICBME-1446: Analysis of Blood Report Images Using General-Purpose Vision-Language Models	
11:15 – 11:30	ICBME-1448: Comparative Evaluation of Deep Learning Architectures for Static American Sign Language Recognition	
11:30 – 11:45	ICBME-1271: A Real-Time Integrated Framework for Face Detection, Gender, and Emotion Recognition Using Convolutional Neural Networks	
11:45 – 12:00	ICBME-1373: چارچوب سلسلهمراتبی مبتنی بر مدل انتشار شرطی و شبکه پیشبینی کننده برای تولید و بازشناسی توامان حالات چهره	











VENUE: Room 4 TIME: 11:00-12:00		
	SESSION CHAIRS: Dr. Jahed and Dr. Makouei	
SE	SESSION SUBJECT: Diagnostic and Monitoring Systems in Medicine	
11:00 – 11:15	ICBME-1180: Continuous non-invasive blood pressure estimation based on impedance plethysmography measurements	
11:15 – 11:30	ICBME-1431: Fixed-Frequency Impedimetric Detection of Sickle Cells Using Interdigitated Electrodes	
11:30 – 11:45	ICBME-1467: سامانه ی یکپارچه و کههزینه برای ثبت پتانسیلهای میدانی محلی (LFP) همگام با ویدئو و تحریک الکتریکی مغز به کمک برچسب گذاری نوری کُدگذاری شده ای رخداد	
11:45 – 12:00	ICBME-1130 :An RZ-OOK Modulation Technique for Joint Data Rate and Output Power Tuning in Biomedical Applications	

VENUE: Room 7 TIME: 11:00 – 12:15	
	SESSION CHAIRS: Dr. Shamekhi and Dr. Zarei
	SESSION SUBJECT: fMRI Signal Processing
11:00 – 11:15	ICBME-1317: Neural Encoding of Outcome Magnitude: Evidence from fMRI
11:15 – 11:30	ICBME-1458: Effective Connectivity Alterations within the Cortico-Basal Ganglia Circuit Associated with Motor Skill Learning
11:30 – 11:45	ICBME-1197: Brain Network Reconfiguration During Creative Playmaking: A Task-fMRI Study
11:45 – 12:00	ICBME-1262: Dynamic Connectivity Reveals Transformative Power of Neurofeedback in Brain Functional Networks
12:00 – 12:15	ICBME-1140: Neural Correlates of Reward and Punishment Processing During Gambling-Based Decision-Making: A Simultaneous EEG-fMRI Study











VENUE: Room 6 TIME: 11:00 – 12:15		
	SESSION CHAIRS: Dr. Motie-Nasrabadi and Dr. Azghani	
SES	SION SUBJECT: EEG Signal Processing, Epilepsy and Motor Control	
11:00 – 11:15	ICBME-1105: Classification of Delta Band Motor Imagery EEG Signals in SCI Patients using the Regularized Common Temporal Pattern Method	
11:15 – 11:30	ICBME-1123: Comparative Analysis of Machine Learning and Deep Learning Models for Epileptic Seizure Detection Using the CHB-MIT EEG Dataset	
11:30 – 11:45	ICBME-1265: Improved Metric for Classification of Nearby Reaching Targets: A Distance-Weighted Accuracy Approach	
11:45 – 12:00	ICBME-1425: A Combined Time-Frequency and Common Spatial-Spectral Pattern Approach for EEG-Based Motor Imagery Classification	
12:00 – 12:15	ICBME-1084: Parkinson's Disease Classification Using EEG and a Hybrid EEGNet-LSTM Architecture	

VENUE: Room 8 TIME: 14:00 - 15:15		
	SESSION CHAIRS: Dr. Ebrahimnezhad and Dr. Jodeiri	
	SESSION SUBJECT: Advanced Medical Imaging Techniques	
14:00 – 14:15	ICBME-1368: Addressing Class Imbalance Using Difficulty-based Oversampling with Variance Control	
14:15 – 14:30	ICBME-1267: Towards Accurate Multimodal Deformable Image Registration via Image Translation and Weak Supervision	
14:30 – 14:45	ICBME-1269: MRI to SPECT Image Translation for Parkinson's Disease Diagnosis	
14:45 – 15:00	ICBME-1242: Comparative Assessment of U-Net and Pix2Pix for Applying Direct Attenuation Correction in the Image Domain in 68Ga-PSMA PET/CT Imaging	
15:00 – 15:15	ICBME-1248: Geometry-Aware Anisotropic Total Variation Regularization for Limited-View Photoacoustic Tomography	











VENUE:	Room 9 TIME: 14:00 - 15:30	
SESSION CHAIRS: Dr. Meshgini and Dr. Shamekhi		
SESSION SUBJECT: Ultrasound and OCT		
14:00 – 14:15	ICBME-1035: Grating Lobe Suppression in Sparse Coprime Array Ultrasound Imaging by Null Alignment	
14:15 – 14:30	ICBME-1414: Fast Reflection-Mode Ultrasound Computed Tomography Versus Conventional Pulse-Echo Technique	
14:30 – 14:45	ICBME-1395: Diagnostic and Classification Analysis of Retinal Diseases Using OCT Imaging: Focus on Diabetic Retinopathy and Overlap with Other Retinal Disorders	
14:45 – 15:00	ICBME-1144: تشخیص بیماری MS با استفاده از EfficientNet-B0 و CycleGAN بر پایه انشههای ضخامت شبکیه	
15:00 – 15:15	ICBME-1166: The Adaptive Approach of Ensemble Deep Learning Model in OCT Image Classification	
15:15 – 15:30	ICBME-1111: Super-Resolution Generative Adversarial Network for Photothermal Optical Coherence Tomography Signal Enhancement	

VENUI	E: Room 4 TIME: 14:00-15:00	
SESSION CHAIRS: Dr. Shamsi and Dr. Golabi		
SESSION SUBJECT: Advanced Artificial Intelligence Methods in Biomedical Sciences		
14:00 – 14:15	ICBME-1007: Leveraging Online Data to Enhance Medical Knowledge in a Small Persian Language Model	
14:15 – 14:30	ICBME-1284: Enhancing Population Diversity and Optimization Efficiency in cat Swarm Optimization Using a Fuzzy Controller	
14:30 – 14:45	ICBME-1115: معرفی معیار کمیسازی الگوهای متیلاسیون DNA در ژنوم	
14:45 – 15:00	ICBME-1059: Enhancing Drug-Target Affinity Prediction with Non-Local Block Graph Neural Networks	











VENUE: Room 6 TIME: 14:00 – 15:15		
SESSION CHAIRS: Dr. Meshgini and Dr. Sheykhivand		
SESSIC	SESSION SUBJECT: EEG Signal Processing, Connectivity, and Brain Networks	
14:00 – 14:15	ICBME-1423: Static and Dynamic WPLI on Stressful Scenarios: an EEG Study	
14:15 – 14:30	ICBME-1179: Modulation of EEG Connectivity by Insular Cortex Stimulation: Frequency-Specific Effects and Interoceptive Implications	
14:30 – 14:45	ICBME-1470: Graph Convolutional Network–Based Surrogate Modeling for MRI-EEG Connectivity Analysis	
14:45 – 15:00	ICBME-1418: EJES: A Diverse Estimator Bank Framework for High-Resolution EEG/MEG Source Localization	
15:00 – 15:15	ICBME-1127: Dynamic Classification of Resting-State EEG Using Adaptive Functional Connectivity in Mild Traumatic Brain Injury	

VENUE: Room 3 TIME: 14:00 – 14:45	
SESSION CHAIRS: Zarei and Dr. Hosseini	
SESSION SUBJECT: Optical Signal Processing	
14:00 – 14:15	ICBME-1295: Robust Glucose Level Classification from NIR-Based PPG Using Morphological Features
14:15 – 14:30	ICBME-1108: Analyzing Blood Glucose Levels with Near Infra-Red Spectroscopy and Chemometric Multivariate Methods
14:30 – 14:45	ICBME-1062: Examination and Analysis of the Influence of Near-Infrared Light Absorption by Hair Melanin on fNIRS Signal











VENUE: Room 7 TIME: 14:00 – 15:15		
	SESSION CHAIRS: Dr. Motie-Nasrabadi and Dr. Molaeezadeh	
SESSION SUBJECT: EEG Signal Processing, Neurological and Mental Diseases		
14:00 – 14:15	ICBME-1367: EEG-based Schizophrenia Detection Using Spectral, Entropy, and Graph Connectivity Features with Machine Learning	
14:15 – 14:30	ICBME-1321: EEG-Based Classification of Schizophrenia and Healthy Controls Subjects Using Statistical and Nonlinear Features with Emphasis on Fuzzy Entropy	
14:30 – 14:45	ICBME-1286: Deep Learning and Fuzzy Entropy in Parkinson's Diagnosis: a Framework Based on Task-Based EEG Signals	
14:45 – 15:00	ICBME-1276: Phase-Amplitude Coupling of Event-Related Potentials during VCPT Task in Dyslexic Subjects	
15:00 – 15:15	ICBME-1380: EEG Graph Construction: A Comparative Analysis for Classification Application	

VENUE: Room 8 TIME: 16:00 - 17:15		
	SESSION CHAIRS: Dr. Jodeiri and Dr. Fahmi Jafargholkhanloo	
	SESSION SUBJECT: Brain Neuroimaging and Pathology	
16:00 – 16:15	ICBME-1392: Leveraging Normal White Matter Hyperintensity Context for Enhanced Pathological Segmentation via Multi-Class Deep Learning	
16:15 – 16:30	ICBME-1057: مدل ترکیبی مبتنی بر ،DenseNetالگوریتم ژنتیک و GAN برای تشخیص آلزایمر از ساویر IMR	
16:30 – 16:45	ICBME-1066: Multi-Modal Brain Tumor Diagnosis via Hybrid Vision Transformers and CNNs: A Deep Learning Approach	
16:45 – 17:00	ICBME-1301: بخشبندی دقیق تومورهای مغزی با رویکرد ترکیبی EfficientNetB4 و ترنسفورمر بینایی	
17:00 – 17:15	ICBME-1440: Multi-View 2.5D Attention U-Net with 3D Fusion for Efficient Stroke Lesion Segmentation from T1-Weighted MRI	











VENUE: Hall B TIME: 16:00-17:30	
SESSION CHAIRS: Dr. Boostani and Dr. Jahani	
SESSION SUBJECT: Artificial Intelligence in Clinical Medicine and prediction of complications	
16:00 – 16:30	Keynote: New Horizons in Brain-Computer Interfaces (BCI) and the Future of Smart Health Dr. Reza Boostani
16:30 – 16:45	ICBME-1219: Comparative Evaluation of Feature Selection Techniques for Six- Month Mortality Prediction in Heart Failure Patients
16:45 – 17:00	ICBME-1042: پیشبینی وقوع سکته مغزی با استفاده از دادههای پروندههای الکترونیکی مراقبتهای بهداشتی بیماران و شبکههای عصبی
17:00 – 17:15	ICBME-1172: Multiclass ICU Length-of-Stay Prediction Using Tree-Based Machine Learning Techniques
17:15 – 17:30	ICBME-1064: Modeling Attention Performance Across Female Reproductive Aging Using Logistic Regression

VENUE: Room 4 TIME: 16:00-17:00	
SESSION CHAIRS: Dr. Towhidkhah and Dr. Hosseini	
SESSION SUBJECT: Multiscale modeling and simulation in biomedical engineering	
16:00 – 16:15	ICBME-1240: همآوایی در شبکهای جهان کوچک و متشکل از نورونهای ممریستوری
16:15 – 16:30	ICBME-1251: A Comparative Analysis of Simulated and Experimental Acoustic and Thermal Behavior of HIFU
16:30 – 16:45	ICBME-1143: طراحی چهارچوب شخصی سازی شده درمان بیماری MS مبتنی بر یادگیری عمیق SAC
16:45 – 17:00	ICBME-1098: Silver Nanodisc Metasurface As Geometrical Tunable Absorber for Tailored Thermal Emission











VENUE: Room 6 TIME: 16:00 – 17:15	
VENUE	E: Room 6 TIME: 16:00 – 17:15
SESSION CHAIRS: Dr. Jahed and Dr. Azghani	
SESSION SUBJECT: EEG Signal Processing, Advanced Methods and Biometrics	
16:00 – 16:15	ICBME-1070: Dual-View Data Representation and Contrastive Learning for Robust EEG-Based Person Identification
16:15 – 16:30	ICBME-1384: Hierarchical Task-Structured GNN Meta-Learning for Few-Shot EEG Motor Imagery Decoding
16:30 – 16:45	ICBME-1462: Mental Workload Classification using Bidirectional LSTM Networks with Multi-Feature Fusion
16:45 – 17:00	ICBME-1400: Phase-Amplitude Coupling Reflects Functional Cortical Engagement During Dynamic and Static Motor Tasks
17:00 – 17:15	ICBME-1153: Mapping Epileptic Networks: IED-Triggered Hemodynamic Changes Identified via Simultaneous EEG-fMRI Recordings

VENUE: Room 7 TIME: 16:00 – 17:15	
SESSION CHAIRS: Dr. Rahimi and Dr. Hashemi Oskouei	
SESSION SUBJECT: Neuromuscular and Biomechanical Signal Processing in Motor	
Assessment	
16:00 – 16:15	ICBME-1241: Investigating Real-time sEMG-based Approaches for Grasping Recognition
16:15 – 16:30	ICBME-1449: BiLSTM-Transformer: A Novel Hybrid Model for Accurate Prediction of Hand Joint Angles from sEMG Signals
16:30 – 16:45	ICBME-1208: Goniometry and Electromyography Data Analysis for Knee Health Diagnosis using Machine Learning
16:45 – 17:00	ICBME-1045: طراحی یک سیستم تشخیص سطح لرزش برای بیماران پارکینسون بر اساس توپولوژی سری زمانی لرزش در فضای فاز جغرافیایی
17:00 – 17:15	ICBME-1060: Unsupervised Gait Anomaly Detection Using Generative Adversarial Networks: A Feasibility Study











VENUE: Room 9 TIME: 16:00 – 1	
SESSION CHAIRS: Dr. Shamsi and Dr. Danandeh	
SESSION SUBJECT: Musculoskeletal Imaging	
16:00 – 16:15	ICBME-1370: 2D Residual U-Net for Accurate Lumbar Vertebrae Segmentation in MRI-Based Low Back Pain Diagnosis using the SPIDER Dataset
16:15 – 16:30	ICBME-1244: BiLSTM-Transformer: A Novel Hybrid Model for Accurate Prediction of Hand Joint Angles from sEMG Signals
16:30 – 16:45	ICBME-1364: Automated Tibial Bone Segmentation using 2D Swin-Unet on Knee X-ray Images
16:45 – 17:00	ICBME-1378: Patch-Based detection of proximal caries on bitewing radiographs
17:00 – 17:15	ICBME-1215: Enhancing Dental Disease Detection: Leveraging Swin Transformer and DenseNet with Attention-Guided Fusion in Dental Panoramic Imaging











ORAL SESSION SCHEDULE: Bioelectrics

Thursday, 20 November

VENUE	E: Room 8 TIME: 11:00 - 12:00	
	SESSION CHAIRS: Dr. Shamsi and Dr. Fahmi Jafargholkhanloo	
SESSION SUBJECT: Cerebrovascular and Brain Imaging		
11:00 - 11:15	ICBME-1266: Benchmarking Class Activation Map Methods for Explainable Brain Hemorrhage Classification on Hemorica Dataset	
11:15 - 11:30	ICBME-1069: Quantitative Mapping of Perivascular Spaces Across MRI Modalities Using Vesselness Filtering and Morphometric Analysis	
11:30 - 11:45	ICBME-1168: Accurate Brain Vessel Segmentation in T1-Weighted MRI based on UNETR: Improving Neurosurgical Planning	
11:45 - 12:00	ICBME-1465: Accelerated Diffusion-Weighted Imaging via Diffusion Gradient Alternation in Radial k-Space Sampling	

VENUE: Room 7 TIME: 11:00 – 12:30	
SESSION CHAIRS: Dr. Shamsollahi and Dr. Hosseini	
SESSION SUBJECT: ECG Signal Processing	
11:00 – 11:15	ICBME-1018: Prediction of cardiac arrhythmia via an improved hierarchical fused fuzzy deep learning
11:15 – 11:30	ICBME-1424: A Novel AR-Based Kalman Filtering Framework for ECG Enhancement
11:30 – 11:45	ICBME-1285: ECG-Based Detection of Acute Myocardial Infarction Using a Wrist-Worn Device: a Machine Learning Approach
11:45 – 12:00	ICBME-1453: بهبود تخمین ضربان قلب در دستگاههای پوشیدنی تجاری با استفاده از فیلتر کالمن و مدلهای رگرسیون
12:00 – 12:15	ICBME-1125: Dynamics modeling of cardiac electromechanical intervals and hysteresis analysis
12:15 – 12:30	ICBME-1231: Predicting Sleep Efficiency and Apnea Index Using ECG-Derived and Sleep Quality Features: A Machine Learning Approach











VENUE: Room 6 TIME: 11:00 – 11:4	
SESSION CHAIRS: Dr. Ebrahimi and Dr. Zarei	
SESSION SUBJECT: EEG Signal Processing, Preprocessing and Artifacts	
11:00 – 11:15	ICBME-1322: An Automatic Pipeline for Simultaneous EEG-fMRI Artifact-removal (SEFA)
11:15 – 11:30	ICBME-1389: Semi-Automatic Multi-Stage Artifact Removal in EEG During Subthreshold GVS: A Machine Learning Approach for Neuromodulation Studies
11:30 – 11:45	ICBME-1421: Personalized EEG Source Estimation in a Shape Drawing Task

VENUI	E: Room 4 TIME: 14:00-14:45		
	SESSION CHAIRS: Dr. Jahed and Dr. Sheykhivand		
SESSIC	SESSION SUBJECT: Interventional and Therapeutic Technologies in Medicine		
14:00 – 14:15	ICBME-1436: Magnetic Catheter Robot with Reduced Friction for Endovascular Minimally Invasive Access		
14:15 – 14:30	ICBME-1279: Design and Development of A Focal Vibrating Massager with Wide Frequency Range and Real-Time Control		
14:30 – 14:45	ICBME-1025: A Telemedicine Approach to Therapist-Free VR Exposure Therapy for Acrophobia: A pilot study		











	VENUE	E: Room 8 TIME: 14:00 - 15:15	
	SESSION CHAIRS: Dr. Ebrahimi and Dr. Danandeh		
I	SESSION SUBJECT: Cardiovascular Imaging		
	14:00 – 14:15	ICBME-1255: ارزیابی کارایی روشهای اصلاح پراکندگی در تصویربرداری SPECT قلب همزمان دو ایزوتویی	
	14:15 – 14:30	ICBME-1224: Attentive Temporal Fusion Network (ATFNet) for Multi-frame Coronary Vessel Segmentation in X-ray Angiography	
	14:30 – 14:45	ICBME-1192: CRAFT-Flow: Cross-Attentional Refinement for Robust Optical Flow Estimation in Cardiac MRI via Deep Learning	
	14:45 – 15:00	ICBME-1335: Hybrid Active Learning–Driven Subset Dataset Selection Enables Near-Optimal Cardiac X-Ray Segmentation with Less Training Data	
	15:00 – 15:15	ICBME-1302: Robust Speckle Noise Reduction in IVUS Imaging: Advancing Autoencoders and Non-Local Means with Particle Swarm Optimization	

VENUE: Ro	oom 7 TIME: 14:00 – 15:15	
	SESSION CHAIRS: Dr. Shamsollahi and Dr. Afrouzian	
SESSI	SESSION SUBJECT: EEG Signal Processing, Emotion and Cognition	
14:00 - 14:15	ICBME-1336: From Handcrafted to Deep Representations: ReliefF and DANN Feature Fusion for EEG Emotion Classification	
14:15 - 14:30	ICBME-1129: Binary Discrete Emotion Detection with Peripheral and Fp1-Fp2 EEG Signals on PEEFS Dataset	
14:30 - 14:45	ICBME-1246: Vision Transformer-Based Emotion Recognition in EEG Using Pseudo-Image Construction	
14:45 - 15:00	ICBME-1374: Graph Attention Networks for EEG-Based Emotion Recognition: Focus on Channel-Level Attention	
15:00 - 15:15	ICBME-1150: Region-Specific EEG Channel-Based Emotion Detection using Bi-directional Deep Neural Networks	











VENUE: Room 6		E: Room 6 TIME: 14:00 – 14:45
	SESSION CHAIRS: Dr. Boostani and Dr. Hosseini	
I	SESSION SUBJECT: Sound and Speech Processing	
	14:00 – 14:15	ICBME-1139: Comparative Analysis of Time-Frequency Representations for Pediatric Respiratory Sound Classification Using Deep Learning
	14:15 – 14:30	ICBME-1473: Natural Language Processing and Speech Processing Integration: Toward A Point-of-Care Framework for Early Detection of Alzheimer's Disease
	14:30 – 14:45	ICBME-1034: HEALTH: Hyperbolic Embedding and Acoustic-based Learning for Topological Hierarchies in Parkinson's Disease











POSTER PRESENTATION: Biomaterial

Wednesday, 19 November

D'		
Biomaterials and Tissue Engineering		
ICBME-1341	3D printing of novel bioactive polycaprolactone nanocomposites for	
TODIVIL 1941	prospective osteoporotic bone defect engineering	
ICBME-1471	Shape memory polymer-based scaffolds for bone tissue engineering	
ICBME-1247	Cerium-based MOFs incorporated into zwitterionic polymers for disruption of bacterial biofilms: Toward next-generation antimicrobial surfaces	
ICBME-1443	Evaluation of mechanical and biological properties of PCL-coated magnesium scaffolds	
ICBME-1161	Freeze-dried oxidized alginate—gelatin scaffold coated with reduced graphene oxide for bone tissue engineering	
ICBME-1131	بررسی خواص مکانیکی داربستهای متشکل از نانوسلولز، ژلاتین و ماتریس خارجسلولی برای کاربرد در مهندسی بافت استخوان	
ICBME-1361	Fused deposition modeling in bone tissue engineering: A comprehensive review	
ICBME-1291	کامپوزیتهای پایه بیوپلیمری تقویتشده با الیاف طبیعی: مروری بر کاربردها در مهندسی بافت استخوان	
ICBME-1198	Comparative evaluation of two keratin extraction methods from kurdish sheep wool and their application in the fabrication of biocompatible hydrogels with gelation time analysis	
ICBME-1264	آلیاژهای حافظهدار نیکل–تیتانیم در مهندسی پزشکی: نوآوریها، چالشها و کاربردهای پزشکی	
ICBME-1293	نقش کلیدی نانولولههای کربنی در بهبود همزمان خواص مکانیکی، ضدباکتریایی و زیست سازگاری پوششهای HA-Ta2O5 بر روی آلیاژهای حافظه دار NiTi	
ICBME-1310	ایجاد پوشش کامپوزیتی HA-TiO2 بر روی آلیاژ زیستتخریبپذیر منیزیم به روش رسوبدهی الکتروفورتیک	
ICBME-1117	In silico evaluation of PAMAM dendrimers as nanocarriers for targeted carmustine delivery in glioma therapy	
ICBME-1238	بهینهسازی ساختار نانوالیافی داربست پلیمری با دندریمر پلی آمیدو آمین برای استفاده در مهندسی بافت عصب	











	Diameterials and Tissue Engineering (Continue)	
Biomaterials and Tissue Engineering (Continue)		
ICBME-1434	A quantitative approach to assess Rhus coriaria nanophytosomes in ketamine-induced liver injury	
ICBME-1296	Biomedical applications of pectin nanomaterials: Progress and perspectives	
ICBME-1405	Engineering pH-responsive hybrid hydrogels via inverse suspension polymerization for novel drug delivery systems	
ICBME-1383	DMAEMA-based photocrosslinkable hydrogels with injectable capabilities for smart drug delivery systems in implant infections	
ICBME-1019	Argeted cancer treatment through tissue engineering and biomaterial-based drug delivery systems:	
ICBME-1225	ساخت و مشخصهیابی هیدروژل بر پایه ژلاتین/صمغ عربی حاوی مقادیر مختلف آگارز به منظور کاربرد در ترمیم زخم	
ICBME-1100	هیدروژلهای طبیعی مبتنی بر زیستمواد برای بهبود زخم: طراحی، پیشرفتهای اخیر و دیدگاههای مهندسی بافت	
ICBME-1469	Curcumin-loaded carboxymethyl cellulose/polyvinyl alcohol smart wound dressing: A biosensor approach for pH-responsive monitoring and healing	
ICBME-1021	Conductive hydrogels in biomedical engineering: Current status and challenges	
ICBME-1147	Electrospun chitosan-gelatin/ZIF-8 nanofibers scaffolds for enhanced wound healing	
ICBME-1274	مطالعه کامپوزیتهای سرامیکی هیدروکسی آپاتیت جهت استفاده در کاشتنیهای استخوانی	
ICBME-1256	هیدروژلهای نانوکامپوزیتی تقویتشده با نانوالیاف آرامید عاملدار شده: راهبردی نوآورانه در راستای گسترش ساختارهای پیشرفته مورد استفاده در پزشکی بازساختی	
ICBME-1347	Influence of PEG/PCL soft segments composition on the wettability and water absorption of polyurethane based scaffolds	
ICBME-1433	Perfluorocarbon-based oxygenation systems: From foundational principles to revolutionary applications in cancer therapy and tissue engineering	
ICBME-1016	Structural insights into the molecular mechanism of cancer regulator BRCA1 methylation	











POSTER PRESENTATION: Biomaterial

Thursday, 20 November

	Diti-1t		
	Biomaterials and Tissue Engineering		
ICBME-1439	Induced pluripotent stem cells-derived dopaminergic neuron transplantation for Parkinson's disease		
ICBME-1004	A brief review of the applications of stem and mesenchymal cell-derived exosomes for targeted therapy and cancer drug resistance:		
ICBME-1048	Stem cell engineering in tissue repair: A Review of therapeutic perspectives		
ICBME-1298	کاربرد داربست زیستی سهبعدی در مدلسازی in vitro فیبروز کبدی ناشی از NAFL درموش سوری نر نژاد 6/C57BL		
ICBME-1068	A Review of the Impact of visible spectrum electromagnetic wavelengths on cellular behaviors		
ICBME-1189	Electrochemical biosensors based on polyaniline nanostructures: An analysis of advances, performance challenges, and the outlook for smart systems		
ICBME-1252	Preparation and characterization of silicone hydrogel contact lenses based on TRIS-HEMA		
ICBME-1290	تهیه نانوحامل ژلاتین گالاکتوزیله شده با هدف کاربرد در دارورسانی هدفمند به بافت کبد سرطانی		
ICBME-1305	مطالعه مروری طراحی و ساخت نانوحاملهای هوشمند برای تحویل هدفمند داروهای ضدسرطان به تومورهای لوزالمعده		
ICBME-1023	Metal-Organic Frameworks: A promising class of materials for next- generation antibacterial drug delivery systems		
ICBME-1432	Preparation of pH sensitive carboxymethyl cellulose/polyvinylpyrrolidone based hydrogels for drug delivery applications		
ICBME-1360	Synthesis and swelling behavior of pH-sensitive chitosan/polyvinylpyrrolidone hydrogels for drug delivery applications		
ICBME-1121	Smart injectable hydrogels: From in-situ gelation to on-demand drug release in regenerative medicine		
ICBME-1250	توسعه هیدروژلهای زیست تقلیدی مبتنی بر یوتکتوژل برای کاربردهای پزشکی		
ICBME-1381	هیدروژل ژل شونده آنزیمی بر پایه ژلاتین برای استفاده در کاربردهای مهندسی بافت		
ICBME-1318	GelMA synthesis and experimental challenges		











POSTER PRESENTATION: Biomechanics

Wednesday, 19 November

	Biomechanics
ICBME-1188	Skin Thermomechanical Modeling: Assessing the Influence of Water and Ambient Air
ICBME-1345	A vortex-promoting cross-junction microchannel for efficient hydroporation in immunotherapy applications
ICBME-1334	Microfluidic Flow-Focusing Systems for Alginate Microcapsule Preparation: Tuning Droplet Size and Frequency
ICBME-1416	Optimization of an Integrated Filter Photometric system and a Centrifugal Microfluidic System for Biochemical Analysis
ICBME-1260	Carbon Nanotube Mediated Hyperthermia for Cancer Therapy
ICBME-1304	Effect of ph changes on thermal and mechanical properties of polyacrylamide hydrogel using molecular dynamics simulation
ICBME-1230	Finite Element Analysis of Lumbar Spine Biomechanics Following Cement Augmentation with Different PMMA Volumes: A Comparison with Intact Spine
ICBME-1175	Functionally Graded Material Vertebroplasty Screws: A Finite Element Biomechanical Study
ICBME-1102	Vibration-Based Assessment of Dental Implants: A Finite Element Study on Bone Quality and Boundary Conditions
ICBME-1366	Effect of Aimlabs Software on Sustained Attention, Reaction Time, and Hand- Eye Coordination in Stroke Patients: A Preliminary Study
ICBME-1342	Biomechanical Analysis of Blindfold Training for Backward Running in Handball Athletes
ICBME-1227	Postural Responses to Mediolateral Perturbations: Contributions of Surface, Vision, and Cognitive Load
ICBME-1174	Neuromuscular Coordination in Badminton Smashes: Validation of Musculoskeletal Models
ICBME-1338	Gait-Triggered Neuromuscular Electrical Stimulation with Unloader Knee Braces: A Feasibility Study
ICBME-1391	Deep Neural Network–Based Adaptive Global Logarithmic Sliding Mode Control for Lower-Limb Rehabilitation Exoskeletons
ICBME-1173	Exponential sliding mode controller to track the human upper limb during Topspin Forehand in Table Tennis











Biomechanics (Continue)	
ICBME-1282	DDQN-Learning of Hill-Type Musculoskeletal Arm Model for Elbow Motor Control
ICBME-1348	عصر جدید مدلسازی بیومکانیکی با یادگیری ماشین آگاه از فیزیک
ICBME-1039	مدلسازی عددی اندرکنش آکوستیک - سیال برای بهبود کیفیت اختلاط در میکروکانال سامانههای زیستی
ICBME-1397	ارزیابی بیومکانیکی دو ایمپلنت باریک در مقابل یک ایمپلنت برای جایگزینی دندان آسیای اول فک پایین: یک تحلیل المان محدود تحت بارگذاری استاتیک و دینامیک
ICBME-1376	کاربرد بیومکانیک و آنالیز راهرفتن در بهینهسازی درمان کودکان مبتلا به فلج مغزی: مرور ادبیات











POSTER PRESENTATION: Biomechanics

Thursday, 20 November

	Biomechanics
ICBME-1183	Non-Invasive Detection of Atherosclerosis and Aneurysm via Electrical Impedance Spectroscopy: A Finite Element Simulation Study
ICBME-1142	Multi-Objective Optimization of the Impeller of a mini Blood Pump: Balancing Outlet Pressure and Scalar Shear Stress
ICBME-1071	Simulation and evaluation of the impact of magnetic source geometry on mechanical stress and magnetic flux distribution in cancerous tumors
ICBME-1124	Numerical investigation of the effectiveness of cryosurgery on a liver tumor
ICBME-1411	Mechanical properties of cancer cells as potential predictive biomarkers
ICBME-1118	Experimental and Theoretical Analysis of the Mechanical Performance of 3D-Printed Biomedical Splints Made of PLA/CF with Structural Geometric Variations
ICBME-1452	An AI-Assisted Approach to Patient-specific 3D Modeling and Stress Analysis of the Temporomandibular Joint from CBCT Images
ICBME-1112	Assessing the Risk of Musculoskeletal Injuries of Workers at the Warehousing Workstation of Iran Tire Company
ICBME-1216	Finite Element Analysis of Ankle-Foot Orthosis (AFO): Influence of Shell and Insole Thickness Across Material Variants
ICBME-1204	Fuzzy Estimator of the Soleus Activation during Heel-raising Motion using OpenSim-MATLAB
ICBME-1363	Experimental Framework for Quantifying Muscle Force-Length Behavior in Dynamic Exercise
ICBME-1213	Simulations of Body-Exoskeleton Interaction using OpenSim-MATLAB Interface
ICBME-1222	مقایسه روشهای مختلف دوخت تاندون فلکسور دست با استفاده از آنالیز اجزای محدود
ICBME-1237	ارزیابی و مقایسه بیومکانیکی تثبیت <i>ک</i> نندههای ستون فقرات در ناحیه (L3-L4) کمری به روش المان محدود
ICBME-1346	طراحی آتل شخصی سازی شده با روش نیمه خودکار پردازش تصاویر DICOM
ICBME-1217	تحلیل بیومکانیکی تعادل ایستایی در جوانان و سالمندان بر روی سطوح پایدار و ناپایدار با استفاده از شاخصهای سینتیکی نیروی واکنشی زمین
ICBME-1399	تاثیر تمرین با تردمیل آبی بر کینماتیک پرش- فرود فوتسالیستهای حرفهای
ICBME-1186	شبیه سازی افزایش نفوذ دارو در لوله مویرگی با غشا نفوذپذیر به کمک اثر نانوذرات مغناطیسی



POSTER PRESENTATION: Bioelectric

Wednesday, 19 November

	51.1.1
	Bioelectrics
ICBME-1325	Design and fabrication of a cost-effective dry electrode for electroencephalography (EEG) signal acquisition
ICBME-1327	Design and Evaluation of a Low-Cost Dry Electrode for Physiological Signal Acquisition
ICBME-1209	Toward Precision Psychiatry: Differentiating Depression and Psychosis Using EEG-Based Machine Learning Models
ICBME-1280	Improving Effectivity of repetitive Transcranial Magnetic Stimulation in Treatment of Amyotrophic Lateral Sclerosis by Designing New Protocol and Using Machine Learning
ICBME-1193	Investigation of the presence of movement intention during sequential hand movements using neurophysiological analyses of EEG signals
ICBME-1396	Dynamic Cross-Frequency Coupling Reveals Task Dependent Neural Engagement During Varying Cognitive Demands
ICBME-1463	Development of an Explainable Random Forest-Based Algorithm for EEG-Based Sleep-Wake Classification Toward Sleep Apnea Detection
ICBME-1445	Emotion Recognition from EEG signal using GA-FLANN with Whale Optimization Algorithm
ICBME-1344	Classification of Excitatory and Inhibitory Neurons in Animal Data Using Machine Learning and CNN Models
ICBME-1354	Deep Learning Approaches for Alzheimer's Disease Diagnosis: A Comprehensive Review
ICBME-1052	GPU-Accelerated GRAPPA: A Fast Implementation Using PyTorch for MRI Reconstruction
ICBME-1207	A Comparative Analysis of CNN Architectures for Histopathology Image Classification: Performance, Efficiency, and Adversarial Robustness
ICBME-1088	Application of Attention Mechanisms in Deep Learning Models for COVID-19 Detection and Classification from Medical Images: A Systematic Review
ICBME-1053	A Comprehensive Review of Machine Learning Techniques for Automatic Skin Disease Detection
ICBME-1343	Robust Binary Differentiation of ALL vs. AML Using Deep Graph Convolutions
ICBME-1055	Multi-transform diagnostic analysis based on gradient-based features for breast cancer detection in thermal imaging
ICBME-1430	Short-term gains vs. long-term Success: Reward strategy design for reinforcement learning in football











Bioelectrics (Continue)	
ICBME-1268	Enhancing Type 2 Diabetes Diagnosis with Evolutionary Algorithms and Machine Learning
ICBME-1162	Predictive Modeling of Astronaut Skin Microbiome Changes Using Machine Learning on NASA Multi-Omics Data
ICBME-1008	Gene expression changes induced by Atorvastatin in breast cancer and stem cells
ICBME-1101	بررسی عملکرد سلولهای Tدر میکرومحیط تومور HGSOCبا رویکرد توالی یابی تکسلولی
ICBME-1429	بررسی آمارههای توصیفی فواصل بین ژنی ژنوم و پاتوژنی در دو سویه K12و O157:H7باکتری E. Coli با رویکرد بیوانفورماتیکی
ICBME-1353	بازسازی و تحلیل سیگنال ECG از نسخههای چاپی نوار قلب بهمنظور طبقهبندی خودکار بیماریهای ایسکمیک قلب با استفاده از شبکههای عصبی کانولوشنی











POSTER PRESENTATION: Bioelectric

Thursday, 20 November

	Bioelectrics
ICBME-1249	Deep Brain Stimulation with a Computational both combined Biphasic and Monophonic square pulse Model for the Essential Tremor of CBGTHC Network of the Parkinson's Disease
ICBME-1365	Integration of High-Speed AFM Nanomechanical Profiling with Deep Spatiotemporal Learning for Early Response Assessment and Tumor Stage Prediction in Oncolytic Virotherapy
ICBME-1040	Diagnosis of Multiple Sclerosis Using Recurrence Plot of EEG
ICBME-1352	Feature-Conditioned WGAN for Generating Alzheimer's EEG: Enabling GAN-Based Synthesis Under Data Scarcity
ICBME-1326	Multi-Level Driver Fatigue Detection Using EEG Signals with CNN-LSTM Models in a Compressed Sensing Framework
ICBME-1278	Distinct Neurophysiological and Psychological Effects of tVNS and Neurofeedback: Insights for EEG-Guided Neuromodulation
ICBME-1236	The Impact of an Interactive Rehabilitation Protocol on Reorganization of Brain Networks in Children with Cerebral Palsy: A Pilot Study
ICBME-1299	Hierarchical STFT based Transformer for Causality discovery
ICBME-1444	Alterations of Brain Activation Maps in Adults with ADHD During Risk-Related Decision-Making Evidence from the Balloon Analogue Risk Task
ICBME-1253	Mitigating MRI Domain Shift in Sex Classification: A Deep Learning Approach with ComBat Harmonization
ICBME-1104	Fibroglandular Tissue Classification in Breast MRI: A Comparative Study of Automated Decision Strategies
ICBME-1358	Late Fusion-Based Deep Learning for Breast Cancer Classification in Mammography
ICBME-1152	TransFuse++: A Hybrid CNN-Transformer Architecture with Cross-Attention, Temporal Modeling, and Uncertainty Estimation for Medical Image Segmentation
ICBME-1164	A Survey on Cardiac MRI Segmentation: From Classical Methods to State-of-the-art Deep Learning
ICBME-1229	Investigating the Self-optimizing nnU-NetV2 for Kidney Tumor Segmentation: Application to the KiTS23 Dataset
ICBME-1307	Added value of synthetic T1/T2-weighted MR images in the segmentation and staging of meningioma
ICBME-1372	Deep Learning-based Segmentation of Human Sperm Heads using YOLOv8 and SAM











20th	Bioelectrics (Continue)
ICBME-1085	A Comprehensive Architecture for Smart Hospitals: Leveraging IoT, AI, and Data Science
ICBME-1311	The Technological Pillars of Smart Hospitals: A 2022–2025 Review of IoMT, Wearables/RTLS/RFID, Robotics (IoRT), and VR/AR
ICBME-1017	تشخیص سرطان پستان از طریق طبقهبندی تصاویر: مروری بر روشها و روندهای فعلی
ICBME-1273	استفاده از یادگیری انتقالی در پاسخ به کمبود طیف در تشخیص بیماری با طیف سنجی رامان
ICBME-1461	ارائه مدل E-UNETR2D جهت قطعه بندی عروق کرونر از روی تصاویر سی تی آنژیوگرافی
ICBME-1099	پایش هوشمند دیابت به کمک اینترنت اشیا و داده کاوی: گامی نوین در مراقبتهای سلامت دیجیتال
ICBME-1049	سامانه هوشمند مبتنی بر بینایی ماشین برای تشخیص افتادن سالمندان: رویکردی ایمن، دقیق و سریع
ICBME-1451	طبقه بندی بیماران پارکینسون و افراد سالم با بهره گیری از ویژگیهای غیرخطی و الگوریتم های یادگیری ماشین
ICBME-1474	ارائه یک مدل ترکیبی برای تشخیص بیماری آلزایمر با استفاده از هوش مصنوعی و منطق فازی











WORKSHOPS PROGRAM

مكان	زمان برگزاری	عنوان کارگاه یا پنل			
Room 2	پنجشنبه ۲۹ آبان، ۹ الی ۱۲	تحول در پزشکی با مدلسازی سهبعدی: کارگاه عملی استفاده از نرمافزار میمیکس برای تحلیل تصاویر پزشکی			
Hall C	سه شنبه ۲۷ آبان، ۱۱ الی ۱۶:۰۰	نقشه مغزی، آشنایی با شبکههای مغز، نحوه اصلاح و تغییر در شبکهها، کاربردهای درمانی و آموزشی، آشنایی با تکنولوژی جدید تحریک مغناطیسی مغز با شدت میدان زیر ۱۵۰ میکرو تسلا	٢		
Room 9	پنجشنبه ۲۹ آبان، ۹ الی ۱۲:۳۰	کارگاه عملی آشنایی با تجهیزات معاینه تشخیصی	٣		
Hall C	چهارشنبه ۲۸ آبان، ۱۴ الی ۱۵:۰۰	تحول دیجیتال در مدیریت تولید	۴		
Hall C	چهارشنبه ۲۸ آبان، ۱۶ الی ۱۷	راهکارهای درآمدزا در خدمات تجهیزات پزشکی	۵		
Room 1	چهارشنبه ۲۸ آبان، ۱۱ الی ۱۲:۳۰	کارگاه بهینهسازی هندسی با ANSYS	۶		
Room 5	پنجشنبه ۲۹ آبان، ۱۴ الی ۱۵:۳۰	کار کاه پهپیناساری هستشی با ۱۵۰ ۱۸۱۸	·		
Room 10	چهارشنبه ۲۸ آبان، ۱۴ الی ۱۵:۳۰	کارگاه آموزشی شبیهسازیهای ماهیچه-رانیده	٧		
Room 10	پنجشنبه ۲۹ آبان، ۹ الی ۱۲:۳۰	به کمک نرمافزار OpenSim	٧		
Hall A	پنجشنبه ۲۹ آبان، ۱۱ الی ۱۲:۳۰	کارگاه ایده شو	٨		
Hall A	چهارشنبه ۲۸ آبان، ۱۴ الی ۱۵	پنل اصول مجوز گیری تجهیزات پزشکی	٩		
Hall A	چهارشنبه ۲۸ آبان، ۱۶ الی ۱۷	پنل آشنایی با گازهای طبی	١٠		
Hall C	پنجشنبه ۲۹ آبان، ۱۱ الی ۱۲	پنل مهندسی پزشکی در طراحی و ساخت ارتزها	11		
Hall A	چهارشنبه ۲۸ آبان، ۱۱ الی ۱۲:۳۰	پنل نقشه مغزی، آشنایی با شبکههای مغز، نحوه اصلاح و تغییر در شبکهها، کاربردهای درمانی و آموزشی، آشنایی با تکنولوژی جدید تحریک مغناطیسی مغز با شدت میدان زیر ۱۵۰ میکرو تسلا	17		











Biomaterial Abstracts: ICBME-

1341	1291	1434	1469	1016	1036	1435	1022	1145	1076
1471	1198	1296	1021	1439	1065	1386	1205	1009	1061
1247	1264	1405	1147	1004	1415	1413	1385	1294	1190
1443	1293	1383	1274	1048	1289	1464	1097	1426	1149
1161	1310	1019	1256	1298	1155	1350	1359	1250	1318
1131	1117	1225	1347	1068	1252	1305	1432	1121	1381
1361	1238	1100	1433	1189	1290	1023	1360		



Article Code: icbme-1036

Article Title: Injectability Enhancement and Optimization of a Biphasic Calcium Phosphate Bone Cement

Abstract: This study presents a novel approach to developing and optimizing injectable biphasic calcium phosphate (BCP)-based bone cement tailored for injectable applications in bone tissue engineering. The BCP powder, synthesized in-house, was characterized using X-ray diffraction (XRD) and Fourier-transform infrared spectroscopy (FTIR), confirming its biphasic nature. A practical injectable cement formulation was achieved with liquid-to-powder ratios (LPR) ranging from 0.55 to 0.7 ml/g. At an optimal LPR of 0.65 ml/g, the cement exhibited 70.85% injectability. However, incorporating 4 wt% carboxymethyl cellulose (CMC) enhanced injectability to 86%, reduced phase separation, and ensured uniform extrusion forces—key requirements for clinical 3D printing applications. Compared to conventional formulations, this cement offers superior injectability and consistency, positioning it as a promising candidate for advanced bone tissue engineering. Future studies will evaluate its biological performance and explore additional biomedical applications.

Keywords: Biphasic calcium phosphate, Bone cement, Injectability, Bone tissue engineering

Authors: Sepehr Larijani - Mitra Asadi-Eydivand - Nabiollah Abolfathi - Mehran Solati-Hashjin











Article Code: icbme-1061

Article Title: Microfluidic Generation of Core-Shell Breast Tumor Spheroids for Evaluating Dose-Dependent Responses to Quercetin

Abstract: Three-dimensional (3D) tumor spheroids produced through microfluidic methods provide a biologically representative platform for studying cancer and assessing drug responses. In this study, we generated uniform water-core alginate shell spheroids composed of MCF-7 breast cancer cells using a droplet-based microfluidic strategy, thereby simulating the in vivo tumor microenvironment. This core-shell configuration helps generate homogenous multicellular tumor spheroids (MCTS) by minimizing the hydrogel's interference with cell-to-cell interactions. Exposure to different concentrations of quercetin—a bioactive flavonoid with established anticancer effects—resulted in a clear dose-dependent outcome. At lower levels, quercetin enhanced cell growth, whereas higher concentrations led to marked cytotoxicity, reflected by reduced cell viability. Although similar dual responses to quercetin have been observed in traditional monolayer cultures, the 3D spheroid model demonstrated these effects more strongly. Moreover, drug resistance in the core-shell spheroids was considerably higher compared to 2D systems, underscoring the model's relevance in replicating the drug resistance in solid tumors.

Keywords: Droplet-based microfluidic, core-shell spheroids, quercetin, breast cancer, dual response, drug resistance.

Authors: Fatemeh Zarei - Mohammad Hashem Molayemat - Amir Shamloo - Mohammad Mehdi Sadeghian











Article Code: icbme-1004

Article Title: A brief review of the applications of stem and mesenchymal cell-derived exosomes for targeted therapy and cancer drug resistance:

Abstract: Mesenchymal stem cell (MSC)-derived exosomes, as small extracellular vesicles carrying diverse bioactive molecules, play a pivotal role in delivering anticancer drugs and repairing radiation-induced tissue damage. Due to their intrinsic ability to target tumor cells, cross physiological barriers such as the blood-brain barrier, and exhibit reduced toxicity compared to free drugs, these exosomes have emerged as promising novel drug delivery vehicles. Numerous preclinical studies have demonstrated that MSC-derived exosomes can selectively deliver chemotherapeutic agents such as doxorubicin, paclitaxel, and bioactive compounds like TRAIL and honokiol to cancer cells, thereby enhancing therapeutic efficacy while minimizing systemic toxicity. This capability is particularly valuable in combating drugresistant cancers such as pancreatic and colorectal cancers. Beyond their antitumor applications, MSC-derived exosomes significantly contribute to accelerating the repair of radiation-induced tissue injuries. By transferring specific microRNAs and cytokines, these vesicles promote cell proliferation, inhibit apoptosis, suppress inflammation and oxidative stress, and mitigate fibrosis progression. Experimental evidence in animal models has shown that MSC-derived exosomes effectively reduce bone loss, facilitate skin repair, and attenuate radiation-induced pulmonary fibrosis. Despite their considerable clinical potential, several challenges hinder the widespread clinical translation of MSC-derived exosomes. These include the lack of standardized protocols for classification, isolation, and storage; limitations in large-scale production; and the need for improved targeting and drug-loading methods. Accordingly, ongoing research focuses on surface engineering of exosomes to enhance targeting specificity, reduce off-target effects, and improve cargo stability. Ultimately, to accelerate the clinical translation of this technology for cancer therapy and tissue regeneration, comprehensive studies including in vivo experiments, long-term safety assessments, and large-scale clinical trials are essential. The development of standardized protocols, scale-up production techniques, and precise targeting strategies remain critical steps toward realizing the full therapeutic potential of MSC-derived exosomes.

Keywords: Mesenchymal stem cell Exosome, Therapy resistance, Cancer, Extracellular vesicles, Drug resistance, Targeted therapy

Authors: Laleh Etemad-Ghazani - Zahra Etemadi - Reza Pashaei











Article Code: icbme-1405

Article Title: Engineering pH-Responsive Hybrid Hydrogels via Inverse Suspension Polymerization for Novel Drug Delivery Systems

Abstract: Hydrogels have attracted considerable attention as advanced platforms for intelligent drug delivery systems owing to their three-dimensional structure, favorable biocompatibility, and ability to encapsulate and release therapeutic agents in a controlled and targeted manner. However, the inherent limitations of natural hydrogels, such as poor mechanical strength, along with the shortcomings of synthetic hydrogels, including lack of biodegradability, restrict their optimal biomedical applications. The development of hybrid hydrogels, which combine natural and synthetic polymers, provides an effective strategy to overcome these drawbacks and to achieve materials with enhanced mechanical integrity, suitable biocompatibility, and efficient responsiveness to physiological stimuli. In this study, a pH-responsive hybrid hydrogel based on chitosan and acrylate monomers was synthesized and characterized via inverse suspension polymerization. The results demonstrated that the obtained spherical microparticles exhibited desirable structural and functional properties, highlighting their significant potential for application in next-generation, targeted drug delivery systems.

Keywords: Chitosan, Drug Delivery, Hydrogel, Inverse suspension polymerization

Authors: Borhan Oghbaei Bonab - Mohammad Ashraf - Sahar Enayati - Alireza Mahjub











Article Code: icbme-1289

Article Title: Plasma Electrolytic Oxidation-Derived HAp-Ta₂O₅ Coatings on Ti6Al4V for Biomedical Applications

Abstract: This study focused on enhancing hydroxyapatite (HAp) coatings by incorporating tantalum pentoxide (Ta₂O₅) nanoparticles at concentrations ranging from 0 to 1.5 g/L into the electrolyte solution. The HAp-Ta₂O₅ composite coatings were applied to Ti6Al4V implants using the plasma electrolytic oxidation (PEO) technique. While increasing Ta₂O₅ concentration did not significantly alter the phase composition, the addition of 1.5 g/L resulted in a denser and more compact coating. In vitro biocompatibility assessments using the MG-63 cell line demonstrated that Ta₂O₅ incorporation improved cell viability and proliferation. Immunofluorescence imaging confirmed more live cells and fewer dead cells on the composite coatings. These results suggest that the HAp-Ta₂O₅ coatings offer a promising approach to

Keywords: Ti6Al4V dental implan, Plasma Electrolytic Oxidation, HAp-Ta2O5 coating ,Biological characteristics

Authors: Milad Hosseini - Jafar Khalil allafi - Mir saman Safavi

developing bioactive metallic implants with enhanced osteoblast compatibility.











Article Code: icbme-1464

Article Title: Proposed Amniotic Membrane/Alginate Dialdehyde Based Injectable Hydrogel as a Biofunctional Scaffold for Soft Tissue Engineering

Abstract: This study proposes a novel biofunctional hydrogel composed of decellularized human amniotic membrane (dHAM) and alginate dialdehyde (ADA) as a potential injectable scaffold for regenerative medicine. Human amniotic membranes (HAM) were decellularized. and histological evaluation using hematoxylin and eosin (H&E) staining, Masson's trichrome (MT) staining, and Alcian blue (AB) staining confirmed the complete removal of cellular material while preserving extracellular matrix components such as collagen and glycosaminoglycans. ADA with a theoretical oxidation degree of 5% was synthesized using sodium metaperiodate, and its oxidation degree and oxidation yield were quantified by ultraviolet visible spectrophotometry and iodometric titration, resulting in mean values of 3.58 ± 0.1% and 71.6%, respectively. The composite hydrogel of dHAM and ADA was prepared via Schiff-base crosslinking between aldehyde groups of ADA and amino groups of solubilized dHAM, combined with ionic gelation mediated by calcium carbonate, calcium sulfate dihydrate, and glucono-δ-lactone. Rheological analysis confirmed the formation of a stable. solid-like three-dimensional network, with the storage modulus (G' = 773 Pa) exceeding the loss modulus (G" = 96-104 Pa) across the frequency range, indicating strong elastic dominance. The hydrogel demonstrated shear-thinning behavior, with viscosity decreasing from 8.75×10^s mPa·s to 1.24×10⁴ mPa·s as frequency increased, ensuring smooth injectability. Thanks to its short gelation time (13.5±2.12 min), this formulation appears promising for in situ hydrogel formation applications. Injectability tests showed continuous and uniform extrusion through a 21-gauge needle without clogging, confirming the material's balanced viscosity and mechanical stability under shear stress. This hybrid hydrogel, introduced for the first time, retained the key biochemical and structural features of native extracellular matrix and demonstrated suitable gelation behavior, highlighting its potential as a promising candidate for tissue engineering applications.

Keywords: Decellularized human amniotic membrane, Alginate dialdehyde, Injectable hydrogel, Tissue engineering, In situ formation, Cardiac tissue engineering

Authors: Yasaman Pahlavanzadeh - Yousef Mohammadi - Maryam Saadatmand











Article Code: icbme-1341

Article Title: 3D Printing of Novel Bioactive Polycaprolactone Nanocomposites for Prospective Osteoporotic Bone Defect Engineering

Abstract: Osteoporotic bone defects pose a major clinical challenge, demanding scaffolds that combine mechanical support with bioactivity to stimulate bone regeneration. In this study, we developed a novel 3D-printed polymeric scaffold coated with APTES-functionalized mesoporous bioactive glass (MBGNPs) nanoparticles to address this need. The scaffold featured a four-layer architecture with 800 µm cubic pores, optimized for potential osteoblast adhesion and proliferation. MBGNPS nanoparticles and surface functionalized MBGNPSs were synthesized and thoroughly characterized by using FE-SEM, EDS, XRD, and FTIR analyses; to confirm their mesoporous structure and chemical composition. Additionally, Scaffold characterization confirmed successful nanoparticle deposition, preservation of pore architecture, and chemical integration of the coating. This study demonstrates a simple and effective strategy to fabricate mechanically robust, bioactive polymeric scaffolds, highlighting their potential as platforms for future osteoporotic bone defect engineering applications.

Keywords: Osteoporosis, 3D printed PCL-based scaffold, mesoporous bioactive glass nanoparticles, bioactive scaffold, Nanocomposites

Authors: Fateme Fathi - Hengameh Zolala - Farhad Esmailzadeh - Shohreh Mashyekhan - Irinia Kurzina











Article Code: icbme-1471

Article Title: Shape Memory Polymer-Based Scaffolds for Bone Tissue Engineering

Abstract: In recent years, bone tissue engineering has become a highly promising approach, in which biomaterial scaffolds play a central role by providing structural and biological support for bone regeneration. Among various scaffolding materials, shape-memory polymers (SMPs) have become widely studied because of their ability to recover their original shape from a temporary form when triggered by external stimuli such as heat. This property enables minimally invasive implantation and conformal fitting into irregular bone defects, thereby enhancing osseointegration and tissue ingrowth, making them excellent candidates for bone tissue engineering scaffolds.

Keywords: Bone tissue engineering, Shape-memory polymers, Scaffold

Authors: Farzad Fereidani Mohammadi - Zahra Mohammadi











Article Code: icbme-1443

Article Title: Evaluation of Mechanical and Biological Properties of PCL-coated Magnesium Scaffolds

Abstract: Magnesium scaffolds, owing to their mechanical properties similar to natural bone and their biodegradability, are considered promising candidates for tissue engineering applications. In this study, Mg–Zn–Ca scaffolds were fabricated using the powder metallurgy method with different porosity agents (10% and 30% urea) and subjected to compression testing. The results showed that the 10% urea samples exhibited significantly higher compressive strength (105 ± 5 MPa) compared to the 30% urea samples (68 ± 4 MPa, p < 0.01). Meanwhile, the higher porosity of the 30% urea samples provided more favorable conditions for tissue ingrowth. To enhance the mechanical and biological performance, polycaprolactone (PCL) coating was applied to the scaffolds. Findings revealed that a single-layer PCL coating increased compressive strength by approximately 10–20%, while a three-layer coating led to an improvement of about 20–30% compared with uncoated samples. Moreover, the PCL coating acted as a protective barrier, reducing the degradation rate and providing more favorable biocompatible conditions. Overall, the results indicate that the application of PCL coating is an effective approach to improve both mechanical stability and biological performance of magnesium scaffolds for bone regeneration applications.

Keywords: Porous magnesium scaffold, Polycaprolactone (PCL), Compressive strength, Biodegradability

Authors: Fatemeh Sharifabadi - Sayed Khatiboleslam Sadrnezhaad











Article Code: icbme-1117

Article Title: In Silico Evaluation of PAMAM Dendrimers as Nanocarriers for Targeted Carmustine Delivery in Glioma Therapy

Abstract: PAMAM dendrimers are hyperbranched, monodisperse nanopolymers extensively studied for brain-targeted drug delivery, particularly in glioma treatment. Although Carmustine is an effective anticancer agent for gliomas, its use in combination with PAMAM dendrimers as a nanocarrier has not been thoroughly investigated. In this study, we explored the potential of PAMAM dendrimers as nanocarriers for the targeted delivery of carmustine. The 3D structures of PAMAM dendrimer generations 1 to 6 were constructed using the Build Dendrimer module in Material Studio and geometry-optimised with the Forceite tool. The structure of carmustine was selected from PubChem (CID: 2578). Molecular dockings were performed using AutoDock4. Our results showed that PAMAM Generations 5 and 6 had the most favorable binding energies with carmustine, with values of -4.89 and -4.09 kcal/mol, respectively. These findings suggest that higher-generation PAMAM dendrimers exhibit stronger binding affinities and more stable interactions with carmustine compared to lower generations, indicating their potential as effective nanocarriers for carmustine delivery.

Keywords: PAMAM dendrimers, Carmustine, Nanocarriers, Drug delivery, Glioma, Molecular docking

Authors: Noora Shaerzadeh - Maryam Azimzadeh Irani - Yeganeh Abbasian











Article Code: icbme-1147

Article Title: Electrospun Chitosan-Gelatin/ZIF-8 Nanofibers Scaffolds for Enhanced Wound Healing

Abstract: Wound healing poses a major public health challenge, exacerbated by the growing burden of chronic diseases and aging populations. Electrospun nanofibrous dressings offer unique advantages enhanced surface-to-volume ratio, controllable porosity, and the potential to administer bioactive compounds to accelerate tissue repair. Herein, we describe the preparation and characterization of chitosan-derived nanofibers incorporating zinc imidazolate framework 8 (ZIF-8) nanoparticles to improve antibacterial activity. ZIF-8 particles were synthesized via coordination of zinc nitrate with 2 methylimidazole, yielding uniform nanoparticles (138 ± 34 nm). Subsequent electrospinning under optimized conditions produced smooth, bead free nanofibers averaging 213 ± 31 nm in diameter. Structural and compositional analyses SEM, FTIR, EDS, and elemental mapping confirmed nanoparticle incorporation without compromising fiber morphology. Antibacterial assay revealed 90% inhibition of Escherichia coli and 10% inhibition of Staphylococcus aureus. Collectively, the present data endorse the suitability of chitosan/ZIF 8 electrospun mats as materials for wound therapy with both infection-preventing and healing-promoting properties.

Keywords: wound dressing, electrospinnig, nanofibers, ZIF-8, chitosan, gelatin

Authors: Maryam Nosrati hashi - Maryam Tajabadi - Fateme Mirzajani - Alireza Khavandi











Article Code: icbme-1385

Article Title: Synthesis and Characterization of an Injectable Magnetic Scaffold Based on Alginate/Chitosan and Zero-Valent Iron for Hyperthermia

Abstract: In this study, we propose an innovative approach for targeted hyperthermia therapy by developing injectable magnetic scaffolds based on alginate/chitosan (CS) composites integrated with Zero-valent Iron Nanoparticles (nZVI), which has not been systematically investigated before. Alginate and CS, both biocompatible and biodegradable materials, were used to create a stable, injectable hydrogel matrix. This study focuses on the synthesis and characterization of a magnetic hydrogel intended for cancer treatment. nZVI nanoparticles were incorporated to enhance the magnetic properties, facilitating targeted heat generation under an external magnetic field. The synthesized hydrogels were characterized through various techniques, including X-ray diffraction (XRD), Fourier-transform infrared spectroscopy (FTIR), vibrating sample magnetometry (VSM), scanning electron microscopy (SEM), and energy-dispersive X-ray spectroscopy (EDX), which confirmed the successful integration of nZVI and the hydrogel matrix. The hydrogel exhibited desirable properties such as high swelling ratios, good stability, and effective degradation profiles, making it suitable for magnetic hyperthermia applications.

Keywords: Magnetic hydrogel, Injectable scaffold, Alginate, Chitosan, Zero-valent Iron Nanoparticle (nZVI), Hyperthermia

Authors: Mohammad Jafari Fashtami - Bahareh Khalilivavdareh - Delaram Dezfoulian - Maryam Tajabadi











Article Code: icbme-1350

Article Title: Development of Folic Acid-Conjugated Iron Oxide Nanoparticles Loaded with Doxorubicin via Arc Discharge: A Novel Approach for Synergistic Photothermal-Chemotherapy of Cancer Using Bacterial Cellulose-Polyvinyl Alcohol Hydrogel

Abstract: The design of multifunctional nanomaterials that combine chemotherapy with photothermal therapy (PTT) has emerged as a promising strategy to overcome the limitations of conventional cancer treatments. Here, we report the fabrication of a novel therapeutic hydrogel system composed of Folic Acid-functionalized iron oxide nanoparticles (IO NPs) synthesized via an arc-discharge method, loaded with doxorubicin (DOX), and embedded within a bacterial cellulose/polyvinyl alcohol (BC/PVA) matrix. The arc-discharge technique produced crystalline FeNPs with high purity and narrow size distribution. Folic acid conjugation enabled tumortargeted delivery, while DOX was efficiently incorporated via electrostatic and π - π stacking interactions. Embedding in the BC/PVA hydrogel facilitated sustained drug release and improved biocompatibility. Structural and functional characterization was conducted using Xray diffraction (XRD), scanning electron microscopy (SEM), UV-Vis spectroscopy, magnetization studies, swelling and rheological analysis, and photothermal heating experiments. In vitro cancer cell studies demonstrated enhanced therapeutic efficacy of the hydrogel system under near-infrared (NIR) irradiation, where synergistic chemo-photothermal effects resulted in significant reduction in cell viability compared to single-mode treatments. This study highlights a multifunctional nanoplatform that integrates targeted delivery, controlled release, and dual therapeutic modalities for effective cancer treatment.

Keywords: Cancer Treatment, Nanomedicine, Drug Delivery System, Hydrogel, Nanocellulose, Photothermal therapy, Chemotherapy, Arc Discharge, Nanoparticles, Wound Healing

Authors: Saeid Orangi - Soodabeh Davaran











Article Code: icbme-1247

Article Title: Cerium-Based MOFs Incorporated into Zwitterionic Polymers for Disruption of

Bacterial Biofilms: Toward Next-Generation Antimicrobial Surfaces

Abstract: A zwitterionic block-copolymer/cerium-MOF composite wound dressing was developed to couple antifouling with active antibacterial function. The film was prepared by integrating room-temperature-synthesized Ce-BTC into P(MAA-co-CouMA)-b-PDMAEMA via solution casting. The targeted composition was verified by FTIR and ^1H NMR, and a homogeneous dispersion of Ce-MOF domains at the examined scales was indicated by SEM (ImageJ-estimated mean domain size ≈0.43 µm). Antibacterial performance against Escherichia coli was enhanced, as a clear inhibition zone and markedly reduced colony formation were observed relative to the neat polymer film. These outcomes are attributed to the combined effects of charge-neutral, ultra-low-fouling surfaces with Ce-mediated antibacterial activity (nanozyme pathways with possible contributory Ce-ion release). Novelty was established through (i) an all-solution, low-temperature route to Ce-BTC/zwitterionic films suitable for scalable processing, (ii) incorporation of photoactive coumarin units enabling future morphology locking by crosslinking, and (iii) a materials-level demonstration that pairing antifouling with Ce-MOF activity yields measurable antibacterial gains over the zwitterionic polymer alone. The findings position Ce-MOF/zwitterionic films as promising, processable candidates for next-generation antimicrobial wound dressings.

Keywords: Zwitterionic polymer, Ce-MOFs, Antibacterial activity, Wound dressing, MOF–polymer composites

Authors: Helia Heydarinasab - Vahid Haddadi Asl - Mahdi Tohidian









Article Code: icbme-1413

Article Title: Gravity-Directed Growth of ZnO Nanorods: Morphological Control via Chemical Bath Deposition

Abstract: The morphology of Zinc Oxide(ZnO) nanorods(NRs) strongly influences their performance in biosensing and cancer cell culture applications. Although chemical bath deposition (CBD) is a cost-effective method for ZnO synthesis, the influence of gravity on nanorod growth remains underexplored due to difficulties in controlling substrate orientation. In this study, we developed a custom-built holder that enables precise upward (against gravity) and downward (with gravity) growth orientations during CBD. Using this setup, we demonstrate that gravity significantly impacts NR morphology, downward growth produced nanorods with smaller, more uniform diameters, improved vertical alignment, and eliminated parasitic microrod clustering. The resulting nanostructured surfaces enhanced cancer cell culture interfaces, highlighting the importance of substrate topography for biological interactions. Our results introduce both a practical tool for orientation, controlled CBD and new insights into gravity, directed nanostructure growth.

Keywords: Zinc Oxide Nanorods, Chemical Bath Deposition (CBD), Gravity-directed Synthesis, Morphological control, Biosensor Platform, Cancer Cell Culture

Authors: Masoud Ghashami - Melisa Daryayi - Mohammad Abdolahad











Article Code: icbme-1296

Article Title: Biomedical Applications of Pectin Nanomaterials: Progress and Perspectives

Abstract: Pectin polysaccharide is a natural biopolymer that has recently emerged as a sustainable platform for the design of functional nanomaterials in biomedical research. Its excellent biocompatibility, biodegradability, low toxicity, chemical versatility, low cost, and ease of availability make it well-suited for nanoscale delivery platforms designed to encapsulate and protect therapeutic agents until they reach the target tissues to be released sustained/controlled. Pectin-based nanomaterials are particularly effective in oral delivery because pectin retains its structure in acidic media of small intestine. On the other hand, pectin and pectin-coated nanomaterials have strong potential in liver cancer-targeted drug delivery through selective binding to hepatocyte cancer cell receptors. While pectin-coated nanocomposites are being explored as non-viral vectors for gene delivery, further clinical validation is needed. In addition, pectin has intrinsic biological properties, including anticancer, antidiabetic, and anti-cholesterol, antioxidant, and antimicrobial activities, that enhance therapeutic effects. Pectin nanomaterials have illustrated significant potential in wound healing by promoting cell proliferation, regulating immune responses, and enhancing tissue regeneration, especially when loaded with therapeutic/pharmaceutical agents. This review highlights recent advances, advantages, limitations, and future directions of pectin-based nanomaterials in biomedical applications, specifically in drug/gene delivery systems and wound healing and theragnostic applications.

Keywords: pectin, biopolymer, nanomaterials, drug delivery, gene delivery, theranostics, wound healing

Authors: Maryam Rajabzadeh-khosroshahi - Ali Baradar Khoshfetrat - Mehdi Salami-Kalajahi











Article Code: icbme-1021

Article Title: Engineering Conductive Hydrogels for Biomedical Applications

Abstract: Hydrogels are rapidly emerging as a pivotal class of materials across diverse disciplines, largely owing to their exceptional attributes such as biocompatibility, biodegradability, and inherent hydrophilicity. Furthermore, their notable adhesive qualities and impressive elasticity enable seamless integration with myriad surfaces. Within their extensive range of applications, particular interest has been directed towards how these substances influence vital biological phenomena, including cellular migration, neovascularization, and the moderation of inflammatory responses. The present paper is dedicated to elucidating the action mechanisms of conductive hydrogels in promoting wound recovery. Concurrently, it offers an overview of advancements in relevant materials and methodologies, discusses prevailing challenges, and forecasts future directions within this specialized domain.

Keywords: Conductive Hydrogels, Wound Healing, Wearable Sensors, Implantable Bioelectronics, Real Time Health Monitoring

Authors: Elham Amiraslani - Zahra Mohammadi









Article Code: icbme-1347

Article Title: Influence of PEG/PCL soft segments composition on the wettability and water absorption of polyurethane based scaffolds

Abstract: Thermoplastic polyurethanes (PUs) with dual soft segments of polycaprolactone (PCL) and polyethylene glycol (PEG) were synthesized to study the effect of soft segment composition on the hydrophilicity of the bulk PU. Three formulations with PCL/PEG ratios of 90:10, 80:20, and 70:30 were prepared. FTIR confirmed urethane bond formation, while water contact angle measurements showed increased hydrophilicity with higher PEG content: 10% PEG scaffold = 62.22° (relatively hydrophobic), 30% PEG scaffold = 27.79° (hydrophilic). The water absorption rate was changed from 8.7% (polyurethane containing 10% PEG) to 57.7% (polyurethane containing 30% PEG) within 24 hours. Finally, the synthesized polyurethanes was electrospun to mimic the extracellular matrix. Adjusting PEG/PCL ratios enables the control of scaffold surface properties, which is essential for cell adhesion and proliferation in tissue engineering.

Keywords: Polyurethane, Scaffold, PEG, PCL, Electrospinning, Hydrophilicity, soft segments, hard segments, polyol.

Authors: Asma Feyzi - Sajjad Moghanlou - Mostafa Rezaei - Farhang Abbasi - Amin Babaie









Article Code: icbme-1383

Article Title: DMAEMA-based photocrosslinkable hydrogels with injectable capabilities for smart drug delivery systems in implant infections

Abstract: A novel class of photocrosslinkable hydrogels with precisely tunable properties was developed for advanced biomedical applications. Using RAFT polymerization, we synthesized two distinct block copolymers, PDMAEMA-b-PMMA-CM, with varying coumarin contents (LCP and HCP). Our structural characterization confirmed the successful incorporation of all monomer units and validated that the HCP polymer contains a significantly higher coumarin content (8.6%) than the LCP sample (4.8%). We systematically investigated the effect of this compositional difference on material performance. Rheological analysis demonstrated that both hydrogels exhibit critical shear-thinning behavior, a key property for minimally invasive injection. Furthermore, the higher coumarin content in HCP led to a superior photodimerization efficiency and a more robust network with enhanced mechanical properties. Ultimately, the hydrogels proved to be a versatile and smart drug delivery platform, allowing for controlled release governed by the network's crosslinking density and a rapid, triggered release in response to acidic environments. This study establishes a clear structure-property relationship, confirming the potential of these injectable materials for targeted therapeutic delivery in applications such as implant-related infection control.

Keywords: Injectable materials, Smart drug delivery hydrogel, Implant infection, photo crosslinking

Authors: Fatemeh Hai Sadeghi - Vahid Haddadi Asl - Hanie Ahmadi











Article Code: icbme-1386

Article Title: Multifunctional Coatings for Biomedical Alloys: Biocompatibility and Antibacterial Activity of Hydroxyapatite with YSZ and Silver on Nitinol

Abstract: Biomedical implants often encounter complications such as infection, cytotoxicity, and limited bioactivity. Nitinol has emerged as a promising candidate due to its favorable mechanical properties. To enhance its biological performance, hydroxyapatite (HA) coatings are commonly applied. However, electrochemically deposited HA coatings exhibit insufficient antibacterial activity and limited protection against the release of toxic ions. In this study, HA coatings were fabricated using pulsed electrochemical deposition at 70 °C, current density of 20 mA/cm², and a deposition time of 20 minutes, with a duty cycle of 10%, to improve these shortcomings by incorporating yttria-stabilized zirconia (YSZ) and silver nanoparticles into HA coatings at various concentrations. YSZ was added at 0.25, 0.5, and 1 g/L, and the resulting samples were characterized using XRD, SEM, and EDS techniques. Nickel ion release analysis indicated reduced ion leaching and lower cytotoxicity at 0.25 and 0.5 g/L concentrations, with 0.5 g/L identified as the optimal formulation. Subsequently, silver was introduced into the optimized coating at 0.1, 0.2, and 0.4 g/L. Antibacterial assays revealed that YSZ enhanced antibacterial efficacy by up to 72%, while silver addition further increased it to 85%. Immersion in simulated body fluid (SBF) for 7 days confirmed complete apatite coverage on the surface, indicating improved bioactivity and apatite nucleation facilitated by the nanoparticles.

Keywords: Antibacterial, Hydroxyapatite, Ion release, Nitinol, Silver, Yttria-Stabilized Zirconia

Authors: Mehdi Hosseini - Mehdi Mozammel - Milad Hosseini - Jafar Khalil-Allafi









Article Code: icbme-1252

Article Title: Preparation and Characterization of Silicone Hydrogel Contact Lenses Based on TRIS-HEMA

Abstract: In this study, silicone-based hydrogel contact lenses were prepared via the free radical polymerization of 3-(methacryloyloxy)propyltris(trimethylsiloxy)silane (TRIS), and 2-hydroxyethylmethacrylate (HEMA) with ethylene glycol dimethacrylate (EGDMA) as the cross-linker and AIBN as the initiator, aiming to enhance the water swelling, wettability and antifouling property. By changing the compositions, the hydrophilicity of the resultant silicone hydrogel lenses can be adjusted. The properties of silicone hydrogel lenses were analyzed such as equilibrium water content, optical transparency, and contact angle. The results showed that the TRIS content in all formulations decreased the equilibrium water content, while HEMA contributed the hydrophilicity of the hydrogels. Water contact angle measurements suggested that the HEMA hydrophilic groups could rearrange on the upper surface of the TRIS containing polymer in the water environment, improving the wettability of the surface. The transmittance of hydrogels contact lenses shows that all hydrogel contact lenses exhibited light transparency in the range 96-97 %.

Keywords: TRIS, HEMA, silicone hydrogel, contact lens

Authors: Mahdiyeh Sedghi - Hakimeh Ghaleh - Sina Hajibababzadeh











Article Code: icbme-1434

Article Title: A Quantitative Approach to Assess Rhus coriaria Nanophytosomes in Ketamine-Induced Liver Injury

Abstract: Background: Ketamine, a widely used anesthetic, can cause hepatotoxicity primarily through elevation of serum liver enzymes. Rhus coriaria (sumac) has antioxidant potential, but its clinical application is limited by poor bioavailability. This study investigates the protective effects of sumac and its nanophytosome formulation against ketamine-induced liver injury in male mice.

Methods: Twenty-five male mice were randomly assigned to five groups: control, nanophytosome control, ketamine (20 mg/kg), sumac-treated, and sumac-nanophytosome-treated. Serum alanine aminotransferase (ALT) and aspartate aminotransferase (AST) levels were measured after 15 days. Sumac nanophytosomes were synthesized and characterized for particle size and encapsulation efficiency.

Results: Ketamine increased ALT to 150 \pm 12 U/L and AST to 180 \pm 15 U/L vs. control (ALT 45 \pm 6, AST 52 \pm 7, p < 0.001). Treatment with sumac nanophytosomes reduced ALT to 68 \pm 9 (p = 0.002, η^2 = 0.62) and AST to 92 \pm 11 (p < 0.001, η^2 = 0.71). Crude sumac extract reduced enzymes less effectively (ALT 102 \pm 13, AST 138 \pm 12).

Conclusion: Sumac nanophytosomes demonstrate significant hepatoprotective effects against ketamine-induced liver injury by reducing ALT and AST levels. This nanotechnology-based formulation offers a promising strategy for managing drug-induced hepatotoxicity and represents the first direct comparison of crude versus nanophytosome sumac in this context.

Keywords: Rhus coriaria, Sumac, Ketamine-induced liver toxicity, Nanophytosome, Hepatoprotection

Authors: Narjes Amin - Akbar Hajizadeh Moghadam - Amin Mohammad Mohammadi - Kimia Mozahheb Yousefi - Fereshteh Mir Mohammadrezaei - Sedigheh Khanjani Jelodar









Article Code: icbme-1068

Article Title: A Review of the Impact of Visible Spectrum Electromagnetic Wavelengths on Cellular Behaviors

Abstract: This review surveys studies published between 2019 and 2023 on how visible-spectrum illumination alters measurable cellular phenotypes under explicitly reported dosimetry. The analysis centers on wavelength (λ), irradiance (mW·cm⁻²), radiant exposure (J·cm⁻²), illumination geometry (distance/angle, beam profile), source type (LED/laser), and cell lineage. Across in vitro and in vivo models, visible light has been shown to regulate morphology, adhesion, migration, proliferation, apoptosis, and metabolism in ways that are jointly wavelength- and dose-dependent. To enable comparable and reproducible findings, reports should disclose λ , irradiance, radiant exposure, source–sample geometry, and cell type in a uniform manner. Rather than restating textbook definitions, this article organizes recent evidence into wavelength–dose–phenotype maps, identifies convergent mechanistic patterns (e.g., red/NIR support of mitochondrial function versus blue-light oxidative stress), and distills practical guidance for experiment design and biomedical applications.

Keywords: Electromagnetic waves, Visible spectrum, Cellular adhesion, Cellular behavior, Cell proliferation, Cell migration

Authors: Arsalan Heidarpanah - Hamid Keshvari - Mehrdad Saviz









Article Code: icbme-1435

Article Title: Antimicrobial and Bioactivity Evaluation of Laser-Modified Biodegradable Magnesium Allov Coated with Chitosan–Graphene Oxide

Abstract: Magnesium alloys are promising for medical implants due to their bone-like elastic modulus and biodegradable nature, which eliminates the need for secondary removal surgery. However, these materials still face limitations in their mechanical properties and biological performance. Therefore, the development of polymeric coatings has been considered an effective strategy to overcome these drawbacks. Chitosan has been employed due to its favorable biocompatibility and mechanical characteristics, while graphene oxide has been incorporated as a bioactivity-enhancing agent owing to its antimicrobial properties. The coatings were fabricated using a dip-coating method, and the effects of different GO concentrations (0, 0.25, 1, and 2 wt%) on antimicrobial and bioactive properties were evaluated. The results indicate that the coating significantly enhanced both the antimicrobial efficacy and bioactivity of the substrate.

Keywords: Akermanite, Antimicrobial, Bioactivity, Chitosan, Coating Graphene oxide, Laser texturing, Magnesium alloy

Authors: Seyed Alireza Ensaniat - Ali Safary - Farid Naeimi - Hamid Reza Bakhsheshi Rad - Monireh Ganjali











Article Code: icbme-1065

Article Title: Engineering Injectable Gelatin-Tyramine/Alginate-Tyramine Hydrogels for Bone Tissue Engineering: A Ratio-Dependent Study of Structure, Mechanics, and Biocompatibility

Abstract: The development of injectable hydrogels with tunable physicochemical and biological properties is critical for advancing minimally invasive strategies in bone tissue engineering (BTE). In this study, enzymatically crosslinked hydrogels composed of tyramine-modified gelatin (GEL-TA) and alginate (ALG-TA) were engineered at three volumetric ratios (70:30, 50:50, 30:70) and systematically evaluated for their structural, mechanical, rheological, and biological performance. The optimized GEL50/ALG50 formulation exhibited a balanced gelation time, an interconnected porous morphology, and superior mechanical properties (Young's modulus: 185.3 ± 12.7 kPa), which can be attributed to enhanced polymer entanglement and crosslinking density. All hydrogels exhibited shear-thinning behavior, desirable for injectability. Human osteosarcoma cell line (MG-63)-based assays confirmed high cytocompatibility, with the GEL50/ALG50 formulation supporting the most favorable cell adhesion, viability, and morphology. These findings highlight the potential of GEL-TA/ALG-TA hydrogels, particularly the 50:50 ratio, as injectable and biocompatible scaffolds for bone regeneration applications.

Keywords: Injectable hydrogel, Tyramine-modified polymers, Enzymatic cross-linking, Bone Tissue engineering

Authors: Melika Mansouri Moghaddam - Soroush Ghofrani Beiragh - Elaheh Jooybar - Rana Imani











Article Code: icbme-1359

Article Title: Dual pH-and glucose-responsive terpolymer based on phenylboronic acid

Abstract: dual pH and glucose responsive terpolymers p(HEMA-PBA-co-HEMA-co-DMAEMA) were synthesized via RAFT polymerization with different DMAEMA ratios. 1H NMR confirmed the successful synthesis. HPHD20 demonstrated the highest glucose responsivity compared to HPHD30 and HPHD40. The terpolymers are used as a biosensing application and insulin delivery systems.

Keywords: Diabetes phenylboronic acid pH- and glucose- responsive p(HEMA-PBA-co-HEMA-co-DMAEMA)

Authors: Fatemeh Ghashghaee - Mahdi Salami hosseini - Mehdi Salami Kalajahi











Article Code: icbme-1121

Article Title: Smart Injectable Hydrogels: From In-Situ Gelation to On-Demand Drug Release

in Regenerative Medicine

Abstract: Injectable hydrogels have emerged as a transformative class of biomaterials, poised to revolutionize regenerative medicine and targeted drug delivery. Their ability to be administered via minimally invasive procedures and form solid scaffolds in situ addresses many limitations of conventional therapies and pre-formed implants. This review focuses on the evolution of these platforms into "smart" systems, which are engineered to respond to specific physiological or external stimuli. We provide a comprehensive overview of the fundamental polymeric components, contrasting the biocompatibility of natural polymers with the tunability of synthetic analogues, and highlighting the rise of hybrid systems. A central focus is placed on the diverse mechanisms of in situ gelation, from reversible physical crosslinking to stable covalent bond formation, which dictate the material's mechanical properties, injectability, and degradation profile. Furthermore, this review systematically details the engineering of stimuliresponsive behaviors—including sensitivity to temperature, pH, light, redox potential, and enzymes—that enable on-demand therapeutic release. We explore how these smart functionalities are being leveraged in cutting-edge applications, including advanced wound healing, cardiac and neural tissue engineering, osteochondral repair, and localized chemotherapy. Finally, we address the persistent challenges facing clinical translation and discuss future perspectives, including the development of multi-responsive systems, 4D bioprinting, and immunomodulatory materials that promise to usher in a new era of personalized and controlled regenerative therapies.

Keywords: Injectable hydrogels, smart materials, in-situ gelation, controlled drug release, regenerative medicine, tissue engineering

Authors: Leyla Mirzaei - Adnan Alizadeh Naeini - Neda Sadat Miragha Babaei











Article Code: icbme-1432

Article Title: Preparation of pH sensitive Carboxymethyl cellulose / Polyvinylpyrrolidone based hydrogels for drug delivery applications

Abstract: Hydrogels are smart materials widely applied in controlled drug delivery systems. In this work, hybrid hydrogels composed of carboxymethyl cellulose (CMC) and polyvinylpyrrolidone (PVP) were prepared through free-radical polymerization. N,N'-Methylene bisacrylamide (NNMBA) served as the crosslinker, while ammonium persulfate (APS) acted as the initiator. The incorporation of CMC and PVP enabled the formation of a composite network with enhanced structural and functional characteristics. Chemical crosslinking was employed to strengthen the mechanical integrity and establish stable covalent bonds within the hydrogel matrix. The swelling performance of the synthesized CMC/PVP hydrogels was evaluated at pH values of 1.5, 4.0, and 7.4, revealing maximum swelling under alkaline conditions. Overall, the findings demonstrate that these polymeric networks hold great promise as carriers for oral drug delivery applications.

Keywords: Hydrogels, pH_sensitive drug delivery, Carboxymethyl cellulose, Polyvinylpyrrolidone

Authors: Masoumeh Olad Mazraeh - Hanieh Shokrkar - Nilufar Nasirpur











Article Code: icbme-1360

Article Title: Synthesis and Swelling Behavior of pH-Sensitive Chitosan/Polyvinylpyrrolidone

Hydrogels for Drug Delivery Applications

Abstract: pH-sensitive hydrogels have attracted considerable attention due to their great potential in targeted drug delivery systems. In this study, a novel composite hydrogel based on chitosan (a natural bioactive polymer) and polyvinylpyrrolidone (PVP, a synthetic polymer that improves mechanical properties) was synthesized via free radical polymerization using N, N'-methylene bisacrylamide (as a crosslinker) and ammonium persulfate (as an initiator). The swelling behavior of the hydrogel was investigated within the physiological pH range (1.5-7.4). The results revealed a strong pH-dependent swelling behavior, with a maximum swelling ratio of 1876% at pH = 1.5 and a minimum of 553% at pH = 7.4. This pronounced sensitivity to pH variations makes the synthesized hydrogel a promising candidate for use as a smart drug delivery carrier, particularly in acidic environments.

Keywords: Swelling, Targeted drug delivery, Polyvinylpyrrolidone, Chitosan, pH-sensitive hydrogel

Authors: Shaghayegh Zameni Nir - Hanieh Shokrkar - Niloofar Nasirpour











Article Code: icbme-1097

Article Title: Photoresponsive Zwitterionic Block Copolymer Nanoparticles Prepared by a One-Step Nanoprecipitation–Photocrosslinking Strategy for Precision Cancer Chemotherapy

Abstract: Targeted polymeric nanocarriers are increasingly explored to enhance the efficacy and safety of anticancer therapeutics. In this study, we report the design and fabrication of photoresponsive block copolymer nanoparticles, P(MAA-co-CouMA)-b-PDMAEMA, synthesized via RAFT polymerization. The copolymer combines the non-fouling characteristics of zwitterionic segments with the light-responsive coumarin moieties, enabling photocrosslinking for enhanced structural stability. A one-pot strategy was employed wherein nanoprecipitation, doxorubicin (DOX) encapsulation, and UV-induced crosslinking occurred simultaneously, simplifying fabrication and improving drug-loading efficiency. Characterization by FTIR and ¹H NMR confirmed successful copolymer synthesis, while SEM and DLS analyses revealed spherical nanoparticles with uniform morphology (~150 nm by SEM; ~250 nm hydrodynamic diameter, PDI < 0.2). In vitro DOX release studies at pH 7.4 and 37 °C demonstrated an initial burst release (~10-12%) followed by sustained release (~35% over 50 h), attributed to the coumarin-crosslinked matrix. This integrated approach offers a versatile platform for controlled and targeted drug delivery in cancer therapy.

Keywords: zwitterionic copolymer, coumarin methacrylate, RAFT polymerization, nanoprecipitation, photocrosslinking, drug delivery nanoparticles, simultaneous encapsulation

Authors: Helia Heydarinasab - Vahid Haddadi Asl - Mahdi Tohidian - Hanie Ahmadi











Article Code: icbme-1022

Article Title: Innovative Biomimetic Skin Repair Strategies Utilizing Barium Titanate

Abstract: Skin healing is guided by endogenous electric fields, and while external electrical stimulation can help, it's impractical due to bulky equipment. Piezoelectric materials like barium titanate offer a self-powered solution by generating electrical signals from body movements. This review highlights barium titanate-based wound dressings, which are biocompatible, flexible, and efficient. When combined with other materials, they enhance healing by promoting cell activity, tissue regeneration, and providing antibacterial and anti-inflammatory effects. These dressings show strong potential for regeneration and repair of chronic and infected wounds without external power sources.

Keywords: Barium titanate, Skin repair, Piezoelectric, Regeneration, biomimetic wound dressing

Authors: Hossein Norouzi Bazmin Abadi - Zahra Mohammadi











Article Code: icbme-1361

Article Title: Fused Deposition Modeling in Bone Tissue Engineering: A Comprehensive

Review

Abstract: Bone tissue engineering has emerged as a promising approach to address the limitations of conventional bone grafting methods, such as autografts, allografts, and xenografts, which are hindered by issues like immunological responses, disease transmission risks, and limited donor availability. Fused Deposition Modeling (FDM), a cost-effective and versatile 3D printing technique, has gained significant attention for fabricating bone scaffolds with precise control over geometry, porosity, and mechanical properties. This paper reviews the role of FDM in bone tissue engineering, focusing on its ability to produce scaffolds that mimic the extracellular matrix (ECM) of bone, facilitating cell migration, proliferation, and differentiation. Key scaffold requirements, including biocompatibility, biodegradability, mechanical stability, and optimal pore size, are discussed alongside the materials used, such as polylactic acid (PLA), polycaprolactone (PCL), and their composites with bioactive ceramics like hydroxyapatite (HA) and tricalcium phosphate (TCP). The FDM process, from CAD design to G-code conversion and layer-by-layer deposition, is detailed, highlighting its accessibility through open-source platforms and low-cost materials. Recent advancements, including the development of bio-based filaments and hybrid polymer-ceramic composites, are explored for their enhanced bioactivity and sustainability. The paper also addresses challenges, such as limited material options and high extrusion temperatures, which restrict direct cell incorporation. By offering patient-specific scaffold designs with tunable properties, FDM demonstrates significant potential for bone regeneration, paving the way for advanced clinical applications in addressing complex bone defects.

Keywords: 3D printing, Fused Deposition Modeling (FDM), Bone tissue engineering, Biocompatibility, Polylactic acid (PLA), regenerative medicine, Bone scaffolds

Authors: Parsa Doaguie - Shima Mirzaie Parsa











Article Code: icbme-1426

Article Title: Chondrocyte-Imprinted Substrates: Promoting MSC Chondrogenesis and Regulating Inflammatory Gene Expression

Abstract: Due to the limitations of using primary chondrocytes, directing stem cells toward chondrogenesis via physical cues has emerged as an efficient strategy for cartilage regeneration. Substrate topography can strongly influence cellular behavior, including differentiation. Here, we investigated the effect of chondrocyte-imprinted substrates on the chondrogenic differentiation of stem cells and dedifferentiated chondrocytes without chemical inducers. Rabbit chondrocytes were isolated, fixed, and used as templates to fabricate patterned polydimethylsiloxane (PDMS) substrates. Rabbit adipose-derived mesenchymal stem cells (ADSCs) and passage 3 dedifferentiated chondrocytes were cultured on these substrates and analyzed using cell staining and real-time PCR for chondrogenic and inflammatory gene expression. Compared to spindle-like control cells, cells on imprinted substrates exhibited round morphologies, enhanced glycosaminoglycan and collagen I/III production, actin fiber rearrangement, and higher expression of chondrogenic genes (collagen II, aggrecan, sox9) with minimal inflammatory gene expression (TNF-α, IL-1, IL-6). These results demonstrate that chondrocyte-imprinted PDMS substrates can effectively induce chondrogenesis without chemical factors, providing a promising tool for cartilage tissue engineering.

Keywords: Chondrogenic differentiation, Cell-imprinted substrate, Topography, Cartilage Tissue, Mesenchymal Stem Cells, Tissue engineering

Authors: Parisa Madani - Sara Derhanbakhsh - Nasrin Salehi - Farzaneh Safshekan - Javad Mohammadi - Shahin Bonakdar











Article Code: icbme-1190

Article Title: Application of Nanomaterials in Biomaterials for the Regeneration of Bone and Cartilage Tissues

Abstract: This study investigates the application of nanomaterials in biomaterials for the regeneration of bone and cartilage tissues. The aim of this research was to design and evaluate nanocomposite scaffolds composed of hydroxyapatite (nHA), poly (lactic-co-glycolic acid) (PLGA), type I collagen, and iron oxide nanoparticles (Fe₃O₄) for use in bone and cartilage tissue engineering. Electrospinning was employed for scaffold fabrication. Experimental results demonstrated that nHA/PLGA nanocomposite scaffolds exhibited excellent mechanical properties, including high compressive strength (20±1.5 MPa), along with superior biological performance such as high biocompatibility and osteoblast viability of 90±5%. Furthermore, collagen/polymer-based scaffolds, due to their outstanding biological characteristics especially in cartilage tissue repair—promoted significant chondrocyte growth and differentiation into adipocyte-like cells. Additionally, iron oxide nanoparticles (Fe₃O₄) imparted magnetic properties to the scaffolds, enabling their use in specialized applications such as targeted drug delivery, scaffold degradation monitoring, and magnetic field-mediated tissue stimulation. Histopathological and microscopic analyses confirmed the successful regeneration of bone and cartilage tissues in animal models. This study highlights that nanomaterials can effectively enhance the performance of biomaterials for tissue engineering applications.

Keywords: nanomaterials, bone tissue regeneration, cartilage tissue regeneration, nanocomposites, hydroxyapatite poly (lactic-co-glycolic acid) (PLGA), type I collagen, iron oxide nanoparticles (Fe₃O₄)

Authors: Behnaz Alijani - Niloufar Kazami











Article Code: icbme-1469

Article Title: Curcumin-Loaded Carboxymethyl Cellulose/Polyvinyl Alcohol Smart Wound Dressing: A Biosensor Approach for pH-Responsive Monitoring and Healing

Abstract: Developing wound dressings that support healing and allow real-time monitoring is a key priority in modern wound care. In this study, we designed a curcumin-loaded carboxymethyl cellulose (CMC)/polyvinyl alcohol (PVA) composite dressing with integrated pH-responsive colorimetric sensing. The films were made by solution blending and freeze-drying. They formed porous, absorbent structures that quickly absorbed fluid and managed wound exudates effectively. Curcumin served as both a therapeutic agent-delivering antioxidant, anti-inflammatory, and antibacterial effects-and a natural colorimetric indicator through its keto-enol tautomerism, enabling reversible pH-dependent transitions visible to the naked eye. UV-Vis spectroscopy confirmed absorbance shifts under acidic and alkaline conditions. It also showed that curcumin remained ~80% stable after 14 days in the polymer matrix FTIR and SEM confirmed successful incorporation and uniform distribution of curcumin within the polymer network. Cytotoxicity assays demonstrated excellent biocompatibility, while disc diffusion and MIC assays revealed significant antibacterial activity of the curcumin-loaded films against Pseudomonas aeruginosa, confirming their potential to reduce bacterial growth. Smartphone-based RGB analysis showed a strong correlation with pH $(R^2 \approx 0.99)$, highlighting the feasibility of low-cost digital wound monitoring. Mechanical testing indicated sufficient tensile strength and flexibility for practical wound application. Quantitative antibacterial data (inhibition zone diameter and MIC) supported strong antimicrobial performance.

The primary objective of this study was to develop a multifunctional wound dressing capable of both protecting and monitoring wounds in real-time. The proposed system is specifically designed for chronic and infected wounds where pH imbalance delays healing. In addition to antimicrobial activity, the fabricated films demonstrated desirable swelling capacity and sustained curcumin release, further highlighting the practical applicability of the dressing in wound care. Cost—benefit analysis demonstrated clear economic advantages over commercial gauze-based and hydrocolloid dressings. The fabrication method is compatible with industrial scale-up, although process optimization is required. Overall, the curcumin-loaded CMC/PVA dressing provides a multifunctional platform that combines biocompatibility, antibacterial activity, pH-responsive biosensing, and cost-effectiveness for next-generation wound care. Future studies will investigate in vivo performance, long-term stability, and clinical translation potential to validate its effectiveness in real-world conditions

Overall, the curcumin-loaded CMC/PVA dressing provides a multifunctional platform that combines biocompatibility, antibacterial activity, pH-responsive biosensing, mechanical stability, and cost-effectiveness for next-generation wound care. Future studies will investigate in vivo performance, long-term stability, and clinical translation potential.

Keywords: Smart Wound Dressing, Carboxymetyl Cellulose, Polyvinyl alcohol, Tissue regeneration, urcumin, Colorimetric Biosensor, Biopolymer, Hydrogel, Biocomaptible, Wound Healing

Authors: Saeid Orangi - Soodabeh Davaran











Article Code: icbme-1048

Article Title: Stem cell engineering in tissue repair: A Review of Therapeutic Perspectives

Abstract: Stem cell engineering represents a transformative frontier in regenerative medicine, offering significant therapeutic potential for the repair and replacement of damaged tissues. This review explores the cellular and molecular mechanisms governing stem cell activity, with a particular emphasis on mesenchymal stem cells (MSCs) and their role in modulating immune responses, promoting angiogenesis, and supporting tissue regeneration. Stem cells operate within dynamic microenvironments known as "niches," where complex interactions with cellular components and the extracellular matrix shape their behavior and function. This article also highlights advanced engineering strategies, such as scaffold-based 3D cultures and geneediting technologies like CRISPR/Cas9, which enhance the therapeutic efficacy and integration of stem cells. Despite current challenges—including tumorigenicity, immune rejection, and ethical concerns—stem cell engineering continues to evolve, promising effective solutions for a wide range of clinical applications, including cardiac, neural, and orthopedic tissue repair.

Keywords: Stem Cell Engineering, Regenerative Medicine, Tissue Repair

Authors: Farnaz Mozayani - Mohammadbagher Kargar











Article Code: icbme-1318

Article Title: GelMA Synthesis and Experimental Challenges

Abstract: Gelatin methacryloyl (GelMA) is a popular material in tissue engineering. It is made from gelatin and methacrylic anhydride (MAA) and capable of being photocrosslinked. GelMA is widely studied in tissue engineering due to its biocompatibility, tunability, and photocrosslinking capability. This study reviews the standard synthesis protocol and reports experimental challenges observed across three laboratory trials. In the first trial, rapid addition of MAA resulted in uneven reaction kinetics, and only 50% of the freeze-dried Falcon tubes yielded usable GelMA powder. In the second trial, dropwise addition improved reaction uniformity; however, overfilled tubes led to incomplete lyophilization, requiring a second cycle to achieve full drying. Re-drying recovered approximately 80% of the material as stable powder. In the third trial, casting into Petri dishes increased surface area and reduced thickness, enabling complete drying in a single cycle with >90% recovery of dry GelMA. These results highlight the critical influence of reagent addition rate, pH stability, and mass-transfer efficiency on product consistency. The findings demonstrate that careful control of reaction and drying conditions is essential for reproducible GelMA suitable for biomedical applications.

Keywords: GelMA, Methacrylation, Lyophilisation, Tissue engineering, Hydrogel

Authors: Mohammad Matin Shirzad - Zahra Mohammadi - Shaghayegh Kohzadi











Article Code: icbme-1023

Article Title: Metal-Organic Frameworks: A Promising Class of Materials for Next-Generation Antibacterial Drug Delivery Systems

Abstract: Bacterial infections that are resistant to drugs represent a significant risk to global public health, highlighting the urgent necessity of developing new antibacterial agents. Metal-Organic Frameworks (MOFs) with their hybrid organic-inorganic composition, large specific surface area, adjustable porosity, biodegradability, and biocompatibility have become highly potential nanomaterial frameworks for future antibacterial applications. This review summarizes the latest advances in the application of MOFs as antibacterial drug delivery systems with an emphasis on their multifaceted antibacterial mechanisms based on physical interaction, metal ion release, organic ligand release, antibiotic and therapeutic gas loading, and catalytic activity.

Keywords: Metal-Organic Frameworks, Antibacterial, Drug Delivery

Authors: Shaghayegh Kohzadi - Zahra Mohammadi











Article Code: icbme-1189

Article Title: Electrochemical Biosensors Based on Polyaniline Nanostructures: An Analysis of Advances, Performance Challenges, and the Outlook for Smart Systems

Abstract: Polyaniline (PANI), as a leading conductive polymer, serves as a fundamental platform for a new generation of electrochemical biosensors owing to its tunable electroactive properties, biocompatibility, and stability. Recent advances in nanotechnology, particularly the use of nanostructures like nanofibers, have enabled the engineering of substrates with exceptionally high specific surface area, which dramatically improves sensor performance. However, despite the high potential of this technology, key challenges such as long-term electrochemical stability and fabrication reproducibility remain significant barriers to commercialization. This review article, while examining the latest advances in the design and application of PANI nanocomposite-based biosensors, provides a critical analysis of their performance. Whereas previous reviews have extensively covered the general applications of polyaniline, this paper specifically focuses on the decisive role of electrospun nanostructures in enhancing sensitivity, lowering the limit of detection, and overcoming functional challenges. In this context, the performance of various sensors for key analytes is compared and analyzed using comparative tables. Finally, by linking existing challenges to emerging solutions, the future outlook for the field is outlined towards smart, self-calibrating biosensing systems.

Keywords: Polyaniline, Electrochemical Biosensor, Nanofibers, Electrospinning, Critical Analysis, Smart Systems

Authors: Nasim Kharazminezhad - Ramez Pourahmad









Article Code: icbme-1439

Article Title: Induced Pluripotent Stem Cells -Derived Dopaminergic Neuron Transplantation

for Parkinson's Disease

Abstract: Parkinson's disease is the second most common age-related neurodegenerative disorder, characterized by the loss of dopaminergic (DA) neurons in the midbrain. Current treatments for the disease only manage its symptoms; however, Cell Replacement Therapy (CRT) is a promising approach for treating Parkinson's disease. This study was conducted with the aim of replacing lost dopamine-producing neurons using sources such as induced pluripotent stem cells (iPSCs).

Keywords: Parkinson's disease, Cell Replacement Therapy, Stem Cells, iPSCs

Authors: Atena Parsaeian - Peyvand Naserisalehabad - Najmeh Najmoddin











Article Code: icbme-1019

Article Title: argeted Cancer Treatment Through Tissue Engineering and Biomaterial-Based Drug Delivery Systems:

Abstract: Targeted cancer therapy has revolutionized oncological treatment by improving drug specificity and minimizing systemic toxicity. This review explores diverse strategies for targeted drug delivery, focusing on antibody-based targeting, nanoparticle-mediated delivery, and RNA interference technologies such as siRNA and miRNA therapeutics. Antibody-drug conjugates (ADCs) have shown promise in specifically binding to tumor cell surface markers like CD44, enhancing selective cytotoxicity. Nanoparticles, particularly those functionalized with ligands such as hvaluronic acid (HA) and chondroitin sulfate (CS), offer improved pharmacokinetics, stability, and tumor targeting via receptor-mediated endocytosis. Recent advances include the use of quantum dots (ODs) engineered for bioimaging and drug delivery, demonstrating enhanced uptake and therapeutic efficacy in CD44-overexpressing tumors. Furthermore, siRNA-loaded nanocarriers provide potent gene-silencing mechanisms, overcoming challenges related to stability and cellular uptake through CD44 targeting. Despite promising preclinical and early clinical outcomes, challenges such as off-target effects, immune responses, and delivery efficiency persist. Future directions emphasize the integration of biomaterial-based drug delivery systems with tissue engineering, refined nanoparticle surface chemistry, and combinational therapies to enhance tumor specificity and therapeutic outcomes. This comprehensive overview highlights the evolving landscape of targeted cancer treatments, emphasizing the critical role of molecular targeting and nanotechnology in developing safer and more effective oncologic therapies.

Keywords: Cancer, method of transmission, medication, targeted therapy, CD44 receptor, Ouantum dots (ODs), siRNA delivery, Targeted cancer therapy, Biomaterials, Gene silencing

Authors: Laleh Etemad-Ghazani - Mina Saddi-Khelejan - Mahdi Hasanpour











Article Code: icbme-1433

Article Title: Perfluorocarbon-Based Oxygenation Systems: From Foundational Principles to

Revolutionary Applications in Cancer Therapy and Tissue Engineering

Abstract: Overcoming oxygen diffusion limitations is critical in tissue engineering and oncology. This review examines perfluorocarbons (PFCs), synthetic compounds with exceptional oxygen solubility, as versatile solutions for oxygen delivery. PFCs' fundamental properties, mechanisms of oxygen transport, and their evolution from blood substitutes to advanced nanoplatforms were explored. Key applications include sustaining cell viability in engineered tissues and enhancing cancer therapies by reversing tumor hypoxia. PFCs improve radiotherapy efficacy, drug delivery, and immunotherapy response by oxygenating tumors and promoting immune cell infiltration. Also, clinical translation challenges, highlighting PFCs' potential to revolutionize therapeutic outcomes across biomedical fields were addressed.

Keywords: Perfluorocarbons, Oxygenation, Tissue Engineering, Cancer Therapy

Authors: Gity Mirzaei - Zeinab Mazloumi - Ali Baradar Khoshfetrat











Article Code: icbme-1016

Article Title: Structural Insights into the Molecular Mechanism of Cancer Regulator BRCA1 Methylation

Abstract: Hypermethylation of the BRCA1 promoter may induce structural alterations that impact gene regulation. This study employed AlphaFold-based structural modeling to examine how methylation affects key DNA conformational parameters. Our findings provide computational insights into how hypermethylation influences the structural features of DNA and interferes with gene expression.

Keywords: DNA methylation, tumor suppressor gene, BRCA1, structural analysis

Authors: Shadi Asadi - Maryam Azimzadeh Irani











Article Code: icbme-1198

Article Title: Comparative Evaluation of Two Keratin Extraction Methods from Kurdish Sheep Wool and Their Application in the Fabrication of Biocompatible Hydrogels with Gelation Time Analysis

Abstract: In this study, keratin was extracted from sheep wool using sodium sulfide hydrate and sodium metabisulfite methods, with urea and sodium dodecyl sulfate (SDS) to enhance solubility. The extraction yield and structural properties were analyzed using Fourier-transform infrared spectroscopy (FTIR), indicating that the metabisulfite method yielded higher purity and structural preservation. Hydrogels were then fabricated using extracted keratin, SF, ADA, and alginate at various ratios to achieve suitable gelation behavior. Rheological analysis confirmed the viscoelastic nature of the hydrogels with stable storage modulus in the linear region. Mechanical compression testing revealed appropriate stiffness for potential bone tissue engineering applications. Overall, keratin type, formulation ratio, and crosslinking conditions critically influenced the gelation behavior, rheological stability, and mechanical performance of the developed hydrogels.

Keywords: Oxidized alginate, inversion test, Schiff base linkage, silk fibroin, keratin, hydrogel

Authors: Sajjad Pourabdal Nergi - Fatemeh Bagheri - Abbas Sheikh











Article Code: icbme-1205

Article Title: Preparation of a plant-based multifunctional nanocomposite hydrogel with conductivity and self-healing property for health monitoring

Abstract: Multifunctional and conductive hydrogels as flexible smart pressure sensors have shown tremendous potential in the areas of biomedical applications, health monitoring, soft robotics, electronic skin, and human-machine interactions. One of the most common forms of these skin-inspired sensors are soft and flexible nanocomposites. A plant-inspired conductive hydrogel possessing zwitterionic side groups was fabricated to form a nanocomposite hydrogel. The chemical structure of the nanocomposite was developed by introducing sulfobetaine methacrylate (SBMA) to the hydroxyethyl cellulose (HEC) and MXene nanosheets were subsequently added to the polymer solutions. The SBMA zwitterionic groups endowed the nanocomposite with decent self-healing and self-adhesion properties. Moreover, the nanocomposite samples revealed tunable mechanical properties. The compressive strength reached 0.93 ± 0.02 MPa and the electrical conductivity of the hydrogel samples reached 1.15 ± 0.16 S/m. The obtained results were satisfactory for human motion sensing to a great extent. The wearable hydrogel can be attached to the human skin owing to the self-adhesion property and diverse human motions including finger bending, wrist bending and pulse rate can be routinely monitored.

Keywords: zwitterionic hydrogel, wearable electronics, hydroxyethyl cellulose, health-monitoring, strain sensor

Authors: Nahid Salimiyan - Roya Sedghi - Sepehr Salighehdar











Article Code: icbme-1076

Article Title: In-silico Molecular Investigation of Caulobacter crescentus Bioadhesive Proteins

Abstract: Caulobacter crescentus, also known as Caulobacter vibrioides, produces a specialized adhesive structure, the holdfast—a polysaccharide-rich matrix located at the stalk tip that enables strong surface attachment. This structure enables strong attachment due to its potent adhesive properties. The "holdfast" in this bacterium is believed to have the highest tensile strength of any known biological adhesive. Three major membrane-associated proteins—HfaA, HfaB, and HfaD—are anchoring components of the holdfast, which enhances its interaction with polysaccharides and thereby reinforces stable surface attachment. In this study, Bioinformatics analyses were performed. BLAST and multiple sequence alignment revealed conserved regions across the proteins. At the same time, phylogenetic analysis indicated a close relationship between Cp19k barnacle's adhesive protein and HfaA, with HfaB forming a more distant group with Cp20k barnacle's adhesive protein variants, which, along with Cp19k, are bioadhesive proteins commonly found in barnacles. Structural modeling using AlphaFold2 showed that HfaA had moderate confidence with flexible regions, in the central and C-terminal domains (pLDDT ~64). HfaB displayed greater stability (pLDDT >75), while HfaD achieved the highest confidence scores (pLDDT >91), with consistent folding across all models. The Epitope prediction using DiscoTope identified multiple B-cell epitope regions in HfaA and HfaB, but limited immunogenicity in HfaD. AlphaFold-Multimer modeling of the protein complex yielded low inter-chain confidence (ipTM <0.20), suggesting weak subunit interaction. These results may lead to the development of biocompatible bioadhesive materials for medical and industrial usage.

Keywords: Holdfast, Bacterial bioadhesive, Protein structure, Immunoinformatics

Authors: Yeganeh Kayalha - Dr.Maryam Azimzadeh Irani











Article Code: icbme-1161

Article Title: Freeze-Dried Oxidized Alginate–Gelatin Scaffold Coated with Reduced Graphene Oxide for Bone Tissue Engineering

Abstract: In this study, a three-dimensional scaffold of oxidized alginate-gelatin (OAL-Gel) was successfully fabricated via a Schiff base reaction. To make the scaffold suitable for bone tissue engineering and create a conductive platform, reduced graphene oxide (rGO), a widely-used conductive material, was applied as a coating. Characterization of the materials and scaffolds began by determining the degree of alginate oxidation (DO) using a titration method. The experimental DO was calculated to be 60%, while the theoretical DO was 50%. Fourier Transform Infrared (FTIR) spectroscopy on the final scaffold and oxidized alginate confirmed the presence of aldehyde groups and Schiff base bonds, validating the successful oxidation of alginate and the intended scaffold fabrication. Furthermore, scanning electron microscopy (SEM) images of the different scaffold groups showed that the alginate-gelatin scaffold cross-linked with calcium chloride had a more organized and uniform network. In contrast, OAL-Gel scaffold exhibited less uniformity due to Schiff base bonds. Overall, this study demonstrates that OAL-Gel scaffold coated with rGO has high potential for use in bone tissue engineering due to its conductivity and biocompatibility.

Keywords: Oxidized Alginate, Schiff Base, Conductive, Bone Tissue

Authors: Mohsen Aghababaei Tafreshi - Sameereh Hashemi-Najafabadi - Nafiseh Baheiraei











كد مقاله: icbme-1225

عنوان مقاله: ساخت ومشخصه یابی هیدروژل بر پایه ژلاتین اصمغ عربی حاوی مقادیر مختلف آگارز به منظور کاربرد در ترمیم زخم

چکده: پوست به عنوان خارجی ترین لایه بدن، نخستین سد دفاعی در برابر عوامل آسیبزا محسوب می شود و ترمیم زخمهای پوستی یکی از چالشهای مهم پزشکی است. هیدروژلها به دلیل تشابه ساختاری با زمینه خارج سلولی و ظرفیت بالای جذب آب، محیطی مرطوب و مناسب برای فعالیت سلولی فراهم می کنند. در این پژوهش، هیدروژلهای مبتنی بر ژلاتین -آگارز -صمغ عربی با مقادیر مختلف آگارز (۱، ۲ و ۳ درصد وزنی) تولید و با استفاده از گلوتارآلدهید کراسلینک شدند. مورفولوژی، خواص مکانیکی، درصد تورم، نرخ تخریب، زیستسازگاری سلولی و فعالیت آنتی اکسیدانی هیدروژلها بررسی شد. نتایج نشان داد با افزایش غلظت آگارز از ۱ تا ۳ درصد، مدول الاستیک هیدروژل ها به ترتیب از -۱۹۵۰ + ۱۹۵۰ + ۱۹۵۰ به -۱۳۰ + ۲۰۳۰ مگاپاسگال و استحکام کششی آن از -۱۰ + ۱۵ به -۱۰ به -۱۶ به ماکرد با درصد تخریب -۲ به ترین از ۲۰ به برای کاربرد در درمان زخمهای مزمن انتخاب شد. نوآوری این پژوهش در را در میان نمونهها داشت و بهعنوان نمونه بهینه برای کاربرد در درمان زخمهای مزمن انتخاب شد. نوآوری این پژوهش در ازیابی سیستماتیک نقش مقادیر مختلف آگارز به عنوان جزء خنثی در تقویت مکانیکی هیدروژلهای زیستسازگار و حفظ فعالیت سلولی و آنتی اکسیدانی آنها است. این رویکرد یک چارچوب علمی و قابل اعتماد برای توسعه زخم پوشهای پیشرفته با عملکرد مکانیکی و زیستی بهینه فراهم میآورد.

كلمات كليدى: زخم پوش،هيدروژل،ژلاتين،آگارز،صمغ عربي،آنتي اكسيدان

نویسندگان: زهرا قاسمی - مهشید خرازیها











كد مقاله: icbme-1256

عنوان مقاله: هیدروژلهای نانوکامپوزیتی تقویتشده با نانوالیاف آرامید عاملدار شده: راهبردی نوآورانه در راستای گسترش ساختارهای پیشرفته مورد استفاده در پزشکی بازساختی

چکیده: هیدروژلها به طور گسترده در پزشکی بازساختی، رباتهای نرم، لوازم الکترونیکی پوشیدنی مورد استفاده قرار می گیرند. با این وجود تهیه هیدروژلهایی با خواص مکانیکی مناسب، روش ساخت آسان و کم هزینه همچنان به عنوان یک چالش بزرگ مطرح می شود. در این مطالعه، هیدروژلهای نانوکامپوزیتی مبتنی بر پلی وینیل الکل (PVA) و نانوالیاف آرامید اصلاح شده به عنوان نانوپُرکنندههای پلیمری جدید با روش تبادل حلال تهیه شده است. همچنین رویکردی نوین به منظور اصلاح سطح نانوالیاف آرامید به وسیله پیوندهای شیمیایی معرفی شده است. هیدروژلهای تهیه شده دارای استحکام کششی 8Pa 39/402 ناوالیاف آرامید به وسیله پیوندهای شیمیایی معرفی شده است. هیدروژلهای تهیه شده دارای استحکام کششی 4Pa میباشند که امکان استفاده از این ترکیبات را در زمینههای گوناگون پزشکی بازساختی بافتهای نرم فراهم می کند.

کلمات کلیدی: پلی وینیل الکل،تبادل حلال،نانوالیاف آرامید،نانوپُر کنندههای پلیمری،هیدروژل نانوکامپوزیتی

نویسندگان: فرهاد اسمعیل زاده - شهره مشایخان - اکبر شجاعی











كد مقاله: icbme-1293

عنوان مقاله: نقش کلیدی نانولوله های کربنی در بهبود همزمان خواص مکانیکی، ضدباکتریایی و زیست سازگاری پوشش های HA-Ta2O5 بر روی آلیاژهای حافظه دار NiTi

چکده: در این پژوهش، پوششهای کامپوزیتی هیدروکسی آپاتیت-اکسید تانتالم-نانولولههای کربنی با موفقیت به روش رسوبدهی الکتروفورتیک بر روی زیرلایه NiTi ایجاد شدند. نتایج نشان داد که افزودن اکسید تانتالم و متعاقباً نانولوله های کربنی منجر به افزایش تراکم ریزساختار پوشش و ایجاد یک شبکه مستحکم میشود. مهمترین یافتهها حاکی از آن است که افزودن نانولولههای کربنی بهطور همزمان خواص مکانیکی و زیستی پوشش را به شکل چشمگیری بهبود میبخشد: چقرمگی شکست پوشش هیدروکسی آپاتیت- اکسیدتانتالم با افزودن ۲ درصد وزنی نانولوله های کربن، به میزان ۱۴۲.۱۱ افزایش یافت. علاوه بر این، پوششهای حاوی نانولوله های کربن به میزان ۱۴۲.۱۱ افزایش یافت. کلی از خود نشان دادند. همچنین، حضور اکسیدتانتالم و به ویژه نانولوله های کربن با بهبود ترشوندگی و شیمی سطح، منجر به افزایش معنادار فعالیت سلولهای استئوبلاست انسانی گردید. نتایج آنالیزهای پراش پرتو ایکس و رامان پایداری فازی ترکیبات و حضور موفقیت آمیز نانولوله های کربن پس از تفجوشی را تأیید کردند. این نتایج نشان میدهد که پوششهای کامپوزیتی حضور موفقیت آمیز نانولوله های کربن پس از تفجوشی را تأیید کردند. این نتایج نشان میدهد که پوششهای کامپوزیتی همدروکسی آپاتیت-اکسید تانتالم-نانولولههای کربنی یک گزینه امیدوارکننده برای بهبود عملکرد کاشتنی های ارتوپدی است.

کلمات کلیدی: آلیاژ حافظهدار NiTi اکسیدتانتالم، چقرمگی شکست، خواص ضدباکتریایی، رسوبدهی الکتروفورتیک، زیستسازگاری، نانولوله های کربن، هیدروکسیآپاتیت

نویسندگان: نازیلا هوراندقدیم - جعفر خلیل علافی











كد مقاله: icbme-1145

عنوان مقاله: بررسی رهایش هوشمند داروی زولدرنیک اسید از نانوذره پلی دوپامین

چکده: هدف از این پژوهش بررسی رهایش هوشمند داروی زولدرونیک اسید بارگذاری شده بر روی نانوذرات پلی دوپامین می باشد. داروی زولدرونیک اسید داروی زولدرونیک اسید (Zln) از جمله داروهای موثر در ترمیم استخوان است که علاوه بر پیشگیری از تخریب استخوان در تمایز سلول های مزانشیمی نیز کارایی خوبی از خود نشان می دهد. استفاده از نانوذرات پلی دوپامین (PDA) که از ماده طبیعی دوپامین (DA) به دست می آید، زیست سازگاری و آب دوستی بالایی داشته و بر اساس حساسیت به نور فروسرخ (NIR) و امواج فراصوت (Ultrasound) می تواند به عنوان حامل Zln رهایش کنترل شده دارو را سبب شود، برای انجام این پژوهش در فاز اول، نانوذرات حاوی دارو ساخته شده و مشخصه یابی نانوذرات ساخته شده انجام شد در ادامه نتایج بارگذاری و رهایش دارو از نانوذرات مورد بررسی قرار گرفت.

در فاز اول که نانوذرات پلی دوپامین ساخته شده، توسط آزمون های DLS و MSE مشخصه یابی شد. در ادامه دارو زولدرونیک اسید بر روی نانوذرات بارگذاری شده و رهایش دارو بررسی شده است. رهایش دارو از نانوذرات به واسطه تحریک توسط محرک های بیرونی، از جمله: لیزر نور فروسرخ (NIR) Near-infrared و امواج فراصوت (Ultra Sonic (US) نیز مورد بررسی قرار گرفت. مطالعات مربوط به رهایش پایدار نشان دادند که حدود % از داروی بارگذاری شده طی % روز بهصورت تجمعی آزاد می گردد، که با رهایش سریع اولیه حدود % در % ساعت نخست همراه بود؛ این رفتار، بیانگر پتانسیل مناسب این سامانه برای کاربردهای درمانی بلندمدت است. تحریک با نور نزدیک به مادون قرمز (NIR) منجر به رهایش پالسی شد که در مجموع بیش از % از دارو طی یک ماه آزاد گردید و این سامانه را برای درمان هدفمند، در موارد لزوم به دوز های بالا را، مناسب می سازد. در مقابل، تحریک با امواج اولتراساوند (US) سبب رهایش سریع اولیه (%) و در ادامه، کاهش تدریجی نرخ رهایش شد که در نهایت به رهایش کامل (%) در مدت حدود % و زنجامید.

كلمات كليدى: بافت استخوان، پلى دوپامين، زولدرونيك اسيد، رهايش كنترل شده، رهايش حساس به نور فروسرخ

نویسندگان: پیام ردایی - فریبا گنجی - شهره مشایخان - منیژه مختاری دیزجی - سید ابراهیم واشقانی فراهانی - فاطمه باقری











كد مقاله: icbme-1238

عنوان مقاله: بهینه سازی ساختار نانوالیافی داربست پلیمری با دندریمر پلی آمیدو آمین برای استفاده در مهندسی بافت عصب

چکده: آسیب به سیستم عصبی از علل اصلی ناتوانی و مرگومیر در جهان است. با وجود پیشرفتها، روشهای درمانی کنونی در این بازسازی کامل عملکرد عصبی ناکارآمد هستند. مهندسی بافت با بهره گیری از داربستهای زیست تقلیدگر، افقهای نوبنی در این زمینه گشوده است. پلی ال لاکتیکاسید (PLLA) پلیمر رایجی در این حوزه است، اما به دلیل آبگریزی، نرخ پایین تخریب، عدم رسانایی و کمبود گروههای عاملی، عملکرد محدودی دارد. در این پژوهش، داربستهای PLLA با دندریمر پلی آمیدوآمین (PAMAM) اصلاح و به روش الکتروریسی ساخته شدند. هدف از این پژوهش، بررسی تاثیر درصدهای مختلف PAMAM بساختار و مورفولوژی داربستها به منظور دستیابی به ترکیب بهینه برای کاربردهای مهندسی بافت عصبی بود. محلولهای الکتروریسی با درصدهای مختلف PAMAM، تهیه شدند و ویژگیهای سطحی و ساختاری داربستها بررسی شد. بر اساس این نتیج، ترکیب حاوی ۵ ٪ پلی آمیدو آمین به عنوان ساختار بهینه از نظر مورفولوژیکی انتخاب شد. این داربستها پتانسیل بالایی برای مطالعات بیشتر در زمینه مهندسی بافت عصب را دارند.

كلمات كليدى: داربست نانوالياف، مهندسى بافت عصبى، الكتروريسى، پلىاللاكتيک اسيد (PLLA)، دندريمر، پلى آميدوآمين (PAMAM)

نویسندگان: حمید جبار، دکتر معصومه حقبین نظرپاک، دکتر عاطفه سلوک، دکتر سمیه اکبری











كد مقاله: icbme-1294

عنوان مقاله: توسعه سامانه میکرونیدلهای هیدروژلی زیستسازگار فیبروئین ابریشم-صمغ عربی با پایداری و کارایی بهبودیافته در دارورسانی

چکیده: فناوری میکرونیدل بهعنوان رویکردی نوین در دارورسانی ترانسدرمال، نیازمند موادی با استحکام مکانیکی و زیستسازگاری بالا است. در این پژوهش، آرایههای میکرونیدل هیدروژلی بر پایه فیبروئین ابریشم (SF) و صمغ عربی (GA) با درصدهای مختلف GA) مختلف (GA) با ۱۸/۰ و ۲ درصد) ساخته و مشخصه یابی شدند. نتایج آزمونهای فیزیکی -شیمیایی نشان داد که افزودن Aموجب ایجاد شبکهای یکنواخت تر و افزایش تخلخلهای باز شد. بررسی مکانیکی نشان داد که غلظت ۱ درصد افزودن Aماستحکام شکست هر سوزن را تا حدود ۱/۰ نیوتن افزایش داد، در حالی که در غلظتهای بالاتر کاهش استحکام مشاهده گردید. آزمون تورمپذیری بیانگر افزایش جذب آب تا حدود ۴۰۰٪ در نمونههای ۲ درصد AG بود و اصلاح فیزیکی با متانول موجب کاهش تورم و بهبود پایداری ساختاری شد. ارزیابی تخریبپذیری نشان داد که نرخ کاهش جرم در نمونههای اصلاح شده طی ۴۳ ساعت به ۱۵–۱۵٪ محدود گردید، در حالی که نمونههای بدون اصلاح تا ۳۰٪ کاهش وزن داشتند. بر اساس تعادل میان استحکام مکانیکی، تورمپذیری و تخریبپذیری، ترکیب SF/1%GA بهینه ترین عملکرد را ارائه داد. این نتایج نوآورانه نشان میدهد که ترکیب GA و AB با اصلاح فیزیکی می تواند مسیر تازهای برای توسعه میکرونیدلهای زیستسازگار و کارآمد در دارورسانی هوشمند فراهم کند.

کلمات کلیدی: دارورسانی هدفمند، میکرونیدلهای هیدروژلی، فیبروئین ابریشم، صمغ عربی، زیستسازگاری، تورمپذیری

نويسندگان: مينو على زاده پيرپشته - فتح اله كريم زاده - مهشيد خرازيها - حميدرضا سليمي جزى











كد مقاله: icbme-1250

عنوان مقاله: توسعه هیدروژل های زیست تقلیدی مبتنی بر یوتکتوژل برای کاربرد های پزشکی

چکده: در این پژوهش، سه نمونه هیدروژل زیست تقلیدی مبتنی بر یوتکتوژل از آکریلیک اسید، آکریل آمید و کولین کلراید در حضور مقادیر مختلف عامل کراس لینکر (MBA) و آغازگر (KPS) سنتز شد. نمونهها با استفاده از آزمونهای FTIR-ATR تورم و تخریب در شرایط فیزیولوژیک و تست مکانیکی فشاری مورد بررسی قرار گرفتند. نتایج طیفسنجی نشان دهند تشکیل پیوندهای هیدروژنی قوی میان اجزای شبکه و بهبود ساختار ژل بود. بررسی خواص فیزیکوشیمیایی نشان داد که افزایش درصد آکریل آمید سبب افزایش ظرفیت تورم و جذب آب می شود، در حالی که حضور کولین کلراید موجب بهبود پایداری ابعادی و کاهش تخریب ژل گردید. آزمون مکانیکی نشان داد که نمونهی بهینه (شامل ترکیب متوسط آکریل آمید و کولین کلراید با غلظت مناسب، کاهش و بهینه (شامل ترکیب متوسط آکریل آمید و کولین کلراید با غلظت مناسب، شاهل و رفتار تورمی متعادل است. این ویژگیها، در کنار زیستسازگاری مناسب، نمونهی بهینه را گزینهای امیدبخش برای کاربردهای زیست پزشکی نظیر همچون رهایش کنترل شده دارو، پانسمان زخم و مهندسی بافت معرفی می کند.

كلمات كليدى: هيدروژل، زيست تقليدى، يوتكتوژل

نویسندگان: فاطمه دهقان بنادکی، مهشید خرازیهای اصفهانی











كد مقاله: icbme-1149

عنوان مقاله: توسعه پوشش چند جزئی بر پایه لیگنین و نانوذرات اکسید سریم بر سطح آلیاژ AZ91 برای استفاده در ایمپلنتهای فلزی

چکده: پوششهای زیستی-معدنی به عنوان راهکاری پیشرفته، نقش مهمی در افزایش دوام و ایجاد خواص زیستی مطلوب در ایمپلنتهای منیزیمی ایفا می کنند. در پژوهش حاضر ، پوششی چندلایه و چندکاره بر پایه ی کامپوزیت لیگنین - اکسید سریم به منظور بهبود خواص سطحی آلیاژ منیزیم، با استفاده از روش پوشش دهی چرخشی طراحی و ساخته شد. جهت ارزیابی ذرات اصلاح شده، از آزمونهای پراش پرتو ایکس و پتانسیل زتا بهره گرفته شد. نتایج، اصلاح موفقیت آمیز ذرات لیگنین و اکسید سریم را تأیید کرده و مقدار پتانسیل زتای نانوذرات اکسید سریم جدید را، به واسطه ی حضور کیتوسان حدود ۲۰+ میلی ولت نشان دادند. یکنواختی پوشش اکسیداسیون میکروقوسی و سطح پوشش سرامیکی با مقدار زبری، ۱۵۰۶۹ میکرومتر توسط تست زبری سنجی تأیید شد. تصاویر میکروسکوپ الکترونی و آزمون طیفسنجی (EDS) نیز نشان دهنده ی پوششی همگن و منسجم از لیگینوسولفونات و ذرات اکسید سریم – کیتوسان بدون تجمع و غیریکنواختی بود. تصاویر میکروسکوپالکترونی روبشی از لیگینو و نانوذرات اکسید سریم حاوی کیتوسان با خواص زیستسازگاری و آنتی اکسیداسی را نشان دادند که ناشی از حضور لیگنین و نانوذرات اکسید سریم حاوی کیتوسان با خواص زیستسازگاری و آنتی اکسیدانی مناسبی را نشان دادند که ناشی و اکسید سریم – کیتوسان، مشاهده نشد. ساخت این پوشش کامپوزیتی دولایه با مواد دارای خواص زیستی ویژه، همچون لیگنین و اکسید سریم – کیتوسان، میتواند گام مهمی در راستای ارتقای پوششهای چندمنظوره برای کاربردهای زیستی ویژه، همچون لیگنین و اکسید سریم – کیتوسان، میتواند گام مهمی در راستای ارتقای پوششهای چندمنظوره برای کاربردهای زیستی ویژه.

کلمات کلیدی: ایمپلنتهای زیست تخریب پذیر، پوشش زیستی - معدنی، پوشش دهی چرخشی، لیگنین، سریم

نویسندگان: هستی عزیزی لمجیری - زهرا قاسمی - مهشید خرازیها











كد مقاله: icbme-1291

عنوان مقاله: کامپوزیت های پایه بیوپلیمری تقویت شده با الیاف طبیعی : مروری بر کاربردها در مهندسی بافت استخوان

چکده: ترمیم نقایص استخوانی یکی از چالشهای جدی پزشکی بازساختی است و مهندسی بافت استخوان نیازمند داربستهایی به طور با استحکام مکانیکی، زیستسازگاری و زیستتخریبپذیری مطلوب میباشد. داربستهای پلیمری سنتزی و طبیعی به طور گسترده در این حوزه به کار گرفته شدهاند، اما اغلب به تنهایی قادر به تأمین الزامات مکانیکی و زیستی مورد نیاز نیستند. به همین دلیل، ترکیب آنها با الیاف طبیعی به عنوان تقویت کننده، رویکردی نوین و امیدبخش معرفی شده است. الیاف گیاهی مانند کتان، جوت، سیسال ، بامبو و سانسوریا به دلیل ویژگیهایی نظیر دسترسپذیری، هزینه پایین، تجدیدپذیری، استحکام کششی و زیستسازگاری بالا، گزینهای مناسب برای بهبود عملکرد داربستها محسوب می شوند. این مقاله مروری به بررسی نقش الیاف طبیعی در بهبود خواص مکانیکی و زیستی داربستهای کامپوزیتی پرداخته و اثر آنها بر افزایش استحکام، قابلیت چسبندگی سلولی، رگزایی و استخوانزایی را تحلیل می کند. همچنین روشهای نوین ساخت مانند الکتروریسی، خشک کردن انجمادی و چاپ سه بعدی به عنوان رویکردهای کلیدی در تولید این داربستها معرفی شده اند. مرور حاضر نشان می دهد که داربستهای تقویت شده با الیاف طبیعی می توانند نسل جدیدی از زیست مواد پایدار و کارآمد برای بازسازی بافت استخوان باشند و زمینه تحقیقات آینده را برای کاربردهای بالینی هموار سازند.

کلمات کلیدی: مهندسی بافت استخوان، داربست های بیوپلیمری، داربست کامپوزیتی، خشک کردن انجمادی، تقویت با الیاف طبیعی، چاپ سه بعدی

نويسندگان: شقايق شكرائي - ناهيد حسن زاده نعمتي - عادله قلي پور كنعاني









كد مقاله: icbme-1131

عنوان مقاله: بررسی خواص مکانیکی داربستهای متشکل از نانوسلولز، ژلاتین و ماتریس خارجسلولی برای کاربرد در مهندسی بافت استخوان

چکیده: در این تحقیق، هیدروژل های ساخته شده به عنوان یک داربست زیست پزشکی از ماتریس خارج سلولی استخوان (ECM) برای کاربرد در مهندسی بافت استخوان ساخته و بررسی شدند. خواص مکانیکی داربست های کامپوزیتی GCE (ECM) در دو حالت خشک و مرطوب توسط تست مکانیکی فشاری مورد ارزیابی قرار گرفت. مدول فشاری با افزایش CNC در حالت مرطوب در کرنش ۹۰ درصد به ۳۱ ۱۸۰۸ مگاپاسکال و در حالت خشک در کرنش ۹۰ درصد به ۴۰ میزان (۱، ۳ و ۵ درصد وزنی) مدول فشاری در حالت مرطوب در کرنش ۹۰ درصد به ترتیب ۶۷/۲۲ ۵/۲۱ و ۲۶ مگاپاسکال و در حالت خشک در کرنش ۸۰ درصد به ترتیب ۶۷/۲۲ ۵/۲۱ و ۱۸۲۵ و ۱۸۲۵ و ۱۸۲۵ مگاپاسکال کاهش یافت استخوان را داربست های شبکه ای GCE پتانسیل استفاده در مهندسی بافت استخوان را دارند.

كلمات كليدى: ماتريس خارج سلولى استخوان، مهندسي بافت استخوان، خواص مكانيكي، نانو سلولز، ژلاتين

نویسندگان ::مهدی درگاهی - معصومه محمودی











كد مقاله: icbme-1290

عنوان مقاله: تهیه نانوحامل ژلاتین گالاکتوزیله شده با هدف کاربرد در دارورسانی هدفمند به بافت کبد سرطانی

چکیده: کارسینوم هپاتوسلولار (HCC) یکی از کشنده ترین سرطانها در جهان است و درمانهای موجود با سمیت دارویی همراهاند. ژلاتین گالاکتوزیله می تواند به عنوان یک نانوحامل مؤثر برای هدفگیری گیرنده های آسیالوگلیکوپروتئین (ASGPR) در سلولهای سرطانی کبد به کار گرفته شود. ژلاتین به دلیل خواصی همچون زیست سازگاری، زیست تخریب پذیری و دارا بودن گروه های عاملی متعدد به عنوان نانوحامل دارورسانی مورد توجه قرار گرفته است. از طرفی نانوحامل های اصلاح شده با گالاکتوز به عنوان لیگاند باعث هدفگیری فعال و اختصاصی به بافت هپاتوسیت های کبدی و افزایش اثر بخشی عامل درمانی می شوند. بدین جهت، در این مطالعه، ژلاتین گالاکتوزیله از طریق واکنش کووالانسی میان گروههای آمینی ژلاتین و گروه های کربوکسیل لاکتوبینیک اسید سنتز شد. نتایج آنالیزهای FT-IR و NMR تشکیل موفق پیوند آمیدی و گالاکتوزیله شدن گرلاتین را تأیید کردند. سپس نانوذرات دارای لیگاند گالاکتوز به روش ضدحلال تکمرحلهای و با تغییر پارامتر نسبت حجمی ضد حلال به حلال ۱۹:۲ اندازه ذرات کوچکتر بوده و اندازه ذرات حدود حلال به حلال ۲:۲ اندازه ذرات کوچکتر بوده و اندازه ذرات حدود انوم براسی کارایی ضدسرطانی این سامانه انجام خواهد شد تا پتانسیل آن در درمان HCC مورد ارزیابی قرار گیرد.

كلمات كليدى: ژلاتين، دارورساني هدفمند، سرطان كبد، لاكتوبيونيك اسيد، نانوحامل، نانوذرات، گالاكتوزيله

نویسندگان: مائده بخشی پور رشته رودی - امیرحسین شریفی - مریم رجب زاده - علی برادر خوش فطرت











كد مقاله: icbme-1155

عنوان مقاله: ساخت و مشخصه یابی چسب زیستالهام برپایه ژلاتین با اتصالات دوگانه آرژنین و اسید کافئیک برای هموستاز سریع

چکیده: در سالهای اخیر، توسعه هیدروژلهای هیبریدی چندمنظوره با چسبندگی قوی و فعالیت هموستاتیک، چالشی مهم در مهندسی زیستپزشکی ایجاد کرده است. در این مطالعه، هیدروژل شبکه پلیمری زیستالهام ژلاتین مزدوج با اسید کافئیک و ال-آرژنین با ۱۲ درصد وزنی آکریلآمید (A-GelCA-12A) ساخته شد. این هیدروژل پیوندهای کووالانسی و برگشتپذیر پویا شامل آمیدی و باز شیف ایجاد کرده و عملکرد مکانیکی و فعالیت بیولوژیکی قابل تنظیم ارائه میدهد. A-GelCA-12A بیشترین استحکام چسبندگی(۱ ۱۵۳ ۱۵۳ کیلوپاسکال)، چسبندگی و هموستاز سریع را نشان داد و حداقل همولیز ۵۰٪و کاهش خونریزی را بهبود داد، که آن را به گزینهای مناسب برای ترمیم زخم، چسب جراحی و کاربردهای بالینی تبدیل می کند.

كلمات كليدى: چسب بافتى، ال-آرژنين، كافئيك اسيد، ژلاتين، عامل هموستاتيك، شبكه پليمرى

نویسندگان: غزل یعقوبی - مهشید خرازیها











كد مقاله: icbme-1415

عنوان مقاله: ساخت داربست پلییورتان گرمانرم-هیدروکسی آپاتیت-اکسید گرافن احیا شده و بررسی رفتار زیست تخریبپذیری و زیستسازگاری آن

چکیده: هدف این پژوهش، طراحی و ساخت داربستهای متخلخل کامپوزیتی بر پایه پلییورتان گرمانرم (TPU) با تقویت همزمان ذرات هیدروکسی آپاتیت (HA) و اکسید گرافن احیا شده (rGO) به روش ریخته گری حلال/شستشوی ذرات است. بدین منظور، با استفاده از طراحی آزمایش طراحی مرکب مرکزی، نسبتهای مختلف از اجزای مذکور بهینهسازی شدند. نمونههای تولید شده از نظر تخلخل، استحکام فشاری، تخریب زیستی و زیستسازگاری سلولی مورد ارزیابی قرار گرفتند. نتایج نشان داد که افزودن HA و rGO منجر به بهبود خواص مکانیکی، کنترل نرخ تخریب، افزایش زیستسازگاری و ارتقای توان القای معدنی شدن در حضور سلولهای استوبلاست (MG-63) شد. به طور خاص، نمونه بهینه دارای تخلخل بالا (حدود ۹۰/)، استحکام فشاری مناسب و زیستسازگاری مطلوب بود که توانست تشکیل رسوبات کلسیمی بیشتری را در مقایسه با نمونه کنترل نشان دهد. در مجموع، این تحقیق نشان می دهد که کامپوزیت TPU/HA/rGO داربست مناسبی برای کاربردهای مهندسی بافت استخوان به شمار می رود.

کلمات کلیدی: اکسید گرافن احیا شده، پلییورتان گرمانرم، داربست متخلخل،هیدروکسی آپاتیت، ریخته *گری* حلال/شستشوی ذرات، مهندسی بافت

نویسندگان: سید امیررضا زارعیان - سید مجتبی زبرجد











كد مقاله: icbme-1310

عنوان مقاله: ایجاد پوشش کامپوزیتی HA-TiO2 بر روی آلیاژ زیست تخریب پذیر منیزیم به روش رسوب دهی الکتروفورتیک

چکده: در ادامه پژوهشهای انجام شده بر روی آلیاژ زیست تخریب پذیر منیزیم، برای حل چالشهای ذاتی آن، روش رسوب دهی الکتروفور تیک بسیار مورد توجه قرار گرفته است. در حالی که تمر کز بسیاری از مطالعات در استفاده از مواد جدید در پوششها است، بهینه سازی و تکمیل پژوهشهای پیشین ضروری به نظر می رسد. مشکلات ذاتی هیدروکسی آپاتیت پس از رسوب روی آلیاژ به طور قابل توجه کیفیت نهایی پوشش را پایین میآورد. استفاده از مواد دیگر در پوشش به همراه آن می تواند پوشش متراکم تر با عیوب کمتر را فراهم کند. علی رغم پیشفت ها، پوششهای تک جزئی هیدروکسی آپاتیت با چالشهای ذاتی نظیر ترک خوردگی ناشی از تنشهای داخلی و چسبندگی ضعیف مواجه هستند که عملکرد محافظتی آنها را تضعیف می کند. این پروهش با هدف غلبه بر این چالشها، بر روی یک پوشش کامپوزیتی مبتنی بر هیدروکسی آپاتیت تیتانیا با استفاده از حلال پروهوتانول تمرکز دارد. در تحقیق حاضر آلیاژ ریختگی Mg / N - Mg / N - Mg به عنوان زیر لایه انتخاب شد. مورفولوژی و ساختار نمونههای پوشش داده شده، توسط میکروسکوپ الکترونی روبشی گسیل میدانی مشخصه یابی شد. نتایج نشان دهنده شکل گیری یک پوشش یکنواخت با تراکم ترک خطی $\frac{\mu m}{\mu m^2}$ به بردی عیل پراش پرتو ایکس نیز حضور موفقیت آمیز فازهای بلوری هیدروکسی آپاتیت و آناتاز تیتانیا را در پوشش تأیید نمود. تست زاویه تماس، خاصیت آبدوستی بالای سطح پوششده را با زاویه متوسط ۱۸۸۴ در مقایسه با نمونه بدون پوشش تأیید کرد.

كلمات كليدى: آبدوستى، آلياژ زيست تخريب پذير منيزيم، ايزوبوتانول، تيتانيا، رسوب دهي الكتروفورتيك، هيدروكسي آپاتيت

نویسندگان: سید محمد مکی - حسن جعفری - فاطمه سادات پیشبین - سلیمان خوشرو











كد مقاله: icbme-1298

عنوان مقاله: کاربرد داربست زیستی سهبعدی در مدلسازی in vitro فیبروز کبدی ناشی از NAFLدرموش سوری نر نژاد C57BL/6

چکده: کبد چرب غیرالکلی (NAFLD) یکی از چالشهای مهم سلامت جهانی است که می تواند به التهاب، فیبروز و سیروز منجر شود. در این پژوهش، با استفاده از موشهای سوری نر و داربست زیستی سهبعدی مبتنی بر نانوبیومتریال، مراحل اولیه آسیب کبدی in vitro بازسازی شد. تغییرات بافتی با رنگ آمیزی H&E و تری کروم ماسون و شاخصهای بالونینگ، هپاتیت، کلستاز و فیبروز بررسی شد. گروه پرچرب بدون عصاره بالونینگ بالای ۹۰٪داشت، درحالی که عصارههای آویشن و کاسنی شدت آسیب را کاهش و تراکم سلولی را حفظ کردند. داربست میکروحیطی مشابه vivo ایجاد و مدلی نوآورانه برای مطالعه و توسعه درمانهای هدفمند فراهم کرد.

كلمات كليدي: أسيبشناسي بافتي،داربست زيستي،كبد چرب غيرالكلي،فيبروز كبدي،رنگ أميزي H&E،نانوبيومتريال،in vitro

نویسندگان: حدیثه شکری - امید وجدان دوست اهرابی











كد مقاله: icbme-1009

عنوان مقاله: بررسی اثر ضد سرطانی لیپوزوم پگیله حاوی ترکیب جنسینوساید Rh2 بر سرطان روده بزرگ در مدل آزمایشگاهی و حیوانی

چکیده: سرطان روده بزرگ (CRC) یک بیماری شایع و کشنده است که با عوارض جانبی شیمی درمانی و مقاومت به دارو مواجه است. این مطالعه با هدف توسعه و ارزیابی اثربخشی ضدسرطانی لیپوزومهای پگیله شده جنسینوساید Rh2 در مدلهای آزمایشگاهی و حیوانی CRC انجام شد. لیپوزومهای یگیله شده حاوی جنسینوساید Rh2 سنتز و مشخص شدند. اثرات ضدسرطانی آنها در ردههای سلولی سرطان کولون و موشهای مبتلا به CRC ارزیابی شد. تجزیه و تحلیل فیزیکوشیمیایی نشان داد که بارگیری دارو باعث افزایش قطر هیدرودینامیکی (از ۱۲۸.۶ به ۱۵۲.۳ نانومتر)، بهبود پتانسیل زتا (از -۲۵.۸ به -۲۸.۴ میلیولت) و حفظ یکنواختی ذرات (PDI < 0.2) شد. FTIR و TEM نشان داد که دارو با موفقیت در لیپوزومها بستهبندی شده و ساختار شیمیایی آن حفظ شده است. فرمولاسیون نهایی کارایی بستهبندی ۸۵۶ درصد و آزادسازی کنترلشده (۲۲.۴ درصد در ۷۲ ساعت) را با پیروی از کینتیک وایبول نشان داد. در آزمایشهای آزمایشگاهی، لیپوزومهای پگیله شده کارایی جنسینوساید Rh2 را ۵۵.۵ درصد افزایش دادند IC50: 18.9 μ M برای داروی آزاد). در مدل های حیوانی، فرمولاسیون حجم تومور را ۷۴ درصد در مقایسه با کنترل ها (۳۲۰ در مقابل ۱۲۵۰ میلی متر مکعب) کاهش داد و عوارض جانبی کبدی کمتری داشت. این یافتهها نشان دهنده موفقیت سیستم نانولیپوزومی در بهبود کارایی و ایمنی جنسینوساید Rh2 برای درمان CRC است. این مطالعه نشان میدهد که جنسینوساید Rh2 پگیله شده لیپوزومی ویژگیهای فیزیکوشیمیایی، زیستدر دسترس بودن و آزادسازی کنترلشده دارو را بهبود می بخشد و اثرات ضدسرطانی قابل توجهی در مدلهای سلولی و حیوانی CRC ایجاد می کند. نانوفورمولاسیون همچنین عوارض جانبی را کاهش می دهد و در عین حال پروفایل ایمنی مطلوبی را حفظ می کند و یک درمان هدفمند امیدبخش برای CRC ارائه می دهد. این نتایج راه را برای كارآزماييهاي باليني آينده هموار ميكند.

كلمات كليدى: سرطان روده بزرگ، ليپوزوم، جنسينوسايد، ضد سرطاني

نویسندگان: محسن زارع - ناهید حسن زاده نعمتی - هادی زارع زردینی











كد مقاله: icbme-1381

عنوان مقاله: هیدروژل ژل شونده آنزیمی بر پایه ژلاتین برای استفاده در کاربردهای مهندسی بافت

چکده: مواد زیستی طبیعی به دلیل زیست تخریب پذیری، زیست سازگاری و ماهیت غیرسمی خود، برای استفاده در مهندسی بافت بسیار مطلوب میباشند. ژلاتین یک ماده زیستی شناخته شده با خواص سل-ژل است که در دمای ۳۷ درجه سانتی گراد به صورت محلول بوده و برای تشکیل هیدروژل، باید پیوند عرضی ایجاد شود. یکی از روشهای جدید برای ایجاد پیوند عرضی صورت محلول بوده و برای تشکیل هیدروژل، باید پیوند عرضی اطلاق شده روژل آنزیمی ژلاتین برای کاربردهای پزشکی انجام شده است. برای این منظور، ژلاتین با استفاده از انزیم ترس گلوتامیناز میکروبی در دمای ۳۷ درجه سانتیگراد و PH خنثی به شکل هیدروژل تهیه و خواص فیزیکی و مکانیکی آن از جمله میزان تورم، زیست تخریب پذیری و استحکام مکانیکی تعیین گردید. نتایج بدست آمده نشان میدهد هیدروژل های حاوی ۲۰ درصد ژلاتین و آنزیم به میزان ۱۰ درصد ژلاتین موجود در ترکیب، بیشترین مقاومت فشاری را از خود نشان میدهند. بررسی میزان رشد سلول های فیبروبلاست حیوانی در سطح هیدروژل ها در مدت ۵ روز نشان داد که این هیدروژلها قابلیت بالای زیستسازگاری داشته و سمیتی برای سلول ندارند. نتایج این تحقیق نشان می دهد هیدروژلهای ژلاتینی ژل شده توسط آنزیم پتانسیل مورد نیاز برای استفاده در مهندسی بافت را دارند.

كلمات كليدى: آنزيم ترنس گلوتاميناز ميكروبي، ژلاتين، هيدروژلهاي ژل شونده آنزيمي

نويسندگان: وحيده ابراهيمي بختور - على برادر خوش فطرت - الهام دهقاني











كد مقاله: ichme-1274

عنوان مقاله: مطالعه کامپوزیتهای سرامیکی هیدروکسی آپاتیت جهت استفاده در کاشتنیهای استخوانی

چکیده: هیدروکسی آپاتیت بهعنوان یک ماده ی معدنی و سرامیک زیستی در دهههای گذشته و به خصوص در سالهای اخیر در پرشکی و دندان پزشکی به طور گسترده ای مورد استفاده قرار گرفته است. هیدروکسی آپاتیت به دلیل زیست سازگاری عالی، زیست فعالی و شباهت به مواد معدنی استخوان انسان، طیف گسترده ای از کاربردها را در زمینههای مختلف دارد. این ماده معدنی به طور گسترده در پیوند استخوان، کاشتنیهای ارتوپدی و دندانی و به عنوان پوششی برای پروتزها برای افزایش ادغام استخوانی استفاده می شود. علی رغم وجود تمام مزایای ذکر شده، مهم ترین نقص این ماده ی سرامیکی، عدم وجود خواص مکانیکی مطلوب و مناسب در شرایط تحت تنش در کاربردهای مفصلی و کاشتنی است. در نتیجه، پژوهشگران با ایجاد کامپوزیتهای مختلف آن با پلیمرها، سرامیکها و فلزات در پی بهبود عملکرد بالینی آن بوده اند.

كلمات كليدى: درمان استخوان، زيستفعالي، زيستمواد، كامپوزيت، هيدروكسي آپاتيت

نویسندگان: میلاد بدر - مهدیه سلطانعلیپور - جعفر خلیل علافی











كد مقاله: icbme-1100

عنوان مقاله: هیدروژل های طبیعی مبتنی بر زیستمواد برای بهبود زخم: طراحی، پیشرفتهای اخیر و دیدگاههای مهندسی بافت

چکیده: هیدروژلهای طبیعی بهعنوان یک نوآوری مهم در مراقبت از زخم، به دلیل جذب بالای رطوبت، زیستسازگاری و قابلیتهای چندگانه، مورد توجه قرار گرفتهاند. این مرور فرایند بیولوژیکی ترمیم زخم را معرفی کرده و به بررسی ترکیب و ویژگیهای هیدروژلهای طبیعی مانند کلاژن، ژلاتین، اسید هیالورونیک، کیتوسان و آلژینات میپردازد. اثرات بیولوژیکی این هیدروژلها، از جمله خواص ضدباکتریایی، آنتیاکسیدانی و ضدالتهایی آنها که در تسریع فرایند ترمیم زخم مؤثرند، مورد بررسی قرار گرفته است. همچنین، چالشها و چشماندازهای آینده در کاربرد عملی این هیدروژلها تحلیل شده و نقش برجسته آنها در درمان زخمهای پیچیده و دیربهبود در حوزه مهندسی بافت برجستهسازی شده است.

كلمات كليدى: بهبود زخم، پانسمان زخم، مواد زيستى، مهندسى بافت، هيدروژل

نویسندگان: محمد عرب چم چنگی - میلاد زارع - سولماز خلیق فرد











كد مقاله: icbme-1305

عنوان مقاله: مطالعه مروری طراحی و ساخت نانوحاملهای هوشمند برای تحویل هدفمند داروهای ضد سرطان به تومورهای لوزالمعده

چکیده: سرطان لوزالمعده یکی از کشنده ترین سرطانها با نرخ بقای پنجساله کمتر از ۱۰٪ است و درمانهای سنتی مانند شیمی درمانی به دلیل مقاومت دارویی و عوارض جانبی شدید، کارایی محدودی دارند. این مقاله مروری بر پیشرفتهای نانوتکنولوژی در تحویل هدفمند داروهای ضدسرطان تمرکز دارد، که با افزایش کارایی داروها (مانند ژمسیتابین و پاکلیتاکسل) و کاهش سمیت، تحول آمیز است. نانوذرات به عنوان ناقلین نوین دارویی، با هدف گیری دقیق سلولهای بیمار، کارایی داروها ر افزایش و عوارض جانبی را کاهش دادهاند. این ذرات با ترکیباتی مانند پلیمرها، لیپوزومها و فلزات برای انتقال داروها و ژنها به سلولهای هدف طراحی شدهاند. نانوذرات با عبور از سدهای بیولوژیکی و هدف گیری گیرندههای سلولی، تحویل دقیق دارو را تضمین می کنند. سیستمهای نانوساختار در درمان سرطان و بیماریهای خودایمنی نتایج امیدوار کنندهای نشان دادهاند. نانومیلههای دارویی نیز رویکردی نوین برای بهبود کارایی و کاهش عوارض هستند. با وجود چالشهایی مانند سمیت و پایداری، نانوذرات پتانسیل بالایی برای تحول در درمان دارند و این مطالعه مروری با هدف جمعآوری پیشرفتهای اخیر، چالشها و مسیرهای آینده، دیدگاه جامعی برای تحقیقات بالینی ارائه میدهد.

كلمات كليدى: نانوذرات،دارورساني هدفمند،سرطان،بيمارهاي خود ايمني،ليپوزومها

نویسندگان: ایدا احمدی - ابوبکر سوری - جعفرصادق مقدس











كد مقاله: ichme-1264

عنوان مقاله: آلیاژهای حافظه دار نیکل-تیتانیم در مهندسی پزشکی: نوآوریها، چالشها و کاربردهای پزشکی

چکیده: افزایش جمعیت سالمندان همراه با افزایش شیوع بیماریهای عروقی مختلف از جمله عروق کرونر قلب بوده، بعلاوه حدود کاه میلیارد نفر از بیماریهای دندانی رنج میبرند. بنابراین، بازار تجهیزات پزشکی همچنان به رشد خود ادامه خواهد داد. با افزایش تقاضا برای جراحیهای کمتهاجمی و درمانها، اهمیت قابلیتهای آلیاژ نیکل-تیتانیم نیز افزایش مییابد. ویژگیهای منحصربهفرد این آلیاژ از جمله حافظهداری و سوپرالاستیسیته، مقاومت در برابر خوردگی به همراه زیستسازگاری خوب آن، بخش تولید تجهیزات پزشکی را متحول کردهاند. خاصیت حافظهداری با ارائهی تحریک چندگانه، کنترل مطلوبی در محدودهی دمای انتقال نزدیک به دمای بدن ارائه می دهد. خاصیت سوپرالاستیسیته، با اعمال نیروهای فیزیولوژیکی سبک و مداوم به اندامهای بدن، انقلابی را در درمان ایجاد کرده و در نتیجه به راحتی بیمار را بهبود می بخشد. خاصیت سوپرالاستیسیته به طور گسترده، برای تولید سیمهای قوسی ارتودنسی، متههای دندانی و استنتها استفاده شده است، زیرا در مقایسه با فولاد زنگنزن معمولی، انعطاف پذیری بیشتری را نشان می دهند. در مقابل، برای کاربردهایی نظیر فیلترهای سایمون، دستگاه انسداد دیوارهی بیندهلیزی و منگنههای از تولیدی از خاصیت حافظهداری این آلیاژ بهره گرفته شده است. این مقاله، عوامل کمتر شناخته شده ای را که در موفقیت پزشکی نیکل - تیتانیم نقش دارند، آشکار می کند و چندین کاربرد پیشرفته را ارائه می دهد.

كلمات كليدى: آلياژهاى حافظهدار نيكل-تيتانيم، زيستسازگارى، عملكرد زيستى، كاربردهاى پزشكى، نايتينول

نویسندگان: مهدیه سلطانعلی پور - میلاد بدر - جعفر خلیل علافی











Biomechanics Abstracts: ICBME-

1188	1366	1039	1452	1217	1442	1135	1316	1460	1211
1345	1342	1397	1112	1399	1417	1315	1457	1408	1235
1334	1227	1376	1216	1186	1377	1441	1393	1422	1375
1416	1174	1183	1204	1134	1306	1081	1221	1472	1339
1260	1338	1142	1363	1195	1275	1151	1170	1107	1314
1304	1391	1071	1213	1287	1371	1169	1406	1126	1194
1230	1173	1124	1222	1437	1156	1132	1239	1420	1181
1175	1282	1411	1237	1178	1238	1427	1106	1475	1228
1102	1348	1118	1346	1308	1309	1050	1390	1382	1212
1379	1159	1058	1120	1082	1148	1312	1090	1355	1428
1313	1187	1096	1206	1154	1362	1095			



Article Code: icbme-1134

Article Title: Kinematic Synergy Reconstruction Analysis for Assessing Gait Complexity and Adaptability in Children With Cerebral Palsy

Abstract: Cerebral palsy is the most common motor disability in childhood, often leading to impaired gait and reduced adaptability in motor control. Quantifying the complexity and variability of joint coordination patterns can provide valuable insight into underlying neuromuscular deficits and inform rehabilitation strategies. This study examined motor coordination and its variability in children with spastic diplegic cerebral palsy compared with typically developing children, using kinematic synergy reconstruction analysis. A total of 150 participants (120 CP, 30 TD; aged 5-13 years) were assessed, with children with cerebral palsy classified into four gait subgroups, including True, Jump, Apparent, and Crouch. Gait kinematic data were analyzed using non-negative matrix factorization, and synergy variability was quantified via variance accounted for (VAF). Results showed that children with CP required fewer synergies than the TD group, with a clear progressive reduction in synergy count across CP subgroups as the severity of gait impairment increased. Moreover, the Crouch and Apparent groups exhibited the lowest synergy counts, highlighting their severe impairment. Regarding adaptability, all CP groups, except the True group, demonstrated significantly lower variability of single-synergy VAF, indicating a more rigid and less adaptable gait patterns. These findings highlight the utility of kinematic synergy analysis for characterizing motor control deficits.

Key Words: Cerebral palsy, gait, Joint coordination, Coordination variability, Kinematic synergy

Authors: Mahshad Nazeri Jeirani, Yasamin Azmi, Mahya Shojaeefard, Masoud Yousefi, Farzam Farahmand











Article Code: icbme-1195

Article Title: Optimal Control and Emergence of Kinematic Synergies in Underactuated Biped Locomotion

Abstract: This study examines the relationship between cost function selection in trajectory optimization and the resulting joint coordination patterns in a planar five-link biped model. The model represents a simplified humanoid with two legs and a torso connected by revolute joints, and a pointed foot that makes the system underactuated. Four cost functions—sum of squared joint torques, sum of squared hip-knee torques, sum of squared joint powers, and squared head acceleration—were optimized using direct collocation combined with a global search strategy in the OptimTrai framework. The resulting optimal kinematics were analyzed using Non-Negative Matrix Factorization (NNMF) to extract kinematic synergies and evaluate coordination through the Variance Accounted For (VAF). Results indicate that the power-squared and headacceleration-squared cost functions produced two synergies, achieving global VAF values of 94% and 88%, respectively, while the torque-squared and hip-knee torque-squared cost functions required three. Across all cost functions, the torso joint exhibited the lowest local VAF, likely due to its periodic motion, which could not be coupled with the motions of other ioints using NNMF. The power-squared cost function demonstrated the highest coordination (global VAF 94% and local VAF 85%), suggesting that energy-based optimization encourages the emergence of more coherent synergy structures. These findings highlight both the influence of optimization objectives on coordination and the need for nonlinear approaches to more accurately model joint synergies in underactuated locomotion.

Key Words: Trajectory optimization, bipedal locomotion, kinematic synergy, Non-Negative Matrix Factorization (NNMF), optimal control

Authors: Mahdi Alipoor, Masoud Yousefi, Farzam Farahmand











Article Code: icbme-1287

Article Title: Excessive and Variable Center of Mass Motion Characterizes Gait Instability in Elderly Women with Obese Knee Osteoarthritis

Abstract: Elderly women with obese knee osteoarthritis (KOA) represent a population at high risk for impaired balance and falls. Quantifying the dynamic stability of their gait is crucial for understanding this risk and developing targeted interventions. Objective: This study compared gait stability and balance between healthy young women and elderly women with obese knee osteoarthritis by analyzing center of mass (COM) kinematics. Methods: Forty elderly women with obese KOA (70±4 yrs, 98.8±7.3 kg, 158.6±7.8 cm) and twenty healthy young women (29±5 yrs, 61.2±6.4 kg, 159.5±6.7 cm) underwent 3D gait analysis. A subject-specific OpenSim model was used to compute the COM trajectory for each participant. Key stability metrics including path, range of motion (ROM), maximum displacement, standard deviation, and their velocity counterparts in the anteroposterior(AP), mediolateral (ML), and vertical (SI) directions—were calculated and normalized to body height. Results: The obese KOA group demonstrated significantly impaired stability across all COM metrics. Specifically, they exhibited a larger COM path, greater ROM, and increased maximum displacement (p<0.05), with the most pronounced differences observed in the ML direction. Furthermore, the obese KOA group showed significantly higher variability, evidenced by greater standard deviation of both COM position and velocity (p<0.05), indicating a less consistent and more unstable gait pattern. Conclusion: Elderly women with obese knee osteoarthritis walk with an unstable gait, exhibiting excessive mediolateral movement of their center of mass. These objective biomechanical findings highlight a significant deficit in dynamic stability, which likely contributes to a heightened fall risk in this population. Rehabilitation strategies should focus on improving mediolateral balance control to mitigate this risk.

Key Words: Gait Analysis; Knee Osteoarthritis; Obesity; Center of Mass; Postural Balance; Stability; Biomechanics

Authors: Diba Chegini, Farhad Tabatabai Ghomsheh, Behzad Yasrebi, Aliakbar Pahlevanian, Siamak Haghipour











Article Code: icbme-1437

Article Title: Backward Walking Under Dual-Task Conditions Among Young Adults: A Potential Tool for Early Detection of Gait Instability and Fall Risk

Abstract: This study aimed to investigate the effect of cognitive and motor dual-task (DT) conditions on gait asymmetry during forward (FW) and backward (BW) walking, and its relationship with fall risk (FR). As a more homogeneous population and to minimize agerelated gait variability, healthy young adults were evaluated under ten different conditions, including FW and BW walking, both in single-task and DT modes (cognitive and motor). The results indicated that there is a main effect of task type (F9,890=20.43, p<0.001) and BW walking produced greater gait asymmetry compared to FW walking, with the highest asymmetry occurring during the task of carrying a cup with the non-dominant hand (NDH). Furthermore, cognitively demanding tasks (e.g., counting BW from 90) significantly increased gait asymmetry in both walking directions. The combination of a challenging walking direction (backward) with high task load exhibited the greatest disruption in gait coordination. These findings suggest that increased gait asymmetry under DT conditions, particularly during BW walking, may serve as a sensitive indicator for detecting motor instability and predicting FR, even in healthy young populations. This provides a foundation for developing screening protocols and preventive interventions to enhance balance and reduce FR.

Key Words: Gait asymmetry, Dual-task, Backward walking, Fall risk, Postural balance

Authors: Zahra Ouni, Hassan Khoudeh, Mina Niknam, Fariborz Rahimi











Article Code: icbme-1178

Article Title: Corrective Insoles Enhance Center of Mass Stability During Stair Descent in Individuals with Leg Length Discrepancy

Abstract: Leg length discrepancy (LLD) is linked to reduced dynamic stability and significant changes in gait biomechanics. This study quantified center of mass (COM) trajectory and sway measures in individuals with leg length discrepancy during stair descent, with and without corrective insoles, to determine whether such orthotic intervention can mitigate postural control deficits and improve stability. Ten male participants with structural leg length discrepancy (30 ± 10 mm) completed stair descent trials with and without custom corrective insoles. Threedimensional kinematics were recorded at 100 Hz using a seven-camera motion capture system. with COM trajectories computed for sagittal, frontal, and transverse planes. The insole height matched the measured discrepancy plus 10%, and trials were repeated three times per condition. Independent t-tests compared sway-related COM parameters between conditions, with significance set at p < 0.05. In the frontal plane, corrective insole usage during stair descent in individuals with leg length discrepancy yielded significant improvements in balance control, with range of motion and maximum deviation of the center of mass reduced by 37.7% and 37.9%, respectively (p < 0.04, p < 0.03). In the transverse plane, decreases of 44.6% in range of motion and 58.1% in maximum deviation (p < 0.030, p < 0.030) indicated enhanced rotational stability. Sagittal plane measures demonstrated small, non-significant reductions (p > 0.05). Although the study included a small pilot sample (n = 10), the findings provide preliminary evidence supporting the use of corrective insoles as a practical strategy to reduce fall risk during stair descent in individuals with leg length discrepancy. Corrective insoles substantially minimized frontal and transverse plane sway, supporting their application as a non-invasive, cost-efficient strategy to enhance dynamic stability in individuals with leg length discrepancy during stair descent.

Key Words: Dynamic Balance, Leg Length Discrepancy, Stair Descent

Authors: Kasra Alborzi, Alireza Hashemi Oskouei, Pouya Mansouri, Seyed Mehran Ayati Najafabadi











Article Code: icbme-1309

Article Title: Phase-Specific Analysis of Arm–Leg Load Sharing in Exoskeleton-Assisted Gait Using Biomechanical Indices

Abstract: This study investigated the redistribution of support between the arms and legs during exoskeleton-assisted gait with forearm crutches, using the Exoped lower-limb exoskeleton. A full-body skeletal model was developed by synchronized motion capture, ground force reaction measurement, and instrumented crutch data to compute phase-specific indices of load sharing. The modeling framework had been previously validated against experimental ground reaction forces, ensuring reliable estimation of joint kinetics and external loads. Results showed that the arms carried approximately 10% of body weight on average (ULSF ≈0.10), with transient peaks of ~0.18 during mid stance. The Vertical Impulse Share (VIS) indicated increased cumulative arm contributions in pre-swing and initial swing (~0.12-0.13), while the Arm Asymmetry Index (AAI) reached values near 1 during loading response (the initial double support phase immediately after heel strike, when the limb begins accepting body weight) and terminal swing, reflecting reliance on a single arm. Peak Support Timing (PST) consistently occurred at \sim 28–30% of the gait cycle, corresponding to late mid stance. These findings demonstrate that although arm forces remain modest in absolute terms, their phase-dependent nature makes them critical for stability and may predispose the upper limbs to repetitive high-load exposure. The proposed framework offers practical insights for safer exoskeleton design and rehabilitation strategies aimed at reducing upper-limb overuse.

Key Words: Exoskeleton-assisted gait, Arm-leg load sharing, Upper-limb support, Load-sharing indices, Upper-limb loading

Authors: Milad Hosseini, Negin Nasirian, Saeed Behzadipour











Article Code: icbme-1135

Article Title: Inverse Dynamics Analysis of the Crutch-Assisted Gait with a Lower-Limb Robotic Exoskeleton

Abstract: This study presents a comprehensive inverse dynamics framework for evaluating upper-limb joint loading during crutch-assisted gait with ExopedTM, a lower-limb robotic exoskeleton. To address the absence of integrated biomechanical models capturing the combined interactions of the user, exoskeleton, and assistive devices, a full-body skeletal model was developed. Motion capture and force plate data were collected from a paraplegic user walking with instrumented forearm crutches, each equipped with a single-axis load cell and reflective markers. The crutch system was validated against force plate measurements, showing high accuracy in vertical ground reaction force (GRF) estimation with a maximum RMS error of 7.01% for axial forces, with shear forces remaining below 10% throughout the gait cycle. The skeletal model was further validated by comparing model output and recorded foot GRFs, demonstrating close agreement in both magnitude and timing of loading patterns with average relative errors of 14.34% for the left foot and 15.86% for the right foot. Inverse dynamics analysis revealed physiologically plausible torques, with peak values of approximately -12 Nm at the elbow and 20 Nm at the shoulder, primarily in the pitch (flexion/extension) and roll (abduction/adduction) axes. These magnitudes align with previously reported ranges for assisted gait and remain within physiological capacity, supporting the model validity. The results identify critical phases of the gait cycle-particularly early and mid-stance-where torque demands peak, providing actionable insights for clinical gait training and exoskeleton control strategies aimed at minimizing upper-limb exhaustion and pathological risks.

Key Words: Inverse dynamics, Crutch-assisted gait, Upper limb biomechanics, Exoskeleton modeling, Joint torque estimation

Authors: Negin Nasirian, Milad Hosseini, Reza Norouzzadeh, Saeed Behzadipour











Article Code: icbme-1315

Article Title: Robotic-Assisted Early Rehabilitation Post Total Knee Arthroplasty: An

Experimental Investigation

Abstract: Total Knee Arthroplasty (TKA) is an orthopedic surgery that requires immediate rehabilitation as a standard practice. Stiffness reduction, Range of Motion (ROM), and functionality restoration can be achieved by Continuous Passive Motion (CPM) devices. Their application in clinical settings is a subject of ongoing debate. In this research, a lightweight onedegree-of-freedom (DOF) knee robotic exoskeleton is proposed to replace CPM devices. The proposed system provides continuous torque delivery of 15 Nm from 0° to 110°, with features such as emergency stop capabilities and multimodal control (position, impedance, torque). Clinical trials were conducted at Al-Zahra Clinic, Marjan Medical Hospital, and Babylon Rehabilitation Center in Iraq. Twenty patients (60% female, 40% male) who had undergone TKA participated in four weekly sessions receiving rehabilitation using the prototype. Clinical outcomes were measured using pain levels (VAS), knee ROM, functional mobility (6MWT), quadriceps strength, and patient-reported outcomes (WOMAC). The findings showed that the robotic exoskeleton was an effective replacement for CPM, allowing for early mobilization in upright, sitting, and partially standing positions. Patients experienced increase in passive ROM. reduced VAS pain scores at rest and during activity, and clinically significant improvements in functional mobility, 6MWT. Low stiffness scores on the WOMAC subscale indicated improved performance in daily activities, high patient compliance, and tolerance. No significant adverse effects were reported. The proposed robotic exoskeleton demonstrated safety, feasibility, clinical benefit for early TKA rehabilitation and scalable alternative to conventional CPM systems.

Key Words: robotic-assisted, rehabilitation, total knee arthroplasty, clinical investigation, experiment

Authors: Raed Abdulameer Mahmood Alalvani, Ali Selk Ghafari











Article Code: icbme-1221

Article Title: Effects of Levodopa and Visual Condition on the Complexity of Postural Control in Parkinson's Disease Patients With and Without Freezing of Gait Through a Multiscale Entropy Approach

Abstract: The subtle ways in which levodopa influences postural control in Parkinson's disease (PD), especially under conditions of altered sensory input, remain a critical topic of exploration. This work analyzed postural sway complexity using a multiscale entropy (MSE) approach in 32 individuals with PD, 13 exhibiting freezing of gait (FoG) and 19 without, evaluated under both medicated (ON) and unmedicated (OFF) conditions, with vision either available or occluded. A primary finding revealed that levodopa significantly reduced medial-lateral postural complexity when visual input was absent (eyes closed) compared to the unmedicated state. While the presence of FoG did not show a significant influence on complexity in this quiet standing task, the results highlight a crucial paradox: standard dopaminergic therapy may inadvertently diminish the system's capacity for adaptive postural regulation. The results emphasize the intricate relationship between pharmacological treatment and sensory integration, indicating that therapeutic strategies should consider how medication influences balance across different environments.

Key Words: Levodopa, Parkinson's Disease, Postural Control, Multiscale Entropy, Complexity, Freezing of Gait

Authors: Kiarash Banan Motarjem, Amirhassan Khalouzadeh Mobarakeh, Aria Behroozi, Elham Shirzad Araghi











Article Code: icbme-1406

Article Title: Gait Retraining of Musculoskeletal Patients Using Deep Learning Techniques

Abstract: Reconstructive surgeries and the use of bone and joint prostheses are among the most common treatments for lower-limb skeletal disorders. Patients undergoing such treatments often face challenges in regaining a proper gait pattern. To overcome these difficulties, they are typically required to participate in rehabilitation programs where correct walking strategies are taught by instructors. However, these programs demand specialized equipment and experienced trainers, which are both costly and time-consuming, and not easily accessible to all patients. In this paper, we propose a novel method for gait extraction, analysis, and correction in musculoskeletal patients using depth-sensing camera (RGBD) and deep learning techniques. The three-dimensional coordinates of anatomical key points in the patient's lower limbs are automatically extracted from gait videos, and the corresponding motion patterns are represented through spatial variation graphs of these key points. Subsequently, inverse kinematics analysis of the motion pattern is performed to derive variations in anatomical indicators (distances and angles) across the main gait phases, including Toe-off, Mid-Stance, Mid-Swing, and Heel-Strike. By comparing these indicators with those of healthy individuals, the system evaluates the extent and nature of gait deviations that require correction. Finally, the proposed framework provides recommendations for adjusting the patient's gait and aligning it more closely with healthy walking patterns. Results from multiple case studies demonstrate that the proposed approach can significantly improve gait performance in the post-surgery phase and substantially reduce musculoskeletal complications caused by improper walking.

Key Words: Skeletal abnormalities, Gait retraining, Depth image processing, Deep learning

Authors: Kourosh Alimadadi, Masoud Shariat Panahi, Morad Karimpour, Hadi Ghattan Kashani











Article Code: icbme-1239

Article Title: Recovery of Hand Motor Function in Children with Hemiparetic Cerebral Palsy using an Interactive Computer Game Combined with Mechanoreceptor Stimulation: A Pilot Study

Abstract: Hemiplegic cerebral palsy (HCP) is a common neurophysiological condition in children, primarily causing motor impairments in the upper extremities. This study investigated the effectiveness of a novel multimodal rehabilitation protocol, which combined computerbased games and mechanoreceptor stimulation of the affected forearm, for improving motor function in children with HCP. Four children (ages 7-9) were selected and participated in 10 half-hour sessions. Clinical motor function of the upper extremity was measured using the Fugl-Meyer Assessment (FMA-UE) before and after the intervention. Hand joint kinematics, including the angles of the shoulder, arm, and wrist of the affected hand, were simultaneously recorded during these rehabilitation tasks. To quantify changes, advanced analytical tools such as Detrended Fluctuation Analysis (DFA) and Power Spectrum Density (PSD) were employed to assess motor stability and inter-joint coordination. The results showed significant clinical improvement in FMA scores which indicates motor enhancement. The kinematic analysis confirmed these clinical findings and provided critical new insights into the underlying quality of movement, highlighting the efficacy of this approach in promoting motor recovery. In conclusion, this multimodal protocol is an effective approach to improve motor recovery in children with cerebral palsy. This study also confirms the necessity of advanced analytical tools and a personalized medicine model to optimize patient outcomes.

Key Words: Cerebral Palsy, Hemiplegia, Motor recovery, Rehabilitation, Mechanoreceptor, Joint Kinematics

Authors: Mobina Ramezani, Shahed Salehzehi, Parisa Hosseini, Zahra Alizadeh Sarborj, Ghazal Mohammadzadeh, Hamid Reza Kobravi, Narges Hashemi, Mehran Beiraghi Toosi, Javad Akhondian











Article Code: icbme-1211

Article Title: OpenSim Musculoskeletal Modeling Framework for sEMG-Based Knee Torque Estimation

Abstract: Active rehabilitation devices use sensors to monitor movement and assess a patient's physiological capacity. Surface electromyography (sEMG) provides a non-invasive method for capturing muscle activity, while musculoskeletal models allow estimation of joint torque without bulky or expensive equipment. In this study, we developed a system that simultaneously records 2-channel sEMG and knee joint angles, integrated with a seated-leg musculoskeletal model in OpenSim via MATLAB. Experimental data were used to estimate muscle forces and compute net knee torque, yielding a peak torque of ~25 N·m, angular impulse of ~50 N·m·s, and average torque of ~12.5 N·m—values consistent with physiological expectations. This integrated approach offers a practical and cost-effective tool for real-time knee torque estimation, enabling improved assessment and monitoring in rehabilitation and biomechanical applications.

Key Words: Active Rehabilitation, Knee Torque Estimation, Hill-Type Musculoskeletal Model, sEMG signals, OpenSim.

Authors: Mohammad-Reza Sayyed Noorani, Mariya A. Vaziry, Seyed Alireza MirTajeddini











Article Code: icbme-1235

Article Title: Optimization Dynamic Stability and Energy Efficiency in Human-Like Bipedal Robot Over a Full Gait Cycle

Abstract: Bipedal robots are crucial for navigating uneven environments where wheeled robots are impractical. This study addresses the dual challenge of ensuring dynamic stability while minimizing energy consumption across a complete gait cycle, including the single support phase (SSP), double support phase (DSP), and switching phase. We developed a simplified 7-link, two-dimensional human model to reduce computational complexity. The optimization objective combined energy consumption and stability, which was maintained by keeping the zero-moment point (ZMP) within its allowable region. Using a two-point foot contact model, joint angles were defined as parametric functions to minimize energy use under kinematic constraints. Experimental human gait data provided initial values and validation for the optimization. Our results demonstrate that considering the complete gait cycle—including the transition phases—yields a distinct and more realistic optimal trajectory. While previous studies achieved a 9% energy reduction by optimizing only SSP and DSP, our simultaneous optimization of all three phases yielded a 3% reduction, a finding that more accurately reflects the system's dynamic limitations.

Key Words: Biped Robot, Gait Prediction, Zero Moment Point, Single Support Phase, Double Support Phase, Switching Phase, Power Consumption Optimization.

Authors: Mahdi Sadeghi, Mostafa Rostami, Soroush Sadeghnezhad











Article Code: icbme-1375

Article Title: Automated Kinematic Analysis of Barbell Curl Using Custom IMU and Deep Learning Techniques

Abstract: In this article, we present a method for monitoring barbell motion during biceps curl exercises to assess movement accuracy and identify excessive stress on the lumbar spine in order to reduce injury risk. A custom IMU sensor was designed, validated, and mounted on the barbell using dedicated clamps. Data were collected from 53 athletes with diverse sporting backgrounds under three conditions: light execution, moderate intensity, and maximum effort. Using a Convolutional Neural Network (CNN), the system achieved an overall accuracy of 92.2%. Specifically, correct repetitions were detected with a precision of 96.6% and a recall of 94.7%, while incorrect repetitions reached a precision of 60% and a recall of 70.6%. These results highlight the potential of sensor-based monitoring as a practical alternative to coach-supervised methods for evaluating exercise performance, while also indicating areas where future improvements are needed. The primary objective of this study was to detect sudden impulses along the anterior–posterior axis, as such loads are known to contribute to intervertebral disc injuries.

Key Words: IMU, Machine Learning, Convolutional Neural Networks, Low Back Injury, Barbell Curl

Authors: Mohammad Khalfe Nilsaz, Elham Shirzad, Ali Fahim











Article Code: icbme-1339

Article Title: Investigating the Impact of Arm Swing on Lower Limb Forces Using Machine Learning Techniques

Abstract: Arm swing is a key component of gait mechanics, influencing joint stability, muscle forces, and locomotion efficiency. Understanding this relationship involves biomechanical complexity. This study investigates how different arm swing amplitudes affect lower limb muscle forces during walking. Motion capture data were collected from 20 healthy participants. with arm swings categorized as large (LA), normal (NA), and small (SA). Muscle force data for 41 muscles were analyzed using OpenSim software. Two approaches were used for classification: (1) statistical feature extraction with machine learning classifiers (Logistic Regression, SVM, Decision Tree, Random Forest, and XGBoost), and (2) time-series analysis using Dynamic Time Warping (DTW) with weighted KNN. Clustering was also performed using algorithms such as OPTICS, Hebbian learning, DBSCAN, SOM, BIRCH, and agglomerative clustering after applying Fourier Transform. The best classification performance in the (LA-NA)-SA scenario was achieved by SVM and Logistic Regression, both reaching 98% accuracy. The DTW-based weighted KNN approach achieved 84% accuracy. Clustering results showed the highest agreement in the (LA-NA)-SA scenario, with the Hebbian learning model achieving a silhouette score of 0.5, and ARI, AMI, and FMI values of 0.44, 0.52, and 0.69, respectively. The results suggest that lower limb muscle force patterns are similar in normal and high arm swing ranges, while low arm swing produces distinct patterns, indicating increased muscular effort. Classification and clustering results were consistent and reinforced each other. This study contributes to the understanding of the importance of arm swing in gait mechanics, with implications for rehabilitation and ergonomic design. The integration of motion capture systems with machine learning models offers a novel and effective approach to human movement analysis.

Key Words: Arm Swing, Force, Lower Limb, Machine Learning

Authors: Mohammad Reza Seidgar, Hadi Farahani, Mostafa Rostami, Elham Naziri, Sadegh Madadi











Article Code: icbme-1314

Article Title: Dynamic Modeling of a Cable-Driven Series Elastic Upper Extremity Exoskeleton for Post-Stroke Rehabilitation

Abstract: This study presents a dynamic modeling framework for simulating human-exoskeleton interaction in upper-extremity movements using Simscape. An open-loop inverse dynamics simulation was conducted with a one-degree-of-freedom exoskeleton designed to assist elbow flexion/extension while allowing natural shoulder motion. The shoulder joint was modeled with compliant properties, and the exoskeleton was actuated via a series elastic actuator (SEA). Simulation results demonstrated close tracking between human and exoskeleton joint angles, with mean errors below ±3°. The SEA provided compensatory torque closely matching the estimated human torque deficit at the elbow, while human–robot interaction forces and torques remained within physiologically acceptable ranges. A cyclogram analysis of shoulder-elbow coordination yielded a correlation coefficient of 0.92, with a 15% reduction in loop area compared to unassisted motion, indicating improved efficiency of assisted movements. These findings validate the proposed model as a reliable tool for analyzing upper-extremity human-exoskeleton dynamics and provide insights for controller design and

Key Words: Human-Robot Interaction, Exoskeleton, Upper-Limb, Series Elastic Actuator,

Simscape, Biomechanics

optimization of assistive strategies.

Authors: Ali Selk Ghafari, Omid Kalantari











Article Code: icbme-1194

Article Title: Effects of laminectomy on active-passive spine loads: a musculoskeletal finite element modeling investigation

Abstract: Lumbar spine pain and disorders, including stenosis, are significant causes of disability, particularly among the elderly, often leading to surgical interventions such as laminectomy with or without facetectomy. It involves the removal of the lamina, spinous process, posterior ligaments, and, in some cases, facet joints, thereby disrupting the normal load-sharing among active and passive spine elements. In the absence of viable in vivo approaches, advanced computational modeling offers insights into the biomechanical mechanisms underlying postoperative complications. This study investigates the biomechanical effects of three surgical procedures, i.e., unilateral laminectomy, full laminectomy, and laminectomy with facetectomy, on active-passive spine load distributions using our validated musculoskeletal-finite element (MS-FE) model. The analysis focuses on preoperative (intact condition) and postoperative simulations of the L4-L5 motion segment during static upright standing posture and forward trunk flexion at 80° (deep flexion). Results show that in the upright standing, negligible differences were observed between intact and postoperative models since ligaments were not tensioned. In contrast, deep flexion induced substantial changes across surgical procedures. Total muscle force increased from 1730 N in the intact model to 1893 N, 2019 N, and 2019 N after unilateral laminectomy, full laminectomy, and laminectomy with facetectomy. Joint compression at L4-L5 increased from 1724 N to 1860 N, 2118 N, and 2118 N across the three procedures. Ligament forces decreased dramatically at L3-L4 and L4-L5 (e.g., 404 N to 12 N, and 399 N to 66 N, respectively) after full laminectomy and facetectomy. Surgical resection of posterior elements had the most pronounced effects on joint compression. ligament forces, and total muscle forces, particularly during deep flexion. Full laminectomy and facetectomy caused greater biomechanical alterations compared to unilateral laminectomy, which led to relatively smaller changes. Unilateral laminectomy should therefore be the preferred approach whenever sufficient decompression can be achieved, especially in cases with unilateral lateral recess stenosis, foraminal stenosis, or focal disc herniation without bilateral symptoms. Understanding these biomechanical changes is essential for optimizing surgical planning, minimizing anatomical disruption, and reducing the risk of postoperative complications.

Key Words: Lumbar spinal stenosis, Spinal surgery, Laminectomy, Finite element modeling, Spinal load distribution

Authors: Aida Ahmadi, Navid Arjmand, Parisa Azimi











Article Code: icbme-1312

Article Title: Impact of Dynamic and Static Sports on Growth and Anthropometric Characteristics (Height, Weight, BMI) in Children and Adolescents

Abstract: Adolescence is crucial for growth and body composition. Physical activity can influence height, weight, and BMI. This study aims to explore how sports of dynamic and static types affect body measurements in teenagers based on sex and age. A cross-sectional study involved 494 participants (256 boys, 238 girls) aged 4-19 years. Participants were categorized as Non-Athletes, Static Athletes, or Dynamic Athletes, Height and weight were measured, BMI was calculated, and sports were classified by physical demand; dynamic (e.g., running, soccer) or static (e.g., archery, voga). Differences among groups were analyzed using one-way ANOVA across three age groups: 4-9, 10-14, 15-19 years. Normality was checked with skewness, kurtosis, and Kolmogorov-Smirnov tests. In early childhood (4-9 years), there were no significant differences in height, weight, or BMI. During pre-adolescence (10-14 years), boys in dynamic sports showed lower weight and BMI compared to Non-Athletes, while girls in both sports groups had significantly higher weight and BMI. In late adolescence (15-19 years), athletes' height and weight were significantly higher in boys than girls, with notable BMI differences between Non-Athletes and Dynamic Athletes. Participation in sports influences growth and body composition in a sex- and age-specific manner. Prevalence of sports participation is low in young children, increases during pre-adolescence, and peaks in late adolescence. Dynamic sports are tied to lower BMI in boys, while static sports are linked to increased fat-free mass. Encouraging organized physical activity supports healthy adolescent development.

Key Words: Adolescence, Athletic Participation, BMI, Height, Weight, Dynamic Sports, Static Sports

Authors: Amin Partovi Fard, Mahmoodreza Azghani, Sadra Jalali, Samin Asghari











Article Code: icbme-1313

Article Title: Effects of Athletic Status on Plantar Pressure Distribution and Biomechanical Foot Health in Children and Adolescents

Abstract: The plantar surface is key for force transmission, shock absorption, and balance. Musculoskeletal development in adolescents can change plantar pressure and injury risk. Few studies compare plantar pressure between physically active and inactive adolescents. This study aims to compare static plantar pressure distribution across eight foot regions in inactive adolescents versus those engaged in static or dynamic sports, stratified by age groups. 494 subjects (256 males, 238 females), aged 4-19, were divided by age (4-9, 10-14, 15-19) and activity level: inactive, static sports (e.g., shooting, archery), and dynamic sports (e.g., soccer, basketball). Static sports focus on stability and minimal lower-limb movement; dynamic sports involve continuous movement and direction changes. Plantar pressure during quiet standing was recorded with the PT-scan® system. Foot type was classified by Arch Index. Pressure was measured in eight areas: left/right forefoot (LF, RF), midfoot (LM, RM), backfoot (LB, RB), and toes (LT, RT). Normality was confirmed before one-way MANOVA. No significant differences, except higher right backfoot pressure in 10–14-year-old girls in static sports (p = 0.021). Other differences were minor and not significant. Physical activity has minimal effect on plantar pressure during static standing in teens. Limitations include the cross-sectional design and static testing. Future studies should include dynamic assessments and longitudinal follow-up to better understand foot development, activity effects, and injury prevention.

Key Words: Athletic Status, Gender, Adolescents, Age, Plantar Pressure

Authors: Amin Partovi Fard, Mahmoodreza Azghani, Sadra Jalali











Article Code: icbme-1154

Article Title: Alterations in Muscle Coordination During Different Gait Phases Following Knee Injury

Abstract: The purpose of this study is to examine muscle coordination patterns around the knee in individuals with post-knee injury, comparing the injured limb to the contralateral limb, as well as to the dominant limb of healthy controls during different gait phases. Surface electromyography (sEMG) signals have been obtained from a public dataset of knee extensor and flexor muscles during walking and analyzed across four temporal gait phases: preparatory, initial stance, initial-to-midstance, and full gait cycle. Two EMG features, Integrated EMG Ratio (IR) and Co-Contraction Index (CCI), have been extracted to quantify muscle activation patterns.

The results have shown significant differences in CCI and IR values in the operated limb compared to the contralateral limb of the injured subjects and the dominant limb of healthy controls during the early stance phases (p<0.05). These findings indicate compensatory neuromuscular changes to improve joint stability after injury, but they may also increase abnormal joint loading and risk of post-traumatic knee osteoarthritis. These findings highlight the need for rehabilitation programs that focus on improving not only muscle strength but also neuromuscular coordination to optimize functional recovery after knee injury.

Key Words: Knee injury, Gait Phases, Co-Contraction Index, Integrated EMG Ratio, Neuromuscular Coordination

Authors: Shaghayegh Hassanzadeh Khanmiri, Alireza Hashemi Oskouei, Peyvand Ghaderyan











Article Code: icbme-1391

Article Title: Deep Neural Network–Based Adaptive Global Logarithmic Sliding Mode Control for Lower-Limb Rehabilitation Exoskeletons

Abstract: Lower-limb rehabilitation exoskeletons have emerged as promising tools to help people with lower-limb disorders. However, designing effective controllers for these systems remains challenging due to their coupled nonlinear dynamics, inherent system uncertainties, and external disturbances. Although classical Sliding Mode Control (SMC) offers robustness, it is often affected by chattering, which can degrade system functionality and performance. To overcome these limitations, we propose a novel control framework called Deep Neural Network (DNN)-Global Logarithmic (GLog)-SMC, which integrates GLog-SMC with an adaptive DNN. The GLog-SMC component enables smooth convergence to the sliding surface while reducing chattering, and the adaptive DNN approximates unknown system dynamics online. A Lyapunov-based adaptation law is used to ensure closed-loop stability. Results on a three-degree-of-freedom exoskeleton show that the suggested approach improves trajectory tracking accuracy, increases robustness, and produces smoother control torques compared to classical SMC.

Key Words: Deep neural networks, Global logarithmic sliding mode control, Rehabilitation exoskeletons, Robustness.

Authors: Masoud Shirzadeh, Ghoncheh Zand, Samim Kamyab











Article Code: icbme-1213

Article Title: Simulations of Body-Exoskeleton Interactionusing OpenSim-MATLAB

Interface

Abstract: Exoskeleton robots are developed for various purposes, including rehabilitation, power augmentation, and movement assistance. This study aims to create some integrated models of the human musculoskeletal system that interact with and are powered by an exoskeleton robot. In fact, we intend to achieve some desired movement scenarios by closed-loop control of the exo-robot via simulations designed using OpenSim-MATLAB Application Programming Interface (API). Here, we examine three scenarios, including knee flexion in a situation where a patient needs a motion assistance service, power augmentation for elbow flexion when the user demands extra power to lift a weight, and a resistive scenario in which elbow flexion is performed against the force applied by a spring. During all three scenarios, the required torque should be applied by the exo-robot, which is calculated based on the PD control law that runs in a closed-loop scheme in MATLAB through receiving motion feedback information provided from the OpenSim solver. The results demonstrate the effectiveness of this integrated framework in accurately simulating human-robot interaction, offering a practical tool for developing advanced assistive motion systems.

Key Words: Human-Robot Interaction, Exoskeleton Robot, Musculoskeletal Model, OpenSim/MATLAB API

Authors: Mohammad-Reza Sayyed Noorani, Hesam Ghasemi Barghi, Shaghayegh

Hassanzadeh Khanmiri











Article Code: icbme-1173

Article Title: Exponential sliding mode controller to track the human upper limb during Topspin Forehand in Table Tennis

Abstract: Understanding and improving the biomechanics of sports movements is essential to both injury prevention and performance optimization. This study presents a control-oriented simulation of the human upper limb during the topspin forehand motion in table tennis. A 4-degree-of-freedom skeletal model of the right arm—comprising the shoulder and elbow joints—is developed using the Denavit–Hartenberg convention. To track experimentally obtained reference trajectories, an exponential sliding mode controller (ESMC) is proposed. The controller ensures finite-time convergence of tracking errors. Simulation results demonstrate high tracking accuracy and proper control torque behavior, indicating the potential of the proposed method in biomechanics and intelligent rehabilitation systems. This framework can be extended to upper-limb exoskeleton control, motion analysis for injury prevention, and intelligent training tools for athletes.

Key Words: Upper limb biomechanics, Table tennis, Exponential sliding mode control, Human motion tracking, Rehabilitation robotics, Injury prevention, Biomechanical simulation

Authors: Erfan Sedaghat, Seyyed Arash Haghpanah











Article Code: icbme-1282

Article Title: DDQN-Learning of Hill-Type Musculoskeletal Arm Model for Elbow Motor

Control

Abstract: This study aimed to develop a model-based reinforcement learning (RL) framework designed to partially emulate central nervous system (CNS) learning processes for goal-directed motor control. The RL model, implemented using a double deep Q-learning (DDQN) algorithm, interacting with a biomechanical arm model served as the simulated environment. The environment comprised a Hill-type musculoskeletal representation of the biceps brachii and triceps brachii muscles, enabling elbow flexion–extension over a range of 10–135°. Within this setup, the RL agent received state information, including elbow joint angle and velocity, from the environment and generated muscle activation signals as control outputs. These signals acted on the Hill-based biomechanical model, allowing the agent to learn reaching toward specified target through iterative episodes. To validate biomechanical realism, forward dynamics simulations were performed in OpenSim using a customized arm model driven by the RL-generated excitations. Results demonstrated that the agent successfully acquired stable and biologically plausible motor strategies.

Key Words: Double Deep Q-learning, Elbow Flexion Control, Hill-Type Musculoskeletal Model, Muscle Activation, OpenSim.

Authors: Mohammad-Reza Sayyed Noorani, Abbas Jafarpour Mahalleh, Kimiya Khojand











Article Code: icbme-1338

Article Title: Gait-Triggered Neuromuscular Electrical Stimulation with Unloader Knee

Braces: A Feasibility Study

Abstract: Knee osteoarthritis (OA) commonly involves the medial compartment of the joint. Valgus unloader braces can reduce joint loading in this region but may also suppress quadriceps activation. Neuromuscular electrical stimulation (NMES) can strengthen quadriceps when voluntary activation is limited. We evaluated the feasibility of a gait-triggered NMES system used in combination with a valgus unloader brace. Accordingly, A portable module was developed incorporating a commercial NMES stimulator, a microcontroller, and an inertial measurement unit (IMU). In real time, gait events (mid-swing, initial contact, and toe-off) were detected in real time to trigger quadriceps stimulation. The system was tested in eight adults with medial knee OA and five healthy controls, each completing a 30-minute supervised walking session. The device operated continuously throughout all sessions. OA patients walked with a significantly slower cadence than controls (1.1 \pm 0.4 vs. 2.0 \pm 0.4 steps·s⁻¹, p = 0.008), and cycle detection accuracy remained high in both groups (91-93%, p = 0.72). No serious adverse events occurred. Overall, This study introduced and evaluated a novel bracecompatible, gait-triggered NMES system for knee OA. The prototype reliably synchronized stimulation with walking, was safe and represented a reproducible model for future clinical translation. Further refinements and multi-week clinical trials are warranted.

Key Words: Knee osteoarthritis; Unloader brace; Neuromuscular electrical stimulation (NMES); Gait event detection

Authors: Mohadeseh Jafarian, Reza Khosrozadeh Sarijalou, Amin Komeili, Kourosh Barati, Navid Arjmand











Article Code: icbme-1204

Article Title: Fuzzy Estimator of the Soleus Activation during Heel-raising Motion using OpenSim–MATLAB

Abstract: In this study, we address muscle-driven simulation for heel-raising motion and estimate the activation of the soleus muscle using a fuzzy inference system (FIS). Surface electromyography (sEMG) signals of the major shank muscles are recorded experimentally, while optical markers attached to anatomical landmarks on the leg are simultaneously tracked using a conventional camera to extract ankle joint kinematics via the Kinovea motion analysis software. Two separate FISs are designed in MATLAB: one based on ankle joint kinematic data and the other on sEMG signals of agonist-antagonist muscles. Both systems were able to estimate the soleus muscle activation. Next, the movement is simulated based on the sEMG signals of four muscles (medial and lateral gastrocnemius, soleus, and tibialis anterior), using the Forward Dynamics tool of OpenSim, with the ankle plantarflexion angle as the output. The error between the maximum experimental and simulated angles serves as the evaluation metric. Although both FISs successfully estimate soleus activation, the EMG-based FIS demonstrates a more physiologically plausible signal pattern and marginally superior performance. It should be noted that without stimulating the soleus, the simulated movement fails to execute correctly.

Key Words: Heel-raising Motion, Muscle-driven Simulation, Fuzzy Estimator, Soleus Activation, OpenSim/MATLAB API.

Authors: Mohammad-Reza Sayyed Noorani, Roghaiyeh Ahmadian Sarand, Nakisa Farshforoush











Article Code: icbme-1363

Article Title: Experimental Framework for Quantifying Muscle Force-Length Behavior in Dynamic Exercise

Abstract: The force-length characteristics of the biceps from resistance exercise training were studied, and the most important role of range of motion (ROM) under three contraction conditions (0-90°, 90-140°, and 0-140° during elbow flexion) was presented during the standing dumbbell biceps curl. Muscle force and mechanical tension are important for Hill-based muscle modeling, and ROM is an important determinant of both. A total of eight controlled repetitions were carried out by five healthy male subjects with a variety of training experiences. Motion capture data were collected with a Motion Analysis system and processed in OpenSim with a modified Arm26 model to extract elbow joint kinematics and normalized biceps muscle lengths. These lengths were filtered and used to calculate the active force-length modifier, which generated continuous force-length curves for the long and short heads of the biceps for all ROMs. The methodology produced stable physiologically realistic force-length relationships and was shown to be a reliable method for use in resistance training analysis. In summary, the workflow provides a practical reference for the quantification of muscle mechanics and can be used to understand the influence of ROM on muscle force in Hill-based models and inform evidence-based training protocols.

Key Words: Musculoskeletal Modeling, Hill-type Model, Force-Length Relationship, Biceps Brachii, Range of Motion.

Authors: Erfan Farahani, Manizheh Zakeri, Mohammad-Reza Sayyed Noorani











Article Code: icbme-1174

Article Title: Neuromuscular Coordination in Badminton Smashes: Validation of

Musculoskeletal Models

Abstract: The badminton forehand overhead smash is a fast, powerful stroke that puts high mechanical stress on the shoulder, raising injury risks. We used non-negative matrix factorization (NMF) to identify shoulder muscle synergies and compared musculoskeletal (MSK) model predictions with electromyography (EMG) recordings from elite athletes. Twenty professional players (age: 24 ± 4 years; experience: 15 ± 4 years) executed maximal smashes, with EMG from 15 shoulder muscles and kinematics via the Vicon system. OpenSim simulated muscle activations. NMF revealed three synergies covering over 90% variance (MANOVA: F(2,19)=2.43, p=0.12, η²p=0.21): scapular support (led by trapezius, 95% EMG / 97% MSK VAF), force generation (pectoralis/anterior deltoid, 97% EMG / 94% MSK, 0.85 ± 0.12 Nm/kg), and deceleration (posterior group, 95% EMG / 98% MSK). Synergy weights correlated highly (0.81–0.88) and activations (0.95–0.98), though trapezius showed lower match (0.77 ± 0.05) from EMG limitations. Signal-to-noise was notable (t(19)=2.81, p<0.05, 0.68). These findings extend our earlier work by emphasizing model accuracy for quick athletic motions, offering fresh perspectives for training optimization and injury mitigation in overhead activities.

Key Words: badminton, muscle synergy, electromyography, musculoskeletal modeling, sports biomechanics

Authors: Raheleh Tajik, Hamed fadaei











Article Code: icbme-1227

Article Title: Postural Responses to Mediolateral Rotations: Contributions of Surface, Vision, and Cognitive Load

Abstract: Maintaining postural stability is a complex process influenced by sensory, motor, and cognitive factors. Dynamic balance tests provide valuable insight into these mechanisms by challenging balance under controlled conditions. This study investigated the effects of surface type, visual availability, and cognitive load on postural control during mediolateral rotational disturbances in healthy young adults. Fifteen participants completed trials on a robotic balance platform under eight conditions combining rigid or foam surfaces, eyes open or closed, and with or without a cognitive task. During each trial, ML platform rotations were applied while Center of pressure (COP) responses were recorded. COP data were analyzed across position, velocity, and frequency domains to capture both static and dynamic aspects of postural control. Analysis of variance revealed that vision significantly affected all COP domains, surface type primarily influenced dynamic and frequency measures, and cognitive load altered static and frequency measures. No significant interactions were observed, indicating that each factor contributed independently to balance regulation. These findings suggest that surface, vision, and cognitive load each impose distinct challenges to postural control during ML disturbances, highlighting the importance of evaluating multiple task constraints when assessing balance performance.

Key Words: Postural Control, Dynamic postural assessment, Mechanical Disturbance, Center of Pressure, COP Measures

Authors: Haniyeh Zahra Budaqi, Ali Mojibi, Saeed Behzadipour











Article Code: icbme-1366

Article Title: Effect of Aimlabs Software on Sustained Attention, Reaction Time, and Hand-Eye Coordination in Stroke Patients: A Preliminary Study

Abstract: Stroke frequently results in cognitive and motor function impairments, including challenges with sustained attention, reaction time, and hand-eye coordination, which significantly affect daily activities and rehabilitation outcomes. This preliminary study explores the potential of Aimlabs, a first-person shooter (FPS)-based training software, in improving these skills among stroke survivors. Twenty participants aged 45-65, diagnosed with ischemic stroke (confirmed via MRI, 3-12 months post-event), engaged in an 8-week intervention, practicing daily for 15-30 minutes on tasks such as Gridshot. Assessment tools were utilized to evaluate outcomes, with the Integrated Visual and Auditory Continuous Performance Test (IVA-CPT) measuring sustained attention through omission errors and reaction time via response speed, while the Purdue Pegboard Test (PPT) assessed hand-eye coordination through assembly scores. Post-intervention results demonstrated substantial enhancements, with IVA-CPT omission errors reducing by 25% (p<0.01), reaction times improving by 18% (p<0.05), and PPT scores rising by 15% (p<0.01). These findings highlight Aimlabs as a cost-effective and engaging tool for neurorehabilitation, combining gamification with traditional therapies. Nonetheless, further randomized controlled trials are necessary to confirm long-term efficacy and broader applicability.

Key Words: Stroke, Aimlabs, attention, reaction time, hand-eye coordination

Authors: Seyed-Ali Bagherzadeh, Leyla Rastgar-Farajzadeh











Article Code: icbme-1342

Article Title: Biomechanical Analysis of Blindfold Training for Backward Running in

Handball Athletes

Abstract: Blindfold training has recently been introduced as a novel approach to enhance proprioceptive control and improve movement coordination in sports performance. In handball, backward running is a critical skill associated with defense, injury prevention, and overall game dynamics. However, the biomechanical mechanisms underlying backward running, particularly under altered sensory conditions, remain poorly understood.

This study aimed to evaluate the effects of blindfold training on joint coordination and stability during backward running in handball players. A total of 24 athletes were recruited and randomly assigned to blindfold training and control groups. Kinematic data were collected using a motion capture system, and dynamic postural indices—including the mean absolute relative phase (MARP) and deviation phase (DP)—were computed to assess inter-joint coordination across ankle, knee, and pelvic segments. Statistical analyses were conducted to examine between-group differences and the effectiveness of the intervention.

The results revealed significant improvements in coordination consistency and controllability in the blindfold training group compared with controls. MARP and DP indices demonstrated that sensory deprivation enhanced proprioceptive feedback, leading to better joint synchronization. These findings suggest that blindfold training may serve as an effective strategy for developing backward running skills in handball, with potential applications in injury prevention and performance optimization. Future research should investigate long-term effects, larger sample sizes, and integration of blindfold training into routine athletic practice.

Key Words: Handball; Backward running; Blindfold training; Proprioception; Joint coordination; Biomechanics.

Authors: Aydin Najipour, Siamak Khorramymehr, Kamran Hassani











Article Code: icbme-1112

Article Title: Assessing the Risk of Musculoskeletal Injuries of Workers at the Warehousing Workstation of Iran Tire Company

Abstract: Repetitive manual material handling (MMH) activities often contribute to the development of musculoskeletal disorders in occupational settings. This study investigates the ergonomic and biomechanical risks associated with tire lifting and loading tasks performed by warehouse workers at Iran Tire Company. To identify the most critical posture, a simplified video-based motion analysis was conducted, followed by simulations using multiple biomechanical modeling platforms. The highest-risk posture produced L4-L5 compression forces of about 4800-5000 N for the 14 kg tire and 3000-3200 N for the 7 kg tire, exceeding the 3400 N safety threshold in most cases. This posture was then evaluated using both biomechanical and ergonomic assessment tools. Based on the results, two interventions were introduced: (1) an engineering control involving a height-adjustable pallet jack to minimize trunk flexion, and (2) an administrative strategy to reduce task frequency, which reduced compression forces to about 2500-2700 N for the 14 kg tire and 1500-1600 N for the 7 kg tire. Post-intervention evaluations revealed a substantial reduction in lumbar spine loading and ergonomic risk scores, highlighting the effectiveness of low-cost ergonomic solutions in enhancing worker safety and reducing the risk of MSDs in manufacturing environments.

Key Words: musculoskeletal risk assessment, tire handling, ergonomic interventions, low back pain, manual material handling

Authors: Mahshad Nazari Jeirani, Amirhossein Mohammadzadeh, Seyedeh Shokouh Azam Mirdamadi, Mohadeseh Sadat Shahangian, Navid Arjmand











Article Code: icbme-1216

Article Title: Finite Element Analysis of Ankle-Foot Orthosis (AFO): Influence of Shell and Insole Thickness Across Material Variants

Abstract: Ankle-Foot Orthoses (AFOs) are essential biomechanical devices designed to enhance gait stability, reduce excessive limb movement, and redistribute load during rehabilitation for individuals with lower limb impairments. To achieve optimal AFO performance, a precise anatomical fit, lightweight construction that does not compromise functionality, mechanical robustness under multi-axial loading, reduced skin pressure, and enhanced user comfort are all required.

This study aimed to develop biomechanically optimized, patient-specific AFOs using advanced technologies such as 3D scanning, additive manufacturing, and topology optimization. A finite element analysis (FEA)-based approach was employed to evaluate the effects of orthotic geometry, material properties, shell and insole thickness, and stiffness under dynamic physiological loading conditions. Four geometric configurations were simulated using patient-specific 3D models, varying shell thicknesses (3 mm and 6 mm) and insole thicknesses (6 mm and 9 mm). Two commonly used materials—polylactic acid (PLA) and polypropylene (PP)—were assessed under a vertical load of 350 N to analyze stress distribution, deformation, and plantar pressure. The results demonstrated that both geometry and material selection significantly influence mechanical performance, including displacement, Von Mises stress, and contact pressure. Thicker shell-insole combinations improved load-bearing capacity, while PP exhibited lower stress concentrations compared to PLA. This integrative simulation framework supports the quantitative evaluation of AFO designs and provides clinically relevant insights for personalized orthotic development and optimization.

Key Words: Ankle-Foot Orthosis, Finite Element Analysis, Shell Thickness, Material Properties, Orthotic Biomechanics

Authors: Maryam Sheikhi, Aisan Rafiei, Nima Jamshidi











Article Code: icbme-1275

Article Title: Anastomosis Angle Effects in Beating-Heart Coronary Bypass Grafts: A Fluid–Structure Interaction Study

Abstract: The geometry of coronary artery bypass grafting (CABG) strongly influences the long-term success of the procedure. Among the geometrical factors, the graft-to-coronary anastomosis angle is one of the most important. Many studies have investigated this parameter using computational fluid dynamics (CFD). However, most of them ignored arterial wall compliance and the displacement of the host coronary artery caused by the beating heart. This limitation reduces the physiological relevance of their findings. In this study, the effect of the anastomosis angle was examined using a fluid-structure interaction (FSI) framework that also included the physiological motion of the host coronary artery during the cardiac cycle. Three angles (30°, 45°, and 60°) were modeled using a 15.2 cm radial artery graft. Hemodynamic and structural parameters were analyzed to provide a more realistic evaluation of graft performance. The results showed that larger anastomosis angles increased coronary outflow, time-averaged wall shear stress (TAWSS), and oscillatory shear index (OSI). At the same time, von Mises stress on the graft wall near the anastomosis decreased with larger angles. These results indicate that higher angles may improve blood supply to myocardium and reduce the risk of mechanical graft failure. However, they also increase the risk of intimal hyperplasia and restenosis at the anastomosis site. Therefore, intermediate angles, such as 45°, provided more balanced outcomes and appears to be the best compromise and may represent a preferable surgical choice. Overall, this study emphasizes the importance of including both vascular wall compliance and coronary motion in graft modeling. The findings may help surgeons select optimal anastomosis geometries for improved CABG outcomes.

Keywords: Fluid-Structure Interaction Method, Radial Artery, Anastomosis Angle, Time-Averaged Wall Shear Stress (TAWSS), Oscillatory Shear Index (OSI), von Mises Stress

Authors: Mohammad Saleh Kazemi, Nasser Fatouraee, Aisa Rassoli











Article Code: icbme-1371

Article Title: Physics-Informed Neural Networks for Cardiac Flow Estimation in 2D

Simplified Human Right Ventricular Geometry

Abstract: One of the significant disorders in the cardiovascular system is pulmonary hypertension associated with the right ventricle, where estimation of pressure resulting from blood flow is critical for assessment. Evaluation of the pressure enhances the diagnostic and therapeutic capacity for the disease. So, pressure measurement without causing wounds or injury to the patient is of paramount importance. 4D magnetic resonance imaging is one of the novel imaging modalities capable of providing useful information to clinicians. However, complete extraction and analysis of blood flow dynamics using existing hardware with raw imaging data is currently not fully accessible. This study demonstrated that non-invasive computation of blood flow pressure in the right ventricle can be achieved using physicsinformed neural networks with minimal data of the velocity field obtained from imaging. This method can estimate the information faster and more accurately compared to conventional methods, eliminating the need to define geometry, mesh, and boundary conditions. The capability of this method was demonstrated through solving two problems: first, the "lid-driven cavity" problem, and second, "steady blood flow within a realistic 2D right ventricular geometry," where the relative errors for pressure field computation were 2.7% and 1.9%, respectively.

Keywords: Blood Pressure Computation, Computational Fluid Dynamics, Medical Imaging, Non-Invasive Measurement, Physics-Informed Neural Networks, Right Ventricle.

Authors: Mohammadmahdi Sekhavatpisheh, Nasser Fatouraee











Article Code: icbme-1156

Article Title: FSI Modeling of Osteocyte Mechanotransduction Under Dynamic Loading

Abstract: Osteocytes, the principal mechanosensors of bone, detect loading primarily through fluid flow shear stress in the lacunar–canalicular network. In this study, an idealized three-dimensional finite element fluid–structure interaction model was developed to investigate, for the first time, the combined effects of loading type and strain magnitude. Dynamic gait-like input was compared with static compression, and peak strains of 3000 and 3500 microstrain were applied. Dynamic loading induced stronger interstitial fluid transport, with more than 50 percent of dendrites experiencing shear stress above the osteogenic threshold, compared with only 33 percent under static loading. This effect was accompanied by higher mean pressure gradients, confirming the role of oscillatory input in broadening dendritic stimulation. Increasing strain magnitude enhanced osteocyte deformation, tissue stress, and energy storage, while fluid responses showed only modest rises in mean pressure and shear stress. These findings demonstrate that dynamic loading provides a more effective stimulus for osteogenic signaling than static compression, whereas elevated strain magnitudes near the upper physiological range may increase the likelihood of microdamage.

Keywords: Fluid-structure interaction, osteocyte, lacunar-canalicular network, fluid flow shear stress, finite element analysis, dynamic loading

Authors: Zahra Rahmani Samani, Hanieh Niroomand-Oscuii, Mohammad Niroobakhsh, Ehsan Alizad Farokhi











Article Code: icbme-1107

Article Title: How Geometric Asymmetry Impacts Aortic Valve Bioprosthesis Performance – A Finite Element Analysis

Abstract: A finite element analysis (FEA) was performed to compare the biomechanical performance of twelve asymmetric aortic valve designs against a symmetric reference, all sharing identical radius and height for geometric consistency. Using Grasshopper for parametric modeling, the study evaluated two key parameters: geometric orifice area (GOA), which affects flow during valve opening, and coaptation area (CA), which impacts sealing during closure. These were tested under simulated physiological conditions to assess the effects of asymmetry. Results showed significant differences in GOA and CA between asymmetric and symmetric designs, highlighting the role of asymmetry in valve opening and closing dynamics. The study identified valve asymmetry ranges (Area Diff % between --9.848 and 31.312) linked to improved performance, offering practical insights for optimizing aortic valve designs. Natural aortic valves, which serve as the benchmark for optimal performance, exhibit inherent asymmetry, with studies showing that one of the three leaflets typically displays statistically significant differences compared to the other two, which have minimal variation. These findings underscore the importance of mimicking such asymmetry in prosthetic valves to enhance efficiency. This analysis provides valuable guidance for advancing prosthetic valve design in clinical and engineering contexts.

Keywords: Asymmetric aortic valve, Geometric orifice area, Coaptation area, Parametric design, Grasshopper, Regurgitation, Prosthetic valve design, Valve dynamics

Authors: Reyhaneh Mosaferchi, Nasser Fatouraee











Article Code: icbme-1126

Article Title: Two-Dimensional FSI Simulation of a Novel SMA-Integrated Bileaflet Mechanical Heart Valve with Comparative Hemodynamic Analysis

Abstract: This study presents a novel hinge-free bileaflet mechanical heart valve actuated by shape memory alloy strips. A two-dimensional fluid–structure interaction (FSI) simulation was carried out in ANSYS Workbench, coupling the fluid and structural solvers through the System Coupling module. Blood was modeled as Newtonian and incompressible under the laminar assumption. The upper leaflet segments were represented as hyperelastic SMA, while the lower portions were modeled as rigid elastic material. The simulations showed physiologically realistic hemodynamics with a peak velocity of approximately 1.6 meters per second during full opening, wall shear stresses generally below 12 pascals with only localized peaks, a maximum transvalvular pressure drop of 1200 pascals (about 9 millimeters of mercury), and an effective orifice area of 2.1 square centimeters. Flow recirculation and vortex formation occurred downstream, but no hinge-related reverse jets were observed. These findings suggest that the hinge-free SMA design can provide performance comparable to conventional bileaflet valves while reducing hinge-associated flow disturbances

Keywords: Mechanical Heart Valve, Shape Memory Alloy, Fluid-Structure Interaction,

Dynamic Mesh, CFD, Hemodynamics

Authors: Ashraf Zareei











Article Code: icbme-1420

Article Title: Comparative Hemodynamic Analysis of Bicuspid and Tricuspid Aortic Valves Through CFD Simulation

Abstract: 4D-MRI imaging offers dynamic visualization of cardiac blood flow, but its limited spatial resolution can restrict the accuracy of hemodynamic quantification. To address this, we present an integrated framework combining 4D-MRI data with computational fluid dynamics (CFD) simulations to enhance the precision of flow analysis in patient-specific aortic geometries. In this study, 4D-MRI data from a patient with bicuspid aortic valve (BAV) disease were used to reconstruct the aortic anatomy. To reduce computational complexity while preserving physiologically relevant flow features, the geometry was simplified by removing nonessential anatomical structures. Idealized valve models were developed for both BAV and tricuspid aortic valve (TAV) configurations. Importantly, both geometries were reconstructed to represent pre-disease anatomy, enabling comparative analysis of baseline hemodynamic conditions. A hybrid valve model was also created by integrating features from both types of valves. CFD simulations were performed under consistent boundary conditions across all configurations. Key hemodynamic metrics—including wall shear stress, oscillatory shear index (OSI), and velocity fields—were quantified and validated against 4D-MRI measurements, demonstrating strong agreement. Comparative results revealed significant differences in shear stress distribution, OSI patterns, and flow organization between valve types, underscoring the influence of valve morphology on aortic hemodynamics. This integrated CFD-4D MRI approach provides novel, patient-specific insights that may inform clinical decision-making, surgical planning, and valve repair strategies.

Keywords: 4D-MRI, Hemodynamics, Cardiac Biomechanics, Oscillatory Shear Index (OSI), Wall Shear Stress (WSS)

Authors: Taha Samiazar, Mouood Allahyari, Reyhaneh Mosaferchi, Julio Garcia Flores, Nasser Fatouraee











Article Code: icbme-1475

Article Title: Impact of Impeller Blade Number on the Hemodynamic Performance of Specially Designed Mini VAD

Abstract: In recent years, the growing prevalence of cardiovascular diseases has highlighted the demand for advanced mechanical circulatory support devices. Ventricular assist devices (VADs) are among the most effective approaches, as they must provide physiologically adequate flow and pressure while minimizing hemolysis and other blood-related complications. The design challenges include device miniaturization, reduced blood residence time, and minimization of shear-induced blood damage. In this study, we present the design and computational analysis of a centrifugal ventricular assist pump with a novel impeller geometry. The impeller, modeled in CATIA based on centrifugal pump theory, has a diameter of 45 mm, which is approximately 14% smaller than comparable designs reported in previous studies. This reduction in size enables integration into applications with strict spatial constraints, such as implantable VADs. Computational fluid dynamics (CFD) simulations were performed at a rotational speed of 2500 rpm and a target flow rate of 5 L/min to assess hydraulic performance and hemocompatibility. Results demonstrate that the proposed design achieves the physiological requirements for pressure head and flow while maintaining hemolysis within acceptable limits. Furthermore, impellers with fewer blades (4 and 5 blades) exhibited lower shear stress and reduced hemolysis, suggesting improved hemodynamic efficiency and safer blood handling characteristics.

Keywords: Ventricular Assist Device, Centrifugal Pump, Hemolysis, Computational fluid dynamics, Impeller design

Authors: Nasser Alizadeh, Hanieh Niroomand-Oscuii, Farzan Ghalichi











Article Code: icbme-1427

Article Title: Comparative Numerical Analysis of Spiral Geometries for Passive Particle Separation in Microfluidic Devices

Abstract: Micro- and nanoparticles play a critical role in chemical, biological, and industrial processes, where consistent particle size and distribution are essential for reliable performance. Microfluidic devices, or lab-on-a-chip (LOC) systems, have been developed to facilitate particle separation and purification. Among these, passive separation devices are often preferred because they rely solely on fluid flow and channel geometry rather than external forces. Spiral microchannels are widely used in such systems, as their curved design induces secondary Dean flows that enhance particle migration and separation. This study numerically investigates the influence of spiral layout and repetition count on particle separation using the Finite Element Method (FEM). Two spiral layouts, circular and square, were analyzed with 2, 4, and 6 repetitions, while maintaining a constant channel cross-section. The simulations focused on the interaction between inertial lift and Dean drag forces to evaluate flow behaviour and particle trajectories. The findings indicate that the square spiral layout provides more precise and reliable separation of particles with different sizes compared to the circular layout.

Keywords: Microfluidics, Lab-on-a-Chip, Particle Separation, Spiral Microchannel, Inertial Focusing Flow

Authors: Yunes Chakeralhoseini, Mohammad Mahdi Tekiyeh, Mahdi Moghimi Zand











Article Code: icbme-1050

Article Title: Parametric study on the separation of extracellular vesicles in a sheathless spiral microfluidic device

Abstract: Extracellular vesicles which carry biological molecules including proteins, RNA, and DNA are emerging as promising biomarkers for non-invasive diagnostics. There are several conventional techniques such as centrifugation, precipitation, and filtration for the manipulation and analysis of extracellular vesicles. However, conventional methods often suffer from a lack of purity and require dedicated handling of trained personnel. In this study, an inertial microfluidic device is proposed to circumvent several steps and isolate extracellular vesicles from a blood sample. Governing equations of motion and particle trajectories are solved by developing a finite element code. A two-dimensional spiral geometry is designed to passively isolate extracellular vesicles from red blood cells, white blood cells, and platelets by incorporating hemodynamic forces including inertial lift and drag forces. The numerical results indicate that extracellular vesicles could be separated from whole blood sample with nearly 83% efficiency, highlighting its potential for robust isolation of extracellular vesicles

Keywords: microfluidic device, spiral microchannels, extracellular vesicles, particle separation

Authors: Mohhammad Mahdi Abdi, Seyedeh Sarah Salehi











Article Code: icbme-1316

Article Title: Acoustofluidic Separation of Circulating Tumor Cells from Semen via Induced Microvortices

Abstract: Prostate cancer detection often relies on invasive or non-specific methods, prompting the need for alternative diagnostic approaches. In this study, we introduce a microfluidic platform designed to isolate circulating tumor cells (CTCs) directly from seminal fluid by leveraging vortex-induced cell separation. By integrating enclosed horseshoe-shaped structures activated by acoustic streaming, the system creates controlled microvortices that selectively trap CTCs. Sperm cells, due to their smaller size and motility, escape the vortex and are gently carried away by a low flow. Unlike conventional methods, this approach requires no preprocessing or chemical labeling. Semen is chosen as the medium because it provides early biological access to prostate-origin cells. Simulation and experimental results confirm stable vortex formation and efficient CTC separation. This label-free technique allows for rapid, gentle, and high-throughput analysis. The platform offers potential as a non-invasive tool for early-stage prostate cancer screening. Its design provides a new direction for liquid biopsy strategies centered on biophysical cell properties.

Keywords: Acoustofluidics, circulating tumor cells (CTCs), microvortex separation, prostate cancer, seminal fluid biopsy

Authors: Ashkan Behrouzi, Sheyda Nadi, Zahra Saeidpour, Majid Badieirostami











Article Code: icbme-1457

Article Title: Development of a spiral microfluidic platform for predicting reduced mechanical damage in oocyte denudation

Abstract: Infertility affects 1 in 6 couples globally, with a 20% prevalence rate in Iran. IVF and ICSI are the most effective treatments, with oocyte denudation being a critical step. Traditional methods like enzymatic and mechanical denudation often damage oocytes. This study investigates microfluidic technology with spiral geometry as a safer alternative for cell separation. Computational fluid dynamics (CFD) simulations were used to analyze shear stress and particle movement in the microfluidic system. The results showed that the spiral design achieved uniform shear stress distribution, with a maximum shear stress of 180 Pascals, which is within the safe range for oocyte preservation. A flow rate of 1 mL/min was used, simulating experimental conditions. Egg yolk was used to model oocytes, with large and small particles representing oocytes and cumulus cells. The study found that larger particles moved toward the channel wall in higher concentrations, consistent with CFD predictions. The spiral geometry increased contact time between the oocyte and the channel wall, ensuring efficient and safe denudation without the need for enzymatic or mechanical methods. These findings suggest that spiral microfluidic designs hold great potential for improving oocyte denudation, offering a promising alternative to traditional methods in assisted reproductive technologies.

Keywords: Infertility, Oocyte Denudation, Microfluidic Technology, CFD Simulations, Spiral Geometry

Authors: Ehsan Nabati, Maryam Saadatmand











Article Code: icbme-1393

Article Title: Investigation of microbubble motion in a microvessel with various obstructions filled with viscous fluid: A finite element modeling study

Abstract: Microbubbles have emerged as powerful agents in biomedical imaging, targeted drug delivery, and ultrasound-mediated therapies due to their unique acoustic and transport properties. However, their motion within microvessels containing irregular structures remains insufficiently understood, particularly under viscous flow conditions where hydrodynamic and surface tension forces compete. Finite element modeling in COMSOL Multiphysics was used to analyze microbubble dynamics in viscous microvessels. Also, the Rayleigh-Plesset equation was applied to study microbubbles, capturing their radius dynamics under pressure, surface tension, and viscosity. The results reveal that obstruction geometry and position significantly influence microbubble trajectories and deformation, with asymmetrical obstructions inducing lateral migration. Changes in horizontal radius had little effect on bubble morphology. Shear stress analysis showed no consistent trend with vertical radius but indicated a clear increase with larger horizontal radii, where a threefold radius increase nearly doubled the maximum shear stress. During 4 microsecond interval period, the microbubble exhibits oscillatory behavior with a maximum radial displacement of approximately 0.4 µm. These findings provide mechanistic insights into microbubble-obstruction interactions, optimization of microbubble-mediated therapies and microfluidic biomedical device design.

Keywords: Microbubbles, vessel, Computational Simulation, Shear stress

Authors: Mahdi Mirzaei, Afsaneh Mojra











Article Code: icbme-1148

Article Title: High-throughput microfluidic electroporation system using 3D-hydrodynamic focusing

Abstract: Electroporation (EP) is a well-established, non-viral method of gene delivery that transiently permeates the cell membrane in response to high fields of applied electric field. Although a successful method, traditional bulk EP systems have major limitations including uneven distribution of the electric field, limited control over exposure of individual cells, and Joule heating which can limit cell viability. Microfluidics have become a valuable tool to overcome these issues of conventional EP by allowing more precise manipulation of fluid movement, localization of the electrified field, and control over individual cells. In this work, we describe a microfluidic electroporation platform that utilizes three-dimensional hydrodynamic focusing to concentrate cells in a narrow stream of fluid measuring 20 x 20 µm at the center of the channel. The vertical and horizontal sheath flow provides orthogonal flow confinement which provides uniform exposure of each cell to the applied electric field. Our electroporation platform has embedded planar electrodes beneath the sheath layers so that the electric field is localized across the focused cell stream while minimizing direct interaction of the electrodes with the cells. Based on numerical simulations in COMSOL Multiphysics it is predicted that flow confinement is stable; concentration profiles developed appropriately; and electric field strengths will be sufficient and under the optimal electroporation window (300-800 V/cm) at an applied voltage below 2 V. The design will provide consistent exposure times on the millisecond time-scale, which is appropriate for mammalian cell electroporation, while avoiding unwanted effects like Joule heating, electrolysis, and pH changes. In comparison to previously documented devices, the system presented has increased field uniformity, lower operating voltages and has better scalability for ongoing flow processes. These results are indicative of the promise that the combination of 3D hydrodynamic focusing and low-voltage microfluidic electroporation has in furthering intracellular delivery for cell therapy production and drug screening, as well as single cell analyzers.

Keywords: electroporation, 3D-hydrodynamic focusing, microfluidic, transfection, intracellular delivery

Authors: Zohre Nazemi Dehkordi, Ali Abouei Mehrizi











Article Code: icbme-1206

Article Title: Finite Element Modeling of Bare-Tip and Cylindrical Diffusing Optical Fibers for Prostate Cancer Focal Laser Ablation

Abstract: Prostate cancer is the second most frequently diagnosed malignancy among men worldwide and remains a major contributor to cancer-related mortality. Standard whole-gland treatments, such as prostatectomy and radiotherapy, achieve effective cancer control but are often accompanied by significant long-term morbidity. Focal laser ablation (FLA) has emerged as a minimally invasive alternative, offering selective tumor destruction with reduced functional side effects. Optical fiber design plays a decisive role in shaping ablation outcomes: bare-tip fibers provide highly concentrated heating suitable for small lesions, whereas cylindrical diffusing fibers distribute energy more evenly, enabling broader and more uniform coverage. This study employs finite element modeling (FEM) to directly compare these two fiber types under controlled conditions in prostate tissue. A spherical prostate model with bioheat transfer and Arrhenius damage formulations was used to simulate two representative scenarios: a baretip fiber at 0.4 W and a cylindrical diffuser at 1 W with 1 cm emission length. Results demonstrated that the bare-tip fiber generated a sharply localized, teardrop-shaped lesion of ~467 mm³, while the diffuser produced a more symmetric, ellipsoidal lesion with a threefold larger damage volume (~1709 mm³) without excessive local overheating. These findings reveal a fundamental trade-off between precision and coverage. Bare-tip fibers may be optimal for small, well-confined tumors, whereas diffusers provide safer margins for larger or irregular lesions. The FEM framework establishes a foundation for MRI-based, patient-specific planning of FLA.

Keywords: Focal Laser Ablation, Laser Therapies, Prostate Cancer, Minimally Invasive Surgery, Finite Element Method

Authors: Sajjad Saadati Rad, Alireza Mehridehnavi, Seyed Mojtaba Karbalaee











Article Code: icbme-1159

Article Title: Simulation of Mechanical Property Changes in Biodegradable Scaffolds under Various Loading Conditions

Abstract: In tissue engineering, biodegradable scaffolds should provide temporary mechanical support while also being able to control their degrading rates to allow tissue regeneration. However, degradation-driven changes under physiological conditions are largely neglected in the literature on static loading. Here, the authors develop a new multiphysics modeling framework focused on encompassing solid mechanics, mass transport, and chemical degradation in COMSOL Multiphysics to assess the scaffold's performance. A Schwarz cubic minimal surface scaffold with 60% porosity and 200–600 μm pore size was designed with three polymers: polycaprolactone (PCL), polylactic acid (PLA), and poly(lactic-co-glycolic acid) (PLGA). Degradation was modeled with stress-enhanced modified Michaelis–Menten kinetics. Both static (0.1–2.0 MPa) and dynamic (1–10 Hz) loading conditions were tested. The results show a nearly linear behavior on the displacement and von Mises stress, with maximum values 72 μm and 3.17 MPa reached at 200 kPa, respectively, while the total load was 3.17 MPa. The overall response suggests the scaffold will become highly predictive in nature.

Keywords: COMSOL Multiphysics, Biodegradable Scaffolds, Mechanical Loading, Finite Element Analysis

Authors: Elnaz Abedini, Mehdi Mehri











Article Code: icbme-1260

Article Title: Carbon Nanotube Mediated Hyperthermia for Cancer Therapy

Abstract: Carbon nanotube (CNT) mediated hyperthermia has emerged as a promising approach for cancer therapy, offering localized heating with high thermal efficiency. This study presents a computational framework that systematically evaluates the effects of CNT concentration and applied power on tumor temperature distribution and necrosis development. An axisymmetric tumor model incorporating interstitial fluid flow, nanoparticle transport, bioheat transfer, and Arrhenius-based damage assessment was employed. The results demonstrate that increasing CNT concentration and power density significantly elevates maximum tumor temperature (up to 52% increase) and accelerates necrosis onset, reducing the time to irreversible tissue damage from over 1000 s to less than 200 s. However, excessive escalation was shown to extend irreversible necrosis into adjacent healthy tissue, highlighting the delicate balance between treatment efficacy and safety. These findings provide clinically relevant insights that support the optimization of CNT dose and power modulation to achieve effective and safe tumor ablation.

Keywords: Carbon nanotubes, hyperthermia, nanoparticle heating, computational modeling, cancer

Authors: Behnam Zeinali, Afsaneh Mojra











Article Code: icbme-1071

Article Title: Simulation and evaluation of the impact of magnetic source geometry on mechanical stress and magnetic flux distribution in cancerous tumors

Abstract: Cancer is one of the most challenging human diseases, and recent research has shown that bio-magnetic systems can be effective in its diagnosis and treatment by influencing pressure distribution, mechanical stress, and the process of cell death in tumor tissues. These systems, due to their magnetic, optical, non-invasive, and controllable properties, have garnered attention as novel tools in the diagnosis, modeling, and treatment of cancer. This study examines the effect of the shape of the magnetic source on the biological and mechanical parameters of tumor tissue. For this purpose, the magnetic field resulting from sources of various shapes has been numerically simulated, and its effect on stress distribution and tumor tissue behavior has been analyzed. The results indicate that changing the shape of the magnetic source can lead to improved field concentration in the target area, reduced damage to healthy tissues, and increased efficiency in non-invasive treatment. This study could be an effective step in the development of magnetic field-based biomedical engineering methods for targeted cancer treatment.

Keywords: Tumor, Magnetic Properties, Cancer, Magnetic Source, Magnetic Nanoparticles

Authors: Alireza Heydari, Borhan Beigzadeh, Mahdi Halabian, Majid Siavashi











Article Code: icbme-1124

Article Title: Numerical Investigation of the Effectiveness of Cryosurgery on a Liver Tumor

Abstract: Cryosurgery provides a minimally invasive treatment option for selected cancers, notably liver tumors. The treatment includes applying an extremely cold procedure by liquid nitrogen or argon gas to eradicate tumors. Indeed, cryosurgery freezes the tissue, leading to the death of the tumor cells. However, it is possible that some parts of the healthy tissue get damaged undesirably during cryosurgery. In this numerical study, the ideal vessel, cryoprobe, and liver tissue, with proper physical characteristics, are considered with the aim of quantifying and assessing the effectiveness of the surgery. Moreover, we investigate how ice-ball formation affects convective heat transfer in the vessel. Physical characteristics of the tumor were added to the model, which contributed to being as accurate as possible. To evaluate the damage rate of the tumor, four parameters are defined: cryoablation coverage ratio (CACR), volume fraction (VF), tissue damage (TD), and ice ball irregularity (IBI). The effectiveness of surgery is reported by the four mentioned parameters. Ultimately, the temperature distribution, the shape of the eventually formed ice ball, and the amount of thermal damage have been analyzed. Hence, the provided graphs as key results in this investigation illustrate that considering tumor properties leads to lessening evaluation parameters of CACR, VF, and TD by 18%, 5%, and 33%, and raising IBI by 100%, respectively. Also, the VF remains constant in these two states. These methods may be utilized to evaluate the cryosurgery procedure.

Keywords: Cryosurgery, Numerical Simulation, Volume Fraction, Necrotic Tissue, Ice Ball Irregularity

Authors: Taha Samiazar, Mahkame Sharbatdar











Article Code: icbme-1345

Article Title: A vortex-promoting cross-junction microchannel for efficient hydroporation in immunotherapy applications

Abstract: Efficient intracellular delivery of therapeutic biomolecules is a critical challenge in biomedical applications, including cancer immunotherapy, gene therapy, and drug delivery. Hydroporation, a mechanoporation-based microfluidic technique, has emerged as a promising method to transiently permeabilize the cell membrane through controlled hydrodynamic stresses. In this study, we present a novel circular cross-junction microchannel with noncolinear inlets designed to generate a mixed extensional-rotational flow, enhancing both shear and vorticity at lower Reynolds numbers compared to conventional square cross-junctions. Three-dimensional numerical simulations were performed across Revnolds numbers 20-366 to analyze flow behavior, including vorticity distribution, recirculation zones, and vortex formation. The results demonstrate that the circular geometry induces stable vortical structures and a well-defined central stagnation point, enabling simultaneous extensional and torsional deformation of cells. Shear stresses in the circular junction were found to be nearly three times higher than in conventional geometries at comparable flow rates, suggesting potential for highefficiency membrane poration while maintaining cell viability. These findings indicate that the proposed design can achieve enhanced hydroporation efficiency with reduced mechanical stress, offering a scalable platform for high-throughput intracellular delivery. Future experimental validation and further optimization of junction geometry may expand its applicability to diverse cell types and therapeutic cargos.

Keywords: hydroporation, cross-junction, intracellular delivery, fluid dynamics, vortex, nanomaterial delivery

Authors: Soheil Mahdavi, Zohre Nazemi Dehkordi, Ali Abouei Mehrizi











Article Code: icbme-1334

Article Title: Microfluidic Flow-Focusing Systems for Alginate Microcapsule Preparation: Tuning Droplet Size and Frequency

Abstract: Microencapsulation is an efficient method for protecting unstable compounds in chemical environments and has wide applications in medicine and tissue engineering. In this study, the formation of alginate microgels in a microfluidic flow-focusing device was numerically simulated using COMSOL Multiphysics 6.3 based on the Level-Set method. The results demonstrated that wall contact angle, flow rate of the phases, and the junction angle of the channels (30°, 60°, 90°, and 120°) significantly affect droplet size and generation frequency. Superhydrophobic channels ($\theta = 150^{\circ}$) facilitated stable W/O droplet formation, while hydrophilic walls failed to produce droplets. Increasing the dispersed phase flow rate (Od) led to larger droplets and plug flow, whereas increasing the continuous phase flow rate (Qc) reduced droplet size due to enhanced shear stress. Overall, the simulation results indicate that the junction angle directly governs the balance between viscous shear forces and interfacial tension. Narrower angles favor shear-dominated breakup with smaller, more monodisperse droplets, whereas wider angles shift the mechanism toward pressure-driven pinch-off, producing larger droplets with lower throughput. Therefore, the channel intersection angle serves as an effective design parameter for tuning droplet size distribution and generation rate in microfluidic systems.

Keywords: Microfluidics, Droplet generation, Flow-focusing, Alginate microdroplets, Level-Set method, Junction angle, Two-phase flow, Numerical simulation

Authors: Meisam Akbari Laleh, Yasaman Pahlevanzadeh, Mina Shafiei, Javad Rahbar Sharouzi











Article Code: icbme-1416

Article Title: Optimization of an Integrated Filter Photometric system and a Centrifugal Microfluidic System for Biochemical Analysis

Abstract: Microfluidic systems are rapidly advancing, particularly when integrated with medical science to enhance laboratory services. Key benefits of microfluidics, such as portability, the ability to multiplex several tests, and low reagent requirements, create a broad research area, especially in laboratory detection systems. Photometer-based analyzers are the most common detectors for medical tests, including absorbance and fluorescence-based detectors that cover a wide range of detection analyses. This study aimed to develop an optimized centrifugal microfluidic system integrated with a custom vertical filter-photometer. The compact design, which incorporates miniaturized filters and lenses, was engineered to achieve a precision and accuracy comparable to commercial autoanalyzers. For this purpose, a centrifugal microfluidic device was designed and optimized with a focus on siphon channel actuation for biochemical analysis. Human serum samples, with previously analyzed biomarker data, were obtained from the Parseh lab. To validate the microfluidic and the optical setup's functionality, three common metabolic tests were selected: glucose, triglycerides, and cholesterol. Human serum was injected into the disc, and the subsequent analysis, along with the calibrator test, was performed on the same disc. The results of light absorbance for these tests on disc microfluidic using the optical setup showed a high correlation (R² above 0.99 for all three tests) with the reported results from the Parseh lab, which served as the reference. Finally, to minimize the bias observed between our results and the reference results, an algorithm was developed to predict optimized data for new tests. Based on the findings, this filter photometer setup has the potential to be enhanced with additional filters for comprehensive biochemical tests analyzed through optical absorbance systems, and along with optimized microfluidic devices, can be introduced for POCT systems.

Keywords: Filter photometers, POCT, Centrifugal microfluidics, Siphon valves, Biochemical markers

Authors: Bahareh Mohammadi Jobani, Amin Dehghan, Zahra Shahsavari, Esmail Pishbin











Article Code: icbme-1188

Article Title: Skin Thermomechanical Modeling: Assessing the Influence of Water and

Ambient Air

Abstract: Skin burn is one of the dangerous incidents that threatens human life on a regular basis. In this study, a thermomechanical model is developed to simulate skin burn by utilizing a multilayer three-dimensional framework of skin that includes the stratum corneum, epidermis, dermis, and subcutaneous tissue. The Pennes model describes bioheat transfer of the tissue. Linear elasticity was utilized for defining skin mechanics. Thermal expansion was incorporated to define the coupling between heat transfer and skin mechanics. In order to investigate the skin cooling response, the influence of ambient air and water on temperature distribution and mechanical response of the skin were analyzed. The findings revealed that that heating causes the top layers of the skin to increase in temperature, but has a minimal impact on the temperature increase of the subcutaneous tissue. Moreover, when water was employed for cooling, the temperature of the skin surface reduced significantly in comparison to the case where ambient air was used. The mechanical behavior illustrated the significant effect of temperature on thermal response. The presented thermomechanical model provides readily implementation with straightforward reproducibility.

Keywords: Bioheat transfer, Thermal stress, Thermomechanical coupling, Burn treatment, Biothermomechanics, Computational biomechanics

Authors: Pezhman Namashiri, Akbar Allahverdizadeh, Fatemeh Khodadoost, Farid Vakili Tahami











Article Code: icbme-1142

Article Title: Multi-Objective Optimization of the Impeller of a mini Blood Pump: Balancing Outlet Pressure and Scalar Shear Stress

Abstract: Cardiovascular diseases are one of the primary causes of mortality globally, and blood pumps along with ventricular assist devices play a crucial role in advanced medical care. To overcome limitations of prior studies, namely the small number of geometric parameters and single objective optimization, we present a hybrid framework that integrates response surface methodology, a neural network surrogate, and a multi objective genetic algorithm to design the impeller of a small blood pump at a specified operating point. Fifteen geometric parameters were varied and 290 computational simulations were performed to construct the database and train the surrogate. The optimization objectives were to maximize outlet pressure and to keep the mean scalar shear stress at 50 Pa.Compared with the baseline impeller, the optimized design achieved a 6-7% increase in outlet pressure and about a 15% increase in static head, while the mean wall shear stress decreased by about 17% and the hemolysis index dropped by nearly 50%. The optimized blade reduced high-shear stress near the leading edge, yielded a more uniform shear field, and exhibited smoother pressure growth and weaker jet-wake structures, indicating more uniform blade loading, better pressure recovery, and lower mixing losses. The neural network correctly captured the improvement trends but showed a modest discrepancy: it overestimated outlet pressure by about 13% and underestimated the shear-stress reduction by about 19% relative to simulation-verified values. Overall, the proposed framework simultaneously improves hydraulic performance and hemocompatibility and offers a practical route for multi-objective optimization of small blood-pump impellers.

Keywords: Blood pump, Computational fluid dynamics, Optimization, Response Surface Methodology, Multi-Objective Genetic Algorithm

Authors: Reza Sahebi-Kuzeh kanan, Hanieh Niroomand-oscuii, Habib Badri Ghavifekr, Farzan Ghalichi











Article Code: icbme-1183

Article Title: Non-Invasive Detection of Atherosclerosis and Aneurysm via Electrical

Impedance Spectroscopy: A Finite Element Simulation Study

Abstract: Atherosclerosis and aneurysm are among the most dangerous and well-known diseases of the cardiovascular system, causing 19.8 million deaths in 2022, of which 85% died due to heart attack or stroke. Therefore, early detection of these conditions can play a significant role in preventing their various complications. In this study, electrical impedance spectroscopy (EIS) was used as a non-invasive method for diagnosing both diseases. The primary objective of this paper is to assess the discriminative capability of EIS between normal tissue, atherosclerotic tissue, and aneurysmal tissue, as well as to investigate how changes in geometric parameters in these two pathological types affect the tissue's impedance response. For this purpose, a three-dimensional model of healthy and diseased tissues was developed using COMSOL software. The results showed that diseased tissues exhibit distinct impedance characteristics compared to normal tissue; Significant increases in electrical impedance are observed in atherosclerosis, while decreases are seen in aneurysm, which are among the identified features. Overall, findings from this study indicate that electrical impedance spectroscopy can be used as a complementary, rapid, cost-effective, and real-time method for detecting both atherosclerosis and aneurysms. Furthermore, accurate numerical modeling can serve as a valuable tool for the initial design of EIS-based diagnostic devices.

Keywords: Atherosclerosis, Aneurysm, Cardiovascular Diseases, Finite Element Simulation, Electrical Impedance Spectroscopy, Non-invasive Diagnosis.

Authors: Shaghayegh Shokri - Rasool Baghbani - Masoomeh Ashoorirad











Article Code: icbme-1283

Article Title: In silico Evaluation of a High-Porosity Titanium Scaffold in a Bioreactor for Bone Tissue Engineering Applications: A Fluid Transport Study

Abstract: This study involves the design and testing of a titanium scaffold with very high porosity, aiming to de- termine its suitability as a bone tissue engineering sub- strate. The structure is based on a modified body-centered cubic (BCC) unit cell with an added vertical strut to im- prove strength while preserving open space. The model was created in Rhinoceros® 3D and achieved a poros- ity of approximately 93.5%, which is a value within the upper range typically reported for bone scaffolds. To understand how this design would behave, a fully coupled fluid-structure interaction (FSI) simulation was per- formed. The scaffold material was modeled as linearly elastic Ti6Al4V and the surrounding fluid as a Newtonian perfusion medium. The results showed very low inter- nal stresses from the flowing fluid (peak von Mises stress ≈ 6.62 kPa) with almost no deformation, confirming that the scaffold maintains its shape under typical perfusion conditions. The flow remained efficient and mostly lami- nar; the average velocity was 1.41 mm/s, within the os- teogenic range 0.16-1.66 mm/s, with local peaks up to 2.7 mm/s in channels aligned with the flow. Overall, the scaffold proposed here will have a mechanical integrity and will have an efficient nutrient transportation at the same time. Such combination makes it encouraging both in re- gard to implants and in regard to bioreactors intended to grow an extra tissue in vitro.

Keywords: Atherosclerosis, Aneurysm, Cardiovascular Diseases, Finite Element Simulation, Electrical Impedance Spectroscopy, Non-invasive Diagnosis.

Authors: Elnaz Khorasani - Setareh Garazhian - Bahman Vahidi











Article Code: icbme-1428

Article Title: Programmable Flow Control in Rotating Microfludic Systems using elastic patch valves

Abstract: We present a compact elastic patch valve (EPV) for centrifugal Lab-on-a-Disc (LoaD) that achieves accurate, fully passive flow control without the need for pneumatic, electrical, or magnetic actuation. The valve is realized as a multilayer PMMA- SILICONadhesive -PMMA stack fabricated through cleanroom-light, rapid-prototyping steps that are compatible with low-cost manufacturing. To evaluate valve performance, we systematically investigated three primary design parameters: source-reservoir volume, radial placement on the disc, and SILICON membrane thickness. Standardized rotation protocols and image-based evidence (disc photographs and time-lapse frames) were employed to compare flow initiation, closure, and stability. The results demonstrate that opening behavior is largely independent of reservoir volume once proper priming is achieved. Placement at larger radii consistently reduced the opening threshold and enabled earlier, more robust flow initiation, while variations in membrane thickness strongly influenced actuation sensitivity: thicker membranes required higher rotational input, whereas thinner membranes opened more readily yet reseated cleanly. Across multiple discs and repeated cycles, the valve exhibited reproducible operation, remained leak-free at rest, and delivered reliable sequencing from semi-open restriction to complete reservoir transfer. Collectively, these findings establish a practical design window—outer-half radial positioning, mid-range volume, and intermediate membrane thickness—that enables programmable on-disc fluid transport, mixing, separation, and washing using rotation alone, without external hardware.

Keywords: Atherosclerosis, Aneurysm, Cardiovascular Diseases, Finite Element Simulation, Electrical Impedance Spectroscopy, Non-invasive Diagnosis.

Authors: Zohreh Mohammadi Zadeh - Amin Dehghan - Esmail Pishbin - Mahdi Navidbakhsh











Article Code: icbme-1081

Article Title: Finite Element Analysis of Mechanical Stability in Hip Joint Implants: A Comparative Study of Ti-6Al-4V and Ti-13Nb-13Zr Alloys

Abstract: In this study, stress and displacement analysis of a titanium hip joint implant was conducted using the Finite Element Method and the Abaqus software. The objective was to examine the effect of design and material composition on the mechanical performance of the implant. The implant design included a solid model created using SolidWorks software. For the simulation, two titanium alloys, TI_6AL_4V and TI_13NB_13ZR, were used, which are suitable for medical applications due to their high biocompatibility. After designing, meshing, and applying boundary conditions and loading similar to walking conditions, the process was completed. The results of relative displacement showed that both materials have displacement values within the permissible range (40 to 150 micrometers), which is beneficial for proper bone growth. In terms of stress distribution, the TI_13NB_13ZR alloy showed better performance compared to TI_6AL_4V. Ultimately, the design with the material TI_13NB_13ZR was introduced as the best option because it generates the least displacement and the lowest stress concentration. Unlike previous studies that overlooked the femoral implant head, this research incorporates its design and analysis, providing a more realistic simulation of implant—bone interaction.

Keywords: Finite element analysis, Titanium alloy, Mechanical strength, Femur, Hip joint implant, Stress distribution, Relative displacement

Authors: Mohammad Amin Parsaei Tashi - Mohammad Hagh Panahi











Article Code: icbme-1120

Article Title: Design and Biomechanical Comparison of a Patient-Specific Anatomical Plate Versus Conventional Plate for Distal Humerus Fractures: A Finite Element Analysis

Abstract: Distal humerus fractures are clinically challenging due to anatomical complexity and complications. In this study, a new anatomical plate was designed and compared with a conventional plate for B1-type distal humerus fractures using finite element analysis. A CTderived 3D humerus model of a 37-year-old female was developed with heterogeneous bone material properties. An anatomically contoured plate was digitally designed to match bone contours and compared with a conventional locking plate under tensile and compressive loadings (100 N). Stress, strain, and displacement analyses revealed similar peak stresses in both designs, while the conventional plate had higher stress near the fracture site. In cancellous bone, the anatomical plate model demonstrated double the stress magnitude compared to the conventional plate, suggesting more effective load transfer. The anatomical plate exhibited reduced strain, whereas cancellous bone showed higher strain within the 100-2000 microstrain range optimal for secondary bone healing. Significantly, despite higher overall hardware displacement, the anatomic plate caused less fracture interface displacement than the conventional plate. This counterintuitive result supports new fracture biomechanics concepts, showing that semi-rigid fixation promotes better healing conditions. The anatomical plate's ability to maintain fracture reduction with controlled micromotion may improve outcomes. supporting anatomically contoured designs for complex periarticular fractures.

Keywords: Biomechanical characteristics, conventional plate, Distal humerus fracture, Finite element method (FEM), Fracture stability, Patient-specific anatomical plate

Authors: Fahime Rezazade - Azadeh Ghouchani - Maryam Amoochi











Article Code: icbme-1132

Article Title: The Influence of Insertion-Induced Prestress and Viscoelastic Properties in Fixational Stability of Pedicle Screws in UHWMPE block: A Finite Element Study

Abstract: Pedicle screws are critical components in spinal fixation systems, and the stiffness of the screw-bone interaction plays a crucial role in implant success. There are various ways to investigate screw-bone bonding strength, one of which is vibration-based diagnosis of screwbone structure. While finite element modeling can reduce the time and give the ability to model different geometries and other conditions, properly modeling the vibration behavior of the screw inside the bone comes with difficulties. This study investigates the influence of insertioninduced prestress and the viscoelastic properties of ultra-high molecular weight polyethylene (UHMWPE) bone-analog material on the natural frequency of a pedicle screw-block assembly using finite element analysis (FEA). Three models were developed: Model I (linear elastic without prestress), Model II (linear elastic with prestress), and Model III (viscoelastic without prestress). A 3D geometry of the screw and UHMWPE block was constructed, and frequency analysis was performed at three insertion depths (10 mm, 20 mm, and 30 mm). Simulation results were compared with previously published experimental data. Model I underestimated the natural frequency at all depths around 14-30%, while Model II, accounting for screw insertioninduced radial prestress, improved prediction accuracy, reducing errors down to under 18%. Model III, which captured UHMWPE's viscoelastic behavior using a Prony series, showed the closest agreement with experimental data, with errors under 7%. The results highlight the importance of modeling both viscoelasticity and insertion-related prestress to accurately predict dynamic behavior. These findings are useful for improving finite element modeling of modal analysis methods to investigate screw stability in spinal implants.

Keywords: Finite element analysis, Natural frequency, Modal analysis, Pedicle screw, UHMWPE, Viscoelasticity, Prestress, Prony series.

Authors: Ahmad Babazadeh Gh - Mohammadjavad (Matin) Einafshar - Ata Hashemi











Article Code: icbme-1169

Article Title: Finite Element Analysis of Spine ProDisc-L Using Titanium, CFR-PEEK and CoCr Endplates with UHMWPE-GUR1020 75kGy RM Core

Abstract: Degenerative disc disease (DDD) frequently affects the L3-L4 segment and may be treated with total disc replacement (TDR). We built a patient-specific L3-L4 finite element model to evaluate ProDisc-L endplates made from Ti-6Al-4V, CFR-PEEK, or CoCrMo paired with an ultra-high-molecular-weight polyethylene (UHMWPE-GUR 1020, 75 kGy) core. Under 150 N preload and 10 N·m flexion, extension, right lateral bending, and left axial rotation, we computed von Mises stresses in bone, plates, and core. Compared to the standard CoCrMo-UHMWPE configuration, the Ti-6Al-4V endplate with UHMWPE-GUR RM core reduced endplate stress by up to 19% for example from 46.64 MPa to 43.97 MPa in bending and core stress by up to 54% for example from 31.94 MPa to 14.96 MPa in extension, while maintaining bone stress within acceptable limits. When compared to CFR-PEEK-UHMWPE GUR RM with Ti-6Al-4V-UHMWPE GUR RM decreased endplate stress by about 5% like 46.23 MPa to 43.97 MPa and core stress by approximately 27% by 17.85 MPa to 13.13 MPa in bending. These improvements indicate that the Ti-6Al-4V and UHMWPE-GUR RM combination more effectively minimizes stress concentrations, enhances load transfer and suggests reduced wear, which may potentially contribute to improved implant longevity. In conclusion, this configuration may represent a biomechanically favorable option for TDR and could potentially improve long-term outcomes, although in vivo studies are required to confirm these findings.

Keywords: Artificial lumbar disc Total disc replacement Finite element analysis Biomechanics Prodisc-L Von mises stress

Authors: Amirali Kashani - Siavash Kazemirad











Article Code: icbme-1187

Article Title: Screws That Hold: Stability Analysis of Distal Tibial Fractures Using FEA and a Novel Fixation Index

Abstract: The biomechanical stability of fracture fixation plays a critical role in postoperative recovery and long-term functional outcomes. This finite element (FE) study compared three screw-based fixation methods for distal tibial fractures, following the AO Surgery Reference guidelines. Patient-specific tibial anatomy was reconstructed from routine clinical CT scans using Mimics software, and fracture models were created to represent a standard extra-articular distal tibial fracture. Each fixation configuration was assessed under physiologically relevant loading conditions. Von Mises stress distributions were calculated for both the intact tibial segment and the fracture fragment, as well as for the fixation screws, In addition, strain and displacement values were determined for each configuration. To provide a single comparative measure, a novel Fixation Stability Index (FSI) was introduced, defined as the product of mean bone stress and strain divided by the maximum fragment displacement. Results showed that medial malleolar split intra-articular fracture yielded the highest FSI (3.77), indicating superior stability, while transverse simple extra-articular fracture had the lowest (1.0). Peak screw stresses were lowest in lateral tibial split intra-articular fracture (61.8 MPa), suggesting reduced implant fatigue risk. Maximum fragment displacement ranged from 0.39 mm to 10.7 mm, and strain distributions were consistent with observed stress patterns. These findings suggest that the FSI provides an effective and quantitative approach for comparing fixation strategies in FEbased orthopedic biomechanics. Incorporating such parameters into preoperative planning may improve fixation choice and enhance patient-specific outcomes.

Keywords: distal tibia fracture, finite element analysis, fixation stability index, screw fixation, biomechanics

Authors: Amirhossein Karami - Mohadese Rajaeirad - Mohamed Elfekky - Nima Jamshidi











Article Code: icbme-1212

Article Title: Role of Protective Pads in Mandibular Biomechanics During Frontal Impact

Abstract: Mandibular fractures are common maxillofacial injuries, frequently resulting from sports, traffic accidents, and violence. Despite advancement in protective strategies, the role of external protective pads in mitigating impact forces to the mandible remains underexplored.

This study develops a computational model of the human jaw to evaluate the biomechanical effectiveness of expanded polystyrene pads in reducing stress concentration during frontal impact. A 3D finite element model of the lower jaw was constructed using high-resolution computed tomography data and assigned density-based heterogenous material properties to it. The mandible was subjected to a frontal impact under three configurations: no protective pad, with a 19mm EPS pad and with a 31mm EPS pad.

Results demonstrated that both EPS pads reduced impact severity. Compared to the unprotected model, the peak impact force decreased by approximately 67% and 71%, respectively, with the 19 mm and 31 mm foams. Maximum first principal stress was reduced from 404 MPa for unprotected mandible to 170 MPa, and 158 MPa for mandibles with EPS foam thicknesses of 19 and 31 mm, respectively.

This research indicated that the application of EPS foam led to an extended impact duration with a reduced peak force, thereby decreasing stress on the mandible. Incorporating a shockabsorbing EPS layer significantly mitigates the risk of mechanical injury during frontal impacts.

Keywords: Mandibular fracture Finite Element Analysis Injury Prevention Impact Expanded Polystyrene foam

Authors: Hosna Olfati - Ata Hashemi











Article Code: icbme-1228

Article Title: Patient-Specific TMJ Implants: A Finite Element Study on Placement and Material Effects

Abstract: The ultimate functional lifespan and clinical efficacy of total TMJ replacements are fundamentally reliant on the structural integrity of the implant and the physiological distribution of forces between the device and the recipient bone. The mechanical performance is primarily dictated by two principal factors: the precise spatial positioning of the implant and the inherent mechanical characteristics of its constituent material. This FEA-based computational investigation sought to quantify and contrast the influence of implant positioning and material selection on the resulting stress fields and overall mechanical resilience of the TMJ reconstruction. A patient-specific total TMJ prosthesis was designed and integrated into a 3D mandibular model reconstructed from high-resolution CT scan data. Two materials were considered: Titanium alloy (Ti-6Al-4V) and Polyetheretherketone (PEEK). For each material, three positioning scenarios were defined: (1) an ideal anatomical reference position, (2) a 2 mm lateral displacement, and (3) a 3 mm medial displacement. The bone-prosthesis assemblies were analyzed in Abagus under a static chewing load of 262.28 N. The results showed that prosthesis positioning significantly impacts the stress distribution pattern. For the titanium model, the lateral position was identified as providing the best combination of mechanical stability (lowest displacement) and host bone protection (lowest bone stress, 90.74 MPa), a configuration that mitigates the risk of fixation failure. Material comparison showed that Titanium (Ti-6Al-4V) implants provided superior stability (lower displacement), whereas PEEK implants, possessing an elastic modulus closer to that of bone, facilitated a more physiological load transfer and mitigated the stress shielding effect. Consequently, the optimal material decision must be patient-specific, balancing the immediate requirement for maximal mechanical stability against the crucial need for long-term host bone viability.

Keywords: Temporomandibular Joint, Finite Element Analysis, Patient-Specific Prosthesis, Stress Distribution, PEEK, Titanium

Authors: Aryana Tavakoulnia - Mohadese Rajaeirad - Nima Jamshidi - Sandipan Roy











Article Code: icbme-1306

Article Title: Cancer-Associated Actin Mutations Enhance Cofilin Binding Affinity: Insights from Steered Molecular Dynamics Simulations

Abstract: Cofilin plays a fundamental role in remodeling of the actin cytoskeleton by binding to actin filaments and facilitating their severing and depolymerization. Alterations in cofilinactin interactions due to actin mutations have been implicated in various cancers, including skin cancer. This study investigates the binding affinity of cofilin to both wild-type (WT) and mutant actin (D288N, G168N, R63Q) using steered molecular dynamics (SMD) simulations. Structural models were constructed and subjected to constant velocity pulling to measure maximum rupture forces and interaction energies. Results demonstrate that all three cancer-associated mutations exhibit increased rupture forces and more negative total energy compared to WT. indicating stronger binding affinities. Notably, the R63Q mutation produced the highest rupture force and most favorable interaction energies, suggesting a significant stabilizing effect on the actin-cofilin complex. Results indicate that R63O increases force-dependent mechanostability at the cofilin-actin interface. This can be leveraged to (i) provide a stabilized control for biochemical and single-filament severing assays and (ii) guide interface-targeted modulators that tune cofilin activity to control filament turnover. These findings provide critical insight into the molecular effects of oncogenic actin mutations and their potential role in cytoskeletal dysregulation during cancer progression.

Keywords: Actin Mutations, Cofilin, Steered Molecular Dynamics (SMD), Interaction Energy, Binding Affinity

Authors: Danial Sedighpour - Farzan Ghalichi - Iman Zoljanahi Oskui











Article Code: icbme-1308

Article Title: Implementation of Anisotropic Hyperelastic Materials in NL-SBFEM

Framework: The HGO Model

Abstract: This paper presents the first implementation of anisotropic hyperelastic materials within the NL-SBFEM framework. The Holzapfel-Gasser-Ogden (HGO) model is integrated through the modular material interface to capture fiber-reinforced tissue behavior. Validation against ABAQUS shows excellent agreement with errors below 2% across different fiber orientations. Parametric studies demonstrate the framework's ability to capture complex anisotropic responses including fiber dispersion effects and nonlinear stiffening behavior. The modular architecture enables future extensions to other anisotropic models and establishes NL-SBFEM as a viable alternative for biomechanical applications requiring boundary-only discretization.

Keywords: NL-SBFEM, Hyperelastic Materials, HGO Model, Anisotropy, Biomechanics

Authors: Seyed Sadjad Abedi-Shahri - Farzan Ghalichi - Iman Zoljanahi Oscui











Article Code: icbme-1355

Article Title: Ultimate Failure Load of Plate-Based Fixation and a Suture Anchor for Rotator Cuff Repair Across Polyurethane Bone Densities

Abstract: Early after rotator cuff repair, the tendon-bone interface is weak; robust time-zero fixation is therefore required to resist oblique loading. To evaluate the time-zero fixation strength of a plate-based approach versus a commercial suture anchor across synthetic cancellous bone densities. Twenty-four tests (four for each combination of method and density) were performed on rigid polyurethane foam blocks with densities of 10, 12, and 15 PCF according to ASTM F1839. The investigational plate-based fixation (AP) and a 4-mm suture anchor (SA) were set up on a custom fixture and pulled to failure at an oblique angle of one hundred twenty degrees under displacement control at one millimeter per second. The primary outcome was the ultimate failure load, defined as the first peak followed by an abrupt drop in load. Independent t-tests were used to compare methods within each density. Mean ultimate failure load for SA was 160 N at 10 PCF, 225 N at 12 PCF, and 400 N at 15 PCF. Mean ultimate failure load for AP was 392 N at 10 PCF, 449 N at 12 PCF, and 455 N at 15 PCF. AP exceeded SA within each density (10 PCF: p less than 0.0001; 12 PCF: p equal to 0.0003; 15 PCF: p equal to 0.0217). Within AP, increasing density from 10 to 12 PCF raised the mean ultimate failure load by about 56 N (p equal to 0.0240); increasing from 12 to 15 PCF did not produce a notable change (p equal to 0.7569). Failures were predominantly anchor pull-out for SA and tape rupture at plate holes for AP; surface indentation beneath the plate was most apparent at 10 PCF. Under a conservative oblique pull of one hundred twenty degrees, the plate-based method provided higher time-zero strength than a suture anchor across 10, 12, and 15 PCF, with the greatest margin at lower density. These density-resolved data may help guide fixation choice when bone quality is limited, pending confirmation under cyclic loading and in cadaveric and clinical studies.

Keywords: Rotator cuff repair; Suture anchor; Plate-based fixation; Synthetic cancellous bone; Ultimate failure load.

Authors: Parviz Ahangar - Solmaz Mojadam Mofrad - Amir Nourani - Amirhasan Amini - Erfan Ahmadpour Joeini - Mohammad nasir Naderi











Article Code: icbme-1362

Article Title: Topology Optimization for Optimal Design of Human Tibial Fixation Plates toward Improving Biomechanical Compatibility

Abstract: Stress shielding is one of the main challenges of using bone fixation plates, caused by the stiffness mismatch between the metallic plates and the natural bone. The goal of this study is to reduce the overall stiffness of tibial fixtures through topology optimization and design of experiments. Effects of four parameters, the number of holes, the hole diameters, the loading condition, and the volume reduction, on the overall stiffness of a tibial fixation plate are investigated using finite element analysis combined with Plackett–Burman and Taguchi design methods. The results show that the loading condition and volume reduction are the most influential factors, while the number and diameter of the holes are less critical. The optimized design, with eight holes, hole diameters of 11 and 13.5 mm, under compressive screw-hole loading, and a 45% volume reduction, achieved an equivalent elastic modulus of 5975 MPa, with a maximum stress well below the titanium yield stress. These results suggest that topology optimization can be used effectively for reducing the stress shielding and improving the biomechanical compatibility of fixation plates.

Keywords: Stress Shielding, Fixation Plates, Tibia, Topology Optimization, Design of Experiments

Authors: Aida Ahmadi - Taha Goudarzi











Article Code: icbme-1377

Article Title: Optimization of the Mechanical Properties of PVA/Gelatin Hydrogel Reinforced with Polycaprolactone Nanofibers Using the Finite Element Method

Abstract: Damage to articular cartilage poses a significant clinical challenge due to its limited self-repair capacity. This study addresses the mechanical inadequacy of hydrogels for load-bearing applications by developing a composite scaffold. Poly(\varepsilon-caprolactone) (PCL) nanofiber-reinforced polyvinyl alcohol/gelatin (PVA/Gelatin) hydrogels were fabricated and mechanically characterized. An inverse finite element (FE) analysis coupled with an optimization algorithm was employed to calibrate an anisotropic Holzapfel hyper-viscoelastic constitutive model against experimental stress-relaxation data. The optimized material parameters, including those for fiber reinforcement and matrix properties, were successfully identified. The FE model demonstrated excellent predictive capability for the scaffold's mechanical response. The results confirm that PCL nanofiber reinforcement effectively tailors the hyper-viscoelastic properties of the PVA/Gelatin hydrogel, making it a highly promising scaffold candidate for articular cartilage repair.

Keywords: Articular cartilage hydrogel hyper-viscoelastic finite element

Authors: Mohadeseh Nazouri - Iman Zoljanahi Oskui - Hadi Taghizadeh











Article Code: icbme-1379

Article Title: Evaluation of Primary Stability of Dental Implants in Synthetic and Natural

Bone: A Comparative Study

Abstract: Rigid polyurethane (PU) foam, commonly referred to as synthetic bone, is widely used in orthopedic and dental implant research due to its uniform properties and ease of use and handling. However, its ability to accurately represent natural bone behavior remains a subject of debate. The aim of this study was to evaluate if PU foam produces comparable primary stability outcomes to those of natural bone. Forty implants from two manufacturers, i.e., Cowellmedi and DRI, with identical dimensions (4 mm diameter × 10 mm length), but different thread and conical designs, were inserted into PU foam blocks (0.2 g/cm³) and also into fresh bovine ribs. Primary stability was assessed using maximum insertion torque (MIT) and resonance frequency analysis (RFA), the latter of which provides implant stability quotient (ISQ). The findings revealed that in natural bone, Cowellmedi implants demonstrated significantly higher MIT compared to DRI, but ISO values did not differ significantly. In contrast, in synthetic bone, both MIT and ISO showed no significant differences between Cowellmedi and DRI implants. These findings highlight that PU foam may not always replicate outcomes observed in natural bone, likely due to different mechanical characteristics and behavior of natural- and synthetic bone. While PU foam remains valuable for controlled testing due to its homogeneity, natural bone surrogates, such as bovine rib, can provide more reliable insights into dental implant performance.

Keywords: Dental implants, Primary stability, Polyurethane foam, Bovine rib, Maximum Insertion torque, Resonance frequency analysis, Implant stability quotient

Authors: Mahdi Farrokhi Kashtiban - Gholamreza Rouhi











Article Code: icbme-1390

Article Title: Biomechanical Contrast Between Native and Decellularized Triple-Negative Breast Tumors in Mice

Abstract: Triple-negative breast cancer (TNBC) is an aggressive subtype that does not have any targeted receptor-based therapies available, for which the 4T1 cell line-based murine model hosted in BALB/c ("Bagg Albino") mice offers a viable syngeneic model. In this work, we provided a comparative assessment of the structural and mechanical properties of native and decellularized tumors induced by the 4T1 cell line (hereafter referred to as 4T1 tumors). Hematoxylin and eosin (H&E) images visually confirmed successful removal of nuclear content with maintenance of the architecture of the cross-linking throughout the extracellular matrix (ECM). Scanning electron microscopy (SEM) displayed hierarchical ultrastructure, with fibrous and porous morphology preserved after decellularization. Atomic force microscopy (AFM) nano-indentation testing illustrated a significant reduction in stiffness following decellularization: the native 4T1 tumor exhibited a mean Young's modulus of 71.3 ± 19.7 kPa, whereas the decellularized ECM measured 10.5 ± 8.6 kPa. This ~7-fold decrease highlights the role of cellular components in conferring tumor rigidity while confirming the preservation of ECM scaffolds. The normality test (Lilliefors) showed p = 0.0181 for native tumor samples and p = 0.0010 for decellularized samples, indicating that data may not be normally distributed (p < 0.05). AFM indentation was performed using a quadratic pyramid probe. Tumors were generated in 8 BALB/c mice, of which 4 samples were subsequently decellularized for analysis. These findings validate the feasibility of decellularized 4T1 tumors as biomimetic scaffolds for studying tumor-stroma interactions, mechanobiology, and therapeutic modeling.

Keywords: 4T1 tumor, triple-negative breast cancer (TNBC), decellularization, extracellular matrix (ECM), atomic force microscopy (AFM), tissue stiffness, tumor microenvironment

Authors: Mohammad Javad Farjam - Saman Asadi - Ashkan Azimzadeh - Saeid Amanpour - AbdolMohammad Kajbafzadeh - Mohammad Ali Nazari











Article Code: icbme-1417

Article Title: Ensemble Learning–Based Surrogate Models for Non-Invasive Estimation of Corneal Mechanical Properties

Abstract: Accurate estimation of corneal mechanical properties is essential for advancing ocular biomechanics and improving the diagnosis of diseases like keratoconus. Conventional inverse finite element methods are often limited by their high computational cost and time requirement. In this study, surrogate models based on Random Forest, XGBoost, and LightGBM were developed to predict third-order Ogden material parameters from simulated corneal apex displacement data. Model performance was rigorously evaluated through mean squared error (MSE), coefficient of determination (R²), and a physics-informed stress–stretch error metric. The results demonstrated strong predictive accuracy in capturing the cornea's mechanical behavior. Among the models, XGBoost achieved the closest match to the mechanical response, Random Forest provided robust overall accuracy, and LightGBM offered the fastest training. This machine learning-based approach effectively bridges the gap between clinical measurement data and intricate biomechanical properties, offering a fast, reliable, and non-invasive alternative to traditional inverse FEM methods.

Keywords: Cornea, Inverse Problem, Machine Learning, Surrogate Modeling, Random Forest, XGBoost, LightGBM, Ogden Material Model

Authors: Seyed Sadjad Abedi Shahri - Mitra Baradari - Iman Zoljanahi Oskui











Article Code: icbme-1472

Article Title: Finite Element Analysis of Polyoxymethylene Hemostatic Clips: Stress

Distribution and Hinge Geometry Optimization

Abstract: Uncontrolled intraoperative bleeding remains a critical surgical challenge. Polyoxymethylene (POM) hemostatic clips are radiolucent and easy to handle, yet hinge-centric stress concentrations can jeopardize their reliability, and quantitative design-level evidence remains limited. We assess how hinge geometry governs the mechanical response of POM clips using nonlinear finite-element analysis (FEA) in ABAQUS/CAE. Four optically reconstructed designs—a solid-hinge baseline, a commercial-type reference, a modified commercial variant with an altered hinge cavity, and a rounded-hinge prototype—were examined under force-controlled closure (2 N and 3 N) and an equal-displacement case (U = 9 mm). Stresses consistently localized at the hinge; under 2 N, peak von Mises values spanned 77–88 MPa across designs. Under 3 N, the rounded-hinge prototype sustained a lower peak (~95 MPa) than the commercial-type (~105 MPa) and exhibited a more homogeneous displacement field. These findings identify hinge architecture as a dominant driver of stress distribution in polymer clips and provide quantitative targets for design optimization and subsequent experimental validation.

Keywords: Finite Element Analysis (FEA), Polyoxymethylene (POM) clips, Hemostatic clip mechanics, Hinge geometry optimization, Structural performance, Stress distribution

Authors: Parastoo Kamali - Hadi Taghizadeh











Article Code: icbme-1102

Article Title: Vibration-Based Assessment of Dental Implants: A Finite Element Study on Bone Quality and Boundary Conditions

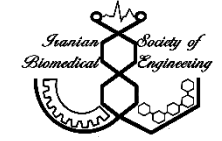
Abstract: Background: Dental implant stability is critical to long-term implant success and is influenced by bone quality, implant geometry, and boundary conditions. Modal analysis provides a non-invasive method to assess implant stability through evaluation of the system's natural frequencies. Objective: This study investigates how boundary constraints, mandible size, bone quality, and bone-substitutive layers affect the natural frequency of dental implants. Materials and Methods: A three-dimensional finite element model of a biphasic healing titanium dental implant—defined here as an implant initially engaging both cortical and cancellous (trabecular) bone—was developed using micro-CT data. Two mandibular geometries ("long" and "short") were modeled. Three boundary conditions were applied by fixing the mandible at (1) mesial/distal sides, (2) the inferior surface, and (3) all three sides. Bone quality was categorized using the Lekholm and Zarb classification:

- Type I: dense cortical bone only
- Type II: thick cortical and dense trabecular bone
- Type III: thin cortical and dense trabecular bone
- Type IV: thin cortical and sparse trabecular bone

Additionally, bone-substitutive layers (magnesium phosphate, hydroxyapatite, PMMA) at two thicknesses (300 μm and 800 μm) were included. *Results*: Natural frequencies were significantly higher in the short mandible model (e.g., 13,959 Hz vs. 3,826 Hz for bone type IV). Increased boundary constraint raised the first mode frequency from 1,786 Hz (one side fixed) to 5,650 Hz (three sides fixed). The highest frequencies occurred in Type I bone (up to 83,958 Hz). Bone-substitutive layers caused frequency changes of <1%, indicating minimal impact. *Conclusions*: Bone quality is a dominant factor in implant stability, with denser bone yielding higher frequencies. Boundary condition modeling significantly affects frequency results. Thin bone-substitute layers do not notably influence vibrational response, although they remain important for osseointegration.

Keywords: Modal analysis, Dental implant stability, Natural frequency, Boundary constraints, Bone quality, Bone substitute materials

Authors: Fatima Wayzani - Mohammadjavad (Matin) Einafshar - Ata Hashemi











Article Code: icbme-1118

Article Title: Experimental and Theoretical Analysis of the Mechanical Performance of 3D-Printed Biomedical Splints Made of PLA/CF with Structural Geometric Variations

Abstract: A biodegradable composite, polylactide (PLA) reinforced with 15% carbon fiber (PLA/CF15%) is becoming more and more employed in 3D-printed biomedical devices via fused deposition modeling (FDM). Few studies, though, have looked at how geometric perforations affect the mechanical integrity of big cylindrical splints. This study examines the compressive and impact performance of solid and perforated PLA/CF15% cylinderical splints produced under same FDM conditions. Axial compression (ASTM D695) and To ascertain ultimate strength, Young's modulus, and absorbed energy, radial drop-weight impact experiments were carried out (n = 5 per design). Higher mechanical resistance was shown by the solid specimens than by the perforated ones; the perforated design, meanwhile, resulted in a significant weight reduction (~33%) and better ventilation. Process-induced flaws like stress concentration close to perforations and porosity were blamed for discrepancies between experimental and theoretical results. Although both designs met fundamental orthopedic splint load criteria (1–1.5 kN), more testing comprising microstructural analysis, fatigue behavior, and adherence to clinical guidelines is advised to guarantee long-term dependability

Keywords: biomedical splint, PLA/CF, FDM 3D printing, mechanical performance, structural geometry

Authors: Elnaz Abedini - Nima Feizlou











Article Code: icbme-1175

Article Title: Functionally Graded Material Vertebroplasty Screws: A Finite Element

Biomechanical Study

Abstract: Vertebroplasty is a minimally invasive treatment for osteoporotic vertebral compression fractures (VCFs), vet conventional titanium screws often induce stress shielding and poor load transfer. This study evaluates the biomechanical performance of a novel functionally graded material (FGM) vertebroplasty screw—comprising a Ti-6Al-4V core and hydroxyapatite (HAP) outer layer—using finite element analysis (FEA. A 3D model of the L2 vertebra was reconstructed from CT data and meshed with over 250,000 elements. Two screw types (homogeneous titanium vs. FGM) were simulated under a 300 N axial load. The FGM screw's radial stiffness gradient was defined by a power-law distribution and implemented via a UMAT subroutine in ABAQUS. Results showed a 14% reduction in peak von Mises stress (12.19 MPa vs. 10.45 MPa) and a 32% decrease in maximum elastic micro-strain (179.9 vs. 121.5) in the FGM screw. Cortical bone stress remained constant (52.20 MPa), while cancellous bone displacement decreased by 36% in the anteroposterior direction (0.02671 mm vs. 0.01702 mm), indicating improved primary stability. Displacement differences between screw types were negligible (<0.00008 mm across all axes), confirming construct integrity. Validation against prior studies showed <10% deviation in stress metrics. The FGM design redistributed internal loads, reduced stress concentrations, and enhanced biomechanical compatibility without compromising cortical integrity. These findings support the potential of graded screws to improve vertebroplasty outcomes by minimizing implant loosening and promoting osseointegration.

Keywords: vertebroplasty; functionally graded materials; finite element analysis; hydroxyapatite; biomechanical compatibility

Authors: Maryam Rahimi - Mohammad Hosein Zadeh-Posti - Aisan Rafiei - Nima Jamshidi











Article Code: icbme-1230

Article Title: Finite Element Analysis of Lumbar Spine Biomechanics Following Cement Augmentation with Different PMMA Volumes: A Comparison with Intact Spine

Abstract: This study presents a finite element analysis (FEA) of lumbar spine biomechanics following cement augmentation with varying volumes of polymethylmethacrylate (PMMA). aiming to identify the optimal volume for vertebral stability while minimizing stress on adjacent segments. A three-dimensional model of the L2-L3 motion segment was constructed from CT scans of a 50-year-old female patient using MIMICS and 3-Matic software. The cortical shell thickness was set to 1 mm, endplates to 0.8 mm, and the intervertebral disc was modeled based on patient anatomy and literature. Cement was idealized as a cylinder coaxial with a pedicle screw and embedded within the trabecular bone. Three cement volumes—1.0 mL, 1.5 mL, and 2.5 mL—were analyzed alongside an intact control model. Boundary conditions included full constraint of L3 and application of compressive and bending loads to L2. Simulations were performed using Abaqus CAE 2022 under dynamic explicit conditions. Results showed that 1.5 mL cement reduced compressive stress by 29.9%, while 2.5 mL yielded the greatest reductions in flexion (56.2%), lateral bending (2.5%), and axial rotation (3.3%). The intact vertebra exhibited maximum von Mises stress of 86.35 MPa under compression, compared to 60.5 MPa and 70.54 MPa for 1.5 mL and 2.5 mL cement, respectively. These findings suggest that moderate cement volumes offer superior biomechanical performance across multiple loading scenarios. Despite modeling simplifications, the study supports the use of simulation-based planning to optimize cement volume and enhance procedural safety in vertebral augmentation.

Keywords: Bone cement augmentation, Vertebral compression fracture, Polymethylmethacrylate (PMMA), Finite element analysis, Spinal biomechanics

Authors: Reihane Yazdani - Mohammdjavad (Matin) EinaAfshar - Azadeh Ghoochani - Nima Jamshidi











Article Code: icbme-1237

Article Title: Biomechanical Evaluation and Comparison of Spinal Fixators in the Lumbar (L3–L4) Region Using the Finite Element Method

Abstract: Treatment of fractures, deviations, and abnormalities of the spine requires precise and appropriate tools based on various concepts such as rigid stabilization systems, semi-rigid stabilization, and dynamic stabilization. In this study, the biomechanical evaluation of different stabilization systems in the lumbar region (L3-L4) was performed using finite element analysis. A healthy spine model without stabilization and three stabilized models with different rods were considered: a conventional simple rod (rigid stabilization), a curved rod (dynamic), and a notched rod. All spinal models were loaded with a compressive force of 400 Newtons and a moment of 10 Newton-meters in four movements: flexion, extension, lateral bending, and axial rotation. The results for range of motion (ROM), percentage reduction in range of motion, von Mises stress, and percentage reduction in von Mises stress were compared. Precision biomechanical tools for the spine are significantly sensitive to geometric features. The obtained results showed that all three rod models used resulted in the fusion of the lumbar vertebrae (L3-L4). However, considering that the stress and strain on the pedicle screw are critical factors in reducing complications and failures of the spinal stabilization system, the notched rod, due to its lower stress compared to other models, has the best performance.

Keywords: Biomechanical Analysis Spinal Fixation Lumbar Spine Finite Element Method Pedicle Screw and Rod

Authors: Nima Moazed - Mohammad Haghpanahi











Article Code: icbme-1304

Article Title: Effect of ph changes on thermal and mechanical properties of polyacrylamide hydrogel using molecular dynamics simulation

Abstract: Hydrogels are three-dimensional polymer grids with cross-links that enable them to imbibe significant amounts of water or biological aqueous without being solved. Common hydrogels are particularly appealing compared to factitious ones due to their diversity, plenty, frugal, non-poisonous, and biocompatibility. This research probes the impact of pH variations on the thermic and mechanical virtues of polyacrylamide hydrogel through molecular dynamics simulations. imitations were conducted using the Lamps software. Prior to examining the final manner of the atomic instances, the equilibrium state was assessed by analyzing changes in thermodynamic items, including temperature, kinetic energy, potential energy, and total energy. As the pH of the simulated atomic samples increased, the values related to the intake of water molecules rose, enhancing the mechanical and thermic virtues of the samples, with the final strength and thermal conductivity coefficient reaching 0.0359 MPa and 0.62 W/m·K.

Keywords: Hydrogel, Molecular Dynamics, Ultimate Strength, Heat Flux, Thermal Conductivity, pH-responsive Hydrogels, Final Strength

Authors: Narges Karimzadeh Dehkordi











Article Code: icbme-1411

Article Title: Mechanical properties of cancer cells as potential predictive biomarkers

Abstract: Cancer, as one of the most complex and multifactorial diseases, remains a major challenge in modern medicine. Progress in therapeutic approaches requires a deeper understanding of cellular behavior and the influence of various factors on cell dynamics. In this context, the mechanical properties of the cellular microenvironment play a critical role in identifying the behavioral patterns of cancer cells and in designing novel therapeutic strategies. The findings of this study demonstrate a strong correlation between biological responses, cellular mechanical behavior, and the predictions obtained through mathematical modeling using the Kelvin-Voigt Fractional Derivative model. This correlation highlights the potential of employing mathematical models based on mechanical parameters to predict the outcomes of biological tests before their actual implementation. Furthermore, such modeling approaches allow the estimation of anticancer drug efficacy on cells in advance of experimental validation. Consequently, integrating mechanical insights with mathematical modeling can significantly reduce the cost and time associated with biological testing while improving the accuracy of designing targeted therapies. These results underline the importance of interdisciplinary strategies that combine biology and engineering, opening new horizons for the development of personalized cancer.

Keywords: Cell Migrating Assay, KVFD Model, Cytoskeleton, Mechanical parameters in cells

Authors: Sayed Reza Ramezani - Afsaneh Mojra











Article Code: icbme-1452

Article Title: An AI-Assisted Approach to Patient-specific 3D Modeling and Stress Analysis of the Temporomandibular Joint from CBCT Images

Abstract: Accurate assessment of temporomandibular joint (TMJ) biomechanics requires patient-specific models that capture anatomical variability with high fidelity. This study presents an AI-assisted method for biomechanical modeling and stress analysis of the TMJ, integrating deep learning—based segmentation and 3D reconstruction from cone-beam computed tomography (CBCT). CBCT scans are processed using a pretrained UNET-R network, fine-tuned with a small dataset to segment the mandible, maxilla, and temporal bone. The segmented geometries are reconstructed into 3D models, converted into volumetric finite element (FE) meshes, and combined with a modeled TMJ disc representing the soft tissue between the mandibular condyle and maxilla. The FE model is then subjected to simulated incisal and unilateral molar loading to estimate stress distribution within the disc. The proposed method enables rapid and reproducible generation of patient-specific TMJ biomechanical models, reducing manual segmentation effort and computational cost while preserving clinical accuracy. This approach demonstrates strong potential for personalized diagnosis, treatment planning, and biomechanical research on TMJ disorders.

Keywords: Temporomandibular joint, finite element analysis, CBCT, deep learning segmentation, patient-specific modeling.

Authors: Mohammad Akhlaghi - Masoud Shariat panahi - Sina Salehpour - Morad Karimpour - Hadi Ghatan Kashani











كد مقاله: ichme-1186

عنوان مقاله: شبیه سازی افزایش نفوذ دارو در لوله مویرگی با غشا نفوذپذیر به کمک اثر نانوذرات مغناطیسی

چکیده: سیستمهای رهایش دارو مبتنی بر میکروفلوئیدیک قطرهای، به دلیل قابلیت کنترل دقیق دوز، در سالهای اخیر توجه محققان زیادی را جلب کرده است. با این حال، محدودیتهای ناشی از مکانیزمهای صرفاً نفوذی، کارایی جذب دارو را کاهش می دهد. در این مطالعه، یک مدل جامع چندفیزیکی در نرمافزار COMSOL توسعه داده شد که شامل دینامیک قطره حاوی نانوذرات مغناطیسی در یک لوله مویرگی با دیواره نیمه تراوا است. شرط مرزی فلاکس برای شبیهسازی عبور دارو از غشا اعمال گردید و اثر میدان مغناطیسی خارجی (فرکانس 400 kHz 400 ، و نانوذرات با قطر ۵ نانومتر بر بهبود انتقال دارو بررسی شد. نتایج نشان داد که اعمال میدان مغناطیسی منجر به افزایش حدود ۲۸٪ در نفوذ دارو به داخل قطره، نسبت به حالت فاقد نانوذرات، می گردد. همچنین، پروفایلهای سرعت، فشار و غلظت دارو در سرعتهای اولیه مختلف قطره استخراج شدند. اضافه کردن فیزیک انتقال حرارت نشان داد که افزایش دما به میزان ۱ کلوین، بر رفتار جریان و توزیع دارو تأثیر قابر توجهی ندارد اما می تواند در رئولوژی محیط در مقیاسهای میکرو مؤثر باشد. این رویکرد می تواند در طراحی سیستمهای رهایش هدفمند دارو، به ویژه در درمان سرطان و توسعه ابزارهای میکروفلوئیدیک با بازده بالا، کاربردهای گستردهای داشته باشد.

كلمات كليدى: رهايش دارو،شبيهسازى،نانوذرات مغناطيسى،ميدان مغناطيسى،لوله مويرگى

نویسندگان: پریماه سلیمی - هامون پورمیرزاآقا - منصور امیری دوگاهه - علی وظیفه دوست صالح - سیده سوده جهانی











كد مقاله: icbme-1095

عنوان مقاله: شبیه سازی عددی انقباض بطن راست قلب جنین انسان به روش تعامل سیال و جامد

چکده: عدم تشخیص به موقع بیماری های قلبی جنینی موجب آسیب به میوکارد، ریه ها، مغز و در نتیجه موجب مرگ می شود. برای تشخیص اختلالات در قلب جنین، امروزه از دستگاه های پیشرفته ای مانند اکوکاردیوگرافی های مخصوص، تصویر برداری رزونانس مغناطیسی و روش های عددی مانند دینامیک سیالات محاسباتی استفاده می شود. هر یک از روش های موجود دارای معایب و محدودیت هایی هستند که نیاز به ارتقای آن ها و دستیابی به اطلاعات دقیق تر و بیشتر داریم، تحقیق حاضر به بررسی الگوی انقباض بطن راست قلب جنین انسان و استخراج پارامتر های همودینامیکی و مکانیکی مرتبط، با بهره گیری از داده های کلینیکی و روش تعامل سیال و جامد پرداخته است. در این مطالعه ابتدا تصاویر اکوکاردیوگرافی قلب جنین و سی تی اسکن قلب نوزاد تازه متولد شده به دست آمد. سپس با استفاده از نرم افزار میمیکس، مقیاسی جهت تبدیل ابعاد بطن نوزاد به بطن جنین صورت گرفت. هندسه نهایی در نرم افزار کتیا به سطوح و حجم های لازم تبدیل شد. در نهایت در نرم افزار انسیس یک مسئله تعامل سیال و جامد برای بطن و جریان خون در آن تعریف شد و در نهایت نتایج با دو مطالعه دیگر مقایسه شد. یکی از نوآوری های این مطالعه اعمال فشار های مختلف به قسمت های متفاوت دیواره بطن بر اساس میزان انقباض پذیری عضله است. نتایج مطالعه حاضر نشان می دهد که با در نظر گرفتن ضخامت بطن و اعمال فشارهای متفاوت به قسمت های مختلف بطن و اعمال شرا مرزی خروجی فشار ۴۰ میلی متر جیوه، نتایج شبیه سازی بسیار نزدیک تر به داده های بالینی خواهد بود. برای بهبود نتایج می توان با تقسیمات بیشتر دیواره بطن و افزودن جزئیات الگوی انقباضی به دیواره بطن به نتایج تجربی نزدیکتر شد.

واژههای کلیدی: الگوی انقباض بطن، بطن راست قلب جنین انسان، پارامتر های همودینامیکی و مکانیکی، تعامل سیال و جامد، دینامیک سیالات محاسباتی

نویسندگان: سیده کیمیا مرتضوی فارسانی، هانیه نیرومند اسکوئی، بهروز جعفرزاده، محمد حسن فردوسی











كد مقاله: icbme-1382

عنوان مقاله: بررسی عددی اثر همزمانی آریتمی قلبی و کلسترول بالا بر تشکیل و رشد پلاگ چربی در آئورت انسان

چکیده: فیبریلاسیون دهلیزی (AF) شایع ترین آریتمی قلبی و عاملی مهم در بروز تغییرات همودینامیکی و اختلال در جریان خون است که می تواندپیشرفت آترواسکلروز را تسریع کند. در این مطالعه، با هدف بررسی اثرات AF بر نفرذ لیپ وپروتئین با چگالی پایین (LDL) و تشکیل فومسل در دیواره آئورت، یک مدل عددی سه بعدی مبتنی بر دینامیک سیالات محاسباتی (CFD) توسعه داده شده است. هندسه واقعی آئورت از دادههای تصویربرداری MRI بازسازی شده و شرایط مرزی خروجی بر اساس مدل ویندکسل تعیین گردیده است. شبیه سازی هادر دو وضعیت فیزیولوژیک شامل ریتم سینوسی نرمال و AF و نیز در دو حالت سطح چربی خون (نرمال و کلسترول بالا یا هایپرلیپیدمیا) انجام شده است. نتایج مدلسازی نشان داده که در حضور AF، میانگین تنش برشی دیواره (TAWSS) کاهش یافته و نواحی با TAWSS پایین مستعد نفرذ بیشتر LDL و تجمع فومسل میشوند. این پدیده در شرایط هایپرلیپیدمیا به طور چشم گیری تشدید شده و اثر همافزایی بین اختلال ضربان قلب و فوامس می شوند. این پدیده در شرایط هایپرلیپیدمیا به طور چشم گیری تشدید شده و اثر همافزایی بین اختلال ضربان قلب نرمال افزایش سطح کلسترول مشاهده شده است. این همزمانی میزان فومسل را ۱۹۴ درصد نسبت به حالت ضربان قلب نرمال افزایش می دهد که ترکیب AF و هایپرلیپیدمیا عاملی پرخطر دو گانه در فرآیند آترواسکلروز محسوب شده و می تواند در طراحی استراتژیهای پیشگیرانه مورد استفاده قرار گیرد.

واژههای کلیدی: آترواسکلروز، آریتمی قلبی، ال دی ال، کلسترول، فوم سل، هایپرلیپیدمیا

نویسندگان: پیمان دوکوهکی، بهار فیروز آبادی











كد مقاله: icbme-1082

عنوان مقاله: ساخت و انتقال ریزقطرات مغناطیسی در تراشه میکروفلویدیک

چکده: تاکنون تحقیقات گستردهای در حوزه تولید ریزقطرات و کنترل حرکت آنها در محیط میکروفلوییدیک صورت گرفته است. این فناوری با کاربردهای زیستی، توجه متخصصان مهندسی پزشکی را به خود جلب کرده است. در این تحقیق، با استفاده از تراشه میکروفلویدیک آشکل، قطرات همگن حاوی نانوذرات مغناطیسی تولید شدند. سپس، تراشهای با فیلم نانومتری مغناطیسی به شکل دایرههای متصل بههم، با روش لیتوگرافی الیفتاف ایجاد گردید. بررسیها نشان دادند در حضور میدان مغناطیسی، این لایه مغناطیسی شده و قطرات مغناطیسی اطراف خود را جذب می کند. چرخش میدان مغناطیسی خارجی باعث جابجایی قطبهای مغناطیسی در مسیر دایره ای میشود که این امر انتقال متوالی قطرات بین دایرههای مجاور را ممکن میسازد و ذرات را در طول مسیر منتقل می کند. نتایج نشان داد که امکان انتقال کنترل شده قطرات، با قابلیت همگامی با فرکانس خارجی اعمال شده تا فرکانس حدود ۱۰۰ میکرومتربر ثانیه، وجود دارد. این قطرات، در ابعاد میکرومتری، قادر به حمل حجمهای دقیقی از دارو در محدوده پیکولیتر تا نانولیتر میباشند و این ویژگی آنها را برای کاربردهای تکسلولی ایدهآل میسازد. این سیستم، با قابلیت انکیسوله کردن مواد مختلف، کاربردهای بالقوهای در حوزههای تحویل هدفمند دارو، تجزیه و تحلیل تکسلولی و سیستمهای آزمایشگاهروی تراشه دارد

واژههای کلیدی: انکپسوله کردن، تراشه مگنتوفورتیک، ریزقطرات مغناطیسی، کنترل مغناطیسی، میکروفلویدیک

نویسندگان: نازنین پژوهیده، روزبه عابدینی نسب، مینا صوفی زمرد











كد مقاله: icbme-1039

عنوان مقاله: مدلسازی عددی اندرکنش آکوستیک - سیال برای بهبود کیفیت اختلاط در میکروکانال سامانههای زیستی

چکیده: فناوری های نوین در حوزه علوم در ابعاد میکرو، از اهمیت فراوانی برخوردار است. سامانه میکرو آکوستیک – سیال علم شناخت و بررسی رفتارهای سیالاتی در تکنولوژی ساخت و کاربرد تجهیزات آکوستیکی در ابعاد میکرو می باشد. در این پژوهش، تغییرات شاخص اختلاط در بستر میکروکانال سامانه زیستی تحت تاثیر میدان آکوستیکی به صورت عددی مطالعه شده است. مدل هندسی، شبکه محاسباتی و معادلات جریان سیال توسط نرم افزار کامسول شبیه سازی شده است. نتایج عددی حاصل از طریق شبیه سازی به منظور صحت سنجی، با نتایج عددی موجود مقایسه شده است. نتایج عددی نشان دادند که با افزایش فشار آکوستیکی، الگوهای گردابهای قوی تری در میدان جریان شکل گرفته و منجر به تداخل بیشتر بین دو سیال ورودی و افزایش اختلاط می گردد. نمودارهای توزیع غلظت در عرض میکروکانالو شاخص کمی اختلاط بیانگر آن هستند که در فشار ۴۲۰ پاسکال، اختلاط تقریباً بهصورت کامل و یکنواخت حاصل شده و شاخص اختلاط به بیش از ۹۹٪ رسیده است. این یافتهها نقس کلیدی میدان آکوستیکی در ارتقاء انتقال جرم و افزایش یکنواختی غلظت در سامانههای میکروسیالی را اثبات می کند.

واژههای کلیدی: سامانههای زیستی، شاخص اختلاط، میکروسیالات، اندر کنش آکوستیک – سیال، کامسول

نویسندگان: رسول عدلی بیله سوار، فرهاد صادق مغانلو، محمد وجدی حکم آباد











كد مقاله: icbme-1348

عنوان مقاله: عصر جدید مدلسازی بیومکانیکی با یادگیری ماشین آگاه از فیزیک

چکیده: رویکردهای مدلسازی سنتی در حوزه مکانیک سیالات زیستی با چالشهایی همچون هزینهبر بودن مطالعات تجربی، نیاز به فرضیات سادهساز در مدلسازی محاسباتی و محدودیتهای مدلهای صرفا دادهمحور مواجه هستند. مدلهای یادگیری ماشین دادهمحور اغلب به دلیلکمبود دادههای برچسبدار و ناسازگاری پیشبینیها با قوانین فیزیکی، از قابلیت تعمیم پذیری کافی برخوردار نیستند. برای حل این مشکلات، یادگیری ماشین آگاه از فیزیک (PIML) قوانین فیزیکی بنیادی را مستقیما در فرآیند یادگیری ماشین ادغام می کند. این رویکرد ترکیبی پایداری، قابلیت تفسیر و دقت مدل را افزایش می دهد و تضمین می کند که ناتیج پیشبینی شده از نظر فیزیکی معقول هستند. این مقاله کاربردهای PIML در غلبه بر چالشهای دیرینه در مدل سازی فرآیندهای فیزیولوژیک مانند همودینامیک و مکانیک بافت نرم را بررسی می کند. با برجسته سازی توانایی PIML در ارائه پیشبینیهای دقیق و اختصاصی برای هر بیمارو حل مسائل معکوس برای استنتاج پارامترهای پنهان، این مقالمه نشان می دهد که چگونه PIML می تواند آینده مدلسازی محاسباتی را در مکانیک سیالات زیستی باز تعریف کرده و پلی میان فیزیک، داده و کاربردهای بالینی ایجاد کند. با وجود چالشهای باقیمانده از جمله پیچیدگیهای محاسباتی و ادغام، PIML به عنوان یک ابزار قدر تمند برای پیشبرد پزشکی دقیق و توسعه دوقلوهای دیجیتال برای بهبود مراقبت از بیمار مطرح می شود.

واژههای کلیدی: بیومکانیک، سیالات زیستی، شبکههای عصبی، یادگیری ماشین ، PINN ،PIML.

نویسندگان: علی یعقوبیان، فائزه یعقوبیان











كد مقاله: icbme-1096

عنوان مقاله: تحلیل پارامترهای کلیدی مؤثر در شکست پچ چسبنده ترمیمی تاندون روتاتورکاف با مدلسازی اجزای محدود

چکیده: پارگی تاندون فوقخاری از شایعترین آسیبهای شانه در افراد بالای ۴۵سال است که باعث درد و محدودیت حرکتی میشود. با توجه به نرخ بالای شکست در درمانهای سنتی مانند بخیهزنی، استفاده از پچهای چسبنده به عنوان روشی نوین مورد توجه قرار گرفته است. در این پژوهش با مدلسازی سهبعدی مفصل شانه، عوامل بیومکانیکی مؤثر در عملکرد پچها شامل ویژگیهای مکانیکی و هندسی استخوان، تاندون و ناحیه چسبنده طی حرکت ابداکشن و چرخش داخلی بررسی شده است. یافتهها نشان دادند که تخصیص ویژگیهای پیچیده استخوانی مانند خواص ناهمگن، باعث کاهش قابل ملاحظه تخریب ناحیه اتصال نسبت به مدلهای همگن و همسانگرد در حرکت ابداکشن و حتی به صفر رسیدن آن در چرخش میشود. المان چسبنده، علیرغم پیچیدگی محاسباتی، در مقایسه با سطح چسبنده الگوهای متفاوتی از شکست ارائه داده و نواحی گسترده تری و کاهش خطر از آشکار می سازد. بررسی ضخامت پچ آشکار کرد که افزایش ضخامت، موجب توزیع یکنواختتر تنش و کاهش خطر گسستگی میشود، بهطوری که پچ با ضخامت ۴/۵ میلی متر، تعادل بهینهٔی بین چسبندگی مؤثر و استقلال حرکتی مفصل شانه ایجاد میکند. این یافتهها می توانند راهنمای طراحی چهای ترمیمی بادوام و کاهش نرخ پـارگی مجـدد تانـدون باشـند، اگرچـه آزمایش های تجربی در مطالعات آینده ضروری است.

کلمات کلیدی: پارگی تاندون فوق خاری، پچ چسبنده، روش اجزای محدود، شکست و آسیب، مدل ناحیه چسبنده.

نويسندگان: شقايق راست قلم - آزاده قوچاني - محسن صراف بيد آباد











كد مقاله: icbme-1151

عنوان مقاله: برنامهریزی قبل از عمل شلفاستابولوپلاستی، با هدف ایجاد یک مفصل کانگروئنت و بررسی ارتباط کانگروئیتی و جذب آلوگرافت

چکیده کانگروئیتی مفصل نقش مهمی در توزیع یکنواخت تنش روی سطوح مفصلی دارد. لـذا در بیماران مبـتلا بـه دیسـپلازی رشدی هیپ، طراحی پیوند قبل از عمل شلفاستابولوپلاستی، بـا هـدف ایجاد مفصـل کانگروئنت، اهمیـت دارد. تـاکنون عمـل شلفاستابولوپلاستی با استفاده از طراحی قبل از عمل، به منظور ایجاد یک مفصل کانگروئنت، انجام نشده است. هدف این مطالعه برنامهریزی قبل از عمل یک بیمار ۱۷ ساله با دیسپلازی شدید مفصل ران، در فضای سهبعدی است، به طوریکه هندسه استخوان پیوند داده شده، تا حد امکان با سطح مفصلی سر فمور همخوانی داشته و باعث توزیع مناسب تنش روی پیوند شـود. مـدلهای سهبعدی استخوانها از تصاویر سی تی اسکن بیمار استخراج گردیده و با استفاده از کد توسعه داده شده در محیط پایتون، سطح زیرین شلف طراحی شد، به طوریکه حداکثر همخوانی با سر فمور را داشته باشد. در ادامه عمل جراحی با استفاده از الگوهای بـه دست آمده از طراحی، انجام شده و توزیع تنش روی پیوند، پارامترهای مورفولوژیکی و کانگروئیتی مفصل، بررسی گردیـده است. نتایج نشان داد طراحی یک مفصل کانگروئنت، نقش مهمی در موفقیت شلف استابولوپلاستی و بقای پیوند دارد و اگرچه نمی توان نامیدوار آلوگرافتی دقیقا مطابق انحنای طراحی شده یافت، اما می توان به پیوندی با کانگروئیتی مناسب در منطقه ی تحمـل وزن امیـدوار بود.

كلمات كليدى: برنامهريزى قبل از عمل، بقاى پيوند، ديسپلازى، شلف استابولوپلاستى، كانگروئيتى

نویسندگان: جعفر نصرآبادی - وحید اربابی - سعید رهنما











كد مقاله: icbme-1181

عنوان مقاله: شبیه سازی المان محدود رفتار ناهمسانگرد لیگامان پریودنتال بر اساس توزیع سهبعدی فیبرهای کلاژن

چکیده: لیگامان پریودنتال بافت همبند نرمی است که مابین دو بافت معدنی دندان و استخوان فک قرار گرفته است. اصلی ترین جزء ریز ساختاری پریودنتال در ایجاد عملکردهای بیومکانیکی، شبکه فیبر کلاژنی گسترده آن میباشد. مهم ترین ویژگی شبکه کلاژنی آن نیز جهت گیری منحصربه فرد الیاف در نواحی مختلف بافت است. از این رو، ارائه مدل های بنیادین مبتنی بر ریز ساختار برای درک رفتار بیومکانیکی لیگامان پریودنتال ضروری است.

در تحقیق حاضر، رفتار ناهمسانگرد لیگامان پریودنتال با درنظر گرفتن جهتگیری سه بعدی الیاف کلاژن (شامل جهتگیری شعاعی و محیطی) براساس ویژگی های ریزساختاری نـواحی آنـاتومیکی مختلف بافت بهوسیله تـابع چگالی انـرژی کرنشی Holzapfel در محیط المان محدود شبیهسازی گردید. سپس الگوهای بیشینه و کمینه تـنش اصلی بـرای شـرایط بارگـذاری ناشی از جویدن (بازه تنشهای کمتر از ۷۰-۱ الی تنشهای بزرگتر از ۵۰۰ مگاپاسکال) استخراج شد. نتایج حاصل بهخوبی تـأثیر جهتگیری الیاف در ایجاد الگوهای تنش موضعی در لیگامان پریودنتال را نشان میدهد. این امر وجود بازسازی موضعی در بافت تحت را تأیید می کند. طبق نتایج، وجود حرکت فیزیولوژیک دندان در جهت مزیال دیستال در اثر تنش موضعی وارده بـه بافت تحت نیروی جویدن مشاهده شدمطالعه این الگوهای تنش و بازسازی در سرتاسر بافت، امکـان شـناخت نـواحی حسـاس بـه آسـیب (زجمله در رأس ریشه) تحت شرایط فیزیولوژیکی و بارگذاری مختلف را فراهم می نماید.

کلمــات کلیــدی: تــابع چگــالی انــرژی کرنشـــی،رفتار ناهمسانگرد،شبیهســـازی اجــزای محــدود،فیبرهای کلاژن،لیگامــان پریودنتال،مدلسازی بنیادین

نویسندگان: محیا بناپور نجاری - علی ولایی - هادی تقیزاده











كد مقاله: icbme-1408

عنوان مقاله: تحلیل المان محدود تنشهای وارده به بافتهای نرم مفصل زانو در درجات مختلف فلکشن

چکیده: مفصل زانو به عنوان یکی از مهمترین مفاصل بدن انسان در فعالیتهای روزمره وظیفه تحمل وزن بدن و حرکت پاها را بر عهده دارد. بدلیل پیچیدگی این مفصل مطالعه تنشهای وارده بر آن در بیماریها، عوارض و حالات گوناگون بوسیله روشهای عهده دارد. بدلیل پیچیدگی این مفصل مطالعه تنشهای وارده بر آن در بیماریها، عوارض و حالات گوناگون بوسیله روشهای بدن آزمایشگاهی کاری دشوار و در بعضی مواقع غیر ممکن است. یکی از روشهای مرسوم در مطالعه توزیع تنش در بافتهای بدن در چنین شرایط پیچیدهای تحلیل به روش المان محدود (FEM) میباشد. این پژوهش به مطالعه توزیع تنش در بافتهای نرم زانو در زوایای مختلف فلکشن این مفصل میپردازد و محلهایی با بیشترین تحمل تنش و احتمال آسیب دیدگی را گزارش می کند. در این راستا مدلهای سه بعدی اجزای مختلف زانو از تصاویر تشدید مغناطیسی استخراج شده سپس با اعمال شرایط بارگذاری مناسب تنشهای وارده به منیسکها و غضروفهای تیبیا و غضروف فمور در بازه زاویهای صفر تا ۱۲۰ درجمه فلکشن زانو مورد بررسی قرار گرفته است. نتایج حاصل از شبیهسازی بیان کننده اعمال بیشتری را تحمل می کنند.

كلمات كليدى: تحليل المان محدود، FEM، زانو، بافت، TKA، بيومكانيك، آسيب، meniscectomy، تنش.

نویسندگان: سروش سیادت - هادی تقی زاده











كد مقاله: icbme-1422

عنوان مقاله!رزیابی بیومکانیکی آسیبپذیری پلاک آترواسکلروتیک و تأثیر مورفولـوژی و خـواص مکـانیکی بـا اسـتفاده از روش اجزاء محدود

چکیده: عملکرد بیومکانیکی شریان کرونر به عنوان یک ساختار انعطاف پذیر برای خونرسانی به عضله قلب و تحمل فشارهای دینامیکی خون ضروری است. حضور پلاک آترواسکلروتیکبا تغییر شرایط بیومکانیکی دینواره، این عملکرد را مختل کرده و ریسک پارگی را افزایش میدهد. جهت ارزیابی این تغییرات، یک مدل اجزای محدود سهبعدی از شریان کرونر با سه مورفولوژی پلاک متفاوت در گرفتگی یکسان و دو حالت سختی (پلاک نرم و پلاک کلسیفیه) شبیهسازی شد. برای توصیف رفتار مکانیکی، دیواره شریان به صورت ماده الاستیک خطی داواره شریان به صورت ماده الاستیک خطی با مدول الاستیک متفاوت در نظر گرفته شدند. برای دستیابی به الگوی توزیع تنش و کرنش، مجموعه شریان پلاک تحت یک فشار داخلی یکنواخت به عنوان نماینده فشار خون قرار گرفت.

نتایج حاصل حاکی از آن است که با افزایش عدم تقارن هندسی پلاک، تنش ماکزیمم در دیواره شریان به شدت افزایش می یابد. به طوری که مدل نامتقارن که لومن به سمت دیواره شریان تمایل دارد،بالاترین سطح تنش را به دیبواره رگ تحمیل می کنید. همچنین، افزایش سختی پلاک از حالت نرم به کلسیفیه، منجر به افزایش قابل توجه تنشهای موضعی در مرز پلاک و دیبواره شریان می گردد. در شبیه سازی حاضر نشان داده شد که عدم تقارن هندسی باعث ایجاد کانون تمرکز تنش در شانه پلاک می شود و کلسیفیکاسیون این تمرکز تنش در شانه پلاک می شود و کلسیفیکاسیون این تمرکز تنش را به شدت تشدید می کند. با توجه به یافتههای این پژوهش، می توان نتیجه گرفت که ترکیب مورفولوژی نامتقارن با سختی بالای پلاک، بحرانی ترین وضعیت بیومکانیکی را ایجاد می کند که مستقیماً ریسک پارگی پلاک را افزایش داده و آسیبپذیری بیمار را تشدید می نماید.

كلمات كليدى: آرترواسكلروز، بيومكانيك، شريان كرونر، تمركزتنش، مورفولوژىپلاك، تحليل اجزاى محدود.

نویسندگان: زهرا غلامحسینی - حامد قدوسی جوهری - احمد حسین زاده - مهدی کلانی - هادی تقی زاده











كد مقاله: icbme-1441

عنوان مقاله: طراحی و تحلیل المان محدود ایمپلنت ماژولار شخصی سازی شده مفصل ران مبتنی بر تصاویر CT: تمرکز بر عملکرد اتصال مخروطی تحت بارهای عملکردی

چکیده: در این پژوهش، یک ایمپلنت ماژولار شخصیسازیشده مفصل ران بر اساس تصاویر DICOM یک بیمار واقعی طراحی و با روش تحلیل المان محدود ارزیابی شد. مدل شامل پنج جزء اصلی (کاپ فلزی، لاینر پلیمری، سر، گردن و ساقه) بوده و از اتصال مخروطی برای بهبود مونتاژ و امکان تعویض مجزای اجزا استفاده شد. هندسه و ابعاد بر مبنای دادههای آناتومیک بیمار و اصل بیومکانیکی تعیین گردید. شبیهسازیهای استاتیک تحت چهار سناریوی بارگذاری شامل راهرفتن، دویدن، برخاستن و نشستن انجام شد. نتایج نشان داد بیشینه تنش فونمایزز در حالت دویدن برابر ۲۵۹MPa و متمرکز در اتصال مخروطی گردن ساقه است. در مقابل، مقادیر بیشینه تنش در حالات راهرفتن (۳۵۴MPa) برخاستن (۲۲۲MPa) و نشستن (۲۲۷MPa) همگی ضریب ایمنی بیش از ۲را تأمین میکنند. بیشینه جابهجایی کل ۴۹۷mm، در دویدن مشاهده شد، در حالی که جابهجایی ساقه و سایر اجزا ناچیز بوده و پایداری مطلوب اتصال مخروطی را تأیید میکند. در مجموع، طراحی حاضر عملکردی ایمن و کارآمد در فعالیتهای روزمره نشان میدهد. با این حال، تمرکز تنش مشاهده شده در حالت دویدن به عنوان یک نقطه بحرانی طراحی مطرح است و لزوم بهینهسازی هندسی برای کاهش تمرکز تنش و افزایش دوام خستگی در نسلهای آینده ایمپلنت را برجسته میسازد.

کلمات کلیدی: اتصال مخروطی، ایمپلنت شخصی سازی شده، ایمپلنت ماژولار، ایمپلنت مفصل ران، تحلیل المان محدود، تعویض کامل مفصل ران

نویسندگان: کبری پیرمحمدی - رسول عابدی - سعد رئیسی











كد مقاله: icbme-1442

عنوان مقاله: طراحی بهینهی پلاکهای ارتوپدی برای ترمیم شکستگی ساب تروکانتریک استخوان ران بر پایهی مدلسازی آماری و روشهای یادگیری ماشین

چکیدهشکستگیهای ناحیهی زیر برآمدگی کوچک استخوان ران از آسیبهای شایع اسکلتی محسوب می شوند که معمولاً با استفاده از پلاکهای ارتوپدی درمان می گردند. انتخاب پلاک مناسب به دلیل تفاوتهای اسکلتی بیماران و شرایط متنوع شکستگی همواره چالشبرانگیز بوده است. در این پژوهش رویکردی جمعیت محور برای طراحی و بهینه سازی پلاک ارائه گردید که بر پایهی مدل سازی آماری شکل توسعه یافته است. بدین منظور، تصاویر سی تی اسکن بیماران، در یک جامعهی آماری متنوع، پردازش شده و ساختار آناتومیکی استخوان، با بهره گیری از مدل سازی آماری شکل، تحلیل و با کشف تفاوتها و خوشههای ساختاری با الگوریتم خوشه بندی بدون نظارت، در پنج گروه متمایز دسته بندی شد. برای هر گروه، یک نمونهی نماینده انتخاب و فرایند طراحی و بهینه سازی پلاک انجام شد. نتایج شبیه سازی های المان محدود نشان داد که پلاک های بهینه شده توانستند بیشینهٔ تنش در استخوان سخت، بافت اسفنجی و مجموعهٔ پلاک پیچ را به ترتیب تا ۴۹/۴٪، ۴۴/۴٪ و ۱۹/۴٪ نسبت به پلاک اولیه (قبل از بهینه سازی) کاهش دهند. این کاهش معنادار در تنش بیانگر بهبود توزیع بار و افزایش پایداری مکانیکی سیستم طراحی کاملاً فردمحور، می تواند به بهبود کارایی بالینی و تسریع روند بهبودی بیماران منجر شود.

کلمات کلیدی: بهینهسازی، پلاکهای شخصیسازی شده، تحلیل المان محدود، خوشهبندی بدون نظـارت، شکسـتگی اسـتخوان ران، طراحی پلاک ارتوپدی، مدلسازی آماری شکل

نویسندگان: ماجده رضائی - مسعود شریعت پناهی - مراد کریم پور - هادی قطان کاشانی











كد مقاله: icbme-1460

عنوان مقاله: تحلیل اثر انشعاب فیبر بر خواص مکانیکی تاندون در محل اتصال به استخوان

چکیده عملکرد صحیح تاندون به عنوان رابط برای انتقال نیرو از عضله به استخوان بسیار ضروری است. همچنین ناحیه اتصال تاندون به استخوان نقش کلیدی در این ارتباط دارد. در واقع به عنوان یک بخش اساسی از بافت تاندون محسوب می شود که کوچک ترین نقص ساختاری در آن منجر به عملکرد نادرست سیستم حرکتی خواهد شد. فیبرها در این قسمت از تاندون از حالت محوری خارج شده و منشعب می شوند. در این مطالعه تاثیر نحوه انشعابات فیبری بر خواص مکانیکی فیبر، در نرم افزار آباکوس شبیه سازی و بررسی شد. همچنین تاثیر جهت گیری فیبریل بر خواص مکانیکی فیبر مورد مطالعه عددی قرار گرفت. نمونه فیبرهای مورد مطالعه به صورت هایپرالاستیک و ناهمسانگرد در نظر گرفته شدند. بارگذاری به صورت کرنش محوری ۱۰ درصدی، به نمونه ها اعمال شد. نیروی عکس العمل ناشی از این بارگذاری برای فیبرها بدست آمد. نتایج حاصل حاکی از آن است، فیبرهایی که در محل انشعاب مجموع مساحت سطح مقطع شاخه های دختر با شاخه اصلی برابر است، مدل مناسبی برای فیبرهای منشعب در ناحیه اتصال تاندون به استخوان هستند. همچنین زاویه جهت گیری فیبریل در این فیبرها نباید بیشتر از ۴۵ فیبرهای منشعب در ناحیه اتصال تاندون به استخوان هستند. همچنین زاویه جهت گیری فیبریل در این فیبرها نباید بیشتر از دحه باشد.

كلمات كليدى: دوشاخگى فيبر، جهت گيرى فيبريل، شبيه سازى عددى، ناحيه اتصال به استخوان، هايپرالاستيک

نویسندگان: فاطمه شهماری میکائیل درسی - هادی تقی زاده











كد مقاله: icbme-1222

عنوان مقاله: مقايسه روشهاى مختلف دوخت تاندون فلكسور دست با استفاده از آناليز اجزاى محدود

چکده: روش ترمیم مناسب آسیبهای تاندون دست به علت شیوع بالای آن مورد توجه بسیاری از پژوهشگران میباشد. روشهای مختلفی برای دوخت تاندون فلکسور دست وجود دارد که هرکدام ویژگی خاص خود را دارند. به منظور مقایسه این روشهای مختلفی برای دوخت تاندون فلکسور و مکانیزم ترمیم آن برای سه روش رایج بخیه ننی چهاررشتهای شامل بکر، کروشیت و کسلر اصلاح شده با روش اجزای محدود در نرمافزار آباکوس انجام شد. به منظور بهبود روشهای فوق، روش جدیدی با ترکیب روشهای بکر و کروشیتدر این مقاله ارائه و توسط روش اجزای محدود مورد بررسی قرار گرفت. نتایج شبیهسازی نشان داد که روش جدید ارائه شده در این مقاله از استحکام بیشتری نسبت به سایر روشها برخوردار است و در جلوگیری از ایجاد فاصله دو میلی متری بین لبههای ترمیمی عملکرد بهتری دارد.

كلمات كليدى: تاندون فلكسور، بخيه زنى، روشهاى مختلف دوخت، آناليز اجزاء محدود.

نویسندگان: امیررضا کاظمی - محمد جعفری گلویک - محمد مهدی جلیلی - سید حسین سعید بنادکی











كد مقاله: icbme-1397

عنوان مقاله: ارزیابی بیومکانیکی دو ایمپلنت باریک در مقابل یک ایمپلنت برای جایگزینی دندان آسیای اول فک پایین: یک تحلیل المان محدود تحت بارگذاری استاتیک و دینامیک

چکده: ایمپلنتهای دندانی بهمنظور جایگزینی دندانهای از دست رفته به کار میروند و بررسی عملکرد بیومکانیکی آنها تحت سناریوهای مختلف بارگذاری، از ملاحظات مهم در برنامهریزی درمان است. هدف این مطالعه، بررسی، تحلیل بیومکانیکی و مقایسه ایمپلنت دندان آسیای اول فک پایین در دو حالت ایمپلنت تکپایه و ایمپلنت دوپایه است. بدین منظور، یک ایمپلنت با قطر بیشتر (۵ میلی متر) متناسب با ابعاد تاج دندان، تحت شرایط بارگذاری استاتیکی و دینامیکی (ضربه) با استفاده از تحلیل المان محدود مورد بررسی قرار گرفت. نتایج هر دو تحلیل نشان داد که دو ایمپلنت ۳ میلی متری در فک پایین ایجاد کردند که بیانگر کاهش تمرکز تنش است. با این حال، بیشترین تنش مشاهده شده در ناحیه گردن ایمپلنت برای ایمپلنت تکپایه کمتر بود که نشان دهنده توزیع بار مطلوب تر در حالت تکپایه است.

كلمات كليدى: ايمپلنت دنداني، ايمپلنت دوتايي، ايمپلنت دندان آسياب، تحليل المان محدود، ضربه

نويسندگان: محدثه سادات حسيني ميانگفشه - سيد عطااله هاشمي











كد مقاله: icbme-1170

عنوان مقاله: تجزیه و تحلیل رفتار بیماران پارکینسون با استفاده از نیروسنج صفحه ای مبتنی بر هوش مصنوعی

چکده: تشخیص زودهنگام بیماری پارکینسون و ارزیابی روند پیشرفت آن، نقشی حیاتی در بهینهسازی توانبخشی و اجرای مداخلات درمانی دارد. در این مطالعه، یک الگوریتم یادگیری ماشین مبتنی بر دادههای نیروسنج صفحهای برای شناسایی خودکار علائم حرکتی در مراحل اولیه بیماری مورد بررسی قرار گرفت. هدف اصلی، استخراج ویژگیهای مرتبط با علائم حرکتی و بهکارگیری آنها بهمنظور تشخیص زودهنگام بیماری بود. دادههای ۱۵ فرد مبتلا به بیماری پارکینسون و ۱۵ فرد سالم برای ارزیابی انتخاب شدند. ویژگیهای مکانی—زمانی بهعنوان ورودی طبقهبندی کننده جنگل تصادفی استفاده شدند. این مدل یادگیری ماشین با استفاده از ویژگیهای استخراجشده از آزمونهای تعادل و ایستادن از حالت نشسته، توانست علائم حرکتی بیماری را با دقت قابل توجه ۸۳٬۳۳٪ شناسایی کند. با وجود محدودیت تعداد نمونهها، این روش پتانسیل بالایی در کاربردهای بالینی برای تشخیص و پایش روند بیماری دارد و می تواند در مطالعات آینده با گسترش دادهها بهبود یابد.

كلمات كليدى: بيمارى پاركينسون، تشخيص بيمارى، خوشهبندى، نيروسنج صفحهاى، يادگيرى ماشين

نویسندگان: شیدا ورزشی، روزبه عابدینی نسب، محمد نجفی آشتیانی، مهراد پوریوسف میاندوآب











كد مقاله: icbme-1106

عنوان مقاله: طراحی ربات نرم پوشیدنی مچ پا با کنترل پیشبین مدل برای توان بخشی پس از سکته

چکیده: افتادگی پا ((Foot Drop)یکی از شایع ترین عوارض حرکتی پس از سکته مغزی است که راه رفتن بیمار را مختل کرده و خطر سقوط را افزایش می دهد. ارتزهای متداول، اگرچه از افتادگی پا جلوگیری می کنند، اما به دلیل ماهیت ایستا و عدم تطابق با نیاز بیمار، منجر به ضعف عضلانی و محدودیت حرکتی می شوند. این مقاله یک راهکار نوین مبتنی بر رباتیک نرم برای این چالش ارائه می دهد. در این پژوهش، یک ربات پوشیدنی نرم برای مفصل مچ پا طراحی شده است که از عملگرهای پارچهای مبتنی بر ماهیچههای مصنوعی پنوماتیکی (RAMsبهره می برد. این طراحی، ضمن تأمین ایمنی و راحتی بیمار، امکان تولید گشتاور کمکی متناسب با فازهای مختلف گامبرداری را فراهم می آورد. برای کنترل دقیق این سیستم با دینامیک شدیداً غیرخطی، یک استراتژی کنترل پیشبین مدل ((MPC فرمول بندی شده است. این کنترل کننده با پیش بینی رفتار آینده سیستم غیرخطی، یک استراتژی کامر پیشبین حرکتی مطلوب را با دقت بالا دنبال کند و محدودیتهای ایمنی مفصل را تضمین نماید. تابیج شبیه سازی های انجام شده در محیط MATLAB/Simulinkشان می دهد که سیستم پیشنهادی قادر است الگوی گامبرداری پاتولوژیک را با موفقیت اصلاح کرده و به مسیر مرجع گامبرداری سالم نزدیک سازد (خطای جذر میانگین مربعات کمتر از ۲ درجه). این نتایج، پتانسیل بالای ترکیب رباتیک نرم و کنترل پیش بین را برای توسعه نسل جدیدی از ابزارهای کمتر از ۲ درجه). این نتایج، پتانسیل بالای ترکیب رباتیک نرم و کنترل پیش بین را برای توسعه نسل جدیدی از ابزارهای هوشمند توان بخشی اثبات می کند.

كلمات كليدى: توان بخشى سكته، ربات پوشيدني، ربات نرم، كنترل پيشبين مدل، ماهيچه مصنوعي پنوماتيكي، مفصل مچ پا

نویسندگان: امیرحسین اختراعی طوسی، یگانه خراشادی زاده









كد مقاله: icbme-1058

عنوان مقاله: محاسبه نیروی عضلانی اندام تحتانی و نیروی تماسی مفصل زانو در بیماران مبتلا به استئوآرتریت زانو

چکده: استئوآرتریت زانو از شایعترین بیماریهای مزمن مفصلی در سالمندان است که با تغییرات عصبی-عضلانی، اختلال در حس عمقی و پایداری مفصل زانو همراه است. این مطالعه با هدف بررسی الگوی فراخوانی عضلات، شاخص همانقباضی (Cl) و نیروی تماسی مفصل زانو در بیماران مبتلا به استئوآرتریت در شرایط مختلف ایستادن انجام شد. دادههای سه بیمار و سه فرد سالم در چهار حالت آزمون (چشم بازابسته و ایستادن روی زمین/صفحه ناپایدار) تحلیل گردید. از ترکیب نرمافزارهای OpenSim با اعمال شرط پایداری مکانیکی هسیان، تخمین نیروهای عضلاتی و مفصلی انجام شد. نتایج نشان داد بیماران در شرایط ناپایدار و حذف بینایی، فعالیت عضلاتی و همانقباضی بیشتری داشتند. در حالت چشمبسته روی سطح ناپایدار، عضلات مرکزی تنه در بیماران بیشینه همانقباضی ۵۳٪ داشتند (در برابر ۳۰٪ در افراد سالم). عضلات مایل شکمی، راسته رانی و تبییالیس قدامی در شرایط ناپایدار بیشترین فعالیت را داشتند. همچنین نسبت نیروی تماسی زانوی غیر در گیر به وزن بدن در بیماران تا ۶۰۲۸ افزایش پایداری و کاهش خطر افتادن در بیماران استئوآرتریت فراهم می کند.

كلمات كليدى: استئوآرتريت زانو، ايستادن، مدلسازى اسكلتى-عضلاني، همانقباضي، نيروى تماسى مفصل

نويسندگان: مجتبي صفري، محمد نجفي آشتياني، فاطمه السادات علوي











كد مقاله: icbme-1090

عنوان مقاله: تحلیل بیومکانیکی موقعیت بهینه زاویه چرخش استابولوم پس از جراحی پریاستابولار استئوتومی گنز با مدلسازی سهبعدی و تحلیل المان محدود

چکیده: دیسپلازی هیپ یکی از شایع ترین ناهنجاریهای مفصل ران است که در صورت عدم درمان مناسب، می تواند به آر تروز زودرس و کاهش عملکرد حرکتی منجر شود. روشهای سنتی سنجش پارامترهای رادیو گرافیک بهدلیل وابستگی به مهارت ناظر و رودرس و کاهش عملکرد حرکتی منجر شود. روشهای سنتی سنجش پارامترهای را دیرازند. این پژوهش با هدف بهینهسازی موقعیت زاویه چرخش استابولوم پس از جراحی پریاستابولار استئوتومی گنز (PAO) با بهره گیری از مدل سازی سهبعدی و تعلیل المان محدود انجام شد. مدل سهبعدی استخوانها و غضروفها از دادههای سیتیاسکن بیمار تهیه و با شبکهبندی تتراهدرال وارد نرمافزار آباکوس شد. بارگذاری بر اساس نقاط آناتومیکی اتصال عضلات و با گام زمانی ۲۰۰۸ ثانیه در طول سیکل گیت انجام گرفت. نتایج تحلیل نشان داد که انتخاب بهینه زوایای چرخش در صفحات کرونال و ساژیتال باعث افزایش سطح تماس غضروفی مفصل به میزان ۱۵٪ و کاهش بیشینه فشار تماسی از 10.00 MPa در حالت اولیه به 9.30 MPa وضعیت بهینه میشود (کاهش حدود ٪۷). این تغییرات موجب توزیع یکنواخت تر بار در مفصل، کاهش خطر فرسایش غضروف و وضعیت بهینه میشود (کاهش حدود ٪۷). این تغییرات موجب توزیع یکنواخت تر بار در مفصل، کاهش خطر فرسایش غضروف و بهبود کارایی مکانیکی مفصل ران میشوند. یافتهها ضرورت استفاده از مدلسازی سهبعدی و تحلیل المان محدود را برای برنامهریزی دقیق جراحیهای اصلاحی در بیماران مبتلا به دیسپلازی هیپ تأیید میکنند.

كلمات كليدى: جراحى گنز، زاويه چرخش استابولوم، درد مزمن، غضروف مفصلى ، مفصل هيپ

نویسندگان: سامرند نانوازاده، دکتر سروش مداح، دکتر سید محمود مدرسی











كد مقاله: icbme-1217

عنوان مقاله: تحلیل بیومکانیکی تعادل ایستایی در جوانان و سالمندان بر روی سطوح پایدار و ناپایدار با استفاده از شاخصهای سینتیکی نیروی واکنشی زمین

چکده: این پژوهش به بررسی تفاوتهای بیومکانیکی تعادل ایستایی میان افراد جوان و سالمند در شرایط مختلف دیداری و سطحی پرداخته است. در این مطالعه، ۳۰ شرکت کننده سالم شامل ۱۶ جوان (۲۰–۱۸ سال) و ۱۴ سالمند (۶۰ سال) شرکت کردند. پس از حذف افرادی با بیماریهای اسکلتی-عضلانی، تعداد نهایی شرکت کنندگان به ۳۰ نفر رسید. شرایط آزمایشی شامل چهار حالت ایستادن (چشم باز/بسته بر روی سطح پایدار/ناپایدار) بود. شاخصهای سینتیکی اصلی شامل انحراف معیار و فرکانس میانه، از مؤلفههای نیروی واکنشی زمین استخراج شد. نرمال بودن دادهها با آزمون شاپیرو-ویلک بررسی شد و در صورت نرمال بودن از آزمون من-ویتنی استفاده شد. نتایج نشان داد که سالمندان در شرایط چالش برانگیز (سطح ناپایدار و چشم بسته) انحراف معیار و فرکانس میانه پایین تری نسبت به جوانان داشتند. این تفاوتها بیشتر در راستای قدامی-خلفی معنادار بود و در سایر راستاها اختلاف چشمگیری مشاهده نشد. این یافتهها نشان دهنده افزایش نوسان در سالمندان است و کاهش کارایی سیستمهای عصبی-عضلانی در حفظ تعادل را نشان میدهد. این نتایج می تواند به پیشگیری از سقوط و طراحی مداخلات توان بخشی کمک کند.

كلمات كليدى: تعادل ايستايي، جوانان، سالمندان، سطوح پايدار و ناپايدار، نيروى واكنشي زمين، شاخصهاي سينتيكي

نویسندگان: فرشته موسوی کنک لو، علیرضا هاشمی اسکویی، شقایق حسن زاده خانمیری











كد مقاله: icbme-1399

عنوان مقاله: تاثیر تمرین با تردمیل آبی بر کینماتیک پرش- فرود فوتبالیستهای حرفهای

چکیده: فرود نامناسب پس از پرش، رایج ترین عامل آسیب رباط صلیبی قدامی زانو است که بهدلیل تکنیک نامناسب، فشار زیادی به این رباط وارد کرده و منجر به پارگی آن میشود. هدف از پژوهش حاضر، بررسی تاثیر ۶ هفته تمرینات تناوبی روی تردمیل آبی برکینماتیک پرش-فرود فوتسالیستهای حرفهای بود. این مطالعه از نوع نیمه تجربی روی بازیکنان تیم فوتسال آلومینیوم اراک بود. جامعه آماری به صورت تصادفی به دو گروه کنترل (n=8) و تجربی (n=8) تقسیم شد در مراحل پیش آزمون و پس آزمون، کینماتیک پرش-فرود آزمودنیها حین اجرای آزمون الدess با بهره گیری از دوربین فیلمبرداری و نرمافزار Kinovea تحلیل شد و پس از پایان دوره تمرینی، دادههای پس آزمون از هر دو گروه جمع آوری گردید. برای تحلیل آماری دادهها، از آزمون تی مستقل جهت مقایسه بین گروهی و آزمون تی زوجی برای مقایسه درون گروهی، با بهره گیری از نرمافزار SPSS و در سطح معنیداری د. ۱۰۰۰ استفاده گردید. نتایج نشان داد که پس از شش هفته تمرینات تناوبی روی تردمیل آبی اختلاف معناداری در کینماتیک پرش-فرود بین گروه کنترل و تجربی مشاهده نشد (20.5≤۲). نتایج بهدستآمده از این تحقیق نشان داد، فوتسالیستهای حرفهای نیاز به اجرای پروتکلهای تمرینی متفاوتی از تحقیق حاضر دارند، تا بتواند بر کینماتیک پرش-فرود آزها مؤثر باشد. بنابراین پیشنهاد می شود در تحقیقات آتی این مورد مدنظر قرار گیرد.

كلمات كليدى: : كينماتيك پرش-فرود، تردميل آبي، تمرينات تناوبي، رباط صليبي قدامي زانو ، فوتساليستهاي حرفهاي

نویسندگان: صفورا قاسمی، مسعود گلیایگانی، امیرحسین نجیمی











كد مقاله: icbme-1376

عنوان مقاله: کاربرد بیومکانیک و آنالیز راهرفتن در بهینهسازی درمان کودکان مبتلا به فلج مغزی: مرور ادبیات

چکیده: فلج مغزی شایع ترین ناتوانی حرکتی دوران کودکی است که در اثر آسیب یا رشد غیرطبیعی مغز ایجاد می شود. اگرچه ماهیت این اختلال عصبی است، پیامدهای آن در حرکت، هماهنگی، تعادل و وضعیت بدن بروز می ابد. عوامل بروز فلج مغزی می توانند در دوره پیش از بارداری، حین بارداری، هنگام تولد یا پس از آن رخ دهند. از نظر بالینی، این بیماری به سه نوع اصلی اسپاستیک (حدود ۸۰٪)، دیسکینتیک (۵۱٪) و آتاکسیک (۵٪) تقسیم می شود. روشهای درمانی گوناگونی برای کاهش عوارض این بیماری وجود دارد و آنالیز راه رفتن شامل ارزیابیهای سینماتیکی، تخمین نیرو و بررسی فعالیت عضلانی، ابزاری کلیدی برای شناسایی ناهنجاریهای حرکتی و انتخاب مناسب ترین رویکرد درمانی است. اهمیت نقش بیومکانیک راه رفتن در این زمینه بهویژه با بهره گیری از فناوریهای نوین آنالیز حرکت برجسته تر می شود. این مقاله مروری به بررسی کاربرد آنالیز حرکت، دسته بندیهای آن ورشهای تخمین نیرو و فعالیت عضلانی و مقایسه آنها با الگوی راه رفتن طبیعی در کودکان مبتلا به فلج دری می پردازد و بر نقش این تحلیلها در بهینه سازی تشخیص و انتخاب مؤثر ترین روش درمانی تأکید دارد.

كلمات كليدى: تحليل حركات بدن، بيومكانيك، تخمين نيروهاى عضلاني، فلج مغزى، راه رفتن.

نویسندگان: علی جعفری، علیرضا هاشمی اسکویی، شقایق حسنزاده خانمیری











كد مقاله: icbme-1346

عنوان مقاله: طراحی آتل شخصی سازی شده با روش نیمه خودکار پردازش تصاویر

چکده: در این پژوهش، یک الگوریتم نوین به منظور طراحی و ساخت آتلهای ارتوپدی شخصیسازیشده بر پایه تصاویر رادیولوژی (DICOM) توسعه داده شده است. الگوریتم ارائه شده که در محیط پایتون پیادهسازی شده، به صورت نیمهخودکار عمل می کند؛ به طوری که کاربر پارامترهایی نظیر ابعاد تصویر، آستانه رنگی بافت پوست و نقاط کلیدی بر روی سطح ناحیه آسیبدیده را مشخص مینماید. در ادامه، این نقاط به نرمافزار CAD)سالیدورکس) منتقل شده و منحنیهای متناظر با سطح پوست، با استفاده از حداقل دو تصویر رادیولوژی با زوایای عمود بر هم، بازسازی میشوند. مدل اولیه تولیدشده ممکن است دارای ناهمواریها و خطاهای اولیه باشد که این موارد از طریق ترسیم دستی منحنیهای هموارساز و اصلاحات نهایی در نرمافزار Meshmixer برطرف می گردند. در نهایت، طرح بهینه برای فرآیند ساخت افزایشی (پرینت سهبعدی) ساخته میشود. نتایج این تحقیق نشان داد که طراحی بهینه آتل برای ساخت، شامل یک ساختار دوتکه با بدنه متخلخل به منظور افزایش کارایی و راحتی کاربر است.

كلمات كليدى: آتل، ابرنقاط، انحنا، پوست، پرينت سه بعدى، طيف خاكسترى.

نویسندگان: محمد مهدی صفاری، محمدرضا سجادی











Bioelectric Abstracts: ICBME-

1325	1354	1162	1326	1229	1049	1271	1262	1269	1007
1327	1052	1008	1278	1307	1451	1373	1140	1242	1284
1209	1207	1101	1299	1372	1474	1180	1105	1248	1115
1280	1088	1429	1444	1085	1243	1431	1123	1035	1059
1193	1053	1353	1253	1311	1046	1467	1265	1414	1423
1396	1343	1249	1104	1017	1226	1130	1425	1395	1179
1463	1055	1365	1358	1273	1196	1317	1084	1144	1470
1445	1430	1040	1152	1461	1446	1458	1368	1166	1418
1344	1268	1352	1164	1099	1448	1197	1267	1111	1127
1295	1057	1143	1208	1069	1286	1042	1400	1364	1285
1108	1066	1098	1045	1168	1276	1172	1153	1378	1453
1062	1301	1070	1060	1465	1380	1064	1241	1215	1125
1367	1440	1384	1370	1018	1392	1251	1449	1266	1231
1321	1219	1462	1244	1424	1322	1279	1192	1129	1139
1389	1025	1335	1246	1473	1421	1255	1302	1374	1034
1436	1224	1336	1150						



Article Code: icbme-1326

Article Title: Multi-Level Driver Fatigue Detection Using EEG Signals with CNN-LSTM Models in a Compressed Sensing Framework

Abstract: Driver fatigue is a major contributor to road accidents, leading to reduced attention, slower reaction times, and impaired decision-making. This study presents a multi-level fatigue detection framework based on electroencephalography (EEG) signals, in which a Convolutional Neural Network (CNN) is employed to extract spatial patterns, and a Long Short-Term Memory (LSTM) network is used to model temporal dynamics in a cascaded architecture. To handle the high dimensionality and redundancy of EEG data, Compressed Sensing (CS) is applied with various compression ratios. Experimental results demonstrate that the proposed system achieves over 90% accuracy and an F1-score above 90% in multi-level fatigue classification. Even at a compression ratio of CR = 40%, the accuracy remains above 90%, while reducing the data volume by approximately 40%. Additional analyses using sensitivity, specificity, Cohen's kappa, and ROC curves confirm the superiority of the proposed approach compared to baseline models (without CS or with simpler architectures). These findings indicate that the proposed framework is well-suited for real-time, portable driver monitoring systems.

Keywords: driver fatigue, multi-level classification, CNN, LSTM, compressed sensing, EEG.

Authors: Sobhan Sheykhivand - Nastaran Khaleghi











Article Code: icbme-1180

Article Title: Continuous non-invasive blood pressure estimation based on impedance plethysmography measurements

Abstract: Continuous blood pressure (BP) monitoring is vital for cardiovascular care, yet existing cuffless methods often suffer from multi-sensor complexity and motion artifacts. This paper presents a novel, simplified approach for non-invasive, continuous BP estimation using a single-channel impedance plethysmography (IPG) system. A mathematically derived model correlates arterial impedance fluctuations directly with BP dynamics, enabled by a two-stage calibration process. To maximize signal fidelity, electrode configuration and injection current frequency (50 kHz) were rigorously optimized using a 3D forearm model in COMSOL Multiphysics, incorporating fluid-structure interaction (FSI) and electrical simulations. The proposed model was validated in MATLAB, demonstrating that an optimized electrode arrangement (29 mm stimulation, 12 mm sensing distance) achieved peak sensitivity ($\Delta Z = 41.47 \text{ m}\Omega$). BP estimation results exhibited exceptional accuracy, with a mean absolute error (MAE) of 0.67 mmHg, a root mean square error (RMSE) of 1.39 mmHg, and a 0.998 correlation to the reference pressure. The system's performance surpasses the AAMI standard, confirming the viability of a single-sensor IPG approach as a low-cost, wearable alternative to complex multi-sensor methods for daily healthcare monitoring.

Keywords: Continuous blood pressure non-invasive monitoring impedance plethysmography (IPG) wearable device mathematical modeling two-stage calibration COMSOL simulation

Authors: Fatemeh Shokri - Masoomeh Ashoorirad - Rasool Baghbani











Article Code: icbme-1431

Article Title: Fixed-Frequency Impedimetric Detection of Sickle Cells Using Interdigitated

Electrodes

Abstract: Sickle cell disease (SCD) causes red blood cells (RBCs) to adopt an abnormal, stiff, crescent-like shape, impairing their ability to flow smoothly through small blood vessels and disrupting normal circulation. These morphological changes are associated with altered blood function and clinical complications, making rapid and accurate detection of sickle cells essential for disease monitoring and management. In this study, we presented an impedimetric detection approach using interdigitated comb electrodes combined with fixed-frequency electrical impedance measurement. As RBCs pass through the sensing region, impedance variations were recorded and analyzed, allowing reliable differentiation between normal and sickle cells. Numerical results demonstrated that sickled RBCs exhibit distinct impedance profiles compared with healthy cells. This label-free, real-time method is well suited for miniaturized platforms and can be seamlessly integrated into lab-on-a-chip devices. The proposed system provides a versatile framework for developing rapid, point-of-care diagnostic tools and offers potential applications in monitoring SCD and other blood disorders. By combining insights from cellular biophysics with microelectrode engineering, this technique highlights the promise of fixedfrequency impedimetric measurements as a scalable and accurate strategy for cellular characterization in biomedical engineering research and applications.

Keywords: Sickle cell disease (SCD), impedimetric detection, red blood cells (RBCs), interdigitated electrodes, fixed-frequency measurement

Authors: Arezoo Savlani - Mobina Ghanbari - Majid Badieirostami - Mohammadjavad Bouloorchi











Article Code: icbme-1130

Article Title: An RZ-OOK Modulation Technique for Joint Data Rate and Output Power Tuning in Biomedical Applications

Abstract: This paper introduces an energy-efficient configuration approach for on-off-keying (OOK) modulation, which is employed in a power amplifier (PA). The presented power amplifier features a dynamic multi-mode design that allows for adjustable data rates and output power in various modes, making it highly suitable for biomedical applications. By tweaking the duty cycle of the input data, the PA achieves an adjustable data rate, generating return-to-zero (RZ) data for RZ-OOK modulation. This modulation method ensures a direct correlation between data rate and power consumption, empowering the transmission of diverse power levels within allocated power constraints. The RZ data is also used to reconfigure the output power. The PA is designed in 180 nm CMOS technology, supports data rates that vary from 0.3 Mb/s to 3 Mb/s, and provides output power levels from -23 dBm to 0 dBm. When adjusting data rates, power dissipation ranges from 0.099 mW to 0.99 mW at an output power of 0 dBm. Moreover, the PA draws between 0.07 mW and 0.99 mW over the tuning range of the output power at the maximum amount of data rate.

Keywords: PA, RZ-OOK, Data Rate, Adjustable, Modulation, Biomedical

Authors: Tayebeh Azadmousavi - Esmaeil Najafiaghdam











Article Code: icbme-1436

Article Title: Magnetic Catheter Robot with Reduced Friction for Endovascular Minimally Invasive Access

Abstract: Endovascular interventions require rapid access and minimal invasiveness to target sites. Catheterization is an effective approach for treating vascular diseases but faces challenges in efficiency and safety within narrow, tortuous vasculature. Here, we present a soft magnetic-polymer catheter robot that combines distributed magnetic actuation with a nanoscale, Hydrogel-based skin to enable active steering and reduced surface friction for minimally invasive endovascular access. The catheter exhibited rapid, large-angle bending in response to low-strength external magnetic fields, allowing safe traversal of confined, convoluted channels. Light-induced hydrogel grafting markedly increased surface hydrophilicity, reducing the water contact angle from $\approx 100^{\circ}$ (uncoated) to $\approx 48^{\circ}$ (coated), and friction measurements in a blood-mimicking fluid (falling-sphere assay) demonstrated lower friction for hydrogel coated samples compared with uncoated controls, indicating reduced insertion and sliding forces. The thin, strongly bonded hydrogel layer preserves the catheter's compliance and magnetic responsiveness, supporting safer, more adaptable navigation and the potential to expand reach in difficult-to-access vasculature.

Keywords: endovascular interventions, magnetic catheter robot, magnetic actuation, minimally invasive access.

Authors: Sina Eskandary - Mohammad Amin Salati - Rezayat Parvizi - Farhang Abbasi











Article Code: icbme-1279

Article Title: Design and Development of A Focal Vibrating Massager with Wide Frequency Range and Real-Time Control

Abstract: Vibration therapy has gained increasing recognition as an effective modality for promoting musculoskeletal health, rehabilitation, and pain management. In this study, we introduce a novel vibration massager equipped with a frequency-controlled actuation system and a dual-peak cam mechanism. The design enables precise modulation of vibration frequency within the therapeutic range of 75-225 Hz while minimizing motor speed requirements, thereby improving energy efficiency and system durability. Frequency stabilization is achieved through a reflective optical sensor in combination with a PID controller, ensuring consistent vibratory output under varying operational conditions. The modular nature of the device further allows for versatile deployment, whether as a handheld tool, fixed to the body via a fixture, or integrated with robotic arms in clinical environments. By combining engineering innovations with adaptability in use, this work provides a foundation for advancing vibration-based therapeutic technologies and opens new pathways for integration in clinical practice.

Keywords: Vibration Therapy, Focal Vibrating Massager, Biomedical Device Design, Mechanoreceptors, Cam and Follower, PID Control

Authors: Ali Bakhshian Talkhoncheh - Mohammad Yousefi - Saeid Niknami - Borhan Beigzadeh











Article Code: icbme-1025

Article Title: A Telemedicine Approach to Therapist-Free VR Exposure Therapy for Acrophobia: A pilot study

Abstract: Acrophobia, an excessive fear of heights, impairs daily functioning and quality of life. While exposure therapy is effective, therapist dependence limits accessibility. This pilot study evaluates a fully automated, therapist-free virtual reality (VR) system that dynamically adjusts exposure intensity using real-time biosignals (heart rate/blood pressure) to treat acrophobia.

Twenty participants with clinically confirmed acrophobia underwent a 27-session protocol featuring three phases: voluntary exploration, adaptive exposure (VR scenarios modulated by physiological feedback), and abrupt stress challenges. The system combined Unity-based VR environments (HTC Vive Pro Eye) with real-time biosignal monitoring (Polar H10, Finapres NOVA) to personalize therapy.

Results demonstrated significant reductions in physiological arousal (mean heart rate 19%, systolic BP 18%) and anxiety (29.3% reduction in STAI-Y1 scores, p<0.001). Retention rates (90%) and safety outcomes surpassed traditional therapist-guided methods.

This study provides first evidence that biosignal-driven, autonomous VR exposure therapy can achieve outcomes comparable to clinician-led approaches, offering a scalable telemedicine solution. Future work should validate efficacy in larger cohorts.

KeyWords: Acrophobia Autonomous VRTherapy Real-time Biosignal Adaptation Telemedicine Exposure Therapy

Authors: Arya Gholipoor Hanizi - Samaneh Minakhani - Poorya Gholipoor











Article Code: icbme-1325

Article Title: Design and fabrication of a cost-effective dry electrode for electroencephalography (EEG) signal acquisition

Abstract: An electrode is a conductive material that, on one side, is connected to a metallic component (such as a copper wire) and, on the other side, to a non-metallic component (such as a semiconductor, electrolyte, or vacuum) within an electrical circuit, establishing a connection between them. Biological electrodes provide a link between the human body and an electrical circuit, ultimately enabling the circuit to transmit useful data to a computer for analysis in various applications.

Various types of electrodes are used for recording bio-potentials, which, based on the type of contact, can be classified into two categories: (1) wet electrodes and (2) dry electrodes. Wet electrodes require the application of conductive materials, such as conductive gel, before attachment to ensure optimal contact. However, these materials can cause inconveniences for both the patient and the operator, such as the need to prepare the skin (e.g., shaving) or to clean the site after signal acquisition. Consequently, dry electrodes have become increasingly popular due to their ease of use for both patients and operators. Nonetheless, one challenge of this type of electrode is the high electrical contact impedance caused by the absence of conductive substances. In this study, a low-cost dry electrode based on a silver-powder sintering process on a copper substrate was designed to enhance EEG signal quality and signal-to-noise ratio (SNR) without requiring conductive gels.

Keywords: Bio-signal, Electroencephalography (EEG), Dry Electrode, Contact Impedance, Sintering Method

Authors: Sobhan Sheykhivand - Nastaran Khaleghi - Lida Zareh Lahijan











Article Code: icbme-1327

Article Title: Design and Evaluation of a Low-Cost Dry Electrode for Physiological Signal Acquisition

Abstract: Electrodes function as conductive interfaces and are generally classified into wet and dry types. While wet electrodes are widely used in physiological signal acquisition, their reliance on conductive gels makes them unsuitable for long-term applications. In contrast, dry electrodes offer a promising alternative for extended monitoring; however, commercially available options are often expensive and less accessible. In this study, we designed and fabricated a cost-effective dry electrode using a sintering-based manufacturing method and selected conductive materials. The proposed electrode was evaluated in various physiological signal acquisition experiments and compared to a standard wet electrode from the OpenBCI brand. Experimental results demonstrate that the fabricated electrode provides an economically viable solution without compromising signal quality, making it suitable for prolonged physiological monitoring.

Keywords: Dry electrode, physiological signals, EEG acquisition, biomedical instrumentation, low-cost design.

Authors: Sobhan Sheykhivand - Nastaran Khaleghi - Maryam Khoshkhabar











Article Code: icbme-1365

Article Title: Integration of High-Speed AFM Nanomechanical Profiling with Deep Spatiotemporal Learning for Early Response Assessment and Tumor Stage Prediction in Oncolytic Virotherapy

Abstract: Oncolytic virotherapy is a promising cancer treatment that selectively targets malignant cells and activates antitumor immunity. However, its clinical progress is limited by the absence of reliable early biomarkers for treatment response. Conventional methods such as imaging and molecular assays provide delayed or indirect feedback, restricting timely therapeutic adjustments. Here, we present a novel framework integrating high-speed atomic force microscopy (AFM) nanomechanical profiling with deep spatiotemporal learning to enable rapid assessment of therapeutic response and tumor stage prediction. Human tumor cell lines infected with clinically relevant oncolytic viruses (HSV-1, VSV, NDV) were analyzed by AFM to capture cellular stiffness, elasticity, topography, and nanovibrational signatures within the first 24 hours post-infection. A hybrid CNN-LSTM architecture was implemented to automatically extract spatial and temporal features from multimodal AFM data. Our results demonstrate that the proposed method distinguishes responders from non-responders with an accuracy of 95.3% (AUC = 0.964) and predicts tumor stage with 92.7% accuracy (AUC = 0.941). Responding cells exhibited early softening, enhanced nanovibrational activity, and membrane roughening, while non-responders showed attenuated changes. The approach consistently outperformed baseline classifiers (SVM, random forest, logistic regression) and achieved reproducible results across biological replicates. This study establishes AFM-AI integration as a rapid, label-free, and non-destructive biomarker platform for real-time monitoring of oncolytic virotherapy. By enabling early response detection and stage prediction, it provides a pathway toward patient stratification and precision oncology.

Keywords: Oncolytic Virotherapy, Atomic Force Microscopy, Nanomechanical Profiling, Deep Learning / CNN-LSTM, Early Response Biomarkers

Authors: Alireza Haghighatjoo - Fatemeh Noori - *Peyman Afshari Bijarbaneh* - Seyed Amirhossein Mousavi











Article Code: icbme-1219

Article Title: Comparative Evaluation of Feature Selection Techniques for Six-Month Mortality Prediction in Heart Failure Patients

Abstract: Heart failure (HF) is a leading cause of hospitalization and mortality worldwide. Accurate early prediction of six-month mortality can support timely and informed clinical decision-making. This study presents a reproducible machine learning pipeline for predicting six-month mortality in HF patients using the MIMIC-III critical care database. We systematically evaluated multiple feature selection methods to identify the most informative features for an XGBoost classifier. Model performance was assessed using recall and ROC-AUC scores within a consistent 10-fold cross-validation framework. Among the tested methods, the L1-based selector achieved the highest performance, with a recall of 0.738 and a ROC-AUC of 0.678.

Beyond performance benchmarking, analysis of the selected features revealed both convergence and diversity across methods. Consistently identified predictors included age, BNP, creatinine, BUN, sodium, hemoglobin, and LVEF, all of which are well-established markers of HF prognosis. Comorbidities such as atrial fibrillation, hypertension, and chronic renal failure were frequently highlighted by Boruta and mutual information, while SHAP emphasized renal markers (creatinine, WRF), BNP, and hemoglobin, aligning closely with clinical evidence. These findings demonstrate that the proposed pipeline not only improves model performance but also yields clinically interpretable insights that are in agreement with established HF risk factors.

Keywords: heart failure, six-month mortality prediction, machine learning, MIMIC-III, feature selection, XGBoost, SMOTEENN

Authors: Parsa Haghighatgoo – Somayeh Afrasiabi











Article Code: icbme-1172

Article Title: Multiclass ICU Length-of-Stay Prediction Using Tree-Based Machine Learning Techniques

Abstract: Accurate prediction of intensive care unit (ICU) length-of-stay (LOS) is essential for patient management and resource planning. This study compares four tree-based machine learning models—Random Forest, XGBoost, LightGBM, and CatBoost—for multiclass LOS prediction using the MIMIC-III database. A total of 42,306 ICU stays were processed with 17 physiologic variables and discretized into 10 ordered LOS classes. Models were evaluated using quadratic-weighted Cohen's kappa (κ) and Mean Absolute Deviation (MAD) to capture ordinal agreement and temporal accuracy.

CatBoost achieved the best performance ($\kappa = 0.444$, MAD = 124.66 hours), effectively predicting both short- and long-stay patients, which are operationally critical. XGBoost and Random Forest provided intermediate results, while LightGBM showed lower temporal precision (MAD = 164.19 hours). The results demonstrate that CatBoost's ordered boosting strategy and native handling of categorical variables enable robust, interpretable predictions suitable for clinical and operational decision-making.

These findings highlight the potential of tree-based machine learning to transform ICU LOS prediction from a retrospective metric into a proactive, reliable and interpretable tool for optimizing patient flow, resource allocation and decision-making. The study provides a foundation for future improvements using richer time-series data, multimodal inputs, and multicenter validation.

Keywords: multi-class prediction, ICU length of stay, CatBoost, MIMIC III, Area Under Curve

Authors: Mahyar Mohammadian - Somayeh Afrasiabi











Article Code: icbme-1064

Article Title: Modeling Attention Performance Across Female Reproductive Aging Using Logistic Regressio

Abstract: Reproductive aging in women is associated with cognitive decline, particularly in attention domains. This study investigates the use of machine learning, specifically logistic regression, to predict attentional performance during different reproductive aging stages. A total of 100 healthy women, 50 premenopausal (mean age = 29.5) and 50 postmenopausal (mean age = 54.8), underwent neuropsychological evaluation using the Montreal Cognitive Assessment (MoCA) and the Integrated Visual and Auditory (IVA-2) test. Among the applied supervised models, logistic regression achieved 95.0% accuracy in 10-fold cross-validation and 100% on the test set. The analysis revealed a strong inverse correlation between reproductive aging and auditory attention subscores. These results suggest that logistic regression offers a reliable, interpretable, and clinically applicable model for early detection of attention decline, supporting its integration into biomedical screening tools.

Keywords: Attention, Reproductive Aging, Logistic Regression, Machine Learning, MoCA, IVA-2

Authors: Zahra Zehtabi - Leila Mehdizadeh Fanid - Pedram Salehpoor - Mahdi Jafari Asl











Article Code: icbme-1007

Article Title: Leveraging Online Data to Enhance Medical Knowledge in a Small Persian Language Model

Abstract: The rapid advancement of language models has demonstrated the potential of artificial intelligence in the healthcare industry. However, small language models struggle with specialized domains in low-resource languages like Persian. While numerous medical-domain websites exist in Persian, no curated dataset or corpus has been available—making ours the first of its kind. This study introduces a newly curated dataset comprising 20k doctor-patient Q&A pairs and 60% of a 90-million-token crawled corpus from medical magazines. Using a parameter-efficient fine-tuning approach, we enhanced the medical knowledge of the baseline model, aya-expanse-8b. Benchmark evaluations demonstrate that the fine-tuned model achieves improved accuracy in medical question answering and successfully passed the Iranian Basic Medical Science Entrance Exam (IBSEE) in September 2023, which the baseline model did not. Additionally, the fine-tuned model improved Persiantranslated MMLU accuracy by an average of 2.67%. This work highlights the potential of leveraging open-access online data to enrich small language models in medical fields, providing a novel solution for Persian medical AI applications suitable for resource-constrained environments. Future research could explore multimodal input to further enhance performance.

Keywords: persian medical question answering, small language model, medical language models, data crawling

Authors: Mehrdad Ghassabi - Pedram Rostami - Hamidreza Baradaran kashani - Amirhossein Poursina - Zahra Kazemi - Milad Tavakoli











Article Code: icbme-1284

Article Title: Enhancing population diversity and optimization efficiency in cat swarm optimization using a fuzzy controllers

Abstract: Optimization plays a critical role in artificial intelligence and various computational tasks. Metaheuristic algorithm such as GA, PSO, and CSO are widely used, yet CSO suffers from low exploration due to rapid convergence. In this study, we propose a fuzzy-based enhancement to CSO to increase population diversity and prevent premature convergence. A fuzzy controller dynamically adjusts agent velocities based on the execution stage and fitness relative to the global best. The proposed method was evaluated on ten complex benchmark functions, each executed 30 times to ensure statistical validity and compared to the standard CSO, Particle Swarm Optimization (PSO) and Genetic Algorithm (GA). Experimental results show that the fuzzy-based CSO significantly improves convergence accuracy and avoids local optima, achieving an average improvement of 12.4% in solution quality over the standard CSO and outperforming PSO and GA in 80% of the test cases. The proposed scheme can be applied in optimization of biomedical data such as learning of weights in deep learning structures and biomedical data analysis.

Keywords: Cat Swarm Optimization, Fuzzy Inference System, Chaotic Operators, Metaheuristic Algorithms, Optimization

Authors: Seyedeh Maryam Rezaei - Reza Boostani











Article Code: icbme-1059

Article Title: Enhancing Drug-Target Affinity Prediction with Non-Local Block Graph Neural Networks

Abstract: Predicting how strongly a drug binds to its protein target is key to speeding up drug discovery. Many graph neural networks excel with local chemical features but often overlook important long-range contacts, particularly when they become deep and challenging to train. In this paper, we present a compact graph neural network model, called NLB-DTA, that adds a single non-local attention block between two light convolutional layers in distinct ligand and protein streams. This block considers the contribution of each atom to other atoms in the molecular downstream and residues in the protein downstream in a single step, capturing distant interactions between atoms and residues. Tested on the widely used Davis dataset, the model achieves state-of-the-art accuracy with high generalization. Since NLB-DTA needs only standard ligand strings and protein sequences, it can run on common GPUs. Our study shows that using a non-local layer is effective in considering the long-range information gap, and so it offers a practical foundation for future virtual screening.

Keywords: Drug target affinity, Graph neural network, Non-local attention, Protein ligand interaction, Virtual screening, Deep learning, Contact maps, Kinase

Authors: Reza Tahmasebi - Eghbal Mansoori - Armin Pishehvar - Abbas Mehrbaniyan









Article Code: icbme-1085

Article Title: A Comprehensive Architecture for Smart Hospitals: Leveraging IoT, AI, and Data Science

Abstract: This paper proposes a novel, comprehensive three-layer architecture for smart hospitals, which tightly integrates the Internet of Things (IoT), Artificial Intelligence (AI), and Data Science. Unlike previous reviews or generalized models, our core scientific contribution is the development of a mathematically supported, security-centric framework designed to solve three critical, coupled challenges in healthcare: data security, system interoperability, and real-time scalability. We demonstrate how this specific integration, leveraging Dijkstra's algorithm for optimized network routing and Bayesian inference for probabilistic diagnostic modeling, moves beyond simple information gathering to provide a functional blueprint for operational efficiency and superior patient outcomes. We also point out privacy flaws and suggest a multi-layered security model, therefore offering a road map for further developments in smart healthcare systems.

Keywords: Internet of Things, Artificial Intelligence, Data Science, Smart Hospital, Healthcare Security, Big Data.

Authors: Jafar Abdollahi - Laya Mahmoudi - Babak Nouri-Moghaddam











Article Code: icbme-1311

Article Title: The Technological Pillars of Smart Hospitals: A 2022–2025 Review of IoMT, Wearables/RTLS/RFID, Robotics (IoRT), and VR/AR

Abstract: Smart hospitals are rapidly evolving into hyper-connected care environments that blend Internet of Medical Things (IoMT), sensing-centric wearables with RTLS/RFID, assistive and soft robotics within the Internet of Robotic Things (IoRT), and immersive VR/AR applications. This review (2022-2025) synthesizes three complementary streams: (i) IoMT architectures and security, highlighting perception-edge/fog-cloud layering and hardwareanchored trust such as PUFs, alongside blockchain-enabled integrity and SDN-based network control; (ii) continuous patient monitoring and operational intelligence via wearable sensors, RFID, and RTLS for asset/patient tracking, workflow optimization, and error reduction; and (iii) robotics / IoRT and VR / AR for telepresence and remote examinations, logistics and UV-based disinfection, personalized soft-robotic rehabilitation, clinician training, analgesia/anxiolysis, and telesutgical use cases. Cross-cutting challenges 5G-enabled interoperability/standardization, privacy/cybersecurity, and explainable AI, cost and changemanagement barriers, and the scarcity of longitudinal, system-level evaluations in real-world hospital deployments. Building on the integrated evidence base, we propose a unified taxonomy and a four-layer system blueprint that links multimodal sensing and edge analytics to governance-grade integration, and we present a consolidated comparison table (advantages vs. challenges) across IoMT, Wearables/RTLS/RFID, IoRT robotics, and VR/AR. We conclude with a forward agenda prioritizing standards-based interoperability, robust security/ethical frameworks, cost-benefit analyses, and prospective clinical evaluations to advance scalable, outcome-driven adoption in smart hospital ecosystems.

Keywords: Smart hospital; Internet of Medical Things (IoMT); Wearables; RFID; RTLS; Internet of Robotic Things (IoRT); Assistive/Soft robotics; VR/AR; Interoperability; Cybersecurity.

Authors: Ali Karami-Nejad - Naeme Kadkhodai Eliaderani - Sahar Jafari - Mahdi Jafari Asl











Article Code: icbme-1008

Article Title: Gene expression changes induced by Atorvastatin in breast cancer and stem cells

Abstract: This research focuses on how atorvastatin influences gene expression in breast cancer cell lines (MCF-7, MDA231, BT474, and SKBR3) and human pluripotent stem cells (iPSCs), using bioinformatics data from the GEO database. The results showed that atorvastatin significantly enhances the expression of key cholesterol metabolism-related genes, such as SQLE, ACAT2, HMGCS1, NSDHL, HMGCR, and DHCR7. Although atorvastatin is widely recognized for its cholesterol-lowering properties and cardiovascular benefits, our findings indicate it may also play a dual role by promoting the proliferation and migration of cancer cells through the upregulation of these genes. To further investigate the biological interactions among the differentially expressed genes, a protein–protein interaction (PPI) network was constructed using the STRING database. The analysis revealed strong interactions among cholesterol biosynthesis proteins, especially HMGCR and DHCR7, which have been associated with heightened growth and migration abilities in gastric and breast cancer cells. These observations raise concerns about atorvastatin's potential carcinogenic effects, highlighting the need for more comprehensive studies to better understand its impact on these genes and its role in cancer development.

Keywords: Atorvastatin, Bioinformatic, Cholesterol Metabolism, Gene Expression, Breast Cancer Cell line& Induced Pluripotent Stem Cells.

Authors: Seyed Mahdi Mousavi - Yaghub Pazhang











Article Code: icbme-1268

Article Title: Enhancing Type 2 Diabetes Diagnosis with Evolutionary Algorithms and Machine Learning

Abstract: Type 2 diabetes is a widespread chronic disease that requires early and accurate diagnosis to prevent serious complications. Traditional diagnostic methods often lack sufficient accuracy, which highlights the need for more reliable computational solutions. In this study, we propose a model that integrates the Random Forest classifier with the Bat Optimization Algorithm for simultaneous feature selection and hyperparameter tuning. The SMOTE-ENN method was first applied to the Pima Indians Diabetes Database to correct class imbalance and remove noisy or ambiguous samples, producing a more balanced and cleaner dataset. The optimized model trained on this refined dataset achieved 89% accuracy, 88% precision, 90% recall, and an F1-score of 89%, clearly outperforming the baseline Random Forest and other existing approaches. These results demonstrate the potential of combining evolutionary algorithms with ensemble learning to provide a practical and cost-effective tool for early detection of type 2 diabetes in clinical practice.

Keywords: Diabetes, Diabetes Diagnosis, Machine Learning, Evolutionary Algorithms, Feature Selection

Authors: Parisa Rezaei - Mohsen Saffar - Hamid Reza Naji - Mohammad Mehdi Faghih - Rasoul Nouriazar











Article Code: icbme-1162

Article Title: Predictive Modeling of Astronaut Skin Microbiome Changes Using Machine Learning on NASA Multi-Omics Data

Abstract: Spaceflight imposes distinct physiological and environmental stresses that disrupt the human skin microbiome a vital interface mediating barrier integrity, immune signaling, and host adaptation. This study introduces a novel integrative machine learning framework that systematically connects NASA multi-omics datasets (GLDS-566 and OSD-574, Inspiration4 mission) to predict spaceflight-associated microbial shifts at a systems level. Using four pre-flight and four post-flight astronaut skin swab samples, microbial abundance profiles were modeled through a hybrid feature selection strategy combining mutual information and recursive feature elimination. Among four tested classifiers Logistic Regression, Random Forest, Support Vector Machine, and Naïve Bayes Logistic Regression achieved the highest performance (accuracy = 0.875, F1 = 0.865) under repeated cross-validation, emphasizing the capability of simpler models to capture subtle microbiological patterns within small, high-dimensional datasets. The framework identified four discriminative Taxonomic IDs (1283, 1654, 2642494, 543736), primarily linked to Staphylococcus and Corynebacterium, which are central to maintaining skin homeostasis. Their differential abundance between pre- and post-flight samples suggests microbial adaptations to spaceflight stressors such as microgravity, radiation, and humidity fluctuations mechanisms analogously observed in biomaterial surface adaptation systems. Unlike prior studies focusing solely on descriptive microbial variation, the present work advances a predictive modeling approach, enabling microbiome-based biomarker discovery for precision astronaut health monitoring. This proof-of-concept demonstrates the feasibility of autonomous microbial surveillance in space environments and establishes a reproducible computational foundation for future integration with broader datasets like the Space Omics and Medical Atlas (SOMA) to enhance long-duration mission healthcare resilience.

Keywords: Machine Learning Microbiome Spaceflight Multi-Omics Logistic

Regression Feature Selection Biomedical Engineering

Authors: Mahdi Ansari - Abolfazl Hajihashemi - Mohammad Rafienia











Article Code: icbme-1251

Article Title: A Comparative Analysis of Simulated and Experimental Acoustic and Thermal Behavior of HIFU

Abstract: High-Intensity Focused Ultrasound (HIFU) represents a promising non-invasive approach for achieving thermal ablation in biomedical applications. Computational models are frequently used to guide the clinical optimization of HIFU; however, thorough experimental validation is necessary to ensure their predictive accuracy. This study provides a validation of a k-Wave-based computational model by contrasting its predictions with experimental data from an ex-vivo porcine liver. Initially, using an appropriate hydrophone, the acoustic pressure field of a HIFU transducer was measured. Next, with the aid of the k-Wave toolbox, numerical simulation of the acoustic field in heterogeneous media was conducted. Subsequently, the thermal ablation effects were evaluated by comparing the dimensions of the physical lesion in the porcine liver to the lesion predicted by a thermal dose model. With a mean percentage difference of 2.7% for the axial length and 33.3% for the transverse width for the lesion dimensions, the experimental and simulated results exhibited good correlation regarding lesion dimensions. These findings confirm the fidelity of the computational model, supporting its use for future HIFU treatment planning and optimization.

KeyWords: AcousticPressur Field Bioheat Transfer numerical Modelling Experimental Validation High-Intensity Focused Ultrasound (HIFU) Thermal Ablation

Authors: Maryam Fazeli - Remi Souchon - Cyril Lafon - Mehran Jahed











Article Code: icbme-1098

Article Title: Silver Nanodisc Metasurface As Geometrical Tunable Absorber for Tailored

Thermal Emission

Abstract: Photothermal therapy (PTT) is a promising, minimally invasive approach, for cancer treatment. PTT relies on nanostructures with optimized light absorption for localized heating. This paper addresses this challenge by designing and analyzing a plasmonic metasurface with a Metal-Insulator-Metal (MIM) configuration for enhanced absorption and thermal emission in the mid-infrared region. Using the FDTD method in Ansys Lumerical software, the spectral response of a silver (Ag) nanodisc array was systematically investigated over a wavelength range of 2 to 6 μ m. The study analyzed the effect of varying the nanodisc diameter (600, 700, 800, and 900 nm). Results reveal that the 600 nm diameter configuration is optimal, exhibiting maximum absorption and emissivity of approximately 61% at a resonant wavelength of 3.7 μ m. In accordance with Kirchhoff's law, this highly selective and efficient absorption makes the engineered metasurface an ideal candidate for PTT applications requiring precise light-to-heat conversion.

Keywords: Tunable Metasurface Silver Nanodiscs Thermal Emission Plasmonic Perfect Absorber Mid-Infrared (Mid-IR)

Authors: Leila Ghasemzadeh - Sajjad Mortazavi - Karim Abbasian











Article Code: icbme-1249

Article Title: A Computational Model of Phase-Delayed Balanced Biphasic Deep Brain Stimulation for Essential Tremor in a Cerebellar-Basal Ganglia-Thalamocortical Network

Abstract: The Essential Tremor is one of the most common movement disorders that significantly reduces life quality of the patients. The Deep brain stimulation (DBS) has been proposed as an effective treatment for this disease, but the selection of optimal stimulation parameters remains a major challenge and is often based on the trial and error. Using comprehensive computational models to simulate brain networks and investigate the effects of different DBS pulses could be an important step in improving the understanding of the disease mechanism and designing more accurate and efficient treatment protocols. For this purpose, in this study, a computational model of cerebellar-basal ganglia thalamocortical (CBGT) network has been developed, including key areas such as basal ganglia with neurons of Subthalamic Nucleus (STN), Globus Pallidus Externa (GPe) and Globus Pallidus Interna (GPi), the striatum with neurons of the D1 Medium Spiny Neuron (D1 MSN), D2 Medium Spiny Neuron (D2 MSN) and Fast Spiking Interneuron (FSI), and the thalamocortical with neurons of the Nucleus Reticularis Thalami (nRT), the Cortex, the Deep Cerebellar Nuclei (DCN), Thalamus (Th), and or the Ventral Intermediate Nucleus of Thalamus (Vim). Then, three types of stimulation, including rectangular monophasic DBS, symmetrical rectangular biphasic DBS, and phasedelayed balanced rectangular biphasic DBS have been simulated on GPi and GPe neurons in Parkinsonian conditions. The results show that phase-delayed balanced rectangular biphasic stimulation at a frequency of 100 Hz and a pulse width of 4 ms is the most effective pattern in reducing beta band oscillations (0.1-0.2) and controlling GPi and GPe burst discharges, and ultimately controlling tremor. On the other hand, phase-delayed balanced rectangular biphasic DBS stimulation has led to a reduction in power loss and heat and causes minimal damage to brain tissue. These findings indicate that the correct selection of pulse type and DBS parameters can provide the greatest therapeutic capability for the patients with essential tremor in Parkinson's disease (PD) by reducing side effects.

Keywords: Essential Tremor (ET), CBGT network model, Monophasic DBS, Biphasic DBS, Parkinson's Disease (PD).

Authors: Shabnam Andalibi Miandoab - Nazlar Ghasemzadeh











Article Code: icbme-1018

Article Title: Prediction of cardiac arrhythmia via an improved hierarchical fused fuzzy deep learning

Abstract: Deep Neural Networks, are widely applied in various fields such as healthcare. Cardiac arrhythmias, particularly non-sinusoidal arrhythmias, represent a critical challenge in cardiovascular diagnostics. As the volume of data generated by humans, including numbers, images, signals, and sounds continues to grow, the importance of DNNs in data analysis becomes more evident. This research focuses on cardiac arrhythmia classification using a Deep Fuzzy Neural Network. The proposed FDNN integrates fuzzy logic (FL) and deep learning (DL) to effectively address traditional deep learning models' limitations in handling data uncertainty and variability. FDNN demonstrates superior performance, achieving high accuracy. precision, and recall, supported by an impressive ROC curve and AUC value of 0.95, outperforming both traditional and advanced neural network-based methods. interpretability of the FDNN model, supported by techniques like SHAP values, integrated gradients, and calibration analysis, further reinforces its potential for clinical adoption and trust in its decision-making process. This paper highlights potential of combining FL with DL for medical applications, particularly in arrhythmia Prediction, offering a robust solution for accurate classification. Extended cross-validation (5- to 30-fold) confirms its robustness, with deep learning models showing consistent gains ($\sim 1-5\%$) over conventional approaches. These results highlight FDNN's potential for reliable arrhythmia detection, emphasizing the advantage of advanced architectures in medical diagnostic.

Keywords: Cardiac arrhythmia, Deep Neural Networks, Non-sinusoidal arrhythmias, Fuzzy Deep Learning, Cardiovascular diagnostics.

Authors: Arman Daliri - Nora Mahdavi











Article Code: icbme-1034

Article Title: HEALTH: Hyperbolic Embedding and Acoustic-based Learning for Topological

Hierarchies in Parkinson's Disease

Abstract: Parkinson's disease (PD) is a neurodegenerative disorder with heterogeneous motor and non-motor features that complicate early diagnosis. Acoustic biomarkers have emerged as non-invasive predictors, yet classical models often fail to capture the hierarchical nature of progression. We introduce HEALTH (Hyperbolic Embedding and Acoustic-based Learning for Topological Hierarchies), a framework that integrates graph-based similarity modeling, hyperbolic geometry, clustering, and explainable classification to analyze dysarthric speech in PD. Sustained phonation recordings were embedded in a two-dimensional Poincaré disk, where hyperbolic distances reflected latent acoustic dissimilarities. Optimization reduced reconstruction loss by ~95%, and silhouette coefficients stabilized near 0.44, indicating robust cluster separation. SHAP analysis highlighted pitch entropy, amplitude variability, and frequency measures as key determinants, enhancing clinical interpretability. Compared to Euclidean approaches, HEALTH achieved superior stratification and explainability. These findings demonstrate the potential of hyperbolic embeddings as scalable, interpretable tools for non-invasive monitoring and precision diagnostics in PD.

Keywords: Parkinson's disease, Hyperbolic embedding, Acoustic biomarkers, Explainable AI, Disease progression modeling.

Authors: Saghar Shafaati - S. Hossein Erfani











Article Code: icbme-1040

Article Title: Diagnosis of Multiple Sclerosis Using Recurrence Plot of EEG

Abstract: Multiple sclerosis (MS) is a chronic disease of the central nervous system, and early diagnosis plays a crucial role in reducing complications and improving patients' quality of life. This study aims to detect MS using EEG signals. The signals include visual responses from three pathways Magno, Parvo, and Konio and were extracted from 9 occipital channels. From this plot, recurrence quantification analysis (RQA) features were extracted and classified using the Random Forest algorithm. The method's performance was evaluated using accuracy, sensitivity, specificity, and AUC metrics. Results showed that the Parvo pathway, in O2 and PO3 channels, achieved the best performance with 90.63% accuracy. Sensitivity was 93.75% and 87.50%, specificity was 87.50% and 93.75%, and AUCs were 93% and 89%, respectively. Sensitivity analysis to the parameter ε indicated that proper tuning plays a key role in improving performance. Overall, the RP method, combined with RQA features and appropriate ε selection, provides an effective tool for MS diagnosis.

Keywords: Electroencephalogram (EEG) Phase Space Reconstruction Multiple Sclerosis (MS) (Recurrence Plot (RP Recurrence Quantification Analysis (RQA)

Authors: Neda Baghestani - Amin Janghorbani











Article Code: icbme-1060

Article Title: Unsupervised Gait Anomaly Detection Using Generative Adversarial Networks: A Feasibility Study

Abstract: Automated classification of human gait, a critical indicator of neuromuscular health, is often hindered by the dependence of supervised machine learning on extensive labeled pathological datasets, which are scarce and difficult to obtain. This paper explores the feasibility of a paradigm towards unsupervised learning, proposing a framework based on a Wasserstein Generative Adversarial Network with Gradient Penalty (WGAN-GP). The WGAN-GP is trained exclusively on healthy gait patterns from a single young subject's shank-mounted inertial measurement unit (IMU) to build a model of healthy movement. The framework utilizes a reconstruction-based anomaly detection strategy, where abnormalities are quantified by the magnitude of the error when attempting to reconstruct a new gait cycle from the learned healthy model. Evaluated using real-world data from healthy subjects (both young and old) and for individuals with Parkinson's disease, the model showed strong performance, achieving an area under the curve (AUC) of 0.96. Notably, the framework also demonstrated sensitivity to nonpathological, age-related variations in gait. This feasibility study demonstrates the ability of the proposed WGAN-GP-based unsupervised detection method as a data-efficient and generalizable alternative. Consequently, it paves the way for future validation on larger clinical datasets to characterize mobility impairments in various disorders and age groups.

Keywords: Gait Analysis, Anomaly Detection, Generative Adversarial Networks (GAN), Unsupervised Learning, Wearable Sensors, Feasibility Study

Authors: S. Hooman Hosseini-Zahraei - Ali Chaibakhsh











Article Code: icbme-1062

Article Title: Examination and Analysis of the Influence of Near-Infrared Light Absorption by Hair Melanin on fNIRS Signal

Abstract: In recent years, the use of functional near-infrared spectroscopy (fNIRS) technology has increased despite its limitations and weaknesses. However, further studies are still needed to assess the quality of the signals it produces. fNIRS utilizes near-infrared (NIR) wavelengths, which are known to be absorbed significantly by melanin, oxygenated hemoglobin (HbO), and deoxygenated hemoglobin (HbR). This presents a challenge for researchers employing fNIRS technology. In this study, we examined the average signal power feature, which changes in proportion to the absorption profile of various chromophores, to analyze how factors such as hair color, length, and density affect fNIRS signals. Due to abnormal data distributions within each group, confirmed by the Anderson-Darling test, we employed the Wilcoxon statistical test to compare group similarities. The p-values obtained from the Wilcoxon test revealed significant differences between the groups: those with dark versus light hair, varying hair densities, and different hair lengths. Our results indicated a decrease in the mean power of HbO, HbR, and optical density (OD) signals in individuals with dark hair, high hair density, and long hair length. Furthermore, we found that hair length and density had a more pronounced effect on the average signal power.

Keywords: Functional near-infrared spectroscopy (fNIRS), Melanin, Impact of skin and hair characteristics, Signal processing.

Authors: Elmira Baghaeifar - Sina Shamekhi











Article Code: icbme-1070

Article Title: Dual-View Data Representation and Contrastive Learning for Robust EEG-

Based Person Identification

Abstract: Person identification using EEG signals has emerged as a promising biometric modality due to the uniqueness and internal nature of brain signals. However, EEG signals are often noisy, task-dependent, and limited in quantity, posing challenges for reliable and generalizable identification. In this paper, we propose a novel dual-view learning framework that integrates both scalp-level spatial features and source-informed neural topology using convolutional and graph neural networks (CNN and GCN). The scalp view captures spatial-spectral representations through a CNN applied to differential entropy (DE) maps, while the neural view models inter-channel relationships via a GCN built on source-localized graphs. To improve generalization across tasks and sessions, we incorporate supervised contrastive learning, encouraging the model to cluster embeddings of the same individual regardless of task conditions. The proposed method is evaluated on the EEG Motor Movement/Imagery Dataset and achieves high accuracy across within-task and cross-task scenarios. Furthermore, it remains effective with reduced training data and benefits significantly from feature normalization. Experimental results and ablation studies confirm the contribution of each component and demonstrate the reliability of the approach for EEG-based biometric identification.

Keywords: Person identification, EEG signal, Dual-view representation, Contrastive learning

Authors: Mahdi Tabatabaei - Mohammad Bagher Shamsollahi











Article Code: icbme-1084

Article Title: Parkinson's Disease Classification Using EEG and a Hybrid EEGNet-LSTM Architecture

Abstract: Parkinson's disease (PD) is a common progressive neurodegenerative disorder that causes motor problems and cognitive-control problems that slowly get worse over time. These problems often show up years before a clinical diagnosis. To meet the need for objective early biomarkers, high-density electroencephalography (EEG) was recorded from 56 subjects (28 PD patients and 28 controls) while they did the Simon Conflict Task 200 times. This task tests how well people can stop themselves from responding when the conditions are the same or different. After a few preprocessing steps, which included 0.1-40 Hz band-pass filtering, commonaverage re-referencing, and independent component analysis (ICA) with ICLabel-guided artifact rejection, one-second epochs that were time-locked to the start of the stimulus were taken out. We then created a hybrid deep-learning framework that combined EEGNet for spatial feature extraction across 64 channels with three stacked bidirectional Long Short-Term Memory (LSTM) layers to capture temporal dynamics. Three shallow supervised models were used to classify the 64-dimensional spatiotemporal representations for each epoch: support vector machine (SVM), k-nearest neighbors (kNN), and an ensemble of SVM and Naïve Bayes. SVM did the best, with 89.7% accuracy, 91.8% sensitivity, and 85.0% specificity. This was a 5-10% improvement over traditional handcrafted-feature classifiers (p < 0.01). These results show that end-to-end spatial-temporal feature learning from task-evoked EEG is a powerful, non-invasive way to accurately separate Parkinson's patients and the control group.

Keywords: Parkinson's Disease, Electroencephalography, Machine Learning, Simon Conflict, Deep Neural Networks

Authors: Pouya Taghipour Langrodi - Amirsadra Khodadadi - Ali Sadat Modaresi - Mohammad Ahadzadeh - Mostafa Rostami - Sadegh Madadi











Article Code: icbme-1105

Article Title: Classification of Delta Band Motor Imagery EEG Signals in SCI Patients using the Regularized Common Temporal Pattern Method

Abstract: Accurate classification of motor imagery tasks is essential for enhancing brain-computer interfaces (BCIs) in spinal cord injury (SCI) rehabilitation. The use of raw time samples often overlooks temporal dependencies in electroencephalography (EEG), limiting classification accuracy. We propose the Regularized Common Temporal Pattern (RCTempP), a novel time-domain feature extraction method that emphasizes discriminative temporal samples. RCTempP was evaluated on EEG recordings from SCI patients imagining five distinct hand movements within the 0.3–3 Hz band. Compared to raw time samples, Common Temporal Pattern (CTP), and Extended CTP (ECTP) approaches, RCTempP yielded statistically significant improvements in eight out of ten class pairs, for which the average accuracy across subjects ranged from 70.4% to 75.1%. Performance was assessed using a fivefold cross-validation protocol to ensure robust and generalizable results. Importantly, RCTempP's significant temporal filters emerged post-cue onset and corresponded to movement-related cortical potential peaks. These findings highlight RCTempP's promise for advancing motor imagery BCIs in SCI rehabilitation.

Key Words: Brain Computer Interface, Spinal Cord Injury, Motor Imagery, Feature Extraction, Regularized Common Temporal Pattern

Authors: Mahdi Babaei - Sorena Shadzinavaz - Sepideh Hajipour Sardouie











Article Code: icbme-1108

Article Title: Analyzing Blood Glucose Levels with Near Infra-Red Spectroscopy and Chemometric Multivariate Methods

Abstract: In this study, near-infrared (NIR) absorbance spectra of blood samples were obtained using the Fourier Transform Infrared (FT-IR) technique. It was observed that multiplying the absorbance spectra by the first derivatives of the water and glucose absorbance profiles efficiently suppresses the interference caused by water in the blood, thus enabling a clearer identification of glucose-specific peaks. When applied in principal component regression (PCR) analysis, this approach yields lower prediction errors compared to PCR based on raw absorbance data, while requiring fewer principal components. Moreover, estimating blood glucose concentration through a linear regression model constructed from glucose molar absorptivity values also provides satisfactory predictive accuracy.

Key Words: Non-invasive glucose monitoring; Near-infrared spectroscopy (NIR); Principal component regression (PCR); Molar absorptivity; Spectroscopic data analysis

Authors: Hadi Barati - Arian Mousavi Madani - Soheil Moradi - Mohammad Mohsen Ebrahimi Seyghalan - Mehdi Fardmanesh











Article Code: icbme-1123

Article Title: Comparative Analysis of Machine Learning and Deep Learning Models for Epileptic Seizure Detection Using the CHB-MIT EEG Dataset

Abstract: Epilepsy is one of the most common neurological disorders that usually comes with sudden and unpredictable seizures and can severely affect the quality of life of patients. This study aims to design and evaluate different artificial approaches for automated seizure detection using EEG signals from the CHB-MIT dataset. This dataset contains 23 patients suffering from epileptic seizures, including boys and girls aged between 1.2 to 22 years old. Feature extraction was performed across time, frequency, and time-frequency domains. Eight classifiers were implemented in this study, including four machine learning algorithms (SVM, KNN, Decision Tree, and naïve Bayes) and four deep learning architectures (Artificial Neural Network, LSTM, TCN, and Transformer). The results demonstrated that the LSTM and TCN models outperformed other classifiers in detecting the preictal and ictal stages, achieving an accuracy of 96.0% and 97.3% with the sensitivity of 93.5% and 90.5%. Moreover, ANN and Transformer achieved 94.8% and 93.2% accuracy. In contrast, SVM, KNN, DT, and NB represented 93.1%, 92.4%, 81.2%, and 71.9% in accuracy. By preparing a uniform data preparation baseline for the CHB-MIT dataset, this study made an identical comparison between machine learning and deep learning models to propose the best approach for epileptic seizure detection.

Key Words: Epilepsy, Neural Networks, Seizure Detection, Electroencephalography, EEG, Deep Learning, Machine Learning, LSTM

Authors: Pouya Taghipour Langrodi - Amirsadra Khodadadi - Mahtab Dastranj - Golnaz Baghdadi











Article Code: icbme-1125

Article Title: Dynamics modeling of cardiac electromechanical intervals and hysteresis analysis

Abstract: This study explores hysteresis in cardiac electrical and mechanical responses to heart rate changes. Specifically, the focus is on the RT interval (as a surrogate for QT) and the systolic interval (S1S2), extracted from ECG and PCG signals, respectively. Long Short-Term Memory (LSTM) models were trained to capture the dynamic relationship between RR intervals and each of these modalities. To evaluate temporal memory, synthetic step-like RR inputs were used, and the corresponding delays in model outputs were analyzed. The results showed clear hysteresis in both RT and S1S2 intervals, with delays increasing at higher workloads (i.e., shorter RR), indicating slower cardiovascular adaptation. In contrast, visual inspection of hysteresis curves revealed that the diastolic interval (S2S1) exhibits negligible delay, suggesting an almost instantaneous response. The low correlation between RT- and S1S2-based delay patterns further implies that electrical and mechanical dynamics reflect complementary aspects of cardiac regulation. These findings highlight the importance of time-aware modeling in characterizing autonomic cardiovascular function.

Key Words: ECG signal, PCG signal, Electromechanical intervals, Dynamic behavior modeling, Hysteresis

Authors: Sina Asadi - Mohammad Bagher Shamsollahi











Article Code: icbme-1127

Article Title: Dynamic Classification of Resting-State EEG Using Adaptive Functional Connectivity in Mild Traumatic Brain Injury

Abstract: Mild Traumatic Brain Injury (mTBI) is a common and potentially life-threatening medical condition that can lead to long-lasting physical and cognitive impairments and accounts for 90% of all TBIs. Brain injury is associated with disrupted connectivity resulting from damage to the axons. This study investigated brain connectivity using resting-state electroencephalogram (EEG) signals in patients with mTBI. Hence, a novel hybrid approach, namely Adaptive Intrinsic Warped Connectivity (AIWC), has been proposed to examine functional connectivity, based on empirical mode decomposition, analytical representation, and dynamic warping techniques. AIWC effectively reveals dynamic, nonlinear coupling patterns that reflect the brain's spontaneous organization and transition states. An analysis has been conducted to compare the detection performance of the proposed connectivity features across symmetrical or asymmetrical channel pairs. The study also examined the effects of several sessions after injury, as well as the utilization of amplitude and phase information through the Recurrent Neural Network as a dynamic mapping procedure. The suggested algorithm has been tested using resting-state EEG signals from the initial session, as well as at two- and four-month follow-ups with 52 individuals diagnosed with mTBI and 31 healthy controls. The results obtained show a high average accuracy rate of 99.22%. The analysis has also demonstrated the proposed feature's higher performance across the frontal lobe, frontal-parietal, frontal-temporal, and frontal-occipital regions.

Key Words: Adaptive Intrinsic Warped Connectivity, Dynamic connectivity feature, Functional Connectivity, Mild Traumatic Brain Injury, Recurrent Neural Network.

Authors: Farzaneh Manzari - Peyvand Ghaderyan











Article Code: icbme-1129

Article Title: Binary Discrete Emotion Detection with Peripheral and Fp1-Fp2 EEG Signals on PEEFS Dataset

Abstract: This study presents a binary discrete emotion detection approach that integrates peripheral physiological signals with EEG recordings from the Fp1 and Fp2 channels, using data from the PEEFS database. Features from both modalities were extracted to classify emotions in two scenarios: 1) individual emotions versus a neutral state, and 2) between discrete emotion pairs. Results indicate that peripheral signals generally outperform EEG alone, particularly in distinguishing emotions such as happiness and sadness from neutral, with F1-scores above 90%. However, EEG proves critical in specific cases; for instance, distinguishing between fear and neutral emotions achieves 88.9% accuracy using EEG alone, and reaches 100% accuracy when combined with peripheral signals. Similarly, emotion pairs involving fear, anger, and disgust benefit substantially from EEG integration, achieving perfect classification accuracy in several instances (e.g., fear-anger, disgust-anger). Overall, the combined modality consistently enhances performance across tasks. These findings highlight the complementary role of minimal EEG alongside peripheral signals in emotion recognition, supporting the development of practical and reliable systems for emotion monitoring applications.

Key Words: Emotion Detection, PEEFS Dataset, Peripheral Physiological Signals, Binary Classification, minimal EEG channels

Authors: Fatemeh Shalchizadeh - Sina Shamekhi - Mahdi Jafari Asl











Article Code: icbme-1139

Article Title: Comparative Analysis of Time-Frequency Representations for Pediatric Respiratory Sound Classification Using Deep Learning

Abstract: Respiratory sound classification has emerged as a promising non-invasive and scalable tool for the early detection of respiratory disorders. While most previous studies have relied on a single feature extraction method—such as Mel-frequency cepstral coefficients (MFCC), Mel-spectrograms, or Short-Time Fourier Transform (STFT)—this study provides a comprehensive comparative analysis of these three approaches, evaluated individually, in pairwise combinations, and in a combined three-method configuration. Experiments are conducted on the SPRSound dataset, a pediatric respiratory sound database comprising 6,656 annotated events from seven unbalanced classes. Three architectures are assessed under identical preprocessing and augmentation strategies: a custom convolutional neural network (CNN), and two pre-trained models (VGG16 and InceptionV3) fine-tuned via transfer learning. Results show that STFT consistently delivers the highest performance for CNN and VGG16 models, while MFCC achieves the best accuracy with InceptionV3. Specifically, VGG16 with STFT attained 93.43% accuracy (score: 0.9545), whereas InceptionV3 with MFCC achieved the top performance within its architecture. These findings highlight the importance of aligning feature extraction techniques with model architecture and provide a systematic benchmark for SPRSound-based respiratory sound classification.

Key Words: respiratory sounds, classification, Deep-learning, Adventitious lung sounds, Convolutional neural network, transfer learning, VGG16, InceptionV3Introduction

Authors: Ghazaleh Shiri - Hanieh Bahrami - Alireza Fallahi











Article Code: icbme-1140

Article Title: Neural Correlates of Reward and Punishment Processing During Gambling-Based Decision-Making: A Simultaneous EEG-fMRI Study

Abstract: Understanding the neural feedback mechanisms that govern cognitive decisionmaking during reward and punishment processing is crucial for deciphering brain function. This study introduces the first simultaneous electroencephalography-functional magnetic resonance imaging (EEG-fMRI) investigation of a modified gambling task, analyzed using a General Linear Model (GLM) framework. In this study, we enrolled 24 participants and acquired simultaneous high-density 65-channel EEG and fMRI recordings to investigate neural correlates of reward and punishment processing during a modified gambling-based decision-making task. We extracted time-series data of event-related potential (ERP) components from EEG signals and modeled them using a Generalized Linear Model (GLM) framework. Unlike conventional sensor-level EEG analyses in EEG-fMRI studies, our method operates directly in the source domain, providing enhanced spatial resolution for identifying neural substrates of decisionmaking processes. Our findings demonstrate robust activation not only in canonical rewardprocessing regions identified in previous studies, but also reveal significant involvement of the olfactory cortex and fusiform gyrus - areas frequently overlooked in such investigations. The data show distinct yet overlapping neural substrates for reward and punishment processing: while the orbitofrontal cortex and insula respond to both winning and losing outcomes, we observed differential activation patterns for each condition. Specifically, winning stimuli preferentially engaged anterior cingulate cortex and the superior orbitofrontal gyrus, whereas losing stimuli activated the cingulate cortex, inferior frontal gyrus and medial superior frontal gyrus. These results provide novel insights into the neural mechanisms of reward processing, advancing our understanding of functional neuroanatomy in decision-making. Furthermore, our ERP-informed fMRI approach establishes a new methodological framework for investigating neurovascular coupling, offering enhanced spatiotemporal precision in mapping cognitive processes to their neural substrates.

Keywords: simultaneous EEG-fMRI, reward processing, gambling-based decision-making, win/loss gambling task, feedback-related negativity (FRN)

Authors: Elias Ebrahimzadeh - Amin Mohammad Mohammadi - Ahmad Hammoud - Lila Rajabion - Hamid Soltanian-Zadeh











Article Code: icbme-1150

Article Title: Region-Specific EEG Channel-Based Emotion Detection using Bi-directional Deep Neural Networks

Abstract: Emotion recognition using EEG signals has garnered significant attention due to its potential applications in affective computing and brain-computer interface technologies. However, the nonlinear and non-stationary nature of EEG signals presents challenges for designing accurate and efficient models. In this work, we propose a hybrid deep neural network that combines a 1D-CNN with a Bi-GRU. The DEAP dataset is utilized for model evaluation, focusing on region-specific channels, particularly those located in the frontal and occipital lobes, which are physiologically and anatomically known to play critical roles in emotional processing. The frontal lobe regulates and interprets emotions, while the occipital lobe contributes to the visual pathways involved in emotional perception. The proposed model achieved 99.9% accuracy with 14 channels and 99.8% with 8 channels, using 1D-CNN-BiGRU in a four-class setting in the test subset. This study demonstrates that selective utilization of physiologically significant EEG regions can lead to robust and efficient emotion recognition models. The proposed approach enhances the feasibility of real-time and wearable affective systems.

Keywords: Emotion Recognition, region-specific channels, EEG, DEAP, Deep Learning, Hybrid Networks, CNN, Bi-GRU

Authors: Mahdi Jafari Asl - Sina Shamekhi - Fatemeh Shalchizadeh











Article Code: icbme-1153

Article Title: Mapping Epileptic Networks: IED-Triggered Hemodynamic Changes Identified via Simultaneous EEG-fMRI Recordings

Abstract: A central goal of the presurgical evaluation for refractory focal epilepsy is the accurate delineation of the epileptogenic zone (EZ)—the cortical region indispensable for generating epileptic seizures. Given that electroencephalography (EEG) provides superior temporal resolution while functional magnetic resonance imaging (fMRI) offers enhanced spatial localization, integrating these modalities holds significant promise for improving epileptic focus identification. In this study, we first derived characteristic spike patterns by detecting and averaging interictal epileptiform discharges (IEDs) from extraoperative EEG recordings. These patterns were then correlated with intracranial EEG data to develop an automated system for precise temporal mapping of seizure activity. Finally, we convolved the resulting temporal regressor with the hemodynamic response function (HRF) within a general linear model (GLM) framework to achieve robust localization of epileptic foci. This study was performed on five medication-resistant epilepsy patients whose neuroimaging and electrophysiological data were acquired at the National Brain Mapping Lab (NBML). Our proposed methodology demonstrated strong concordance with clinical EEG findings across all five cases. Notably, for the three surgical candidates, the approach provided additional localizing information beyond conventional EEG data. Ouantitative analysis revealed statistically significant enhancements in both localization accuracy (p<0.05) and spatial precision (mean ± SEM: 2.3 ± 0.4 mm) compared to current gold-standard techniques reported in recent literature.

Keywords: Epilepsy, Simultaneous EEG-fMRI, Mapping Epileptic Networks, IED-Triggered Hemodynamic, Blood-oxygen-level dependent imaging (BOLD).

Authors: Elias Ebrahimzadeh - Hora Amoozegar - Mostafa Asgarinejad - Melika Akbarimehr - Hamid Soltanian-Zadeh











Article Code: icbme-1179

Article Title: Modulation of EEG Connectivity by Insular Cortex Stimulation: Frequency-Specific Effects and Interoceptive Implications

Abstract: This study examined the impact of targeted insular stimulation on EEG-based brain connectivity across multiple frequency subbands, using both correlation and coherence analyses. EEG data were collected from healthy participants both prior to and following transcranial direct current stimulation (tDCS) targeting the insular cortex. To identify significant channel-to-channel interactions, p-value matrices and heatmaps were generated for each subband. The results revealed that insular stimulation induced notable changes in connectivity, particularly within central and posterior regions, with the alpha and beta subbands showing the highest number of significant connections. Correlation analysis demonstrated greater sensitivity in the alpha and theta bands, while coherence was more effective in detecting changes within the beta and gamma bands, highlighting subband- and method-specific modulation patterns. Beyond its involvement in cognitive and sensory networks, the findings underscore the insula's central role in interoception—integrating bodily signals such as cardiac and visceral inputs to support self-awareness and emotional regulation. Overall, this study demonstrates that targeted insular stimulation can enhance functional interactions within sensory, cognitive, and interoceptive networks, supporting its potential application in neuromodulation-based interventions.

Keywords: EEG connectivity, Insula, Interoception, Brain networks, Neuromodulation, tDCS

Authors: Ramin Aghili Karampour - Alireza Fallahi - Reza Kazemi











Article Code: icbme-1193

Article Title: Investigation of the presence of movement intention during sequential hand movements using neurophysiological analyses of EEG signals

Abstract: Background: A brain–computer interface (BCI) is considered a promising tool in neurorehabilitation. For this purpose, movement intention can be detected from brain signals and used as a control command for a robotic device. In most existing studies, a rest interval is provided before each movement to allow the generation of movement intention. However, daily life activities are performed continuously, without such intervals.

Method: This paper focuses on detecting movement intention during sequential movements, using neurophysiological analyses that include movement-related cortical potentials (MRCP), event-related desynchronization/synchronization (ERD/ERS) patterns, and, for the first time, inter-trial phase coherence (ITC) analysis.

Results: The results showed that during sequential hand movements, including reaching, grasping and lifting objects of various weights, holding the object, lowering it, replacing it, releasing it, and returning the hand to its initial position, two movement intentions were present: the first before starting the hand movement, and the second during the holding phase of the object.

Conclusions: In this study, we demonstrated that it is possible to decode the next movement intention while performing the current movement, which can lead to the development of a new generation of intelligent neural prostheses.

Keywords: brain computer interface (BCI), movement related cortical potentials (MRCP), event related desynchronization (ERD), inter trial coherence (ITC), movement, intention, rehabilitation

Authors: Elnaz Eilbeigi











Article Code: icbme-1197

Article Title: Brain Network Reconfiguration During Creative Playmaking: A Task-fMRI

Study

Abstract: We investigated how large-scale brain networks support creative decision-making in soccer. Thirty-five male players completed the Standardized Video Task in Soccer (SVT), a video-based creativity task during fMRI; professional coaches rated the originality/feasibility of each imagined play. We computed topography-based high-order functional connectivity (tHOFC) between 100 cortical regions during the idea-generation ("Think") periods and compared the High and Low SVT groups across all edges using a max-statistic permutation test. Global connectivity did not differ between groups, but six edges linking a right peripheral-visual node to dorsal and ventral attention hubs were weaker in the High-SVT group. Across individuals, lower visual–attention connectivity correlated with higher creativity scores (r = -0.52, 95% CI -0.76 to -0.17, p = 0.006; significant after FDR correction at q = 0.05). These results indicate that selective decoupling, not global hyperconnectivity, characterizes creative playmaking and aligns with accounts of internally directed cognition. Methodologically, our connectivity analysis with strict permutation testing reveals subtle, task-locked network reconfigurations in sport cognition.

Keywords: Creative decision-making, task-fMRI, topography-based high-order functional connectivity (tHOFC)

Authors: Mohammd Rezaei - Mahdi Siami - Asghar Zarei - Alireza Talesh Jafadideh











Article Code: icbme-1208

Article Title: Goniometry and Electromyography Data Analysis for Knee Health Diagnosis using Machine Learning

Abstract: In this study, we employed the Sánchez dataset [1] comprising synchronized knee goniometric measurements and surface electromyography (sEMG) recordings from major knee flexor and extensor muscles to develop a machine learning-based classification system for knee joint health assessment. The dataset included biomechanical data from 11 healthy controls and 11 participants with diagnosed knee pathologies. Our analysis focused only on the data collected during walking trials. Accordingly, training data prepared through kinematic monitoring of knee joint angles and subsequent segmentation of complete gait cycles - from initial heel-strike through terminal swing phase. Thus, we compiled 48 datasets from healthy controls and 173 datasets from participants with knee abnormalities. Each dataset included synchronized sEMG signals from four major muscles (rectus femoris, biceps femoris long head, vastus medialis, and semitendinosus) along with knee goniometry data, all of them were captured through complete gait cycles. Here, various combinations of statistical, temporal, and wavelet features using SVM, LDA, and KNN classifiers for knee health assessment were evaluated. Goniometric data alone achieved the best index with 97.7% accuracy (LDA/SVM models) when incorporating at least one feature from each type. For sEMG signal combinations, optimal performance (93.8% accuracy with LDA) was obtained using solely semitendinosus muscle data with complete feature sets. Comparative analysis revealed wavelet features as the least effective individually, while combined feature sets consistently yielded superior results. The sEMG signals from other individual muscles or their various combinations, regardless of feature selection approach, consistently demonstrated inferior classification performance.

Keywords: Knee Health Diagnosis, Machine Learning, Feature Extraction, Goniometry, Surface Electromyography.

Authors: Mohammad-Reza Sayyed Noorani - Zahra Mahmoudi Anzabi - Sara Sharifi











Article Code: icbme-1209

Article Title: Toward Precision Psychiatry: Differentiating Depression and Psychosis Using EEG-Based Machine Learning Models

Abstract: Accurate differential diagnosis of major depressive disorder, psychosis, and psychotic depression remains a major challenge in psychiatry due to overlapping clinical symptoms and the reliance on subjective assessment tools. This study aimed to identify objective EEG-based neuromarkers that distinguish between these three diagnostic groups using quantitative EEG features and machine learning. Resting-state EEG was collected from 60 medication-free adult patients clinically diagnosed via DSM-based psychiatric interviews. A total of 26 linear and nonlinear features, including relative power, cordance, alpha peak frequency, Lempel–Ziv complexity, largest Lyapunov exponent, and sample entropy, were extracted across 19 scalp channels. Statistical group comparisons with FDR correction identified significant feature—channel combinations, which were then ranked using the MRMR algorithm. Stepwise feature inclusion and classification with SVM, KNN, and MLP were performed. Results showed that 42 selected features achieved optimal accuracy, with KNN yielding 96.53±0.20% accuracy. These findings highlight the potential of EEG neuromarkers to support precision psychiatry and improve diagnostic specificity.

Keywords: Major Depressive Disorder, Psychosis, Machine Learning, Statistical Analysis, Differential Diagnosis.

Authors: Vahid Asayesh - Mehdi Dehghani - Majid Torabi - Sepideh Akhtari-Khosroshahi - Maedeh Akhtari-Khosroshahi - Sebelan Danishyar











Article Code: icbme-1231

Article Title: Predicting Sleep Efficiency and Apnea Index Using ECG-Derived and Sleep Quality Features: A Machine Learning Approach

Abstract: Sleep quality and obstructive sleep apnea profoundly influence cardiovascular function, cognition, and overall well-being, yet conventional monitoring approaches remain largely invasive or cumbersome, underscoring the imperative for streamlined, non-invasive alternatives. Herein, we present a machine learning framework that synergistically integrates electrocardiogram (ECG)-derived features with sleep quality metrics to forecast sleep efficiency and apnea-hypopnea index (AHI). Drawing upon the ECSMP (A Dataset on Emotion, Cognition, Sleep, and Multi-Modal Physiological Signals) dataset—encompassing recordings from 89 healthy participants—we curated a subset of 33 subjects whose data exhibited complete and unimpaired capture across all ECG-sleep modalities, thereby ensuring analytical fidelity; incomplete records from the remaining participants, attributable to recording artifacts or procedural inconsistencies, were judiciously excluded to uphold data integrity. From these selected recordings, 22 ECG-derived and sleep quality features were extracted and subsequently refined through recursive feature elimination (RFE) to mitigate redundancy and enhance predictive salience. We evaluated three regression models—Ridge Regression, Random Forest, and Gradient Boosting—employing subject-based 5-fold cross-validation to generalizability across individuals. For sleep efficiency, Ridge Regression attained a mean R² of 0.8734, indicating a high degree of explained variance; by comparison, Random Forest registered an R² of 0.2756 for AHI, which underscores the formidable obstacles in modeling sporadic apnea episodes amid constrained empirical resources. Feature importance scrutiny further illuminated wake hours and deep sleep ratio as preeminent correlates for sleep efficiency, complemented by deep sleep ratio and ORS amplitude for AHI. Collectively, this framework lays a promising foundation for non-invasive, individualized sleep monitoring, offering reliable estimates of sleep efficiency and preliminary insights into apnea patterns, albeit within the constraints of a modest sample size.

Keywords: Sleep efficiency, Apnea index, ECG, Machine learning, Feature selection

Authors: Mahla Khodaverdi - Raheleh Davoodi











Article Code: icbme-1236

Article Title: The Impact of an Interactive Rehabilitation Protocol on Reorganization of Brain Networks in Children with Cerebral Palsy: A Pilot Study

Abstract: Hemiparetic cerebral palsy (HCP) is a condition caused by brain damage that affects one side of the body, making it difficult for children to control the muscles on the affected side and affecting their ability to perform daily tasks. Traditional motor rehabilitation methods often lack patient interaction and fail to produce sufficient neuroplastic changes. Therefore, this study presents a new interactive, game-based program enhanced with controlled mechanoreceptor stimulation for upper extremity rehabilitation. Five children with hemiparetic cerebral palsy participated in this rehabilitation intervention, which consisted of 15 sessions of 20 minutes each. The Fugl-Meyer Assessment (FMA) and electroencephalography (EEG) were used to quantify motor improvement and analyze the underlying neural mechanisms, respectively, before and after the intervention. Advanced signal processing techniques, including phaseamplitude coupling (PAC) and phase-phase coupling (PPC), were used to provide a deeper understanding of brain network dynamics and neuroplasticity after the intervention. The results of the FMA scores showed significant improvement in hand motor abilities. These findings were fully correlated with positive neurophysiological changes. PAC analysis showed increased neural efficiency and coordination, while PPC confirmed improved functional connectivity between key cortical regions. This study provides compelling evidence that integrated mechanoreceptor-game therapy not only improves physical function (FMA scores) but, uniquely, demonstrates superior neuroplastic changes (PAC/PPC) compared to traditional methods, validating its use in pediatric neurorehabilitation.

Keywords: neurorehabilitation, neuroplasticity, hemiparetic cerebral palsy (HCP), phase-amplitude coupling (PAC), phase-phase coupling (PPC)

Authors: Shahed Salehzehi - Mahdi Mollaei - Parisa Hosseini - Ali Koohian Mohammad abadi - Mohammad Ebrahim Hashemi - Hamid Reza Kobravi - Narges Hashemi - Mehran Beiraghi Toosi - Javad Akhondian











Article Code: icbme-1241

Article Title: Investigating Real-time sEMG-based Approaches for Grasping Recognition

Abstract: To fully exploit real-time prosthetics and exoskeleton assist devises, human-machine interfaces that can effectively deduce related activity and intent are essential. Surface electromyography (sEMG) provides a well-established non-invasive method for this purpose. yet two key barriers to its broad adoption are attaining recognition latency well below 200ms and preserving accuracy in presence of signal drift. In order to describe an orderly solution to these issues, this paper is a comprehensive assessment of deep learning and conventional algorithms. To establish a comprehensive scheme for targeted gesture, data was meticulously collected from individuals in the biomedical engineering lab. Furthermore, to be able to contrast the proposed method against the already reported work, a well-established publicly available dataset, namely EMG-EPN-612 was utilized, 4 channels were used it contains recording from 100 participants. To achieve appropriate real-time accuracy, commonly used classifiers, namely Support Vector Machine (SVM), Random Forest, and Convolutional Neural Networks (CNN) were implemented and compared based on these metrics. Input was rigorously evaluated in three forms, processed signals, handcrafted features, and Short-Time Fourier Transform (STFT) images, in a bid to determine the optimal strategy. Although all these models were shown to support the required real-time constraint, however only the CNN model applied to the STFT inputs achieved the acceptable 92% accuracy on the EMG-EPN-612 dataset, as compared to SVM applied to handcrafted features of 84% accuracy on the recorded dataset. These results provide first-time explanation and trade-off between model complexity and computation cost, and required accuracy. This research provides useful recommendations that further assist in developing more effective, responsive, and accessible hand assist devices and prosthetics.

Keywords: Hand Grasping Recognition, Surface Electromyography (sEMG), Real-Time Systems, Short-time Fourier Transform (STFT), Convolutional Neural Networks (CNN)

Authors: Monire Ameri Haftador - Ali Akbari - Mehran Jahed











Article Code: icbme-1246

Article Title: Vision Transformer-Based Emotion Recognition in EEG Using Pseudo-Image

Construction

Abstract: Transformer-based models have demonstrated remarkable performance across natural language process- ing and computer vision. Our research aims to extend these models to time-series EEG data, evaluating their effectiveness for feature extraction and pattern recognition. To achieve this, we first transform the EEG data into pseudo-images using autoencoders. This approach enables us to convert multi-channel time-series data into spatiotemporal 2D pseudo-images, which are then processed by a Vision Transformer (ViT) model. Two important features in EEG data that we need to consider are intra- channel features, which represent the dynamics within each individual channel, and inter-channel features, which capture the relationships between different channels. In our method, the autoencoder captures the unique intra- channel features of each EEG channel, while the self- attention mechanism in the ViT uncovers inter-channel de-pendencies, enhancing the model's representational power. Additionally, this approach provides visualizations of active channels during different emotional states, offering insights into brain function and supporting further research in understanding the neural basis of emotions. We evaluated our model on two widely recognized EEG datasets, SEED and DREAMER, achieving promising results: 99.81% ac- curacy on SEED, and 97.17% for valence and 97.50% for arousal on DREAMER, outperforming existing models. These findings suggest that the proposed method effectively extracts rich and meaningful features from EEG data, paying the way for more advanced analysis in neural and affective computing.

Keywords: EEG data, transformers, emotion recog- nition

Authors: Ali Kouchakzadeh - Soheil Moradi - Mohammad Mohsen Ebrahimi Seyghalan - Mehdi Fardmanesh











Article Code: icbme-1262

Article Title: Dynamic Connectivity Reveals Transformative Power of Neurofeedback in Brain Functional Networks

Abstract: The unknown procedure of neurofeedback interaction on brain networks is a critical drawback of this method. In this study, a dynamic functional connectivity (dFC) framework, using spatially constrained independent component analysis, was used to capture transient changes of brain networks due to reality monitoring neurofeedback. As a result of applying the analysis on a fMRI dataset of healthy individuals, four recurring connectivity states involving the default mode (DMN), cognitive control (CC), and sensorimotor (SM) networks were identified. After training, participants showed a significant increase (p<0.05) in time spent in a DMN-integrated state (State 2/Cluster 2), occurring 37% of the time and marked by strong within-DMN coupling, reflecting enhanced internal processing. Conversely, dwell time decreased (p<0.05) in a CC-SM dominated state (State 1/Cluster 1), suggesting reduced reliance on externally driven control or sensorimotor interactions. Transition analyses supported these effects, with increased shifts toward the DMN-integrated state (from 1.5% to 4.5%) and fewer transitions to Cluster 1 (from 1.8% to 0.2%). Overall, this dFC framework effectively captured neurofeedback-induced reorganization, offering a promising tool for optimizing interventions. Its ability to detect subtle, time-varying network changes highlights its potential clinical utility for monitoring and personalizing treatments in some brain disorders.

Keywords: ICA, dFNC, neurofeedback, brain networks, reality-monitoring

Authors: Kasra Momeni - Gholam- Ali Hossein-Zadeh











Article Code: icbme-1265

Article Title: Improved Metric for Classification of Nearby Reaching Targets: A Distance-Weighted Accuracy Approach

Abstract: Accurate classification of reaching targets is critical for upper-limb prosthesis control, rehabilitation robotics, and human-robot interaction. Traditional classification metrics assume uniform misclassification costs, ignoring the spatial relationships between targets. This overlooks significant performance degradation; misclassifications in safety-critical zones (e.g., near obstacles or humans) or those impairing functional outcomes (e.g., failing to grasp a cup) can be far more detrimental than spatially adjacent misclassifications—despite equivalent cost in standard metrics—leading to elevated user workload or complete task failure. To address this, we propose a spatially informed weighted accuracy metric. Misclassification costs are assigned based on the normalized Euclidean distance between the intended target and the misclassified position, penalizing distant errors more heavily than proximal ones. We demonstrate the utility of this metric first using synthetic confusion matrices achieving identical standard accuracy but exhibiting distinct spatial error patterns (far, near and random misclassification error patterns). We then apply it to a real-world reaching target prediction task, comparing two classifiers (Quadratic Kernel SVM vs. Gaussian Kernel SVM) with equal standard accuracy (63%). The proposed metric effectively discriminates classifier performance by imposing higher penalties on distant misclassifications (86.3% for Ouadratic Kernel SVM vs. 85.5% Gaussian Kernel SVM), revealing significant differences masked by standard accuracy. Crucially, the metric explicitly normalizes against the worst-case misclassification cost inherent to the target layout, providing a spatially aware assessment of classification performance essential for real-world deployment.

Keywords: reaching target classification, upper-limb prosthesis control, spatially weighted accuracy, performance evaluation metrics, misclassification cost, motor intention decoding

Authors: Zahra Dayani - Ali Maleki - Ali Fallah











Article Code: icbme-1276

Article Title: Phase-Amplitude Coupling of Event-Related Potentials during VCPT Task in Dyslexic Subjects

Abstract: Dyslexia can be categorized as a learning problem with neurodevelopmental roots. People with dyslexia usually have unexpected problems with reading and deciphering letters and symbols. Such a disorder not only profoundly impacts academic achievements but also affects social and emotional aspects of one's life. For this reason, early detection of dyslexia seems to be necessary to provide dyslexic people with a more appropriate educational curriculum and support. In this study, we provide more support for the capability of the Visual Continuous Performance Task (VCPT) in the early detection of dyslexia. We used Phase-Amplitude Coupling (PAC) to extract biomarkers for dyslexia detection. Besides, we discuss how coupling and connectivity measures are prone to spurious connections and why surrogate corrections need to be performed. Our results revealed that while Delta-Gamma and Theta-Gamma coupling show strong statistical significance, Alpha-Gamma PAC is more effective in distinguishing dyslexic from typically reading subjects, reflecting active top-down attentional control. Cross-frequency coupling patterns highlighted the prominence of temporal and frontal electrodes, whereas occipital electrodes contributed less than expected, suggesting that attention and cognitive control mechanisms play a major role during VCPT. Alpha-Gamma PAC acts as a dynamic gating mechanism, selectively amplifying task-relevant neural activity and suppressing irrelevant signals, thereby supporting efficient performance.

Keywords: Dyslexia, ERP, Phase-Amplitude Coupling, VCPT

Authors: Mahdi Mollaei - Maryam Mohebbi - Reza Rostami











Article Code: icbme-1278

Article Title: Distinct Neurophysiological and Psychological Effects of tVNS and

Neurofeedback: Insights for EEG-Guided Neuromodulation

Abstract: This pilot study investigates the neurophysiological and psychological effects of two emerging non-invasive neuromodulation techniques, transcutaneous vagus nerve stimulation (tVNS) and neurofeedback (NF), in healthy adults. Fifteen participants were allocated to one of three groups: tVNS (applied to the left tragus), NF (Alpha/Theta protocol), or a control group. Each intervention included eight sessions of 30 minutes over a four-week period. Resting-state electroencephalography (EEG) was employed to quantify the alpha/theta power ratio, while psychological outcomes were assessed using the Beck Anxiety Inventory (BAI) and selected subscales of the Millon Clinical Multiaxial Inventory-IV (MCMI-IV). Non-parametric withingroup analyses indicated that tVNS significantly increased the alpha/theta ratio (p = 0.042), reflecting a shift toward neurophysiological relaxation. In contrast, NF significantly reduced anxiety (p = 0.042) and depressive symptoms (p = 0.048). No significant effects were found in the control condition. Interestingly, although NF was expected to exert stronger effects on EEGbased biomarkers, it primarily influenced psychological outcomes, whereas tVNS showed more pronounced modulation of neurophysiological indices. These findings highlight distinct mechanisms of action and underscore the potential of tVNS for EEG-guided neuromodulation, motivating future work toward adaptive closed-loop tVNS systems tailored to individual neural oscillatory dynamics.

Keywords: Neurofeedback, Transcutaneous Vagus Nerve Stimulation, Emotion Regulation, Electroencephalogram, Alpha/Theta Ratio

Authors: Seyedeh Zeinab Molaeizadeh - Aitor Aritzeta Galan











Article Code: icbme-1280

Article Title: Improving Effectivity of repetitive Transcranial Magnetic Stimulation in Treatment of Amyotrophic Lateral Sclerosis by Designing New Protocol and Using Machine Learning

Abstract: rTMS can help ALS, but response differs widely between patients. We asked whether pre-treatment EEG could forecast who benefits. A practical way forward is to predict response before stimulation in maximizing the therapeutic efficacy. EEG-based features, when integrated with machine learning, offer a workable route to modeling response. Results demonstrate the effectiveness of EEG-derived features in identifying rTMS responders and non-responders by means of a Support Vector Machine (SVM) model. TWe enrolled 34 ALS participants (NP: 18; OP: 16). We recorded pre-treatment resting-state EEG. Extracted features by using signal processing methods were: time domain (mean amplitude, variance), frequency domain (band power, peak alpha frequency), nonlinear tests (Hjorth parameters, fractal dimension, Hurst exponent). We trained an RBF-SVM on these features. A Support Vector Machine trained on band-power, zero-crossing and fractal-dimension features reached 97.3% accuracy (AUC = 0.99). ROC analysis indicated near-perfect separation between responders and non-responders, with an AUC of 0.99, indicating the stability of the selected features for predicting treatment response. These results support EEG-guided, patient-specific rTMS settings.

Keywords: repetitive Transcranial Magnetic Stimulation (rTMS), Machine Learning, Amyotrophic Lateral Sclerosis (ALS), Support Vector Machine (SVM), Electroencephalography (EEG).

Authors: Ali Abedi - Gholamreza Moradi - Reza Sarraf Shirazi - Mehran Jahed











Article Code: icbme-1285

Article Title: ECG-Based Detection of Acute Myocardial Infarction Using a Wrist-Worn

Device: a Machine Learning Approach

Abstract: Identifying acute myocardial infarction (AMI) at an early stage, particularly outside the hospital, remains one of the most pressing challenges in modern healthcare. While many wearable devices can record electrocardiogram (ECG) signals, most lack the essential precordial leads that are critical for accurate AMI detection. In this study, we evaluate the diagnostic capability of a wrist-worn, two-lead wearable ECG (wECG) device and compare its performance with the clinical standard, the conventional 12-lead ECG. Our analysis is based on a dataset where wECG and standard 12-lead ECG signals were recorded simultaneously from three participant groups: healthy individuals (CTRL), patients diagnosed with AMI, and patients with other cardiovascular diseases (CVD). This paper proposes a framework for diagnosing AMI patients as distinct from healthy individuals. Within this framework, we extracted both statistical features and Hjorth parameters. Then employed four different machine learning classifiers to assess classification performance across various scenarios. Using mutual information and f-test scores, we selected the best lead based on inter-class separation. The standard 12-lead ECG models achieved nearly flawless results, reaching 100% average accuracy. The wECG device also demonstrated impressive capabilities, accurately distinguishing between healthy participants and AMI patients with more than 98% average accuracy. Notably, the V5-LA configuration, when processed with the KNN classifier, achieved perfect average accuracy, highlighting the strong diagnostic power of this single lead. Overall, our results indicate that with careful design, a compact wECG device has the potential to serve as a reliable and highly effective tool for AMI detection in pre-hospital environments.

Keywords: Machine learning, Acute myocardial infarction, ECG, Wrist-worn wearable ECG, Hjorth parameters

Authors: Tania Hossein Khani - Amir hossein Tajarrod - Asghar Zarei - Mousa Shamsi











Article Code: icbme-1286

Article Title: Deep Learning and Fuzzy Entropy in Parkinson's Diagnosis: a Framework Based on Task-Based EEG Signals

Abstract: Parkinson's disease (PD) is the second most common neurodegenerative disorder worldwide, characterized by reduced dopamine levels in the central nervous system. Electroencephalography (EEG) signals have emerged as a promising tool for diagnosing PD due to their non-invasive nature, low cost, and high temporal resolution. This paper proposes a framework for diagnosing PD in healthy individuals. The proposed framework involves the extraction of fuzzy entropy from sub-bands of wavelets, combined with deep learning networks to classify EEG signals obtained under an auditory oddball paradigm. The deep learning networks used in this study include the EEG Network (EEGNet), Residual Networks within EEG (ResNetEEG), EEG Transformer, and Long Short-Term Memory Fully Convolutional Network (LSTMFCN). Four classification scenarios were explored: healthy control (CTRL) vs. PD patients off medication (PD-OFF), CTRL vs. PD patients on medication (PD-ON), PD-ON vs. PD-OFF, and a multi-class. The results indicated that the ResNetEEG network achieved the best average accuracy of 99.78% for the CTRL vs. PD-OFF classification. In contrast, the LSTMFCN network demonstrated optimal performance for the other classifications, with average accuracies of 99.81% for CTRL vs. PD-ON, 99.38% for PD-ON vs. PD-OFF, and 99.85% for the multi-class scenario. Both the EEGNet and EEG Transformer networks also showed comparable performance. Even the ROC curves for these networks showed AUC values of 1.0, further confirming the effectiveness of the implemented networks. These results emphasize the significant potential of utilizing EEG-derived features and deep learning techniques for the accurate detection of PD across various clinical scenarios.

Keywords: Deep learning, Parkinson's disease, EEG, Fuzzy entropy, LSTMFCN

Authors: Amir Hossein Tajarrod - Tania Hossein Khani - Asghar Zarei - Mousa Shamsi











Article Code: icbme-1295

Article Title: Robust Glucose Level Classification from NIR-Based PPG Using Morphological Features

Abstract: Diabetes is a primary global health concern, and noninvasive monitoring could be critical for its early detection and management. This study presents a noninvasive approach to blood glucose classification using photoplethysmography (PPG) signal and machine learning approaches. However, PPG signals are biological signals that, similar to their counterparts, suffer from considerable environmental noise and patient-to-patient variability. Here, we propose a morphology-based framework for robust PPG-based Glucose classification. For this purpose, a custom-designed optical finger sensor operating at 940 nm was used to record two independent 30 s signals from fasting participants, including both healthy and diabetic subjects. After excluding low-quality signals, the final dataset included 159 subjects. Signals also underwent multi-stage filtering, normalization, and cycle-based template-matching quality control before feature extraction. We then employed the proposed framework to identify consistent cycle-shape patterns within each acquisition and verify their stability across repeated recordings. Two feature sets were compared including the cycle-based morphological and global signal-based features. Correlation analysis showed that morphology-based features were more robust and reproducible, while global signal features were less reliable under shortduration acquisitions. Multiple classifiers were tested, with Gradient Boosting achieving the highest accuracy (93.75%) using morphological features, compared to 84.38% with nonmorphological features. These findings suggest that morphology-based signal analysis provides robust and salient features from short PPG signals, enabling practical and accurate noninvasive diabetes screening.

Keywords: Diabetes classification, Photoplethysmography (PPG), Near-infrared spectroscopy (NIRS), Biomedical signal processing, Morphological features, Machine learning

Authors: Arian Mesforoosh-M.- Yeganeh Binafar - Mohammad-R. Akbarzadeh-T.











Article Code: icbme-1299

Article Title: Hierarchical STFT based Transformer for Causality discovery

Abstract: Electroencephalogram (EEG) signal analysis is essential for understanding brain dynamics and functional connectivity. Classical causality estimators such as Granger causality. Partial Directed Coherence (PDC), and Directed Transfer Function (DTF) are based on linear autoregressive models and often fail to capture nonlinear dependencies in neural time series. Meanwhile, deep learning models—including CNNs, RNNs, and Transformers—have achieved strong results in EEG decoding tasks, but they primarily model correlations rather than true causal interactions. To overcome these limitations, we propose the Hierarchical Causal-STFT Transformer (H-STFT-T), a novel framework that integrates causal short-time Fourier transform (STFT) representations with a multi-level hierarchical Transformer. The model enforces causality in the spectral domain through lag-stacked STFT features and leverages local convolutions and multi-band causal attention across time and channels. Causal relevance scores are extracted via a gradient × attention (RRP) mechanism, and statistically significant connections are determined through surrogate-based testing and Benjamini-Hochberg FDR correction, yielding interpretable directed graphs. Evaluations on both synthetic datasets and real EEG benchmarks demonstrate that H-STFT-T outperforms classical causal estimators and deep non-causal baselines, as well as modern causal discovery methods, in recovering groundtruth causal links and lag structures—revealing physiologically meaningful directed connectivity.

Keywords: EEG, causal discovery, Transformers, connectivity, time-frequency analysis

Authors: Sahar Semsarha - Mohammad bagher Shamsolahi











Article Code: icbme-1317

Article Title: Neural Encoding of Outcome Magnitude: Evidence from fMRI

Abstract: Reward and punishment outcomes play a central role in adaptive decision-making, vet while the effects of outcome valence have been extensively studied, the neural encoding of outcome magnitude remains less well understood. Previous neuroimaging research has typically examined reward magnitude in isolation, often with only two outcome levels, limiting the precision of magnitude-related findings. To address this gap, we conducted a functional MRI (fMRI) study using a modified monetary gambling task designed to parametrically vary both gain and loss magnitudes. Twenty-four healthy participants performed 100 randomized trials while undergoing 3 Tesla fMRI scanning. Outcome magnitudes were modeled as parametric modulators within the general linear model framework, allowing us to identify brain regions whose blood-oxygen-level-dependent (BOLD) responses scaled with feedback size. Grouplevel analyses revealed significant magnitude-related activations in a distributed network including the dorsal anterior cingulate cortex (dACC), Rolandic Operculum extending into the insula, bilateral inferior frontal gyrus (IFG), precuneus, and right cerebellum. Notably, the dACC showed robust bilateral engagement, consistent with its role in evaluating outcome salience and encoding motivationally relevant information. These findings demonstrate that outcome magnitude, across both rewards and punishments, recruits neural circuits beyond classical reward areas, engaging regions involved in cognitive control, interoceptive processing, and adaptive behavioral regulation. Our results advance the understanding of how the human brain encodes the quantitative features of feedback and highlight the importance of considering magnitude alongside valence in models of decision-making and reinforcement learning.

Keywords: fMRI, decision-making, gambling, monetary incentive, reward magnitude, punishment magnitude, feedback processing, parametric modulation, dorsal anterior cingulate cortex (dACC).

Authors: Amin Mohammad Mohammadi - Shaghayegh Mahmoudi - Narjes Amin - Farid Hosseinzadeh - Elias Ebrahimzadeh - Hamid Soltanian-Zadeh











Article Code: icbme-1321

Article Title: EEG-Based Classification of Schizophrenia and Healthy Controls Subjects Using Statistical and Nonlinear Features with Emphasis on Fuzzy Entropy

Abstract: Schizophrenia is a severe mental disorder that frequently causes the patient to have numerous problems with normal daily activities, and still, doctors struggle to accurately diagnose it in the early stages. Brain imaging and clinical tests, even if they are sometimes capable of achieving the goal, are often a lengthy procedure, expensive, and can also be somewhat uncomfortable for patients. New scientific work seeks to come up with a less intrusive and cheaper method, which will include the use of the EEG signal and the ML algorithm in identifying abnormalities of the schizophrenic patients as compared with the healthy ones. At first, the Fast Fourier Transform (FFT) was used to decompose the EEG signal into multiple sub-bands of frequency, and it was decided to extract a set of features from each sub-band, where the features included the statistical and nonlinear features - kurtosis, skewness, Shannon entropy, fuzzy entropy, mobility, and complexity. Subsequently, the ReliefF algorithm was utilized for the selection of features, and the significant features thus extracted were used as input for a number of classifiers, including the k-nearest neighbors (KNN), linear support vector machine (SVM), and the random forest (RF), to name but a few. The functional capabilities of the designed system were verified on a genuine EEG dataset that contains recorded signals from schizophrenia patients as well as from healthy subjects. Random forest was identified as the most effective one among the various implemented classifiers, as it achieved the highest performance with an average accuracy of 97.69%. Also, fuzzy entropy was identified to be a constantly discriminative feature, implying it could serve as a sound biomarker for the differentiation of schizophrenia from healthy subjects by utilizing EEG signals.

Keywords: Schizophrenia, Electroencephalogram, Machine Learning, Fuzzy Entropy

Authors: Mahdiyeh Tofighi Milani - Sina Shamekhi - Asghar Zarei











Article Code: icbme-1322

Article Title: An Automatic Pipeline for Simultaneous EEG-fMRI Artifact-removal (SEFA)

Abstract: Simultaneous EEG-fMRI provides complementary temporal and spatial information about brain function, but its utility is hindered by severe scanner-induced artifacts such as gradient and ballistocardiographic (BCG) noise. Manual artifact correction is effective but labor-intensive, inconsistent, and difficult to scale. We introduce SEFA, a fully automated twostage preprocessing pipeline for simultaneous EEG-fMRI that integrates MRI-specific artifact correction (average artifact subtraction, optimal basis set, and PCA/OBS modeling) with stateof-the-art EEG cleaning techniques adapted from a previous popular standard EEG preprocessing pipeline, HAPPE, including automated independent component classification (MARA and ICLabel), bad-channel detection, multitaper regression for line noise, and segmentlevel quality control. Validation against manually corrected datasets from a reward-based decision-making task demonstrated that SEFA achieves near-perfect equivalence with expert preprocessing. Event-related potentials (ERPs) from both approaches indistinguishable morphology, latency, and amplitude, with mean channel-wise correlations of r = 0.91 ± 0.14, and 72% of electrodes exceeding r > 0.90. Signal-to-noise ratio (SNR) improved from ~0.8 dB in raw data to 6.7 dB with SEFA, matching manual performance (6.9 dB). Statistical testing confirmed no significant differences in ERP amplitude or latency between automated and manual methods (all p > 0.1). By reducing operator bias and cutting processing time from hours to minutes, SEFA enables reproducible, scalable, and clinically feasible preprocessing of simultaneous EEG-fMRI data.

Keywords: Simultaneous EEG-fMRI, EEG, preprocessing, artifact removal, automation, pipeline, SEFA.

Authors: Farid Hosseinzadeh - Amin Mohammad Mohammadi - Mehrdad Anvarifard - Sasan Keshavarz - Elias Ebrahimzadeh - Hamid Soltanian-Zadeh











Article Code: icbme-1336

Article Title: From Handcrafted to Deep Representations: ReliefF and DANN Feature Fusion for EEG Emotion Classification

Abstract: Emotion recognition from EEG signals is challenged by noise, variability, and high dimensionality. This study introduces a hybrid framework that combines handcrafted feature optimization with deep representation learning through a Domain-Adversarial Neural Network (DANN). Using the ECSMP database, EEG signals were preprocessed and a diverse set of temporal, spectral, time–frequency, and nonlinear features were extracted. ReliefF reduced these to 43 discriminative indices, which were benchmarked against DANN-derived latent representations across multiple classifiers, including Random Forest, SVM, MLP, and gradient boosting models. Results show that DANN features substantially improved balance and reduced class bias, achieving up to 97.3% accuracy with MLP, CatBoost, and LightGBM. Interpretability was addressed using SHAP, which highlighted the importance of wavelet- and amplitude-based measures (e.g., wavelet length, MAV, Willison amplitude). Unlike prior ECSMP studies requiring extensive multimodal features, our approach achieves competitive six-class classification using only seven EEG channels and a few number of features, highlighting the value of combining optimized handcrafted indices, DANN-based deep representations, and explainable AI for lightweight and interpretable affective computing.

Keywords: EEG, DANN, ECSMP, emotion recognition, machine learning

Authors: Zahra Mahdinezhad - Raheleh Davoodi











Article Code: icbme-1344

Article Title: Classification of Excitatory and Inhibitory Neurons in Animal Data Using Machine Learning and CNN Models

Abstract: Automatically distinguishing excitatory from inhibitory (E/I) neurons in extracellular recordings is a fundamental challenge in neuroscience, as it enables accurate circuit dissection and more reliable spike sorting outcomes. In this study, we developed and evaluated models for cell-type classification based on extracellular action potentials (EAPs). Hippocampal recordings from the Buzsáki Lab, including 26 opto-tagged inhibitory neurons and matched excitatory neurons, were used to benchmark performance. Three classifiers were implemented: Support Vector Machine (SVM), Linear Discriminant Analysis (LDA), and Convolutional Neural Networks (CNNs), trained on either raw spike waveforms or their two-dimensional wavelet transforms. A leave-one-out cross-validation scheme was applied to assess generalization. Among all tested models, CNNs achieved the highest accuracy (94.32%), outperforming both SVM (~92%) and LDA (~87%). Interestingly, CNNs performed slightly better on raw waveforms compared with wavelet inputs. While our results are slightly below those reported for CNNs on simulated data (~99%), they highlight the robustness of deep learning approaches when applied to real neuronal datasets. This work supports the growing evidence that deep networks can automatically extract informative features from extracellular recordings without hand-crafted metrics.

Keywords: Machine Learning, Deep Learning, Wavelet Transform, Neuron Classification, Hippocampal Mouse Data

Authors: Mahdi Mollaei - Amirhossein Mashghdoust - Ali Khadem











Article Code: icbme-1352

Article Title: Feature-Conditioned WGAN for Generating Alzheimer's EEG: Enabling GAN-Based Synthesis Under Data Scarcity

Abstract: Alzheimer's disease (AD) significantly impairs cognitive function, making early detection and personalized care crucial. Electroencephalography (EEG) provides a noninvasive, low-cost window into cortical oscillations and is sensitive to AD-related spectral slowing and reduced temporal complexity. However, acquiring high-quality EEG data is often limited by factors such as patient fatigue, session variability, and logistical challenges, especially in environments like socially assistive robots (SARs). These constraints make it difficult to gather sufficient data for training reliable deep models for AD detection. To address this challenge, we propose a feature-conditioned Wasserstein generative adversarial network (fc-WGAN) that generates class and subject specific EEG segments from minimal training data. We first analyze a broad set of time-domain and frequency-domain EEG features to identify those most discriminative between AD and cognitively normal groups. Notably, features like nonlinear energy and band powers consistently demonstrate high separability, fc-WGAN aligns the mean and variance of these features between real and generated EEG batches, enhancing physiological realism and class consistency. Starting from only 200 overlapping 3-second segments per subject, our method improves EEGNet classification accuracy from 87.5±4.5% to 96.2±4.4% by effectively augmenting the training dataset. These results underscore the power of feature-aligned generation in overcoming data scarcity and demonstrate the practical utility of fc-WGAN for SAR-based cognitive assessment and early AD detection in real-world settings.

Keywords: Alzheimer's disease, Electroencephalography, Conditional Wasserstein GAN, Feature matching, Synthetic data generation

Authors: Parsa Bahramsari - Alireza Taheri











Article Code: icbme-1354

Article Title: Deep Learning Approaches for Alzheimer's Disease Diagnosis: A Comprehensive Review

Abstract: Alzheimer's disease (AD) is a progressive neurodegenerative disorder that severely affects memory, cognition, and daily functioning. Early and reliable diagnosis plays a critical role in improving treatment strategies and patient quality of life. In recent years, deep learning (DL) techniques have shown remarkable potential in medical imaging and neurophysiological signal analysis, enabling automated and accurate detection of AD and related conditions such as mild cognitive impairment (MCI) and frontotemporal dementia (FTD). This paper provides a comprehensive review of 17 recent studies published between 2023 and 2025, which applied various DL architectures, including convolutional neural networks (CNNs), recurrent neural networks (RNNs), transformers, and hybrid models, to electroencephalography (EEG), magnetic resonance imaging (MRI), and multimodal datasets. The reviewed works adopted diverse feature extraction strategies such as discrete wavelet transform (DWT), synchrosqueezing, power spectral density (PSD), and intrinsic time-scale decomposition (ITD), combined with advanced classifiers and interpretable AI frameworks. A comparative analysis highlights the strengths and limitations of each approach, dataset availability, and diagnostic accuracy. Finally, key challenges, including limited dataset diversity, lack of interpretability, and generalization issues, are discussed, along with future directions such as explainable AI, federated learning, and multimodal fusion, which hold promise for advancing AD diagnosis.

KeyWords: Alzheimer's disease (AD), Mild Cognitive Impairment (MCI), Electroencephalography (EEG), Magnetic Resonance Imaging (MRI), Deep Learning (DL), Convolutional Neural Networks (CNNs), Recurrent Neural Networks (RNN), Transformers, Multimodal analysis

Authors: Mahdi Jafari Asl - Saba Haji Molla Rabie











Article Code: icbme-1367

Article Title: EEG-based Schizophrenia Detection Using Spectral, Entropy, and Graph Connectivity Features with Machine Learning

Abstract: Schizophrenia is a serious mental disorder that changes the way people think, perceive, and manage daily life. Getting the diagnosis right is critical for proper treatment, but in practice it is often difficult. Current evaluations depend mostly on a clinician's judgment, and the overlap of symptoms with bipolar disorder or major depression makes the task even harder. EEG offers a safe and noninvasive way to study brain activity, yet no single EEG feature has been reliable enough to stand on its own. This makes it important to look at integrative approaches that bring together different aspects of brain dynamics. In this study, we analyzed EEG features to distinguish patients with schizophrenia from healthy controls. Spectral power was measured across δ , θ , α , β , and γ bands. Temporal irregularity was quantified with Multiscale Permutation Entropy (MPE), which to our knowledge represents the first application of MPE to EEG in schizophrenia. Functional connectivity was estimated with the weighted Phase Lag Index in θ , α , and β bands, followed by extraction of graph measures including global efficiency, clustering coefficient, characteristic path length, and mean strength. These features were used to train Random Forest, Multi-Layer Perceptron, and Support Vector Machine classifiers. Among the models, Random Forest achieved the most reliable performance, reaching 99.7% accuracy under stratified 5-fold validation and 99.6% under leave-one-subject-out validation. Feature analysis showed that connectivity in θ and α bands contributed most strongly to classification. Topographic maps of θ , α , and β activity also revealed regional group differences. Overall, the results suggest that combining spectral, entropy, and connectivity measures offers a promising framework for EEG-based detection of schizophrenia. Nevertheless, these findings are preliminary given the limited sample size (N=28), and replication in larger and more diverse cohorts is required before clinical translation.

Keywords: Artificial Intelligence, Bandpower, EEG, Functional Connectivity, Graph Features, Machine Learning, Multiscale Permutation Entropy, Schizophrenia Detection

Authors: Nazila Ahmadi Daryakenari - Seyed Kamaledin Setarehdan











Article Code: icbme-1374

Article Title: Graph Attention Networks for EEG-Based Emotion Recognition: Focus on

Channel Level Attention

Abstract: We investigate the specific contribution of channel-level attention to EEG-based emotion recognition by introducing Channel-GAT, a compact two-layer graph attention network that operates on the 10–20 sensor graph. Each 1-s window is represented as a 32-node graph with differential-entropy band features; edges capture spatial proximity and, when reliable, functional connectivity. On the DEAP dataset, Channel-GAT consistently outperforms non-attention graph models and common grid-based baselines while remaining lightweight, reaching around 93% accuracy for valence and 92% for arousal in subject-dependent evaluation and competitive performance under leave-one-subject-out testing. Ablations show that attention yields a clear gain over a plain GCN, and that using an explicit graph structure substantially improves over MLPs without topology. Attention maps emphasize frontal regions for valence and parietal—occipital regions for high arousal, frequently highlighting F3/F4, T7/T8, and Pz/Oz—patterns that align with affective neurophysiology and support principled channel selection for low-density wearables. The resulting pipeline is reproducible, trains within minutes per fold on a single GPU, and offers an interpretable, deployment-friendly pathway to real-time affect monitoring.

Keywords: EEG, emotion recognition, graph attention networks, channel-level attention, differential entropy, functional connectivity, DEAP.

Authors: Akbar Asgharzadeh-Bonab - Hamid Bigdeli - Mohammad Javad Heidari











Article Code: icbme-1380

Article Title: EEG Graph Construction: A Comparative Analysis for Classification Application

Abstract: Schizophrenia is associated with disrupted neural connectivity and abnormal brain dynamics that can be captured through electroencephalogram (EEG) analysis. However, traditional EEG analysis methods often fail to represent the complex spatial and temporal dependencies in brain activity. This paper addresses this challenge by modeling EEG signals as graph signals and comparing three graph construction strategies for schizophrenia classification: a Gaussian kernel-based similarity graph, a functional-causal fusion graph, and a Semilocal graph. EEG recordings from healthy controls and schizophrenia patients were preprocessed, band-pass filtered into canonical frequency bands (delta, theta, alpha, beta, gamma), and represented as graphs according to each construction method. Graph-based features were extracted and used for classification with a support vector machine under five-fold stratified cross-validation. Experimental results demonstrate that the functional-causal fusion graph consistently achieved the highest accuracy across all frequency bands, reaching perfect classification in several cases, while the Gaussian kernel and Semilocal graphs produced slightly lower but competitive results. These findings indicate that integrating functional and causal connectivity information provides a more discriminative graph representation for schizophrenia EEG classification and emphasize the importance of graph construction strategy in EEG analysis using graph signal processing.

Keywords: Electroencephalogram (EEG), Graph Signal Processing (GSP), Graph Construction, Classification, Schizophrenia

Authors: Kiana Kalantari - Mohammad Bagher Shamsollahi











Article Code: icbme-1384

Article Title: Hierarchical Task-Structured GNN Meta-Learning for Few-Shot EEG Motor Imagery Decoding

Abstract: Motor imagery classification from electroencephalogram (EEG) signals is a core challenge in brain–computer interface (BCI) systems. Yet, strong inter-subject variability, where each subject follows a distinct distribution, renders conventional learning approaches poorly suited for generalization to unseen subjects. Few-shot meta-learning offers a promising alternative by enabling rapid adaptation to new subjects with only limited labeled data. At the same time, neuroscience evidence emphasizes that EEG decoding should leverage network-level interactions rather than treating electrodes as independent sources, motivating graph-based representations. In this work, to leverage network-level structure, We propose a principled graph construction pipeline to represent EEG data. Also to enable subject-level adaptation in few-shot settings, we use a meta-learning framework that learns Hierarchical Task Structures, through which we exploit inter-subject correlations, and employ GNN architectures as the learner. Experiments on the motor imagery dataset show that our method achieves over 10% higher accuracy than baseline models, while reducing variance across subjects by roughly 10\%. This demonstrates that combining graph-based representations with few-shot meta-learning yields more reliable and subject-adaptive BCI systems.

Keywords: EEG Signals, Meta-learning, BCI Decoding, Graph Neural Networks (GNNs), Subject-level Adaptation, Hierarchical Task Structures

Authors: Mohammad Armin Dehghan - Mohammad Mohammadianbisheh - Mohammad Bagher Shamsollahi











Article Code: icbme-1389

Article Title: Semi-Automatic Multi-Stage Artifact Removal in EEG During Subthreshold GVS: A Machine Learning Approach for Neuromodulation Studies

Abstract: Parkinson's disease (PD) is characterized by widespread disruptions in neural oscillations and network dynamics, which can be captured through resting-state EEG biomarkers. Galvanic vestibular stimulation (GVS) has emerged as a promising noninvasive neuromodulation technique to modulate these neural patterns. However, EEG recordings during GVS are severely contaminated by high-amplitude stimulation artifacts, especially when exploring a wide range of stimulation protocols. In this study, we designed a data acquisition protocol involving 304 distinct subthreshold GVS waveforms, each with a unique temporal profile, to investigate their effects on brain activity. These stimuli induced strong artifacts in the EEG signal, particularly during the stimulation interval. To recover clean EEG signals, we developed a multi-stage preprocessing pipeline combining regression-based artifact suppression, canonical correlation analysis (CCA), and independent component analysis (ICA), supported by machine learning classifiers for automatic detection and removal of GVS, EOG, and EMG artifacts. We evaluated the effectiveness of this pipeline through classification of EEG signals from PD patients and healthy controls across three temporal segments: prestimulation (Pre-stim), stimulation (Stim), and post-stimulation (Post-stim). Despite the intense artifacts in the Stim interval, classification accuracy reached 82.46%, closely matching the performance in Pre-stim (85.06%) and Post-stim (91.67%) intervals. This confirms that the artifact removal process successfully preserved disease-relevant neural information even during active stimulation. Beyond classification, we conducted additional evaluations including temporal consistency analysis of biomarkers, correlation of model coefficients across intervals, and visual inspection of signal quality. These assessments demonstrated that the cleaned EEG signals retained physiologically meaningful patterns and stable biomarker profiles across time. Our findings show that EEG signals recorded during GVS can be reliably cleaned and analyzed, enabling rapid screening of stimulation protocols and paving the way for personalized neuromodulation strategies in Parkinson's disease.

Keywords: Parkinson's disease, Galvanic vestibular stimulation, Neuromodulation, Artifact removal, EEG biomarkers, Machine learning

Authors: Mahdi Babaei - Sepideh Hajipour Sardouie - Martin Keung - Varsha Sreenivasan - Hanaa Diab - Maryam S. Mirian - Martin J. McKeown









Article Code: icbme-1396

Article Title: Dynamic Cross-Frequency Coupling Reveals Task-Dependent Neural Engagement During Varying Cognitive Demands

Abstract: Phase-amplitude coupling (PAC), reflecting cross-frequency interactions between neural oscillations, underlies cognitive processing, attention, and working memory. This study examined workload-dependent PAC across prefrontal, frontal, parietal, temporal, motor regions during low-, medium-, and high-load cognitive tasks compared to baseline using Electroencephalography (EEG) of 17 healthy participants. PAC was quantified via comodulograms and regional peak values, focusing on theta-gamma and beta-gamma interactions. Baseline PAC was minimal across regions (mean MI ~0.07-0.09). Low-load tasks elicited significant theta-gamma PAC in prefrontal (0.40) and frontal (0.32) regions, with minor increases in parietal (0.18) and temporal (0.12) cortices. Medium-load tasks recruited parietal cortex more strongly (0.45) alongside prefrontal (0.60) and frontal (0.58) regions, while temporal PAC rose to 0.25. High-load tasks induced robust, multi-frequency PAC: prefrontal (0.85), parietal (0.82), frontal (0.75), temporal (0.50), and motor (0.30) regions remained low, while occipital PAC (0.10). A repeated-measures ANOVA revealed significant effects of workload (F=15.23, p-value<0.001), region (F=18.46, p-value<0.001), and their interaction (F=20.90, p-value<0.001). These region- and frequency-specific patterns reflect executive control, attention, working memory, and motor planning. The findings demonstrate that PAC is significantly sensitive to cognitive workload and highlight it as a potential index of neural engagement during complex tasks.

Keywords: Phase-amplitude coupling, cognitive workload, Electroencephalography, thetagamma coupling, beta-gamma coupling

Authors: Seyed Saman Sajadi - Babak Fazli - Fateme Karbasi - Ehsan Garosi - Milad Jalilian - Soheila Hosseinzadeh - Amir Homayoun Jafari - Seyed Abolfazl Zakerian











Article Code: icbme-1400

Article Title: Phase-Amplitude Coupling Reflects Functional Cortical Engagement During Dynamic and Static Motor Tasks

Abstract: Phase–amplitude coupling (PAC) links slow oscillatory phases with fast rhythmic amplitudes, offering insight into hierarchical brain coordination during movement. We investigated PAC across cortical regions during static and dynamic hand and foot contractions in fifteen healthy adults using EEG. PAC was quantified with the modulation index and validated through surrogate testing across 24 electrodes spanning frontal, premotor, motor, and occipital regions. Results revealed distinct task- and effector-specific coupling patterns. Static tasks were dominated by beta-gamma PAC (phase \approx 18-20 Hz; amplitude \approx 65-70 Hz) in contralateral motor and premotor regions, reflecting sustained force control. Dynamic tasks elicited stronger theta-gamma PAC (phase $\approx 6-8$ Hz; amplitude $\approx 55-60$ Hz), particularly in motor (MI = 0.82 ± 0.12) and premotor (MI = 0.84 ± 0.13) areas (p < 0.01), consistent with sequencing and planning demands. Occipital theta-gamma PAC increased selectively during dynamic hand movements, indicating visuomotor integration, while foot tasks engaged mainly midline motor regions. Repeated-measures ANOVA showed significant main effects of Region (F = 18.72, p-value < 0.001) and Task (F = 6.85, p-value = 0.001), confirming stronger coupling during dynamic versus static movements. These findings delineate the spectral and spatial organization of motor PAC, highlighting its role in flexible motor control can be interpreted as preliminary but suggestive of reproducible cortical engagement patterns relevant to motor neuroscience and neurological disorders.

Keywords: Beta-Gamma Coupling, Theta-Gamma Coupling, Electroencephalography, Muscle Contraction, Motor Control

Authors: Seyed Saman Sajadi - Ahmad Reza Keihani - Fateme Karbasi - Mohammad Amin Fathollahi - Shahriar Nafissi - Erfan Azizi - Amir Homayoun Jafari











Article Code: icbme-1418

Article Title: EJES: A Diverse Estimator Bank Framework for High-Resolution EEG/MEG

Source Localization

Abstract: Brain source reconstruction from electroencephalography (EEG) magnetoencephalography (MEG) signals is a central inverse problem in neuroscience. Classical localization algorithms, however, are highly sensitive to realistic conditions such as limited data length, low signal-to-noise ratios, and structured interference, which greatly restricts their reliability in clinical and research applications. To address this limitation, we introduce the Ensemble of Joint Estimation Strategy (EJES), a novel framework for robust source localization. EJES leverages algorithmic diversity by constructing a heterogeneous bank of estimators drawn from two distinct families; subspace-based approaches, implemented as weighted Multiple Signal Classification (MUSIC) estimators, and spatial filtering approaches, implemented as beamformers operating on different powers of the data covariance matrix. A final, stable source estimate is obtained by selectively integrating the outputs of these estimators through a robust consensus mechanism. The performance of the EJES framework was quantitatively evaluated against standard, single-algorithm approaches through extensive Monte Carlo simulations. Results consistently demonstrate that EJES provides significantly more accurate and stable localization than conventional single-algorithm methods, particularly under challenging scenarios combining short data segments, low signal quality, and high interference. These findings underscore the potential of ensemble strategies to improve the robustness of neuroelectromagnetic source reconstruction, providing a more reliable tool for noninvasive brain imaging.

Keywords: Brain Source Reconstruction, Inverse Problem, Localization, Estimator Bank, MUSIC, LCMV.

Authors: Reza Khajehsarvi - Sayed Mahmoud Sakhaei - Sadegh Jamshidpour











Article Code: icbme-1421

Article Title: Personalized EEG Source Estimation in a Shape Drawing Task

Abstract: We investigated individual neural signatures during visuomotor learning using subject-specific EEG source localization. Five adults learned foot-drawing of geometric shapes across seven sessions, with EEG recorded during Sessions 1 and 7. Subject-specific MLP networks localized activity to 116 brain regions. Analysis of 145 trials revealed three distinct neural phenotypes: cognitive-control (cingulate-dominant), executive-planning (PFC-dominant), and visual-processing (V1-dominant). Unexpectedly, cingulate cortex showed highest activation probability (24.0%) over motor areas (19.5%). Learning patterns varied by shape: Star required 16.8% more total activation (summed across dominant regions), while B showed 4.1% reduction, indicating neural efficiency. Critically, no brain regions were active across >2 subjects (maximum 40% overlap, Jaccard=0.23). Within-subject trial-to-trial consistency (0.71 ± 0.06) significantly exceeded between-subject consistency (0.59 ± 0.09), p<0.001, demonstrating that individuals maintain stable personal neural strategies rather than converging on universal patterns. These findings demonstrate motor learning relies on individual-specific neural solutions rather than universal mechanisms, mandating personalized approaches for BCIs and rehabilitation.

Keywords: EEG source localization, individual neural phenotypes, visuomotor learning, subject-specific modeling

Authors: Zakieh Hassanzadeh - Melisa Daryayi - Navid Entezari - Fariba Bahrami











Article Code: icbme-1423

Article Title: Static and Dynamic WPLI on Stressful Scenarios: an EEG Study

Abstract: Analyzing brain signals can provide valuable insights into the complexities of anxiety and contribute to improve mental health. In this paper, we used the DASPS dataset, which contains EEG recordings from 23 healthy individuals in a resting state with eyes closed. Participants were presented with descriptions of 6 stressful scenarios and assessed their emotional states through questionnaires. Functional connectivity was estimated using the Weighted Phase Lag Index (WPLI), and dynamic analysis was conducted through clustering methods to detect change points between different mental states. Above static and dynamic features were used for statistical analysis and classification on the 6 scenarios. Statistical tests revealed significant differences across all frequency bands between the verbal abuse scenario and the witnessing a fatal accident, while no significant difference was observed among the remaining scenarios. Classification was performed using a Support Vector Machine (SVM), and model performance was evaluated through 5-fold cross-validation. The best accuracy in the sixclass classification was achieved in the gamma band, 42.02%, after applying a proposed majority voting approach. Our analysis suggests that static features showed relatively better classification performance than dynamic features in this dataset, although overall accuracies remained modest across all bands.

Keywords: Anxiety, stress, EEG, functional connectivity, dynamic connectivity, WPLI

Authors: Nasrin Dehghani - Negin Joghataei - Zahra Ghanbari - Mohammad Hassan Moradi











Article Code: icbme-1424

Article Title: A Novel AR-Based Kalman Filtering Framework for ECG Enhancement

Abstract: Model-based Bayesian methods, while effective for preserving ECG morphology, often demand extensive preprocessing (e.g., R-peak detection, phase assignment, offline parameter optimization), hindering their real-world use. Our prior adaptive Kalman filter bank reduced preprocessing to R-peak detection but introduced computational complexity and iterative parameter adjustments via expectation maximization. To address these limitations, we introduce a novel approach: an autoregressive (AR) state model embedded within a two-stage Kalman filter framework for ECG denoising and parameter estimation. Critically, this method eliminates the need for any preprocessing, including R-peak detection. It achieves this by adaptively estimating model parameters and dynamically adjusting state and measurement noise covariances based on intrinsic noise characteristics. Extensive evaluations on benchmark datasets (MIT-BIH Normal Sinus Rhythm, Arrhythmia; Creighton University Ventricular Tachyarrhythmia; Sudden Cardiac Death Holter) reveal that our proposed AR-based Kalman smoother (AR-KS) surpasses state-of-the-art model-based adaptive Kalman filter banks, particularly for signal-to-noise ratios (SNRs) above 0 dB.

Keywords: ECG denoising, autoregressive model, Kalman filter

Authors: Hamed Danandeh Hesar











Article Code: icbme-1425

Article Title: A Combined Time-Frequency and Common Spatial-Spectral Pattern Approach for EEG-Based Motor Imagery Classification

Abstract: Brain-Computer Interfaces (BCIs) are revolutionizing neurorehabilitation, providing crucial communication and control for individuals with severe motor impairments from conditions like ALS, spinal cord injuries, or stroke. By creating direct links between brain activity and external devices, BCIs bypass damaged neural pathways, thus restoring motor function and significantly enhancing quality of life. Electroencephalography (EEG) is a favored BCI modality due to its accessibility and cost-effectiveness. However, a major challenge lies in the substantial impact of cognitive and individual differences on motor imagery (MI) task performance and overall BCI accuracy. This research introduces a novel method to overcome these challenges, focusing on enhanced MI classification. Our approach synergistically integrates Common Spatial-Spectral Pattern filters with the Tunable-Q Wavelet Transform. This powerful combination was applied to the extensive CHO-2017 database (52 participants), which uniquely captures significant inter-individual cognitive variations, specifically to distinguish between left and right-hand MI tasks. A critical aspect of our method is the utilization of only the top 10 most discriminative features extracted through this hybrid technique. This deliberate streamlining maximizes classification efficacy while maintaining computational efficiency. This tailored feature set demonstrated remarkable effectiveness, performing across 99% of participants. When integrated with a K-Nearest Neighbors classifier, this approach achieved an outstanding accuracy of 98.84%, notably surpassing existing state-of-the-art methods in the field. These findings hold significant promise for developing more accurate and robust BCI systems capable of extracting optimal commands for diverse MI applications, ultimately advancing neurorehabilitation outcomes.

Keywords: Motor Imagery Tasks, Common Spatial-Spectral Patterns, Tunable-Q Wavelet Transform

Authors: Reza Nejati - Hamed Danandeh Hesar











Article Code: icbme-1445

Article Title: Emotion Recognition from EEG signal using GA-FLANN with Whale Optimization Algorithm

Abstract: Non-verbal cues—such as intentions and emotions—are central to human communication. Electroencephalogram (EEG) signals, which record the brain's electrical activity, offer a direct and culture-independent basis for emotion recognition. We propose a compact and efficient pipeline that uses the Whale Optimization Algorithm (WOA) as a wrapper-based feature selector and a Genetic-Algorithm-trained Functional Link Artificial Neural Network (GA-FLANN) as the classifier. EEG signals are band-pass filtered (4–40 Hz), segmented, and transformed into spectral and connectivity descriptors; WOA searches for an optimal sparse subset of discriminative features that maximizes classification performance, while GA-FLANN performs the final emotion classification. Experiments were conducted on the SJTU Emotion EEG Dataset (SEED) comprising 15 subjects, each with 64 EEG channels sampled at 1000 Hz, and involving three emotion classes (positive, neutral, negative), with comparisons against radial basis function (RBF) and Improved Self-Organizing FLANN (ISO-FLANN) baselines. On SEED, the proposed WOA–GA-FLANN achieves 98.73% accuracy and 98.13% macro-F1, improving over radial basis function (RBF) and Improved Self-Organizing FLANN (ISO-FLANN) by approximately +4.7% and +3.9%, respectively.

Keywords: EEG signal Emotion recognition GA-FLANN Classification Whale Optimization Algorithm (WOA)

Authors: Mohammadamir Razmi - Pouya Faridfar - Seyed Amirreza Navali Hosseini alavi











Article Code: icbme-1449

Article Title: BiLSTM-Transformer: A Novel Hybrid Model for Accurate Prediction of Hand

Joint Angles from sEMG Signals

Abstract: Surface electromyography (sEMG) signals offer a non-invasive pathway for advancing human-machine interfaces, yet predicting continuous hand joint angles is challenging due to signal variability and complexity. This study proposes a novel hybrid model integrating bidirectional long short-term memory (BiLSTM) and Transformer architectures to accurately predict 10 degrees of freedom (DOF) in hand joints—metacarpophalangeal (MCP) and proximal interphalangeal (PIP)—using the NinaPro DB8 dataset. The model captures temporal muscle dynamics through BiLSTM and models long-range dependencies with a Transformer encoder, enhanced by residual connections for training stability. To enhance efficiency, a comprehensive preprocessing pipeline extracts time-domain features, applies dimensionality reduction, and employs standardization to optimize performance. A custom regularized loss function mitigates overfitting, ensuring robust predictions. The model achieves a mean absolute error of 8.2° across all 10 joints, with 6.8° for metacarpophalangeal joints and 9.7° for proximal interphalangeal joints, outperforming prior benchmarks focused on fewer aggregated joint angles. This approach enables precise, naturalistic hand pose reconstruction for prosthetic control, offering scalability and personalization for rehabilitation applications.

Keywords: surface electromyography, sEMG, hand kinematics, time series, Joint estimation, BiLSTM-Transformer, NinaPro DB8, Regression, Human-machine interfaces

Authors: Anita Sadat Sadati Rostami - Alireza Nazari - Mohammadreza Nayeri











Article Code: icbme-1458

Article Title: Effective Connectivity Alterations within the Cortico–Basal Ganglia Circuit Associated with Motor Skill Learning

Abstract: We studied whether a short time training program leaves directionally specific changes within the resting-state cortico—basal ganglia network. Thirteen healthy adults trained for two weeks to draw shapes with their foot (mainly using knee joint movement). Speed rose by ~24% and distance-to-target fell by ~15% as reported in another study on the same dataset [1]. Resting-state fMRI was acquired before and after training periods. Using spectral dynamic causal modeling, we estimated directed coupling within a hypothesis-driven motor area, including supplementary motor area (SMA), primary motor cortex (M1), dorsal premotor cortex, thalamus, caudate, putamen, pallidum, and a cerebellar relay. Group analysis revealed selective changes: stronger right SMA→left M1 influence, stronger thalamus→striatal drive (to caudate and putamen), and stronger putamen→pallidum coupling; in contrast, left M1→left putamen decreased. These shifts suggest that practice increases top-down drive from planning to execution and reinforces basal ganglia pathways that favor the trained action, while down-weighting less efficient cortico-striatal routes. The results provide directional evidence that even brief practice reorganizes cortico—basal ganglia communication at rest and align with models in which reinforcement- and error-based processes jointly shape skill.

Keywords: motor learning, resting-state fMRI, spectral dynamic causal modeling, effective connectivity, neurorehabilitation.

Authors: Mohammad Rezaei - Alireza Talesh Jafadideh - Fariba Bahrami - Shahzad Tahmasebi Boroujeni











Article Code: icbme-1462

Article Title: Mental Workload Classification using Bidirectional LSTM Networks with Multi-Feature Fusion

Abstract: Mental workload assessment is crucial for optimizing human performance in various domains including brain-computer interfaces (BCI) and cognitive load monitoring systems. This paper presents a novel approach for mental workload classification using Bidirectional Long Short-Term Memory (BiLSTM) networks with comprehensive feature extraction from EEG signals. Our method incorporates multiple feature types including spectral power analysis, entropy measures, and Hjorth parameters to create rich temporal sequences for classification. We evaluate two BiLSTM architectures - basic and advanced - on the STEW dataset containing high and low mental workload conditions from 48 subjects. The advanced BiLSTM model achieves exceptional performance with 99.97% 5-fold accuracy and 99.84% test accuracy, demonstrating the effectiveness of temporal sequence modeling for mental workload classification. The proposed approach shows significant improvements over traditional machine learning methods and provides a robust classification framework suitable for practical applications.

Keywords: Mental workload, EEG, BiLSTM, Deep learning, Feature extraction, Temporal classification

Authors: Fatemeh Farokhshad - Sepideh Bahri Hampa - Amirhesam Ghasri - Sara Bagherzadeh











Article Code: icbme-1463

Article Title: Development of an Explainable Random Forest-Based Algorithm for EEG-Based Sleep-Wake Classification Toward Sleep Apnea Detection

Abstract: Automatic sleep stage classification allows separating sleep stages without human experts. Many existing algorithms rely on multi-channel physiological signals such as EEG, EOG, and EMG. However, because of the complex equipment and required expertise, these methods usually need specialized laboratory settings. Therefore, developing a high-accuracy classification algorithm using a single signal remains a key challenge in sleep research, as it could enable portable devices and home-based sleep monitoring systems. Sleep stage classification is essential for detecting and managing sleep disorders such as sleep apnea. This study presents an optimized and clinically interpretable pipeline for sleep stage classification and apnea detection using EEG signals. The proposed approach is based on a simple, interpretable Random Forest framework and is intended to serve as a valuable tool for both clinical and research-oriented applications in sleep apnea detection. It integrates optimized preprocessing, data cleaning, algorithmic optimization, and class balancing to enhance accuracy and interpretability. Notably, our optimized Random Forest pipeline outperforms more complex deep-learning models, especially on 6-class sleep staging, sleep-wake discrimination and Apnea detection. The proposed method achieved accuracy, sensitivity, and specificity of 99.30%, 97.59%, and 99.68%, respectively, for distinguishing sleep from wakefulness, and 87.18%, 85.19%, and 89.16%, respectively, for apnea detection.

Keywords: Polysomnography, EEG signal, Sleep stage classification, Sleep apnea detection, Random Forest, Machine learning

Authors: Pargol Sharifi - Mohammad Fakharzadeh











Article Code: icbme-1470

Article Title: Graph Attention Networks for EEG-Based Emotion Recognition: Focus on

Channel Level Attention

Abstract: We Multimodal neuroimaging data, comprising Magnetic Resonance Imaging (MRI) and Electroencephalography (EEG), provide complementary spatial and temporal perspectives on neural dynamics. Conventional multimodal connectivity estimation, however, is computationally demanding and often limited by incomplete or noisy inputs. This study presents a Graph Convolutional Network (GCN)-based framework for efficient approximation of connectivity patterns across MRI and EEG. The model exploits graph-structured representations from one modality to predict connectivity maps of the other, enabling bidirectional MRI—EEG and EEG—MRI inference. By embedding spatial dependencies among brain regions, the framework preserves both topological and spectral characteristics while substantially reducing computational cost Experiments on multimodal datasets demonstrate that the GCN reliably reproduces full-model outputs, offering a scalable and robust solution for real-time, data-limited brain connectivity analysis.

Keywords: Graph Convolutional Network (GCN), Magnetic Resonance Imaging (MRI), Electroencephalography (EEG), Brain Connectivity

Authors: Arshia Rezaei - Bahareh Abbaszadeh











Article Code: icbme-1473

Article Title: Natural Language Processing and Speech Processing Integration: Toward A Point-of-Care Framework for Early Detection of Alzheimer's Disease

Abstract: Alzheimer's disease (AD) is a major global health concern, with no definitive cure currently available. Recent medical advances have introduced pharmacological interventions that may slow neurodegenerative progression, particularly in the stage of mild cognitive impairment (MCI). However, existing biomarkers require specialized clinical facilities, making largescale MCI screening challenging. To address this limitation, we propose a fully automatic framework for MCI detection that integrates linguistic and acoustic features extracted from spontaneous picture description tasks. A Large Language Model (LLM) has been used to analyze the semantic and syntactic structure of speech, capturing representations of semantic. episodic, and working memory, as well as emotional cues affected by AD. Simultaneously, acoustic processing has been adopted to quantify changes in voice quality associated with neurodegeneration. The fused feature set is evaluated using three well-established classifiers. Validation in the TAUKADIAL Challenge dataset demonstrates that the proposed framework achieves an accuracy of 0.8 under a Leave-One Subject-Out cross-validation approach, representing the highest reported performance on the test set. Importantly, the framework relies on a single picture description task, utilizes a compact LLM, and is built entirely on opensource packages, making the framework user-friendly and suitable for real-world point-of-care applications.

Keywords: Alzheimer's disease Speech processing Large Language Model Machine Learning Mild Cognitive Impairment Natural Language Processing

Authors: Aslan Modir - Fatemeh Shalchizadeh - Armin Ghasimi - Sina Shamekhi











Article Code: icbme-1045

Article Title: Designing a tremor level detection system for Parkinson's patients based on the topology of tremor time series in geographical phase space

Abstract: We believe that the geometric structures or topologies of points reconstructed from time series in phase space contain richer information for classifying nonlinear time series; However, there is a lack of analytical tools to extract such information. In this study, a novel processing space based on geographical directions is presented, utilizing reconstructed trajectories from time series in phase space. Therefore, this geographic phase space provides a platform for extracting cartographical patterns related to different problems. This space was utilized in designing a tremor detection system for Parkinson's disease that classifies tremor signal into two levels; high-amplitude tremor and low-amplitude tremor. The findings of this study showed that a pattern consisting of north, east, and northwest directions reconstructed from the tremor signal was directly related to the severity of Parkinson's disease. Using the knearest neighbors classifier, the metrics of accuracy, sensitivity, and positive predictive value were calculated for training data equal to 100% while these metrics were obtained for the test data with accuracy = 96.55%, sensitivity = 98.25%, and positive predictive value = 95.44%. While the application of this new space is promising for identifying abnormal geographical directions associated with tremor severity in Parkinson's disease scenarios, it is recommended that future research examine the computational efficiency of the proposed space in processing other biomedical signals.

Keywords: Compass direction, Geographical phase space, Cartographical pattern, Tremor severity

Authors: Mahdi Zolfagharzadeh-Kermani - Saeid Rashidi - Maryam Asaseh











Article Code: icbme-1035

Article Title: Null-Alignment Grating-Lobe Suppression in Coprime Sparse Ultrasound

Arrays:A Hardware-Efficient Imaging Approach

Abstract: Synthetic Transmit Aperture (STA) ultrasound imaging achieves high resolution and contrast by employing all transducer elements for both transmission and reception, enabling two-way dynamic focusing. However, this comes at the cost of increased hardware complexity and reduced frame rates. Sparse array techniques have been explored to mitigate these limitations by reducing the number of active channels, and transmission events. In this work, we propose a Grating-Lobe Suppressed Array (GLSA) method that achieves superior contrast compared to conventional periodic and coprime sparse arrays, while also providing a wider field of view compared to the micro-beamforming approach, which reduces digital receive channels by summing signals from grouped transducer elements. Experimental results on a CIRS phantom for lateral cysts demonstrate that GLSA increases mean gCNR by 6.7× over periodic sparse arrays, 5.4× over coprime sparse arrays, and substantially over the micro-beamforming approach, including regions where this method failed to provide reliable measurements due to its limited field of view—while retaining 81.4% of non-sparse performance.

Keywords: Synthetic transmit aperture, Grating Lobe Suppression, sub-array beamforming, Frame rate improvement.

Authors: Mina Ezati - Vahid Amin Nili - Zahra Kavehvash











Article Code: icbme-1046

Article Title: An Attention-Guided Convolutional Neural Network for Predicting Neoadjuvant Chemotherapy Response in Breast Cancer Patients

Abstract: Among women worldwide, breast cancer continues to represent one of the most critical and challenging medical conditions, demanding ongoing improvements in diagnostic and therapeutic strategies. Due to factors like tumor adhesion or large volume making some patients initially ineligible for surgery, neoadiuvant chemotherapy (NAC) aims to shrink tumors and enable breast-conserving surgery while assessing early treatment response. However, accurately forecasting an individual's response to NAC remains a major clinical challenge. It critically impacts personalized treatment planning, patient prognosis, and survival rates. It is also essential for minimizing unnecessary treatment-related toxicity. In this work, we designed an attention-based dual-branch convolutional network (AG-CNN) that analyzes dynamic contrast-enhanced MRI scans to forecast the likelihood of achieving a pathological complete response (PCR) before therapy. Our framework integrates global contextual learning with region-specific analysis by employing attention maps that guide the network toward clinically informative tumor subregions. When evaluated on the selected dataset, the architecture demonstrated strong predictive power, reaching an overall accuracy near 96%, with sensitivity exceeding 97% and specificity close to 96%. The model outperformed baseline methods lacking attention mechanisms, demonstrating the significant advantage of integrating attention in clinical outcome prediction. These results highlight the potential of attention-driven MRI analysis to guide personalized therapy planning.

Keywords: breast Cancer, pathological complete response, neoadjuvant chemotherapy (NAC), attention mechanism, convolutional neural network (CNN), dynamic contrast-enhanced magnetic resonance imaging (DCE-MRI), early detection of breast cancer, malignant lesion diagnosis.

Authors: Parisa Donyaei - Javad Haddadnia











Article Code: icbme-1052

Article Title: GPU-Accelerated GRAPPA: A Fast Implementation Using PyTorch for MRI

Reconstruction

Abstract: GeneRalized Autocalibrating Partial Parallel Acquisition (GRAPPA) is a widely used algorithm in MRI parallel imaging that reconstructs accelerated MRI scans by estimating the unknown phase-encoding lines omitted during k-space data acquisition. Unlike SENSE (Sensitivity Encoding), which operates in the image domain, GRAPPA directly processes kspace data and offers high reconstruction quality without requiring prior knowledge of coil sensitivity maps, making it one of the most commonly used algorithms for MRI reconstruction in clinical practice. Recent MRI reconstruction trends increasingly combine classical methods with deep learning, either as end-to-end trainable networks or hybrid pipelines that use physicsbased operators within learning frameworks. GRAPPA is often employed as a preprocessing step before feeding slice information into deep learning models for MRI reconstruction. Despite its effectiveness, GRAPPA is typically a time-consuming part of the training process. In this work, we leverage the GPU capabilities of the PyTorch library and employ several optimization techniques to accelerate the GRAPPA algorithm. Our implementation is compared against the PvGRAPPA repository, developed by Nicholas McKibben, using a subset of the NYU fastMRI dataset. The results demonstrate that our optimized implementation achieves more than 40-fold speedup, which is statistically significant (p < 0.01) while maintaining equivalent image quality with no significant differences in reconstruction metrics (p > 0.05).

Keywords: GRAPPA, MRI Reconstruction, Deep Learning, FastMRI, GPU acceleration.

Authors: Mehrdad Anvari-Fard - Mahdi Bazargani - Mohammad Javad Heidari - Hamid Soltanian-Zadeh











Article Code: icbme-1053

Article Title: A Comprehensive Review of Machine Learning Techniques for Automatic Skin Disease Detection

Abstract: This study offers a thorough analysis of machine learning (ML) methods for automatically identifying skin conditions, emphasizing developments in both technology and algorithms. Medical imaging and the increasing incidence of dermatological disorders have made ML crucial for precise and effective diagnosis. We examine and highlight the advantages and disadvantages of deep learning architectures, conventional machine learning algorithms, and new hybrid approaches. Evaluation metrics, preprocessing methods, and datasets utilized in the field are all covered in the review. Important issues like data imbalance, computational complexity, and model generalizability are addressed, along with potential future paths to increase algorithmic effectiveness and practicality. For researchers looking to develop automated dermatological diagnostics, this study is a valuable technical resource.

Keywords: Machine Learning, Deep Learning, Skin Disease Detection, Computer Vision, Medical Imaging.

Authors: Mahdie Naseri - Azita Shirazipour - Seyed Javad Mirabedini











Article Code: icbme-1055

Article Title: Multi-Transform Diagnostic Analysis Based on Gradient-Based Features for Breast Cancer Detection in Thermal Imaging

Abstract: Breast cancer is one of the most common causes of death in women, and early diagnosis plays a key role in successful treatment. Thermal imaging is a non-invasive and radiation-free technique, but its effectiveness depends on extracting reliable features for classification. In this work, we compare three spatial-frequency transforms, including 2D Fast Fourier Transform (2D-FFT), 2D Empirical Wavelet Transform (2D-EWT), and 2D Discrete Orthonormal Stockwell Transform (2D-DOST), together with gradient-based descriptors such as SIFT, HOG, Gradient Local Ternary Pattern (GLTP), Gradient Entropy (GradEn). The experiments are performed on breast thermograms from the DMR-IR database. After preprocessing and ROI extraction, features are reduced by principal component analysis (PCA) and classified with a Random Forest (RF) classifier using stratified 5-fold cross-validation. To handle class imbalance, balanced sampling was applied. The results show that the combination of 2D-DOST with HOG features provides the best performance with 97% accuracy, 95% sensitivity, 99% specificity, 97% F1-score and an AUC of 0.96721. The findings indicate that combining multi-transform analysis with gradient-based features can improve the diagnostic potential of breast thermography.

Keywords: Breast Cancer, Spatial-Frequency Transform, Gradient-Based Feature, 2D-FFT, 2D-EWT, 2D-DOST; SIFT, HOG, GLTP, GradEn.

Authors: Ainaz Daneshdoust - Sedigheh Ghofrani - Mahdi Eslami - Iman Ahanian











Article Code: icbme-1066

Article Title: Multi-Modal Brain Tumor Diagnosis via Hybrid Vision Transformers and CNNs: A Deep Learning Approach

Abstract: In this study, we propose a hybrid deep learning framework that integrates Convolutional Neural Networks (CNNs) with Vision Transformers (ViTs) for multimodal MRI-based brain tumor diagnosis. The model was trained and evaluated on public datasets, achieving higher accuracy and robustness compared to conventional CNN and ViT models. Our approach improved classification accuracy by 3–5% over recent state-of-the-art baselines. These findings suggest that hybrid architectures can effectively capture both local and global features, making them promising tools for reliable brain tumor diagnosis.

Keywords: Brain Tumor Segmentation, Deep Learning, Vision Transformer, 3D ResNet, Medical Image Analysis.

Authors: Alireza Haghighatjoo - Fatemeh Noori - Peyman Afshari Bijarbaneh - Seyed Amirhossein Mousavi











Article Code: icbme-1069

Article Title: Quantitative Mapping of Perivascular Spaces Across MRI Modalities Using Vesselness Filtering and Morphometric Analysis

Abstract: Perivascular spaces (PVS), fluid-filled structures around cerebral vessels, are key markers of glymphatic function. We compared T1-weighted (T1w), T2-weighted (T2w), and Enhanced PVS Contrast (EPC) MRI for automated PVS segmentation and quantification. We used high-resolution MRI data from 50 healthy Human Connectome Project (HCP) participants. We applied denoising and vesselness filtering to enhance PVS structures. PVS masks were generated and refined using thresholding and skeletonization. We extracted volume, count, diameter, and contrast metrics for comparison. T2w yielded the highest PVS volume and count; EPC showed the largest diameters. All modalities differed significantly across most metrics (p < 0.001). Skeletonization reduced volume and count but preserved relative differences. EPC consistently produced the largest diameter estimates, both before and after skeletonization, suggesting improved structural delineation of central PVS regions. While contrast-based metrics showed weaker and less consistent differences, mean diameter and volume remained the most discriminative. T2w and EPC offer complementary strengths, with EPC excelling in PVS detail.

Keywords: Glymphatic, Vesselness Filtering, Perivascular Space (PVS), Structural MRI, Human Connectome Project (HCP), Enhanced Perivascular Contrast (EPC).

Authors: Razieh Salesi - Hamid Soltanian-Zadeh











Article Code: icbme-1088

Article Title: Application of Attention Mechanisms in Deep Learning Models for COVID-19 Detection and Classification from Medical Images: A Systematic Review

Abstract: The COVID-19 pandemic, declared by the World Health Organization in March 2020, strained healthcare systems globally, highlighting the urgent need for rapid and accurate diagnosis to control its spread and optimize treatment. This systematic review investigates recent advancements in attention-based deep learning models for detecting and classifying COVID-19 using medical images, primarily chest X-rays and CT scans. We explore key attention mechanisms—spatial, channel, and self-attention—assessing their roles, strengths, and limitations in improving diagnostic precision. The study reviews their integration with architectures like convolutional neural networks (CNNs), Vision Transformers, and our proposed hybrid model, RMT-Net, through a comparative analysis of performance on public datasets such as COVIDx. Leading models achieve accuracies above 95%, demonstrating their efficacy. Clinically, these tools enhance triage and decision-making, yet challenges like data scarcity and interpretability persist. Future research should focus on improving data quality, developing interpretable models, and integrating multi-modal data. This review underscores the potential of attention mechanisms to revolutionize computer-aided diagnosis for COVID-19, offering a foundation for future innovations in medical imaging.

Keywords: COVID-19, Deep Learning, Attention Mechanisms, Medical Image Analysis, Chest X-ray, CT scan, Disease Classification.

Authors: Jafar Abdollahi - Babak Nouri-Moghaddam - Abbas Mirzaei











Article Code: icbme-1111

Article Title: Super-Resolution Generative Adversarial Network for Photothermal Optical Coherence Tomography Signal Enhancement

Abstract: Photothermal Optical Coherence Tomography is an emerging functional imaging modality that combines the high spatial resolution of OCT with molecular specificity through photothermal contrast. However, PT-OCT signals typically require extensive temporal averaging to achieve adequate signal-to-noise ratios, limiting imaging speed and real-time applications. This work presents a novel one-dimensional Super-Resolution Generative Adversarial Network (1D-SRGAN) that reconstructs full-length PT-OCT temporal responses (176 data points) from truncated initial signal segments (22 data points), achieving an 8× temporal super-resolution while preserving critical spectral characteristics at the modulation frequency. The proposed architecture employs a deep residual generator with skip connections and adversarial training, validated through comprehensive frequency-domain analysis. Statistical evaluation demonstrates significant improvement in signal reconstruction fidelity, with preserved modulation frequency characteristics and enhanced signal-to-noise ratios compared to conventional interpolation methods.

Keywords: Optical Coherence Tomography, Photothermal Imaging, biomedical imaging, generative adversarial networks, signal processing, super resolution.

Authors: Amirhossein Osooli - Mohammadhossein Salimi











Article Code: icbme-1152

Article Title: TransFuse++: A Hybrid CNN-Transformer Architecture with Cross-Attention, Temporal Modeling, and Uncertainty Estimation for Medical Image Segmentation

Abstract: Similar to any automated image analysis, precise and credible segmentation is indispensable; however, current convolutional or transformer-based networks alone cannot produce the necessary satisfactory spatial resolution, paired with anatomical global thought and volumetric consistency, in medical practice. We introduce TransFuse++, a promising step that offers incremental improvements to the TransFuse architecture, which closely integrates a CNN branch for local texture representation and a Vision Transformer branch for long-term context encoding. The model is further improved with three new modules: a cross-attention mechanism that explicitly aligns the slices, a model with a gated recurrent unit (GRU) that propagates time through stacked sequences, and Monte Carlo dropout that produces pixel-based uncertainty maps. Furthermore, context-dependent cross-skip attention fusion, along with an enhanced BiFusion head, enables more precise boundary delineation without a notable increase in computational cost in the default (no-MC) configuration. When trained in an end-to-end manner on a cardiac X-ray (1.717 frames), a lung CT (6.766 slices) and MR of cirrhotic liver (more than 600 volumes) datasets with an identical 5-fold cross validation protocol, we observe improvements of up to 4.1 percentage points in terms of Dice coefficient and 4.3 percentage points in terms of mIoU, obtaining Dice = 0.972 ± 0.002 (X-ray), 0.989 ± 0.001 (CT) and 0.923± 0.061 (MRI). The analysis using Spearman correlation revealed that the per-image Dice coefficients of competing models were either not related to each other ($|\rho| \le 0.06$, Bonferroniadjusted p > 0.005) or that they introduced complementary specific errors in addition to existing architectures. Ablation experiments validate that cross-attention, temporal modeling, and crossskipping fusion are key contributors to these incremental improvements. Meanwhile, the uncertainty maps help identify ambiguous areas, making TransFuse++ a promising step toward a confidence-aware segmentation approach for multimodal radiology.

Keywords: Hybrid CNN-Transformer Architecture, Medical Image Segmentation, Cross-Attention Mechanism, Temporal Modeling, Uncertainty Estimation, Deep Learning.

Authors: Masoud Noroozi - Sayna Jamaati - Hamed Aghapanah - Ali Saeeidi Rad - Mahsa Asadi Anar - Ali Darzi - Mahla Shokouhfar - Helia Sadat Kazemi - Mohammadreza Ghahari -Mohammad Saeed Soleimani Meigoli - Jafar Majidpour - Hossein Arabi - Ali Reza Karimian











Article Code: icbme-1164

Article Title: A Survey on Cardiac MRI Segmentation: From Classical Methods to State-of-the-art Deep Learning

Abstract: Accurate and timely diagnosis of cardiac pathologies relies heavily on Cardiovascular Magnetic Resonance (CMR) imaging, the gold standard for assessing myocardial structure, function, and tissue characteristics. A critical step in CMR analysis is the segmentation of heart chambers—particularly the left ventricle, right ventricle, and myocardium—to derive essential clinical parameters such as ejection fraction, ventricular volumes, and myocardial mass. Manual segmentation, while accurate, is labor-intensive and subject to inter-observer variability, limiting its scalability in clinical practice. This has driven the need for automated, reliable, and reproducible segmentation methods. Classical approaches, including active contours and level sets, struggle with noise and low contrast. In contrast, deep learning models—especially U-Net variants, transformers, and hybrid architectures—have achieved expert-level accuracy, enabling fully automated quantification. However, challenges remain in generalizability across scanners and centers, robustness to artifacts, model interpretability, and integration into clinical workflows. This review addresses these gaps by systematically evaluating contemporary techniques, highlighting advances in deep and hybrid models, public benchmarks, and emerging solutions such as explainable AI and federated learning. This work emphasizes the importance of translating methodological advances into clinically viable solutions, fostering the adoption of secure, interpretable, and scalable AI-based CMR segmentation in routine practice.

Keywords: Cardiac MRI Segmentation, Deep Learning, Hybrid Methods, Machine Learning Methods, Survey.

Authors: Hamed Aghapanah Roudsari - Reza Saboori Amleshi - Ali Saeeidi Rad - Masoud Noroozi











Article Code: icbme-1166

Article Title: The Adaptive Approach of Ensemble Deep Learning Model in OCT Image Classification

Abstract: Currently, there exists a global population of over 2.2 billion individuals with visual impairments, among which at least 1 billion could potentially avoid or treat their vision-related issues. The domain of eye care encounters significant challenges on a worldwide scale. Disparities persist in the accessibility, quality, and reach of treatment and rehabilitation services. Integrating eve care within healthcare systems and a scarcity of skilled eve care professionals compound these challenges. The early screening of fundus images offers an economical and accessible means of preventing blindness stemming from ocular disorders. Manual diagnostic approaches are time-consuming and can lead to delayed treatment due to limited medical resources. The advent of deep learning has yielded promising outcomes in the study of eye diseases, although most of these endeavors have focused on specific conditions. Pioneering research demonstrates the cost-effectiveness and efficacy of early eye diagnosis for mitigating blindness due to conditions such as diabetes, glaucoma, and cataracts. This study emplovs various deep learning architectures. including VGG16. MobileNetV3Small, showcasing their synergistic integration to outperform individual models. The fundus image recognition task entails categorizing images into four classes, achieving an average recognition accuracy of 96.3%, and precision of 95.63%.

Keywords: Adaptive Ensemble Models, Deep Learning, OCT Images.

Authors: Hamed Aghapanah Roudsari - Ali Ghaderian - Mrteza Choubin











Article Code: icbme-1168

Article Title: Accurate Brain Vessel Segmentation in T1-Weighted MRI based on UNETR: Improving Neurosurgical Planning

Abstract: Preoperative planning for brain tumor surgeries is highly challenging and requires precise identification of vascular anatomy to minimize the risk of complications. While T1-weighted contrast-enhanced (T1CE) MRI is routinely used for preoperative assessment, automated vessel segmentation from these scans remains a significant challenge. The absence of reliable vessel maps can disrupt surgical workflows and may compromise patient safety, especially in settings where specialized angiographic imaging is not available. In this study, we propose a transformer-based UNETR model that leverages global contextual information to address the complexity of brain vessel segmentation. After standardized preprocessing, the model was trained and validated on 30 expert-annotated T1CE MRI scans. The approach achieved high performance, with a Dice score of 87%, IoU of 0.98, sensitivity of 0.99, and specificity of 0.99, showing strong capability in detecting both major vessels and smaller vascular branches. These findings highlight the potential of attention-based architectures to enhance routine clinical imaging by providing accurate vessel maps directly from standard MRI sequences already acquired for tumor evaluation. Such a framework could support safer and more efficient preoperative planning without requiring additional imaging resources.

Keywords: Brain Vessels Segmentation, T1CE MRI images, Deep Learning, Neurosurgical Pre-Planning.

Authors: Fatemeh Gholizadeh - Mahdiyeh Rahmani - Ahmad Pour-Rashidi - Ebrahim Najafzadeh - Parastoo Farnia - Alireza Ahmadian











Article Code: icbme-1192

Article Title: CRAFT-Flow: Cross-Attentional Refinement for Robust Optical Flow Estimation in Cardiac MRI via Deep Learning

Abstract: Optical flow estimation in medical imaging, particularly in dynamic cardiac MRI (CMRI), presents significant challenges due to complex non-rigid motion, low contrast, and absence of ground-truth labels. While deep learning has revolutionized optical flow in natural scenes, its application to medical sequences remains limited by model generalization and noise sensitivity. In this work, we propose CRAFT-Flow, a novel deep architecture that integrates cross-attentional transformers with a refined PWC-Net backbone to achieve robust, highprecision motion estimation in synthetic and real cardiac MRI sequences. Inspired by the CRAFT model's success in large-displacement flow estimation, we redesign the correlation mechanism using cross-attention transformers, replacing classical correlation volumes to enhance long-range correspondence and reduce noise artifacts. Our model is trained on synthetic 4D cardiac phantoms generated via MRXCAT and XCAT, enabling supervision under realistic motion patterns. We further introduce a multi-scale warping and unsupervised refinement framework to adapt the model to unlabeled clinical CMRI data. Extensive experiments on Sintel, KITTI, and a custom cardiac dataset demonstrate that CRAFT-Flow achieves competitive performance, with a 21% reduction in EPE compared to PWC-Net on cardiac MRI, while demonstrating superior robustness under motion blur and noise. On Sintelclean, our EPE (2.22) is higher than RAFT (1.83), indicating room for improvement in natural scene benchmarks, but our model excels in medical-specific metrics and efficiency and superior robustness under motion blur and noise. The proposed framework opens new pathways for motion-aware analysis in cardiac imaging, autonomous driving, and video understanding.

Keywords: Cardiac MRI, Cross-Attention, Deep Learning, Motion Estimation, Optical Flow, Transformer Networks, Unsupervised Learning.

Authors: Hamed Aghapanah Roudsari - Reza Ashiri Gudarzi - Morteza Choubin











Article Code: icbme-1196

Article Title: Lightweight 3D U-Net for Robust Liver Segmentation in Multi-Institutional CT Datasets

Abstract: A computed tomography (CT) image of the liver and surrounding structures provide detailed cross-sectional images, which highlight anatomical variations and pathological conditions. Using CT and U-Net networks to segment the liver is a well-known method for accurate diagnosis, treatment planning, and surgery. Although, the high computational demands of recent 3D U-Net-based architectures prevent their deployment in resource-constrained environments. A lightweight 3D U-Net optimized for liver segmentation is proposed in this study, maintaining high performance while reducing computational complexity drastically, Several institutional datasets of 250 abdominal CT volumes were compiled from public benchmarks (LiTS, IRCAD) and local clinical sources, encompassing anatomical, pathological, and protocol variations. An isotropic resampling procedure was used to resample, normalize intensity, standardize crops, and augment data on-the-fly. With fewer than two million parameters, the proposed model retains the encoder-decoder and skip-connection designs of conventional 3D U-Nets. An evaluation of a 30% independent set of tests achieved Dice similarity coefficients of 0.85 ± 0.02, intersect-over-unions of 0.82 ± 0.03, inference times under 0.7 s and GPU memory consumption below 2 GB. The performance was consistent across public and local datasets, highlighting the importance of heterogeneous training data. Even though the proposed model is slightly less accurate than heavy architecture, it delivers nearreal-time segmentation with minimal resource consumption, so it can be integrated into clinical workflows, especially in environments where computational resources are limited.

Keywords: Liver, Segmentation, 3D U-Net, Computed Tomography (CT).

Authors: Seyyed Mohammad Hosseini - Faeze Salahshour - Ahmadreza Sebzari - Masoomeh Safaei - Hossein Ghadiri Harvani











Article Code: icbme-1207

Article Title: A Comparative Analysis of CNN Architectures for Histopathology Image Classification: Performance. Efficiency, and Adversarial Robustness

Abstract: The integration of Convolutional Neural Networks (CNNs) into histopathology promises to revolutionize diagnostics, yet their vulnerability to adversarial attacks poses a significant risk to clinical deployment. This study investigates the relationship between CNN architecture, performance, and adversarial robustness. We benchmarked five distinct architectures (VGG16, ResNet-50, MobileNetV3-Large, EfficientNet-B4, and ConvNeXt-Tiny) on the PathMNIST dataset for classification accuracy, efficiency, and robustness against both Projected Gradient Descent (PGD) and Fast Gradient Sign Method (FGSM) attacks. Our results, averaged over five runs, show that while ConvNeXt-Tiny achieved the highest clean accuracy (93.07%±0.88%), its performance collapsed under low-strength attacks. Adversarial training significantly enhanced resilience, maintaining 62.14%±0.65% accuracy under a PGD attack that reduced the standard model's accuracy to nearly zero. This highlights a critical trade-off between standard accuracy and adversarial robustness, underscoring the need to evaluate models for both safety and reliability before clinical adoption.

Keywords: Convolutional Neural Networks, CNN, Histopathology, Adversarial Robustness, Adversarial Training, Medical Imaging, Image Classification.

Authors: Moein Akbari Shahpar - Mohsen Akbari-Shahpar











Article Code: icbme-1215

Article Title: Enhancing Dental Disease Detection: Leveraging Swin Transformer and DenseNet with Attention-Guided Fusion in Dental Panoramic Imaging

Abstract: The automatic identification of dental diseases and anomalies in panoramic radiographs poses a significant challenge, primarily due to the vast array of dental conditions that can manifest. The synergistic integration of multiple deep learning architectures has the potential to enhance overall performance, as each model compensates for the limitations present in the others. In the context of deep learning, the choice of backbone architecture is critical for effective feature extraction. Consequently, employing diverse feature extraction techniques can substantially augment the model's capability to accurately identify dental conditions. This paper introduces an approach for detecting diseases and abnormalities in panoramic dental images through the application of an Attention-Guided Fusion technique, which integrates features extracted from two distinct architectures: DenseNet and Swin Transformer. The DenseNet framework excels in capturing local features, while the Swin Transformer is proficient in obtaining global contextual information. By adaptively fusing these features, the proposed method which achieved an F1-score of 0.621 effectively highlights critical regions within the images. The performance of the proposed model was rigorously evaluated using a publicly available dataset, demonstrating a significant improvement in accuracy compared to several established methodologies, including Faster R-CNN, Combined DINO and YOLOv8, DETR, YOLOrtho, HierarchicalDet, and DiffusionDet.

Keywords: Dental Disease Detection, Panoramic Dental X-ray Images, DenseNet, Swin Transformer, Guided Fusion technique.

Authors: Mahdieh Dehghani - Reza Aghaeizadeh Zoroofi











Article Code: icbme-1224

Article Title: Attentive Temporal Fusion Network (ATFNet) for Multi-frame Coronary Vessel Segmentation in X-ray Angiography

Abstract: X-ray coronary angiography remains the clinical gold standard for visualizing coronary lumen but presents major challenges for automated analysis: low vessel contrast, overlapping anatomy, catheter occlusion, breathing/heartbeat motion and extremely thin branching vessels that fracture easily in segmentation maps. To address these issues we propose ATFNet (Attentive Temporal Fusion Network), a compact UNet++-inspired architecture that ingests short temporal stacks (four successive frames) and fuses motion and appearance cues into a single 2-D prediction. Key components are (i) SATS (Spatial Attention Temporal Squeeze), a per-frame directional spatial attention and learned temporal fusion that compresses four frames into a channel-recalibrated 2-D representation; (ii) SE ResBlock3D/2D units that provide residual learning with squeeze-and-excitation attention in the 3D encoder and 2D decoder; (iii) DSF (Deep Supervision Fusion), which combines coarse (spatial merge) and attentive (channel-reweighted) fine kernels from multiple decoder depths into one robust output; and (iv) a topology-aware StructuredSparsityLoss (BCE-Dice base + multi-scale tree norm) together with the Lion optimizer and scheduler to stabilise and accelerate training on modest clinical data. On a manually annotated clinical XCA set, ATFNet produces noticeably more continuous, less fragmented vessel masks and improved temporal stability compared with single-frame baselines; ablation studies confirm that SATS, DSF, SE-Res blocks and the Lion optimizer each contribute to the observed gains. These results indicate that compact, attentionaugmented temporal fusion, combined with a tree-aware loss, can substantially improve coronary vessel continuity and segmentation fidelity in angiographic sequences.

Keywords: Attentive Temporal Fusion Network, Coronary vessel segmentation, X-ray coronary angiography, Spatial Attention Temporal Squeeze, Structured sparsity loss.

Authors: Pouya Babaei - Farshad Almasganj











Article Code: icbme-1226

Article Title: Benchmarking nnU-Net vs. Custom 3D U-Net for Kidney Tumor Segmentation: A Controlled Study on KiTS19 Dataset

Abstract: This study presents a controlled comparison between nnU-Net and a custom three-dimensional U-Net architecture for kidney and tumor segmentation using the KiTS19 dataset. Both models were trained under identical conditions, using the same preprocessing, data augmentation, and training protocols to isolate the effects of architecture and optimization strategies. Evaluation was conducted on 210 labeled cases, with 140 used for training and 70 for testing, using the Dice similarity coefficient and intersection over union metrics. The nnU-Net achieved Dice scores of 0.9683 for kidney and 0.8166 for tumor, while the custom U-Net obtained scores of 0.9450 and 0.6296, respectively. Similarly, intersection over union scores were 0.9390 and 0.7176 for nnU-Net, compared to 0.8997 and 0.5167 for the custom model. A non-parametric Wilcoxon signed-rank test confirmed that these differences were statistically significant, with a p-value that was extremely small and very close to zero. These findings highlight the role of deep supervision, architectural scaling, and automated configuration in enhancing segmentation accuracy for challenging medical imaging tasks.

Keywords: deep learning, medical image segmentation, 3D U-Net, nnU-Net, kidney tumor.

Authors: Ariya Soleimany - Masoud Noroozi - Mohammad Saber Azimi - Alireza Karimian - Jafar Majidpour - Hossein Arabi











Article Code: icbme-1229

Article Title: Investigating the Self-optimizing nnU-NetV2 for Kidney Tumor Segmentation: Application to the KiTS23 Dataset

Abstract: Kidney cancer ranks among the top 10 most prevalent cancers, with renal cell carcinoma (RCC) being the dominant form, accounting for approximately 90% of all kidney cancer cases. As computer technology advances unprecedentedly, its integration into the medical field, particularly in computer-aided diagnostics and treatment, has grown significantly. In this work, we evaluate the nnU-NetV2 segmentation model on the kidney tumor segmentation dataset (KiTS2023). The 3D nnU-NetV2 model was trained for 300 Epochs with single-fold validation, using 320 CT scans from the retrospective KiTS23 dataset, with 80 cases for validation and 89 cases for testing. The evaluation metrics Dice Similarity Coefficient (DSC), IoU (Intersection over Union), sensitivity, and specificity were applied to assess performance in both region-based and foreground segmentation. Test-set DSC values were 0.8334 (Kidney+Tumor+Cyst), 0.6678 (Tumor+Cyst), and 0.6009 (Tumor); IoU scores were 0.7705, 0.5621, and 0.5078, respectively. Sensitivity values were 0.7915, 0.6743, and 0.6459, respectively, and specificity remained consistently high at 0.99 across all regions. For foreground segmentation on the test set, DSC was 0.7007, and IoU was 0.6135. Despite using a relatively low number of epochs and single-fold validation, comparison with the benchmark results demonstrates that the nnU-Net model remains a robust tool for automatic kidney tumor segmentation.

Keywords: Deep Learning, Medical Image Segmentation, nnU-NetV2, Kidney Tumor Segmentation.

Authors: Sanam Doostinia - Masoud Noroozi - Mohammad Saber Azimi - Jafar Majidpour - Hossein Arabi











Article Code: icbme-1242

Article Title: Comparative Assessment of U-Net and Pix2Pix for Applying Direct Attenuation Correction in the Image Domain in 68Ga-PSMA PET/CT Imaging

Abstract: Accurate quantitative positron emission tomography (PET) imaging needs effective attenuation correction (AC). This remains a challenge in dedicated PET systems that lack concurrent computed tomography (CT). Recent research has investigated deep learning (DL) methods for AC, but direct comparisons between models are still limited. This study systematically compares the performance of two widely used DL architectures, U-Net and Pix2Pix, for direct AC of whole-body 68Ga-PSMA PET images using a consistent set of 95 patient data sets. Both models are evaluated under identical conditions. For each data set, CTbased attenuation-corrected PET (PET-CTAC) was used as the reference. Quantitative evaluation included mean error (ME) of mean of standardized uptake value (SUVmean), normalized root mean square error (NRMSE), structural similarity index (SSIM), and peak signal-to-noise ratio (PSNR). Both U-Net and Pix2Pix generate PET images with visual quality similar to PET-CTAC, but Pix2Pix generally showed better quantitative metrics. Specifically, U-Net achieved ME, NRMSE, SSIM, and PSNR values of 0.037 ± 0.02, 0.006 ± 0.005, 12.88 ± 2.73, and 0.98 ± 0.14, respectively, whereas Pix2Pix achieved 0.015 ± 0.015, 0.005 ± 0.004, 13.93 ± 2.48, and 0.99 ± 0.004. Statistical analyses are conducted using paired t-test or Wilcoxon signed-rank tests, selected based on the normality of the data, demonstrated that Pix2Pix produced SUV estimates closer to those of PET-CTAC, with lower bias and variability than U-Net. In conclusion, both DL models enabled direct AC of whole-body 68Ga-PSMA PET, but Pix2Pix provided more accurate and reliable AC when the two models were directly compared, indicating Pix2Pix is the stronger candidate for clinical use in dedicated PET systems without CT imaging.

Keywords: Attenuation Correction, PET/CT, PSMA, Deep Learning, U-Net, Pix2Pix.

Authors: Negin Hamidiyan - Hadi Taleshi Ahangari - Pardis Ghafarian - Hossein Arabi - Mohammad Reza Ay











Article Code: icbme-1243

Article Title: A survey over deep learning methods for early detection in mammogram images

Abstract: Breast cancer is the second most common cancer in the world. If cancerous masses are not detected in a proper time interval, they can jeopardize patients' lives. Breast cancer can be detected in different ways, such as X-Ray, ultrasound, histopathological imaging, and genetic sequencing. Deep learning (DL) plays a vital role in medical imaging research, such as convolutional neural networks (CNNs), graph neural networks (GNNs), and transformer-based models. We also reviewed previous research on DL methods for detecting and classifying breast cancer. We focus on studies of previous DL methods, preprocessing, datasets, evaluation, and limitations. CNN and hybrid models increase performance compared to traditional machine learning. Transformer-based and graph- based models enhance feature representation. In this research, we use ScienceDirect, IEEE Xplore, Springer, and Google Scholar databases. This survey focuses on new DL-based architectures for just X-Ray mammograms as well as multimodal fusion DL-based methods to make researchers familiar with state-of-the-art DL-based methods in breast cancer detection methods. We have briefly introduced the efficient DL-based schemes and compared their results on different publicly available datasets and discussed the pros and cons of the investigated methods.

Keywords: Breast cancer, Deep learning, Convolutional neural networks, Graph neural networks, Transformer.

Authors: Zeinab Shirkool - Mohammad Ali Tabarzad - Reza Boostani











Article Code: icbme-1244

Article Title: Improving Generalization in MRI-Based Deep Learning Models for Total Knee Replacement Prediction

Abstract: Knee osteoarthritis (KOA) is a common joint disease that causes pain and mobility issues. While MRI-based deep learning models have demonstrated superior performance in predicting total knee replacement (TKR) and disease progression, their generalizability remains challenging, particularly when applied to imaging data from different sources. In this study, we show that replacing batch normalization with instance normalization, using data augmentation, and applying contrastive loss improves generalization. For training and evaluation, we used MRI data from the Osteoarthritis Initiative (OAI) database, considering sagittal fat-suppressed intermediate-weighted turbo spin-echo (FS-IW-TSE) images as the source domain and sagittal fat-suppressed three-dimensional (3D) dual-echo in steady state (DESS) images as the target domain. The results demonstrated a statistically significant improvement in classification metrics across both domains by replacing batch normalization with instance normalization in the baseline model, generating augmented input views using the Global Intensity Non-linear (GIN) augmentation method, and incorporating a supervised contrastive loss alongside the classification loss to align representations of samples with the same label. In the source domain, this approach achieved an accuracy of 74.12 ± 2.90, an F1 score of 74.57 ± 3.33, and a ROC AUC of 80.65 ± 2.83, outperforming the baseline model, which scored 71.29 ± 4.43, 69.76 ± 4.58, and 77.79 ± 4.66, respectively. In the target domain, the method achieved an accuracy of 70.04 ± 2.49, F1 score of 67.30 ± 3.57, and ROC AUC of 78.12 ± 1.97, compared to the baseline's 52.87 ± 3.17 , 18.98 ± 16.89 , and 59.33 ± 6.20 . The GIN method with contrastive loss performed better than all evaluated single-source domain generalization methods when using 3D instance normalization. Comparing GIN with and without contrastive loss (for both normalization types) showed that adding contrastive loss consistently led to better performance.

Keywords: knee osteoarthritis, deep learning, medical image analysis, MRI, total knee replacement prediction, model generalization.

Authors: Ehsan Karami - Hamid Soltanian-Zadeh











Article Code: icbme-1248

Article Title: Geometry-Aware Anisotropic Total Variation Regularization for Limited-View Photoacoustic Tomography

Abstract: Photoacoustic tomography (PAT) is a hybrid imaging modality that combines optical absorption contrast with ultrasonic detection, providing high-resolution visualization of tissue structures. However, PAT reconstructions often suffer from artifacts under limited-view acquisition due to incomplete angular sampling. Conventional isotropic total variation (TV) applies uniform smoothing, which can blur structural details, while image-adaptive anisotropic methods overlook the measurement geometry, potentially amplifying artifacts along poorly sampled orientations. We propose a geometry-aware anisotropic total variation (GA-TV) regularization that incorporates the angular sensitivity of the sensor array into the reconstruction process. GA-TV computes directional derivatives and applies geometry-derived weights to selectively suppress gradients in under-sampled directions while preserving edges in well-sampled orientations. The method integrates seamlessly with model-based (MB) reconstruction frameworks. Simulations with vessel and brain phantoms using full-ring, half-ring, and linear arrays show that GA-TV improves artifact suppression and structural fidelity. Quantitative evaluation using SSIM and ASR confirms superior reconstruction quality, achieving a 27% improvement in ASR and higher SSIM compared to conventional methods.

Keywords: Photoacoustic Tomography, Limited-View, Model-Based Reconstruction, Artifact Suppression.

Authors: Amirreza Jodeiry - Zahra Kavehvash











Article Code: icbme-1253

Article Title: Mitigating MRI Domain Shift in Sex Classification: A Deep Learning Approach

with ComBat Harmonization

Abstract: Deep learning models for medical image analysis often suffer from performance degradation when applied to data from different scanners or protocols, a phenomenon known as domain shift. This study investigates this challenge in the context of sex classification from 3D T1-weighted brain magnetic resonance imaging (MRI) scans using the IXI and OASIS3 datasets. While models achieved high within-domain accuracy (around 0.95) when trained and tested on a single dataset (IXI or OASIS3), we demonstrate a significant performance drop to chance level (about 0.50) when models trained on one dataset are tested on the other, highlighting the presence of a strong domain shift. To address this, we employed the ComBat harmonization technique to align the feature distributions of the two datasets. We evaluated three state-of-the-art 3D deep learning architectures (3D ResNet18, 3D DenseNet, and 3D EfficientNet) across multiple training strategies. Our results show that ComBat harmonization effectively reduces the domain shift, leading to a substantial improvement in cross-domain classification performance. For instance, the cross-domain balanced accuracy of our best model (ResNet18 3D with Attention) improved from approximately 0.50 (chance level) to 0.61 after harmonization. t-SNE visualization of extracted features provides clear qualitative evidence of the reduced domain discrepancy post-harmonization. Cross-domain balanced accuracy improved from ~0.50 to 0.61 after ComBat, a modest yet meaningful gain that moves the model from chance-level failure toward more reliable generalization while remaining below clinical utility. This work underscores the critical importance of domain adaptation techniques for building robust and generalizable neuroimaging AI models.

Keywords: Deep Learning, Sex Classification, Combat Harmonization, Domain Adaptation, Magnetic Resonance Imaging.

Authors: Peyman Sharifian - Mohammad Saber Azimi - Masoud Noroozi - Alireza Karimian - Hossein Arabi











Article Code: icbme-1266

Article Title: Benchmarking Class Activation Map Methods for Explainable Brain Hemorrhage Classification on Hemorica Dataset

Abstract: Explainable Artificial Intelligence (XAI) has become an essential component of medical imaging research, aiming to increase transparency and clinical trust in deep learning models. This study investigates brain hemorrhage diagnosis with a focus on explainability through Class Activation Mapping (CAM) techniques. A pipeline was developed to extract pixel-level segmentation and detection annotations from classification mod- els using nine stateof-the-art CAM algorithms, applied across multiple network stages, and quantitatively evaluated on the Hemorica dataset, which uniquely provides both slice-level labels and highquality segmentation masks. Metrics including Dice, IoU, and pixel-wise overlap were employed to benchmark CAM variants. Results show that the strongest localization performance occurred at stage five of EfficientNetV2-S, with HiResCAM yielding the highest bounding-box alignment and AblationCAM achieving the best pixel-level Dice (≈ 0.57) and IoU (\approx 0.40), representing strong accuracy given that models were trained solely for classification without segmentation supervision. To the best of current knowledge, this is among the first works to quanti- tatively compare CAM methods for brain hemorrhage detection, establishing a reproducible benchmark and underscoring the potential of XAI-driven pipelines for clinically meaningful AI- assisted diagnosis.

Keywords: Explainable Artificial Intelligence (XAI), Class Activation Map (CAM), Brain Hemorrhage Classification, Deep Learning.

Authors: Zahra Rafati - Mohamad Hoseyni - Javad Khoramdel - Amirhossein Nikoofard











Article Code: icbme-1267

Article Title: Towards Accurate Multimodal Defformable Image Registration via Image Translation and Weak Supervision

Abstract: This study proposes a weakly supervised learning strategy for training deep learning models on multimodal registration tasks, using loss functions based on monomodal similarity metrics. Since monomodal metrics are generally more reliable and robust than their multimodal counterparts, this strategy stabilizes the training process and tends to produce more plausible outcomes. The approach is implemented using synthetic image generation models that convert images from one modality to another to reduce intensity inconsistencies across domains. We apply this method to MRI-to-CT deformable registration, which is a critical component of the radiotherapy planning process. The results demonstrate significant improvement in image alignment while preserving their realistic appearance. In addition, we compare this learning strategy with an unsupervised approach trained using multimodal similarity metrics. The comparison indicates a more stable training process. Quantitative results show notable improvements in both SSIM (from 0.8429 to 0.8510) and the mean Dice score (from 0.7750 to 0.7985).

Keywords: deformable image registration, image-to-image translation, weakly supervised learning, computed tomography, magnetic resonance imaging.

Authors: Maryam Nasr - Mohammadreza Yazdchi - Mohsen Safdari











Article Code: icbme-1269

Article Title: MRI to SPECT Image Translation for Parkinson's Disease Diagnosis

Abstract: Parkinson's disease, the second most common neurological disorder worldwide, results from the degeneration of dopaminergic neurons in the substantia nigra, making early diagnosis complex and challenging. Although MRI images are widely accessible, they lack the sensitivity required to detect early changes. Conversely, DaTscan images provide higher accuracy by directly visualizing dopaminergic activity, but their use is limited by cost and complexity. This study employs a deep learning-based generative model, CycleGAN, to convert MRI images of patients and healthy individuals into DaTSPECT-like images. Subsequently, a Convolutional Neural Network (CNN) classifies patients and healthy subjects using the transformed images. This approach combines the advantages of both MRI and DaTscan modalities while addressing the scarcity of DaTscan data. Data were obtained from the PPMI dataset, which includes DaTSPECT and MRI images of patients and healthy controls. Results demonstrate that incorporating synthetic images with the original data increases classification accuracy to 85% and recall to 82.5%, reflecting improvements of 8.75% and 17.5%, respectively, over using only original DaTscan images. These findings confirm the effectiveness of the proposed method in enhancing Parkinson's disease diagnosis.

Keywords: CNN, CycleGAN, Data Augmentation, DaTSPECT, MRI, Parkinson's disease.

Authors: Pegah Zandian PourEsfahani - Abolfazl Adib Almojahedi - Seyyede Zohreh Seyyed Salehi











Article Code: icbme-1271

Article Title: A Real-Time Integrated Framework for Face Detection, Gender, and Emotion Recognition Using Convolutional Neural Networks

Abstract: This paper presents a real-time convolutional neural network (CNN) framework for simultaneous facial emotion and gender recognition. The proposed architecture is designed to process facial images and classify them into six basic emotion categories (happiness, sadness, anger, fear, surprise, disgust) and two gender classes (male, female). The model employs a series of convolutional, pooling, and fully connected layers to hierarchically extract and classify discriminative facial features. When evaluated on publicly available benchmarks, the system achieves state-of-the-art performance, reporting 85% accuracy on the FER-2013 emotion recognition dataset. To enhance interpretability, a guided backpropagation visualization technique is integrated, enabling real-time analysis of learned features and weight dynamics across layers. We demonstrate that combining modern CNN design, advanced regularization, and visual explainability is essential for bridging the gap between offline performance and realtime deployment. The framework is validated through implementation in an integrated vision system capable of unified face detection, gender classification, and emotion recognition in a single forward pass. With applications in social robotics, human-computer interaction, and affective computing, this work provides both a scalable CNN architecture and an open-source implementation to support further innovation in real-time affective vision systems.

Keywords: Facial expressions, Gender Classification, Convolutional neural networks, Facial Emotion Recognition, Deep Learning.

Authors: Mostafa Asgarinejad - Elias Ebrahimzadeh - Vida Mirabolfathi - Lila Rajabion - Hamid Soltanian-Zadeh











Article Code: icbme-1302

Article Title: Robust Speckle Noise Reduction in IVUS Imaging: Advancing Autoencoders and Non-Local Means with Particle Swarm Optimization

Abstract: Speckle noise in Intravascular Ultrasound (IVUS) images poses a significant challenge, necessitating early elimination of these artifacts. In this study, two novel methods were designed: a denoising convolutional autoencoder and a modified non-local means algorithm using particle swarm optimization (PSO) for automatic parameter selection. This research delved into assessing the efficacy of various denoising models, encompassing spatial domain techniques (median filter, non-local means, optimized non-local means), transform domain methods (wavelet, curvelet), and deep learning approaches (denoising autoencoder). A wide array of data augmentation techniques was employed during the training of the autoencoder model. Evaluation was conducted using two key metrics: Structural Similarity Index Measure (SSIM) and Peak Signal-to-Noise Ratio (PSNR). The findings indicate the robustness of the autoencoder model with the proposed augmentation strategy across different speckle noise variances, highlighting its superiority over traditional methods. Moreover, the study underscores the enhanced performance of modified non-local means with particle swarm optimization (PSO) compared to manual non-local means.

Keywords: Intravascular Ultrasound (IVUS), Speckle Noise, Convolutional Autoencoder, Non-Local Means, particle swarm optimization (PSO), Data Augmentation.

Authors: Shirin Ashtari Tondashti - Navid Adib - Mehran Alyali - Mahdis Yaghoubi - Seyed Kamaledin Setarehdan











Article Code: icbme-1307

Article Title: Added value of synthetic T1/T2-weighted MR images in the segmentation and staging of meningioma

Abstract: Accurate pre-operative classification and volumetric definition of intracranial meningiomas are paramount to the development of appropriate surveillance, surgical, and radiotherapeutic approaches. The traditional post-contrast T1-weighted MRI (T1c) is used clinically but is time-consuming to contour and not always available or against indications. To assess how a bias-corrected native-T1/ T2-weighted ratio (T1(n)/T2(w)) map, combined with fully automated segmentation and grading networks, can enhance meningioma work-up without gadolinium. The novelty of this research lies in the use of T1n/T2w information to generate synthetic images, replacing the need for four separate MRI sequences. The BraTS-MEN multicentre dataset (685 scans to be segmented and 868 scans to be graded) was skull-stripped and registered to the atlas. A 3-D nnU-Net V2 was trained to segment tumors using (i) T1c and (ii) T1n/T2w volumes. The resulting masks were either presented directly or supplemented with the four mpMRI channels in a 3-D ResNet-18 to predict WHO grades 1-2. Performance was measured as Dice, IoU, accuracy, and class-based sensitivity/specificity. T1c performed the best in terms of geometry Dice (92.12 ± 4.14 %) and IoU (86.35 ± 11.3 %). The T1n/T2w map nonetheless maintained a clinically satisfactory Dice of 82.1 ± 11.68 with decreased falsepositive voxels in neighboring dura. The ratio-based pipeline was superior to the T1c model in all global measures (accuracy 0.61 vs 0.427; mean Dice 0.558 vs 0.425) and the sensitivity of high-grade (>= WHO II) tumor was over twofold higher (0.70 vs 0.31). The T1n/T2w ratio map, as a gadolinium-free contrast agent, and the nnU-Net V2 in segmentation and ResNet-18 in the classifier demonstrate strength in automated grade assessment accuracy and preventing the under-treatment of aggressive meningiomas. An open-source, hardware-light, and easily reproducible workflow indicates a potential avenue of non-invasive, contrast-sparing preoperative assessment that could be validated in a multi-institutional prospective setting.

Keywords: Meningioma, T1/T2 Ratio Imaging, nnU-Net, Segmentation, Automated WHO Grading, Deep Learning.

Authors: Masoud Noroozi - Sayna Jamaati - Peyman Sharifian - Mahsa Karbasi - Esmaeil Gharepapagh - Alireza Karimian - Hossein Arabi - Sahar Rezaei











Article Code: icbme-1335

Article Title: Hybrid Active Learning–Driven Subset Dataset Selection Enables Near-Optimal Cardiac X-Ray Segmentation with Less Training Data

Abstract: Deep neural networks deliver state-of-the-art performance in medical-image segmentation but demand exhaustive pixel-level annotation, a major barrier in data-limited clinical settings. We introduce a single-shot hybrid subset-selection scheme that uses only 15% of the available training images (206 of 1,373; i.e., 85% reduction) while maintaining accuracy close to a full-data baseline. A U-Net with a ResNet-50 encoder is trained on 512×512 cardiac radiographs. To curate a compact training set, we combine (i) an uncertainty-aware active branch that converts class-probability vectors into a label-free pool-scoring uncertainty proxy via a lightweight ResNet-18 regressor, and (ii) a geometry-preserving coreset branch that applies k-center greedy search to Global-Average-Pooled (GAP) bottleneck features. The two branches are deduplicated and budgeted to 206 images (15%) before training the segmenter de novo with the same recipe as the baseline. With the fixed 15% budget, Active-only and Coresetonly training achieve Dice scores of 0.916 and 0.929, respectively; the Hybrid selection attains Dice 0.950, accuracy 0.984, sensitivity 0.950, and specificity 0.990, with no statistically significant difference from the full-data model (paired two-sided t-tests, p>0.05). The proposed mask-agnostic (at pool-scoring) and modular hybrid selector enables near-optimal segmentation at a fraction of labeling cost and is readily adaptable to other backbones and representation spaces.

Keywords: Active Learning, Coreset Selection, Cardiac X-Ray Segmentation, Data Efficiency, Uncertainty Estimation, Deep Learning.

Authors: Sayna Jamaati - Masoud Noroozi - Hossein Arabi - Alireza Karimian











Article Code: icbme-1343

Article Title: Robust Binary Differentiation of ALL vs. AML Using Deep Graph Convolutions

Abstract: Early triage of acute leukemia remains challenging due to subtle morphologic differences between lymphoid and myeloid blasts and the time-consuming nature of manual review. This study introduces a comprehensive computational pipeline that combines graphbased image representation with deep convolutional modeling to automatically distinguish between ALL and AML samples. A curated dataset of 44 patient smears was utilized, preprocessed through resizing and normalization. To balance class representation, synthetic data were generated using a generative network, and the images were further converted into graph structures where nodes captured localized intensity characteristics. A six-layer graph convolutional backbone with batch normalization, dropout, and a terminal softmax performs binary classification. Under a 70/20/10 split with 5-fold cross-validation, the model achieves strong and consistent performance (Accuracy 99.4%, Specificity 97.3%, Kappa 0.85), and remains robust when synthetic white noise is added (accuracy >90% at SNR = 0 dB). Comparative analyses against standard CNN/ResNet/VGG baselines indicate superior accuracy and stability, supporting the efficiency of graph-enhanced representations for this task. These results suggest a practical tool to support pathologists in rapid screening and referral. Subsequent research may focus on expanding the framework toward multi-class analysis involving additional leukemia subtypes and investigating new data augmentation mechanisms beyond GAN-based synthesis.

Keywords: Acute leukemia; ALL, AML, graph convolutional networks, microscopic smear analysis, robust classification.

Authors: Mahsanr Rahmani - Saeed Meshgini - Reza Afrouzian











Article Code: icbme-1358

Article Title: Late Fusion-Based Deep Learning for Breast Cancer Classification in

Mammography

Abstract: This study investigates a late fusion framework for breast cancer classification in mammography using deep learning. Two EfficientNet-B0 models were trained independently on craniocaudal (CC) and mediolateral oblique (MLO) mammographic views. Their outputs were integrated via a fully connected late fusion layer. Experimental evaluation on a dataset collected from two hospitals showed that single-view models achieved 82.14% accuracy with perfect sensitivity but limited specificity, while the late fusion model improved performance to 92.86% accuracy, 1.000 sensitivity, and 0.8667 specificity. The proposed lightweight fusion framework is computationally efficient and particularly suitable for small, clinically curated datasets. These results confirm that multi-view late fusion reduces false positives and enhances diagnostic reliability in computer-aided mammography. Moreover, our deterministic and lightweight fusion enables faster inference compared with probabilistic or transformer-based fusion methods.

Keywords: Breast cancer, mammography, deep learning, late fusion, BI RADS.

Authors: Mehdi Baharloo - Ata Jodeiri











Article Code: icbme-1364

Article Title: Automated Tibial Bone Segmentation using 2D Swin-Unet on Knee X-ray

Images

Abstract: Tibial plateau fractures (TPFs) comprise roughly 1% of all bone fractures and represent a complex subset of knee injuries with significant clinical implications if not accurately diagnosed and managed. The accurate diagnosis of TPFs from radiographs is challenged by subtle fracture lines and significant inter-observer variability in manual segmentation. To overcome the aforementioned limitations, this study evaluates the performance of a Transformer-based deep learning architecture, Swin-Unet, for automated and precise tibial segmentation. A retrospective dataset comprising 958 anterior-posterior and lateral radiographs from 220 patients with TPFs was curated. Ground truth masks of the tibia bone were manually annotated and validated through a multi-stage review by orthopedic surgeons. Following preprocessing steps, including resizing, adaptive contrast enhancement, and normalization, a 2D Swin-Unet architecture featuring patch-based self-attention mechanisms was trained. Quantitative assessment of the optimized Swin-Unet model on the validation dataset vielded a mean Dice Similarity Coefficient of 0.8314 ± 0.15, a mean Intersection over Union of 0.7374 ± 0.16, and an overall accuracy of 0.9735. Qualitative analysis confirmed the model's ability to accurately delineate tibial boundaries. In conclusion, this study validates the Swin-Unet model as a robust and efficient framework for automated tibial segmentation. By mitigating the challenges of manual delineation, this approach holds significant promise for improving the consistency of orthopedic diagnostic workflows. It serves as a foundation for AIdriven clinical decision support in musculoskeletal imaging.

Keywords: Tibial Plateau Fracture, Medical Image Segmentation, Swin-Unet, X-ray Imaging, Deep Learning.

Authors: Ali Kazemi - Abolfazl Zamanirad - Soodabeh Esfandiary - Ebrahim Najafzadeh - Mohammad Hossein Nabian - Parastoo Farnia - Alireza Ahmadian











Article Code: icbme-1368

Article Title: Addressing Class Imbalance Using Difficulty-based Oversampling with Variance

Control

Abstract: Learning from imbalanced data is one of the difficult challenges in the field of deep learning and computer vision. Despite continuous research progress in the last few decades, learning from data with an imbalanced distribution of classes remains an important and active area of research. In real-world problems, imbalanced data often limits the applicability and practicality of deep models. The aim of this paper is to introduce a novel solution to deal with this problem in a targeted and applicable format for classification. This paper presents an innovative oversampling strategy that operates directly in feature space, rather than in pixel space. Unlike common methods such as SMOTE or ADASYN, this approach utilizes Instance Hardness level and Adversarial Neighborhood standard deviation to generate artificial instances that are aware of and fit the embedding distribution. Experimental results on three known image datasets show that this approach improves minority class recall and increases overall classification stability. The proposed approach is evaluated using deep learning architectures as embedding extractors and emphasizes the importance of different feature-embedding representations. The approach is model-independent and offers superior performance in terms of both effectiveness and computational efficiency compared to similar approaches.

Keywords: Medical image classification, Oversampling, Class imbalance, Deep learning.

Authors: Zahra Asgharzadeh Bonab - Sina Shamekhi











Article Code: icbme-1370

Article Title: 2D Residual U-Net for Accurate Lumbar Vertebrae Segmentation in MRI-Based Low Back Pain Diagnosis using the SPIDER Dataset

Abstract: Low back pain affects roughly 12% of people worldwide and continues to be a principal cause of disability. Precise visualization of lumbar vertebrae and intervertebral discs is critical for detecting pathological changes and guiding clinical interventions. Robust structure segmentation is essential to ensure trustworthy diagnosis and informed treatment plans. Compared to X-ray or CT scans, magnetic resonance imaging (MRI) provides superior softtissue contrast, making it the preferred modality for comprehensive spinal assessments. However, manual segmentation of vertebrae is labor-intensive and prone to inter-observer variability. At the same time, semi-automatic approaches are often time-consuming and lack robustness in accurately identifying vertebral anatomical structures, particularly when applied to low-quality or diverse clinical MRI data. In this study, we propose a 2D Residual U-Net for vertebral segmentation on the SPIDER dataset. The pipeline includes reorientation, resolution standardization, and morphological mask refinement, along with a hybrid Dice-Binary Cross-Entropy loss to address class imbalance, particularly in non-vertebral structures. The proposed model achieved a Dice score of 0.946 and an IoU of 0.897, slightly surpassing a standard 2D U-Net with Dice = 0.931 and IoU = 0.823. These results demonstrate that accurate 2D segmentation enables reliable 3D reconstruction, providing an efficient and clinically applicable solution for spinal analysis and LBP diagnosis.

Keywords: Low Back Pain, Magnetic Resonance Imaging, Segmentation, Deep Learning, Residual U-Net.

Authors: Armita Rahimi Borgi - Abdollah Zohrabi - Ali Kazemi - Mostafa Abdolghaffar - Ramin Kordi - Parastoo Farnia - Alireza Ahmadian











Article Code: icbme-1372

Article Title: Deep Learning-based Segmentation of Human Sperm Heads using YOLOv8 and

SAM

Abstract: Accurate assessment of sperm quality is critical for diagnosing male infertility, with precise segmentation of sperm heads in microscopic images posing a significant challenge due to its traditional manual execution, which is time-consuming and error-prone. This study proposes a hybrid deep learning framework that integrates YOLOv8 for initial sperm-head localization with the Segment Anything Model (SAM) for refined mask generation. Evaluated on a dataset of 305 bright-field images from six donors, the YOLOv8—SAM approach achieved an IoU of 78.62% and a Dice score of 70.78%, surpassing standalone YOLOv8 (IoU: 66.69%, Dice: 70.01%) and SAM (IoU: 40.46%, Dice: 57.62%). The results show promising potential, though certain limitations exist. The framework's generalizability is constrained by a small donor pool, lack of SAM fine-tuning, and a focus on sperm-head segmentation. Future work will address these limitations to improve cross-domain performance and clinical applicability.

Keywords: Sperm segmentation, YOLOv8, Segment Anything Model (SAM), Deep learning.

Authors: Hadis Aligoo Zanjany - Maryam Pashaiasl - Ata Jodeiri











Article Code: icbme-1378

Article Title: Patch-Based detection of proximal caries on bitewing radiographs

Abstract: Proximal caries lesions, also known as interproximal caries, were identified as cavities forming on the contact surfaces between adjacent teeth—areas challenging to clean and prone to early-stage decay. This study proposed a deep learning-based framework for automatic proximal caries detection using bitewing radiographs. A patch-based classification strategy was employed to localize lesion-centered regions that are often overlooked in global image analysis. To enhance diagnostic performance, an attention-based Multiple-Instance Learning (MIL) approach was applied to aggregate patch-level features into robust image-level predictions. We trained and evaluated the system on a dataset of 1,084 bitewing radiographs. The proposed MIL model achieved a test accuracy of 93.1%, significantly outperforming both global image classification (64.1%) and patch-only methods (66.2%). These results demonstrated the effectiveness of attention-based MIL in learning fine-grained features associated with caries. The system was designed to support diagnostic decision-making and facilitate early, non-invasive intervention in clinical dental practice.

Keywords: Proximal Caries, Bitewing Radiographs, Deep Learning, Patch-based classification, Medical image analysis.

Authors: Sana Esmaeili - Parnian Alizadeh oskoee - Tahmineh Razi - Asiyeh Dadghar - Kasra Rahimipour - Ata Jodeiri











Article Code: icbme-1392

Article Title: Leveraging Normal White Matter Hyperintensity Context for Enhanced Pathological Segmentation via Multi-Class Deep Learning

Abstract: White matter hyperintensities (WMHs) on FLAIR MRI are critical indicators of cerebrovascular dysfunction associated with elevated risks of stroke, dementia, and death. Current automated segmentation methods suffer from false positive detection in periventricular regions, failing to distinguish normal aging-related hyperintensities from pathologically significant lesions, which reduces clinical applicability and diagnostic accuracy. This study investigates whether training deep learning models to explicitly differentiate between normal and abnormal WMH improves pathological WMH segmentation performance compared to traditional binary approaches. Four state-of-the-art architectures (U-Net, Attention U-Net, DeepLabV3Plus, Trans-U-Net) were evaluated across two training scenarios using 1,974 FLAIR images from 100 MS patients with expert-annotated ground truths. Scenario 1 employed binary training (background vs abnormal WMH), while Scenario 2 utilized three-class training (background, normal WMH, abnormal WMH). Statistical analysis included paired t-tests and Cohen's d effect size calculations. U-Net achieved the most substantial improvement in Scenario 2 with 55.6% increase in Dice coefficient (0.693 vs 0.443) and 131% precision enhancement (p < 0.0001, Cohen's d = 0.971). Traditional CNN-based architectures demonstrated larger effect sizes than transformer-based models. The three-class training approach significantly enhances pathological WMH segmentation while maintaining clinical feasibility, providing a validated framework for improving automated neuroimaging tools' diagnostic utility.

Keywords: White matter hyperintensities (WMH), deep learning, medical image segmentation, FLAIR MRI, multi-class classification, U-Net, pathological segmentation, neuroimaging.

Authors: Mahdi Bashiri Bawil - Mousa Shamsi - Ali Fahmi Jafargholkhanloo - Abolhassan Shakeri Bavil











Article Code: icbme-1395

Article Title: Diagnostic and Classification Analysis of Retinal Diseases Using OCT Imaging: Focus on Diabetic Retinopathy and Overlap with Other Retinal Disorders

Abstract: Diabetic retinopathy (DR) is a leading cause of vision loss, requiring early detection to prevent disease progression using optical coherence tomography (OCT) imaging. Challenges like class imbalance and overlapping retinal conditions complicate accurate diagnosis. This study proposes a customized Vision Transformer (ViT base patch16 224) enhanced with a novel Multi Scale Attention Module, processing image patches at scales (1, 2, 4) to capture both local and global features for improved DR detection. For fair comparison, we evaluated our model against DenseNet121, ResNet50, and EfficientNet B0, all augmented with Mixup and Focal Loss to address data imbalance. Using 4-fold cross-validation on a single center OCT dataset, our model achieved a validation accuracy of 90.80% ± 0.93% for non overlapping cases and 90.75% ± 1.74% for overlapping cases (381 images), outperforming the baseline models. Grad-CAM visualizations highlighted the model's focus on clinically relevant regions, enhancing interpretability. Limitations include data from a single center and a limited number of overlapping cases. These findings underscore the potential of our approach for automated DR screening, with future validation needed on multi-center and lower-quality OCT datasets.

Keywords: Optical coherence tomography (OCT), diabetic retinopathy (DR), deep learning (DL), Vision Transformer (ViT), data imbalance, disease overlap, early detection.

Authors: Fatemeh Reyhani - Yashar Amizadeh - Ata Jodeiri











Article Code: icbme-1414

Article Title: Fast Reflection-Mode Ultrasound Computed Tomography Versus Conventional Pulse-Echo Technique

Abstract: Conventional pulse—echo ultrasound limits boundary depiction and contrast. We propose a dual-probe, phased-array reflection ultrasound computed tomography (RUCT) scheme in which one probe transmits diverging waves and the opposing probe records oblique echoes, providing near 360 ° angular coverage. The approach is evaluated in numerical simulations on generic heterogeneous 2-D phantoms under matched acquisition budgets. Images are reconstructed with delay-and-sum beamforming and compared with linear and single-probe phased acquisitions. The dual-probe, diverging configuration yields crisper delineation of convex and concave boundaries, stronger target-to-background separation, and more uniform intraregion intensity. The region-of-interest SNR and CNR increase consistently, while the diverging transmission reduces the number of shots, thereby decreasing the scan time and data volume required for comparable coverage. Although limited to simulations, the results indicate a practical route to fast, high contrast reflection tomography compatible with clinical arrays.

Keywords: Reflection ultrasound computed tomography (RUCT), pulse-echo ultrasound (US), dual-probe phased arrays, diverging-wave transmission, Delay-and-Sum beamforming.

Authors: Elnaz Rostami Siahpoush - Haniye Fathi - Zahra Kavehvash











Article Code: icbme-1440

Article Title: Multi-View 2.5D Attention U-Net with 3D Fusion for Efficient Stroke Lesion Segmentation from T1-Weighted MRI

Abstract: Automatic stroke lesion segmentation from Magnetic Resonance Imaging (MRI) scans is essential for clinical decision-making and patient prognosis. However, stroke lesion segmentation from mono-spectral MRI such as T1-weighted (T1w) images suffers from similar gray level characteristics of brain tissues and heterogeneity of lesion properties (e.g., shape and size). Deep learning methods have emerged as the leading approach for medical image segmentation. In this context, 2D architectures neglect inter-slice dependencies, whereas 3D counterparts demand high computational resources. This study presents a 2.5D multi-view framework that employs three 2D U-Nets for intra-slice lesion segmentation across axial, coronal, and sagittal views. The resulting probability maps are then fused using a 3D convolutional neural network (CNN). The 2D U-Nets incorporated residual blocks in the encoder—decoder and attention blocks in the skip connections, while the 3D CNN with attention mechanisms produced the final segmentation. We assessed the performance of the proposed model using the ATLAS V2.0 dataset for stroke lesion segmentation, resulting in an average Dice score of 0.64±0.27 outperforming 2D approaches and comparable to 3D models, while requiring fewer parameters, making it practical for resource-constrained settings.

Keywords: Stroke Lesion, MRI, 2.5D Segmentation, Deep Learning, Attention mechanism, multi-view.

Authors: Fatemeh Salahshourinejad - Kamran Kazemi - Negar Noorizadeh - Mohammad Sadegh Helfroush - Ardalan Aarabi











Article Code: icbme-1444

Article Title: Alterations of Brain Activation Maps in Adults with ADHD During Risk-Related Decision-Making: Evidence from the Balloon Analogue Risk Task

Abstract: Attention-Deficit-Hyperactivity Disorder (ADHD) is a widespread neurological developmental disorder characterised by impulsivity, lack of focus, and inadequate control of impulses. For the purpose of exploring possible mechanisms, we examined functional magnetic resonance imaging (fMRI) data acquired during the Balloon Analogue Risk Task (BART). Our analysis has been conducted at both the participant and group levels. We conducted an analysis of two contrasts: Balloon>Control and Control>Balloon, which revealed the engagement disparities between the task and control conditions. The participants in the group comparison consisted of 38 individuals with ADHD and 38 healthy control subjects who were matched. Our study results revealed that participants with ADHD demonstrated increased brain activation maps in the Visual Network (VN) and the Default Mode Network (DMN) compared to the control group. The alterations arise from motor restlessness, increased reactivity to external stimuli, as well as the integration of trivial ideas via focused objective procedures. In addition, we noticed that both executive control and sensory attentional (VN, DMN) networks, which have been linked to ADHD, are fundamentally deficient. In clinical terms, our findings bolster the beneficial effects of interventions that improve cognitive control and impulse regulation, and they underscore the importance of task-based paradigms like BART in improving our comprehension of the neural processes associated with ADHD.

Keywords: Attention-Deficit-Hyperactivity Disorder, Balloon Analogue Risk Task, FMRI data, Connectivity Networks.

Authors: Bahar Kermani - Mahdi Mirzaee Barzegar - Alireza Shirazinodeh











Article Code: icbme-1446

Article Title: Analysis of Blood Report Images Using General-Purpose Vision-Language

Models

Abstract: The reliable analysis of blood reports is important for health knowledge, but individuals often struggle with interpretation, leading to anxiety and overlooked issues. We look for the potential of general-purpose Vision-Language Models (VLMs) to address this challenge by automatically analyzing blood report images. We conduct a comparative evaluation of three VLMs—Owen-VL-Max, Gemini 2.5 Pro, and Llama 4 Maverick—determining their performance on a dataset of 100 diverse blood report images. Each model was prompted with clinically relevant questions adapted to each blood report. The answers were then processed using Sentence-BERT to compare and evaluate how closely the models responded. The findings suggest that general-purpose VLMs are a practical and promising technology for developing patient-facing tools for preliminary blood report analysis. Their ability to provide clear interpretations directly from images can improve health literacy and reduce the limitations to understanding complex medical information. This work establishes a foundation for the future development of reliable and accessible AI-assisted healthcare applications. While results are encouraging, they should be interpreted cautiously given the limited dataset size. The similarity between the answers is also very high. The similarities are calculated pairwise and across all responses. This suggests that VLMs have a shared understanding of how to process and reason about structured clinical data presented in images, specifically blood report images.

Keywords: Vision-Language Models, VLM, Health Care AI, Blood Report Analysis, Multimodal AI.

Authors: Nadia Bakhsheshi - Hamid Beigy











Article Code: icbme-1448

Article Title: Comparative Evaluation of Deep Learning Architectures for Static American

Sign Language Recognition

Abstract: Sign language is a vital form of non-verbal communication for individuals with hearing and speech impairments, yet its interpretation remains challenging. This study optimizes four deep learning models—Convolutional Neural Networks (CNN), Autoencoder Classifier Networks (AEC), modified LeNet-5, and Long Short-Term Memory (LSTM)—for static American Sign Language (ASL) recognition. Performance and generalization were enhanced using Batch Normalization, Dropout, Global Average Pooling, Learning Rate Scheduling, and alternative optimizers such as SGD and AdamW. Experimental results show that CNN-9 achieved the highest performance (99.05%), followed by AEC-7 (94.88%), LeNet-9 (91.03%), and LSTM (88.32%). These findings demonstrate the effectiveness of deep learning architectures for static ASL recognition and highlight the impact of architectural and training adjustments. Ensemble strategies further improved results: Soft Voting combining CNN-9 and AEC-7 achieved the best outcome, Weighted Soft Voting ensembles excluding LSTM-1 performed best, and Hard Voting with CNN-9, AEC-7, and LSTM-1 outperformed other configurations. Overall, ensemble methods enhance accuracy and robustness beyond individual models.

Keywords: Sign Language Recognition, Convolutional Neural Networks (CNN), Long Short-Term Memory (LSTM), Modified LeNet-5, Autoencoder Classifier Network (AEC), Ensemble Strategies.

Authors: Shamim Najafi - Sedigheh Dehghani











Article Code: icbme-1465

point-of-care stroke diagnosis.

Article Title: Accelerated Diffusion-Weighted Imaging via Diffusion Gradient Alternation in Radial k-Space Sampling

Abstract: Diffusion-weighted imaging (DWI) is essential for stroke diagnosis but remains limited by long acquisition times, particularly in portable and ultra-low-field MRI systems where reduced signal-to-noise ratio (SNR) exacerbates this challenge. Conventional DWI requires at least four full k-space acquisitions, restricting its practicality in time-critical or resource-limited settings. We propose a two-acquisition DWI framework that employs radial kspace sampling with alternating diffusion gradient directions, requiring only one non-diffusionweighted (S₀) and one diffusion-weighted acquisition. Simulations were performed using a realistic brain phantom in MRiLab with a customized diffusion modeling pipeline and nonuniform FFT reconstruction. Results show a two-fold reduction in acquisition time while maintaining strong agreement with conventional DWI, with relative root-mean-square errors of 3.9-4.2%. Stroke-relevant tissue boundaries remained clearly visible, and error maps confirmed minimal structural distortion. Unlike cartesian undersampling, radial sampling eliminates foldover aliasing artifacts, further supporting robust image quality. This acquisition-level acceleration is independent and can be combined with parallel imaging or compressed sensing to achieve additional gains. The method offers a practical solution for low-field and portable MRI, enabling faster and more reliable diffusion imaging in urgent clinical scenarios such as

Keywords: Stroke diagnosis, Signal-to-noise ratio (SNR) enhancement, Apparent diffusion coefficient (ADC), Non-uniform FFT (NUFFT) reconstruction, Portable MRI, Ultra-low-field MRI.

Authors: Fateme Hoseini Rashkani - Abbas Nasiraei Moghaddam











Article Code: icbme-1430

Article Title: Short-term gains vs. long-term Success: Reward strategy design for reinforcement learning in football

Abstract: Reinforcement learning in complex games like soccer relies heavily on how you define your reward function and environment. In this work, we developed a custom 3v3 soccer environment and implemented two RL-based teams with distinct learning trends: one with a fast convergence but limited long-term adaptation, and another with a slower yet more robust learning trajectory. Simulation shows that despite performing better at the start, the short-term agents fall short of the performance of the long-term agents in the long run, and after passing 50% of the episodes, the win rate of long-term agents rises from 30% in the beginning to 50%.

Keywords: Reinforcement Learning, Multi-agent systems, Soccer Simulation.

Authors: Mohammad Pashaei - Amirhossein Tayebi - Hadi Amiri - Ali Fahim











كد مقاله: icbme-1467

عنوان مقاله: سامانه ی یکپارچه و کمهزینه برای ثبت پتانسیلهای میدانی محلی (LFP) همگام با ویدئو و تحریک الکتریکیِ مغز به کمک برچسب گذاری نوری کُدگذاری شده ی رخداد

چکده: در پژوهشهای علوم اعصاب، ثبت همزمان سیگنالهای مغزی و رفتار برای درک ارتباط بین فعالیت عصبی و رفتار حیاتی است. در این پژوهش یک سامانهی یکپارچه و کمهزینه برای ثبت و تحریک سیگنالهای مغزی همزمان با ضبط ویدئو معرفی می شود که مسئلهی همگامسازی و برچسب گذاری رویدادها را بدون اتصال فیزیکی میان سامانهی ثبت و تحریک سیگنال مغزی و دوربین حل می کند. هستهی روش، یک نشانگر نوری کنترلشونده و الگوریتم پردازش تصویر است که بستههای نوری کدگذاری شده با BCH را از ویدئو استخراج کرده و زمان و نوع رویدادها را با دقت یک فریم بازیابی می کند. سامانهی بومی طراحی و ساخته شد و در آزمایش حیوانی روی موش صحرایی، همراه با ثبت پتانسیل میدان محلی (LFP) و اعمال تحریک الکتریکی، ارزیابی گردید. نتایج نشان داد برچسبگذاری خودکار رخدادها پایدار بوده و بازیابی بستهها ،حتی در شرایط نویزی، کامل انجام می شود؛ از این رو تطبیق رفتار با سیگنالهای عصبی سریعتر و قابل اعتمادتر شده و زمان تحلیل ویدئو به طور محسوسی کاهش می یابد. معماری پیشنهادی قابل توسعه است و با طیفی از دوربینهای رایج کار می کند. این پژوهش یک محسوسی کاهش می یابد. معماری پیشنهادی قابل توسعه است و با طیفی از دوربینهای رایج کار می کند. این پژوهش یک مقرون به صرفه برطرف می کند.

کلمات کلیدی: الگوریتم پردازش تصویر، برچسبگذاری رویداد، تحریک الکتریکی، پتانسیل میدان محلی (LFP)، سیگنال عصبی، فیلمبرداری ویدئویی، کد BCH، نشانگر نوری، همگامسازی نوری دادههای الکتروفیزیولوژی و ویدئو

نويسندگان: حنيف صولت نيا - بيژن وثوقي وحدت











كد مقاله: icbme-1042

عنوان مقاله: پیشبینی وقوع سکته مغزی با استفاده از دادههای پروندههای الکترونیکی مراقبتهای بهداشتی بیماران و شبکههای عصبی

چکیده: پیش بینی زودهنگام سکته مغزی به عنوان یکی از راهکارهای حیاتی برای کاهش مرگ و میر ناشی از این بیماری، نقش محوری در مدیریت بهداشتی افراد دارد. لذا، در این پژوهش به بررسی ویژگیهای مختلف موجود در پرونده الکترونیکی پزشکی افراد و نقش هر کدام در پیش بینی سکته مغزی به کمک روشهای مختلف انتخاب ویژگی و انواع شبکههای عصبی پرداخته شده است. بر این اساس، دو روش انتخاب ویژگی مبتنی بر همبستگی و است. بر این اساس، دو روش انتخاب ویژگی، شامل روش مجموعههای ناهموار و روش رتبهبندی ویژگی مبتنی بر همبستگی و چهار نوع شبکه عصبی، شامل شبکه پرسپترون چندلایه، شبکه رگرسیون تعمیمیافته، شبکه پیشرو آبشاری و شبکه بازگشتی، بمنظور شناسایی عوامل مؤثر در بروز سکته مغزی، استفاده شدهاند. مطابق نتایج حاصل، ویژگیهای سن، فشار خون بالا، بیماری قلبی و میانگین سطح گلوکز به ترتیب به عنوان موثر ترین ویژگیها در پیش بینی سکته مغزی شناسایی شدهاند. همچنین شبکه عصبی پیشرو آبشاری بهترین عملکرد را با صحت پیش بینی ۱۱/۷۰ درصد، برای ویژگی سن، ارائه داده است. چنین یافتههایی می توانند به عنوان پایهای برای توسعه مدلهای هوشمند پیش بینی سکته مغزی و بهبود مدیریت این بیماری در کاربردهای کلینیکی مورد استفاده قرار گیرند.

كلمات كليدى: پيشبيني، سكته مغزى، شبكه عصبي، مجموعههاى ناهموار، همبستگى، يادگيرى ماشين.

نویسندگان: عارفه یعقوبی، افشین ابراهیمی، پیوند قادریان











كد مقاله: icbme-1115

عنوان مقاله :معرفی معیار کمیسازی الگوهای متیلاسیون DNA در ژنوم

چکیده :متیلاسیون DNA به عنوان یکی از مهم ترین مکانیسمهای اپیژنتیکی، نقش کلیدی در تنظیم بیان ژنها ایفا می کند. تغییرات الگوهای متیلاسیون در نواحی CpG ژنومی با طیف وسیعی از بیماریها از جمله سرطان و بیماریهای عصبی مرتبط است. این ویژگی، متیلاسیون DNA را به ابزاری ارزشمند در تشخیص بیماریها و مطالعات اپیژنومیک تبدیل کرده است. در این مطالعه، معیار جدیدی به نام شاخص یکپارچگی الگوی متیلاسیون، MPCI معرفی شده است که با تحلیل همزمان این مطالعه، معیار و غیرمتیله در سطح تکخوانشهای حاصل از توالی یابی، امکان ارزیابی جامعی از الگوهای متیلاسیون را فراهم می آورد. این روش با در نظر گرفتن همبستگی بین CpGهای مجاور و محاسبه یکپارچگی الگوها در خوانشهای مختلف، می آورد. این روش های مرسوم مانند بار هپلوتایپ متیلاسیون به نام MHL را مرتفع میسازد. نتایج نشان می دهد که تمایز انواع سلولهای نزدیک به هم (مانند لنفوسیتهای D4 و CD8 با بهبود ۱۲/۱۸٪ در صحت تشخیص، عملکردی برتر از مطالع دارد. همچنین در سناریوهای بیوپسی مایع در غلظتهای کم ، این روش میانگین صحت را ۵/۱۱٪ افزایش می دهد که نشان دهنده دقت بالاتر آن در تشخیص زودهنگام بیماریهاست. این مطالعه بر اهمیت تحلیل الگوهای متیلاسیون به جای تمرکز برتک سایتهای CpG تأکید دارد و نشان می دهد که MPCI با کمیسازی الگوی متیلاسیون در خوانشها، ابزاری ارزشمند برای کشف نشانگرهای زیستی، طبقهبندی بافتهای مختلف و تشخیص بیماری در بیوپسی مایع محسوب می شود.

كلمات كليدى :متيلاسيون DNA، توالى يابى نسل جديد، بيوپسى مايع، طبقه بندى، كشف بيوماركر

نویسندگان: نغمه سادات ناظر کاخکی ، نرجس الهدی محمدزاده، محیا مهرمحمدی











كد مقاله: icbme-1099

عنوان مقاله : پایش هوشمند دیابت به کمک اینترنت اشیا و داده کاوی: گامی نوین در مراقبتهای سلامت دیجیتال

چکده :دیابت به عنوان یکی از شایعترین بیماریهای مزمن، تأثیر قابل توجهی بر سلامت و کیفیت زندگی افراد دارد. ازاینرو، توسعه راهکارهای هوشمند و پیشگیرانه برای تشخیص زودهنگام و مدیریت مؤثر این بیماری ضروری است. در این راستا، سامانههای نظارت دیجیتال مبتنی بر اینترنت اشیاء (IoT) قادرند دادههای سلامت بیماران، از جمله سطح گلوکز خون، دمای بدن و موقعیت جغرافیایی را بهصورت بلادرنگ جمعآوری و با کمک الگوریتمهای هوش مصنوعی پردازش و تحلیل کنند. این اطلاعات سپس در اختیار تیم پزشکی قرار می گیرد تا تصمیم گیریهای درمانی بهینه صورت پذیرد. مقاله حاضر یک سیستم نوین برای پایش بیماران دیابتی معرفی می کند و با استفاده از هشت الگوریتم یادگیری ماشین(بیز، جنگل تصادفی، درخت تصمیم، نزدیکترین همسایگی K، شبکه عصبی، رأی گیری، رگرسیون و ماشین بردار پشتیبان)، به پیش بینی و ارزیابی دیابت می پردازد. کارایی این الگوریتمها بر اساس معیارهای استاندارد مقایسه و تحلیل شده اند. نتایج نشان می دهد که شبکه عصبی با استفاده از ویژگیهای کلیدی شناسایی شده (سابقه خانوادگی، میزان گلوکز خون، سن و شاخص توده بدنی)، می تواند میانگین صحت و دقت ۸۸/۷۹ درصد را برای پیش بینی بیماری دیابت فراهم کند.

کلمات کلیدی :داده کاوی، تشخیص، دیابت، مدل سازی، Rapidminer

نویسندگان :سیده عارفه رضوی، وحید جمشیدی، محبوبه طالبی، ملیکا ناصری











كد مقاله: icbme-1049

عنوان مقاله :سامانه هوشمند مبتنی بر بینایی ماشین برای تشخیص افتادن سالمندان: رویکردی ایمن، دقیق و سریع

چکیده :در این مقاله، یک سامانه هوشمند و یکپارچه برای پایش سلامت سالمندان مبتنی بر دوربین مداربسته طراحی و پیادهسازی شده است. این سامانه از سه بخش اصلی شامل دستگاه تشخیص افتادن، سرور مرکزی و اپلیکیشن موبایل تشکیل شده است. الگوریتم تشخیص افتادن بهصورت بلادرنگ روی برد Raspberry Pi 3B اجرا می شود و ترکیبی از روشهای کلاسیک و یادگیری عمیق است؛ به گونه ای SVM کلاسیک و مدلهای شبکه عصبی چندلایه (MLP) و کلاسیک و مدلهای شبکه عصبی چندلایه (MLP) و مصوصی، از رمزنگاری MoveNet در بخش عمیق برای افزایش دقت به کار گرفته شده اند. سامانه به منظور حفظ امنیت و حریم خصوصی، از رمزنگاری End-to-End و ارتباطات امن مبتنی بر Flutter بهره می برد. اپلیکیشن موبایل نیز با فریمورک Flutter توسعه داده شده و به صورت مستقیم با سرور پیادهسازی شده بر پایه Flask در تعامل است. نتایج ارزیابی عملکرد بر روی سه دیتاست معتبر نشان می دهد که سامانه پیشنهادی با دقت ۹۶٪ قادر به تشخیص افتادن بوده و با سرعتی فراتر از نیازهای پردازش بلادرنگ اجرا می شود. از جمله ویژگیهای برجسته سامانه می توان به طراحی جامع، دقت بالا، امنیت ارتباطی، استفاده از هوش مصنوعی و قابلیت اجرای صنعتی اشاره کرد که آن را به گزینه ای کارآمد برای مراقبت از راه دور سالمندان تبدیل می سازد.

کلمات کلیدی :امنیت ارتباطات، اپلیکیشن موبایل، بینایی ماشین، پایش سلامت سالمندان، تحلیل ویدیو، تشخیص افتادن، سامانه هوشمند، مراقبت از راه دور، یادگیری ماشین، رزبری پای

نویسندگان :سیدحسن نوری، هدی محمدزاده











كد مقاله: icbme-1101

عنوان مقاله :بررسی عملکرد سلولهای T در میکرومحیط تومور HGSOC با رویکرد توالی یابی تکسلولی

چکیده :سرطان تخمدان یکی از مرگبارترین سرطانها در میان زنان است و ناهمگونی سلولی در میکرومحیط تومور (Microenvironment – TME (Microenvironment – TME) نقش مهمی در پیشرفت بیماری دارد. در این مطالعه، بهمنظور تحلیل دقیق میکرومحیط توموری در سرطان سروز با درجه بالا (High-Grade Serous Ovarian Carcinoma – HGSOC)، دادههای توالی یابی RNA تکسلولی از نمونههای سالم و سرطانی، مورد بررسی قرار گرفتند. پس از پالایش دادهها، انواع سلولها با استفاده از نشانگرهای ژنی شناسایی و برچسبگذاری شدند. نتایج خوشه بندی و تحلیل فضایی نشان داد که سلولهای T. B. فیبروبلاست، اندوتلیال، اپی تلیال و سایر انواع سلولی در نمونهها حضور داشتند. ترکیب سلولی در نمونههای سالم و بیمار تفاوت معناداری نشان داد. بهویژه، سلولهای T در نمونههای توموری فراوانی بیشتری داشتند. با این حال، بررسی عملکرد این سلولها با استفاده از تحلیل غنی سازی مجموعه ژنی تکنمونهای (single-sample Gene Set Enrichment Analysis – ssGSEA) داشان داد که افزایش تعداد آنها با کاهش کارایی ایمنی همراه بود. مسیرهای مرتبط با فعال سازی ایمنی کاهش یافته و مسیرهای مرتبط با فعال سازی ایمنی کاهش عافته و مسیرهای مرتبط با فعال مهمی در جهت طراحی مسیرهای مؤثر تر علیه سرطان تخمدان باشد.

کلمات کلیدی :سرطان تخمدان سروز با درجه بالا، توالی یابی RNA تکسلولی، هوش مصنوعی، میکرومحیط توموری، خستگی عملکردی

نویسندگان :زهرا زندی، روزبه عابدینی نسب











كد مقاله: icbme-1429

عنوان مقاله :بررسی آمارههای توصیفی فواصل بین ژنی ژنوم و پاتوژنی در دو سویه K12 و O157:H7 باکتری E. Coli با درویکرد بیوانفورماتیکی

چکیده :مطالعه انجام شده به مقایسه ساختار ژنومی سویههای ای کولای K12 و پاتوژن O157:H7 پرداخته است. نتایج نشان میدهد سویه C157:H7 با داشتن ژنوم پیچیده تر، توزیع نامنظم تر فواصل بین ژنی و همپوشانیهای بزرگ تر، ظرفیت بالاتری برای بیماریزایی و سازگاری محیطی دارد. تفاوتهای معنادار در طول و توزیع ژنها و پراکندگی فواصل بین ژنی، انعطاف پذیری زیستی بیشتر O157:H7 را نشان میدهد. همچنین پیشبینیهای مدل PathogenFinder2 احتمال بالای پاتوژنیسیته این سویه را با دقت نزدیک به ۹۹٪ تأیید کرده است. این تحقیق اهمیت تحلیل دقیق ژنومی و آماری را در فهم تفاوتهای زیستی و عملکردی سویهها برجسته میسازد و می تواند راهنمای مهمی برای مطالعات آینده و کاربردهای بالینی باشد.

کلمات کلیدی:فاصله بین ژنی، پاتوژن، ای کولای، پاتوژنیسیته، تحلیل ژنومی

نویسندگان :علی دژبرد، مرتضی علیزاده، محمد حاجی تبار، رحمان خدادادی گله











كد مقاله: icbme-1240

عنوان مقاله :هم آوایی در شبکهای جهان کوچک و متشکل از نورونهای ممریستوری

چکده این مقاله نقش اتصالات الکتریکی و میدان را در همآوایی شبکه نورونهای ممریستوری با ساختار جهان کوچک بررسی می کند. سنجش تحلیلی نشان می دهد که دو نوع اتصال می توانند همآوایی کامل را منجر شوند؛ اما شبیه سازی ها نشان می دهند که در عمل تنها تحت اتصالات الکتریکی همآوایی کامل محقق می شود. در اتصالات میدان، به علت توزیع مقادیر ویژه، دستیابی به همآوایی ممکن نیست. همچنین، در اتصال الکتریکی نورونها ابتدا به همآوایی فاز و سپس دامنه می رسند، حال آن که در اتصالات میدان الگویی مشابه با تأخیرهای غیر یکنواخت بروز می یابد. این نتایج در کی عمیق تر از پویایی شبکههای نورونی ارائه می دهد.

کلمات کلیدی :همآوایی،نورون،شبکه،ممریستور،جهان کوچک

نویسندگان :محمدمهدی شیرزاد - مهتاب مهراب بیک - سجاد جعفری











كد مقاله: icbme-1143

عنوان مقاله :طراحی چارچوب شخصی سازی شده درمان بیماری MS مبتنی بر یادگیری تقویتی عمیق SAC

چکده :مولتیپل اسکلروزیس (MS) یک بیماری خودایمنی مزمن سیستم عصبی مرکزی است که با تخریب پیشرونده غلاف میلین و پاسخهای التهابی غیرطبیعی همراه است. محدودیت درمانهای فعلی در انطباق با وضعیت پویای بیماران، نیاز به راهکارهای هوشمند و انعطافپذیر را برجسته میسازد. در این پژوهش، برای نخستینبار یک چارچوب کنترلی تطبیقی مبتنی بر یادگیری تقویتی عمیق توسعه داده شده است که دوز داروی تعدیل کننده سیستم ایمنی را بهصورت شخصیسازی شده تنظیم میکند. این چارچوب از الگوریتم بازیگر منتقد نرم (SAC) بهره میبرد و بر مدلی زیستی متشکل از شش معادله دیفرانسیل معمولی (ODE) برای گرههای لنفی استوار است. نوآوری کلیدی در افزودن یک ترم کنترلی به معادلات است که اثر داروی هدف گیرنده سلولهای B را شبیهسازی میکند. تا آنجا که اطلاع داریم، این نخستین کاربرد یادگیری تقویتی عمیق در کنترل تطبیقی دارو بر پایه مدل چند مقیاسی در MS است. نتایج شبیهسازی در بازه نازد داروزه نشان داد که سیاست بهینه استخراجشده منجر به کاهش التهاب، تثبیت پاسخ ایمنی و کاهش وابستگی به دوز ثابت دارویی شد.

کلمات کلیدی :الگوریتم SAC، کنترل دارویی شخصی سازی شده، مدل ریاضی زیستی، مولتیپل اسکلروزیس، یادگیری تقویتی عمیق

نویسندگان :مریم سبزهیان، محبوبه سبزهیان، امین نوری، ماندانا سادات غفوریان











کد مقاله: icbme-1017

عنوان مقاله: تشخیص سرطان پستان از طریق طبقهبندی تصاویر: مروری بر روشها و روندهای فعلی

چکیده: شناسایی زودهنگام سرطان پستان یکی از ارکان کلیدی در پیشگیری و موفقیت درمان این بیماری بهشمار میآید. همگام با پیشرفتهای چشمگیر در حوزههای یادگیری ماشین و بهویژه یادگیری عمیق، کاربرد روشهای نوین طبقهبندی تصویر در تشخیص این نوع سرطان، رشد قابل توجهی یافته است. این مقاله مروری، نگاهی جامع به تازهترین رویکردهای تحلیل تصاویر پزشکی از جمله ماموگرافی، تصاویر بافتشناسی و سونوگرافی دارد. تکنیکهایی نظیر شبکههای عصبی کانولوشنی (CNN)، یادگیری انتقالی، یادگیری چندنمونهای و مدلهای ترکیبی مبتنی بر ادغام چند معماری مورد بررسی قرار گرفتهاند. همچنین، پایگاههای داده پرکاربردی چون BreakHis، CBIS-DDSM و BUSI معرفی شدهاند. در ادامه، با مقایسه عملکرد مدل ها از نظر شاخصهایی نظیر دقت، حساسیت و نرخ مثبت کاذب، تلاش شده است تا نقاط قوت و چالشهای فعلی روشن تر گردد. در پایان نیز مسیرهایی برای ارتقاء دقت، کاهش مصرف منابع و بهبود تفسیرپذیری مدلها پیشنهاد شده است.

كلمات كليدى: سرطان پستان، طبقهبندى تصوير، يادگيرى عميق، CNN، ماموگرافى، هيستوپاتولوژى، سونوگرافى، شبكه عصبى، تشخيص زودهنگام، دادهپزشكى.

نویسندگان: ریحانه ابراهیمینسب - آزیتا شیرازیپور - سید جواد میرعابدینی









كد مقاله: icbme-1057

عنوان مقاله: مدل تركيبي مبتني بر ،DenseNetالگوريتم ژنتيک و GAN براي تشخيص اَلزايمر از تصاوير MRI

چکده: در این پژوهش، یک چارچوب ترکیبی مبتنی بر شبکه عصبی کانولوشن ،(CNN – DenseNet) الگوریتم ژنتیک و شبکه مولد متخاصم (GAN) برای تشخیص بیماری آلزایمر با استفاده از دادههای MRI ارائه شده است. دادههای مورد استفاده از پایگاه داده MIRIAD شامل تصاویر MRI بیماران مبتلا به آلزایمر و افراد سالم استخراج گردید. در مدل پیشنهادی، الگوریتم ژنتیک جهت بهینهسازی فراپارامترهای CNN و شبکه GAN برای رفع مشکل عدم توازن دادهها به کار گرفته شد. یافتههای تجربی نشان داد که مدل ترکیبی پیشنهادی در مقایسه با روشهای متداول نظیر درخت تصمیم، ماشین بردار (SVM) و مدلهای مبتنی بر تقویت گرادیان، عملکرد برتری داشته است. این مدل به دقت ،90% (Recall) پشتیبان (Recall) و ضریب F1 90% دست یافت که بالاتر از سایر مدلهای مقایسهای حساسیت (Imaginal بیانگر آن است که رویکرد ترکیبی پیشنهادی می تواند بهعنوان ابزاری هوشمند و قابل اعتماد در تشخیص دقیق و زودهنگام آلزایمر به کار رود و زمینه ساز ارتقاء سامانههای بالینی گردد.

کلمات کلیدی: اَلزایمر، تصاویر ،MRIتشخیص بیماری، یادگیری ماشین، یادگیری عمیق، شبکه عصبی کانولوشن ،(CNN) الگوریتم ژنتیک، شبکه مولد متخاصم (GAN).

نویسندگان: محمد قنبری صباغ - محسن کرمی طلایی











كد مقاله: ichme-1144

عنوان مقاله: تشخيص بيماري MS با استفاده از EfficientNet-B و CycleGAN بر پايه نقشههاي ضخامت شبكيه

چکده: بیماری مولتیپل اسکلروزیس (MS) یکی از اختلالات مزمن و پیشرونده سیستم عصبی است که شناسایی زودهنگام آن میتواند به بهبود فرایند درمان و کاهش آسیبهای عصبی کمک کند. تصویربرداری توموگرافی انسجام نوری (OCT) در سالهای اخیر بهعنوان ابزاری غیرتهاجمی برای بررسی تغییرات ساختاری شبکیه در بیماران MS مطرح شده است. در این پژوهش، یک سامانه یادگیری عمیق جهت طبقهبندی بیماران مبتنی بر نقشههای ضخامت شبکیه توسعه داده شده است. این سامانه از معماری EfficientNet-B0 بهره میبرد که با استفاده از تکنیک افزایش داده مبتنی بر شبکههای مولد تخاصمی چرخهای ،(CycleGAN)دادهها را غنیسازی کرده است. عملکرد مدل پیشنهادی در مقایسه با معماریهای مرسوم از جمله VGG-19 و ResNet-50.ResNet-101 مورد ارزیابی قرار گرفت. یافتهها نشان میدهد که مدل پیشنهادی با دستیابی به دقت ۹۹.۶۳٪، امتیاز F1 معادل ۹۹.۶۱٪ و سطح زیر منحنی (AUC) برابر با ۲۰۰٪، از سایر معماریها عملکرد دقیق تری داشته است. تا آنجا که بررسیها نشان میدهد، این نخستین مطالعهای است که از ترکیب EfficientNet-B0 با نقشههای داشته است. تا آنجا که بررسیها نشان میدهد، این نخستین مطالعهای است که از ترکیب EfficientNet-B0 با نقشههای ضخامت لایههای کلینیکی و شرایط محدودیت داده برجسته میسازد.

کلمات کلیدی: افزایش داده ،CycleGanتشخیص بیماری، مولتیپل اسکلروزیس، نقشه ضخامت شبکیه، یادگیری انتقالی، EfficientNet-B

نویسندگان: محبوبه سبزهیان - مریم سبزهیان - ماندانا سادات غفوریان - امین نوری











كد مقاله: icbme-1255

عنوان مقاله: ارزیابی کارایی روشهای اصلاح پراکندگی در تصویربرداری SPECT قلب همزمان دو ایزوتوپی

چکیده: مقطع نگاری رایانهای گسیل تک فوتون (SPECT) قلب با استفاده از دو رادیوایزوتوپ تکنسیوم (Tc-99m) و m99 (Tc-99m) در اراد-120). ۲۰۱ (Tl-201)، دلیل مزایای تشخیصی خود، کاربرد بالینی گستردهای دارد. یکی از مشکلات اصلی در تصویربرداری همزمان دو ایزوتوپی (SDI)، افزایش سهم فوتونهای پراکنده به دلیل تفاوت در انرژی فوتونهای گسیل شده از دو رادیوایزوتوپ و در نتیجه، کاهش کنتراست تصاویر و نیز برآورد نادرست توزیع اکتیویته است. در این مطالعه، در گام اول، به منظور تعیین بازه انرژی اصلی بهینه، کسر پراکندگی در بازههای ۳۰٪-۲۵٪ با مراکز انرژی 80-80 keV برای رادیوایزوتوپ 201 Tc-99m بازههای انرژی اصلی بهینه، کسر پراکندگی در بازههای برای رادیوایزوتوپ Tc-99m مورد ارزیابی قرار گرفت. در گام بعد، با تنظیم یک بازه انرژی ثانویه در بخش کامپتونی طیف و نیز دو بازه انرژی باریک در دو سمت بازه اصلی بهینه، کارایی روشهای اصلاحی دو بازه انرژی (DEW) و سه بازه انرژی (TEW) در برآورد سهم پراکندگی بازه انرژی اصلی و بهبود کنتراست تصویری در هر دو روش انرژی (DEW) و تصویربرداری تک ایزوتوپی جداگانه، ارزیابی و مقایسه شد. نتایج حاصل از این مطالعه نشان میدهد که استفاده از روشهای اصلاحی DEW و TC-99m منجر به بهبود کنتراست تصویری برای هر دو رادیوایزوتوپ DEW کنتراست برای هر دو رادیوایزوتوپ دو جداگانه میشود. همچنین، افزایش نسبی کنتراست برای هر دو رادیوایزوتوپ در روش همزمانی بیش از روش جداگانه و برای رادیوایزوتوپ در روش همزمانی بیش از روش جداگانه و برای رادیوایزوتوپ در روش همزمانی بیش از روش جداگانه و برای رادیوایزوتوپ TC-99m بیش از روش همزمانی بیش از روش جداگانه و برای رادیوایزوتوپ TC-99m بیش از روش جداگانه و برای رادیوایزوتوپ TC-99m بیش از روش جداگانه و برای رادیوایزوتوپ TC-99m بیش از روش جداگانه و TC-99m بیش از روش جداگانه و TC-99m بیش از روش جداگانه و TC-99m بیش از TC-99m بیش از TC-99m بیش از TC-99m بیش و TC-99m بیش از TC-99m بیش و
کلمات کلیدی: ، SPECT تصویربرداری همزمان، اصلاح پراکندگی، تکنسیوم- ،99ستالیوم-۲۰۱.

نویسندگان: بهاره جودی ثمرین - مهسا نوری اصل











كد مقاله: icbme-1273

عنوان مقاله: استفاده از یادگیری انتقالی در پاسخ به کمبود طیف در تشخیص بیماری با طیف سنجی رامان

چکیده: کاربرد طیفسنجی رامان در ترکیب با مدلهای یادگیری عمیق، پتانسیل عظیمی برای تشخیص غیرتهاجمی سرطان پستان نشان داده است؛ با این حال، کمبود مجموعه دادههای بالینی برچسبدار، یک مانع جدی در مسیر توسعه مدلهای دقیق و قابل اعتماد به شمار می رود. پژوهش حاضر، با هدف غلبه بر این چالش، کارایی یک پارادایم نوآورانه یادگیری انتقالی بین- دامنهای را از یک منبع کاملاً غیربیولوژیک ارزیابی می کند؛ در این راستا، یک مدل شبکه عصبی کانولوشنی یک بعدی (-LD دامنهای بر روی مجموعه داده بالینی بافت (CNN1) بر روی مجموعه داده بالینی بافت پستان (AllBreast) شامل سه کلاس (نرمال، خوشخیم و سرطانی) تنظیم دقیق گردید. نتایج مقایسه این مدل با یک مدل مشابه که از ابتدا آموزش دیده بود، یک جهش عملکردی چشمگیر را به اثبات رساند: دقت کلی طبقهبندی از ۵۰.۰۰٪ به ۸۵.۲۹ رسید. ۸۵.۲۹ این یافت، کارایی بالای یادگیری انتقالی را نه تنها در جبران کمبود داده، بلکه در افزایش قدرت تعمیمپذیری و حساسیت تشخیصی مدل در کاربردهای حساس پزشکی اثبات می کند.

کلمات کلیدی: سرطان پستان، شبکه عصبی کانولوشنی، طیفبندی بافت، طیفسنجی رامان، کمبود داده، یادگیری انتقالی، یادگیری عمیق

نویسندگان: آرام زندی - زهره دهقانی بیدگلی











كد مقاله: icbme-1301

عنوان مقاله: طبقهبندی دقیق تومورهای مغزی با رویکرد ترکیبی EfficientNetB4 و ترنسفورمر بینایی

چکده: در این مطالعه، یک مدل ترکیبی به نام FusionNet برای طبقهبندی تومورهای مغزی از تصاویر MRI ارائه شد. FusionNet شامل EfficientNetB4 و ترنسفورمر بینایی است که ویژگیهای محلی و وابستگیهای بلندبرد تصاویر را وی یک پایگاه داده معتبر نشان داد که این مدل با دقت ۹۹.۲۶٪ عملکردی بهتر نسبت به معماریهای پایه دارد و سه نوع تومور مغزی رایج را با دقت و شاخص F1 بالا شناسایی میکند. تحلیل نتایج نشان میدهد ترکیب ویژگیهای محلی EfficientNetB4 با توانایی ترنسفورمر در درک روابط سراسری تصویر نقش کلیدی در بهبود عملکرد دارد. این یافتهها حاکی از آن است که FusionNet می تواند به عنوان یک ابزار تشخیص خودکار تومور مغزی با کارایی بالا و قابلیت استفاده در محیطهای بالینی کاربرد داشته باشد.

كلمات كليدى: ترنسفورمر بينايي، تومور مغزى، شبكه عصبي كانولوشني، مدل هيبريدي، يادگيري عميق، EfficientNetB.

نويسندگان: الهه الهي پرست باقرى - افشين ابراهيمي











كد مقاله: icbme-1353

عنوان مقاله: بازسازی و تحلیل سیگنال ECG از نسخههای چاپی نوار قلب بهمنظور طبقهبندی خودکار بیماریهای ایسکمیک قلب با استفاده از شبکههای عصبی کانولوشنی

چکده: بیماریهای قلبیعروقی بهعنوان یکی از مهم ترین علل مرگومیر در جهان شناخته می شوند و تشخیص به موقع آنها نقش بسزایی در پایش فعالیت الکتریکی قلب است، اما در بسیاری از موارد تنها نسخه چاپی یا تصویری آن در دسترس می باشد که تحلیل خودکار آن را با چالش مواجه می کند. بر این در بسیاری از موارد تنها نسخه چاپی یا تصویری آن در دسترس می باشد که تحلیل خودکار آن را با چالش مواجه می کند. بر این اساس، هدف این پژوهش توسعه روشی هوشمند و نوآورانه برای بازسازی دیجیتال و تحلیل خودکار سیگنال ECG از تصاویر اسکناده اسکنشده است. در این مطالعه، از مجموعه داده عمومی Mendeley Data شامل ۹۲۹ تصویر ECG در چهار دسته بالینی (نرمال، غیرنرمال، تاریخچه انفارکتوس میوکارد و انفارکتوس میوکارد) استفاده شد. در مرحله پیش پردازش، شبکه گرید قرمز با استفاده از تکنیکهای پردازش تصویر حذف گردید و مسیر موج سیگنال پس از باریکسازی و کالیبراسیون به سیگنال دیجیتال زمان و تالیبراسیون به سیگنال های استفاده آورش داده شد. تقسیم بندی داده ها به صورت ۷۵٪ آموزش، ۱۰٪ اعتبار سنجی و ۱۵٪ آزمون انجام گرفت. نتایج بازسازی شده داده مدل پیشنهادی توانست با دقت بین ۹۳٬۵۶٪ تا ۹۵٬۵۶٪ عملکردی قابل توجه ارائه دهد. این یافته ها بیانگر پتانسیل بالای بینایی ماشین و یادگیری عمیق در استخراج و تفسیر داده های زیستی از منابع غیرمستقیم همچون تصاویر نوار قلب است.

کلمات کلیدی: بازسازی سیگنال زیستی، پردازش تصویر ،ECGتشخیص بیماری قلبی، شبکه عصبی کانولوشنی ،(CNN) سیگنال دیجیتال نوار قلب، طبقهبندی بیماری قلبی.

نويسندگان: فاطمه كيخا - مهديه قاسمي - سيد مهدي صالحي











كد مقاله: icbme-1373

عنوان مقاله: چارچوب سلسلهمراتبی مبتنی بر مدل انتشار شرطی و شبکه پیشبینی کننده برای تولید و بازشناسی توامان حالات چهره

چکیده: حالات چهره از مهمترین ابزارهای ارتباط غیرکلامی انسان هستند و سرنخهای ارزشمندی برای ارزیابی وضعیتهای عاطفی و شناختی فراهم می کنند. پژوهش ها نشان دادهاند که افراد دارای اختلال طیف اوتیسم نسبت به افراد عادی شدت و تنوع کمتری در حالات دارند؛ شاخصی که می تواند در تشخیص زودهنگام، بهویژه در کودکان، سودمند باشد. با این حال، جمعآوری دادههای تصویری از کودکان با محدودیتهای اخلاقی و عملی همراه است. در این مقاله چارچوبی سلسلهمراتبی معرفی می شود که بهطور همزمان وظیفه تولید و بازشناسی حالات چهره را انجام می دهد. هسته اصلی این چارچوب یک مدل انتشار نرم شرطی است که تصاویر واقع گرایانه چهره را بر اساس مقادیر پیوسته ظرفیت-انگیختگی تولید کرده و تنوع داده را در شرایط کمداده افزایش می دهد. در کنار آن، شبکهای پیش بینی کننده بهصورت انتها به انتها با مدل مولد آموزش داده می شود تا مقادیر ظرفیت-انگیختگی را تخمین زده و دقت بازشناسی حالات ظریف را ارتقا دهد. نتایج پژوهش نشان می دهد که رویکرد پیشنهادی علاوه بر بهبود کیفیت تصاویر تولیدی، موجب افزایش قابل توجه دقت شبکه پیش بین می شود. این چارچوب می تواند در مهندسی پزشکی و بایش باینی، از جمله اختلالات عصبی و روانپزشکی و بهویژه اوتیسم، ابزاری کمکی برای تقویت مجموعهدادههای محدود کودکان و کمک به تشخیص زودهنگام باشد.

كلمات كليدى: يادگيرى عميق، بازشناسى حالات چهره، توليد حالات چهره، مدلهاى انتشار.

نویسندگان: علی محمدپزنده - عمادالدین فاطمیزاده











كد مقاله: icbme-1461

عنوان مقاله: ارائه مدل E-UNETR2D جهت قطعهبندی عروق کرونر از روی تصاویر سی تی آنژیو گرافی

چکیده: بیماریهای عروق کرونری بهعنوان یکی از علل اصلی مرگ و میر در سطح جهانی مطرح هستند. نیاز به روشهای پیشرفته جهت تشخیص، ارزیابی دقیق و مداخله به موقع جهت درمان در این بیماریها امری ضروری است. سی تی آنژیوگرافی بهعنوان یکی از ابزارهای کلیدی برای تصویربرداری از شریانهای کرونری تبدیل شده است و بینش دقیقی از ناهنجاریهای عروقی ارائه می دهد. با این حال، تحلیل دستی تصاویر سی تی آنژیوگرافی متخصصان را با چالشهای زیادی روبهرو می کند و مسالهای زمان بر است. در این پژوهش روش جدیدی با استفاده از بهبود شبکههای ترنسفرمر UNETR و خطاهای ترکیبی جهت قطعه بندی عروق کرونر ارائه شده است و نتایج ارزیابی نشان می دهد که مدل توانسته است به دقت %DiceScore 87 برسد. مقایسه خروجیهای مدل با برچسبهای واقعی نشان از تفکیک خوب عروق کرونر توسط مدل دارد.

كلمات كليدى: بيمارىهاى عروق كرونر، سىتى آنژيو گرافى، قطعهبندى، شبكه، UNet، شبكه، ترنسفرمر.

نویسندگان: مصطفی رجبزاده - فواد قادری - حمیدرضا پورعلی اکبر - نصرالله مقدم چرکری











كد مقاله: icbme-1474

عنوان مقاله: ارائه یک مدل ترکیبی برای تشخیص بیماری آلزایمر با استفاده از هوش مصنوعی و منطق فازی

چکده: بیماری آلزایمر یکی از چالشهای مهم سلامت جهانی است و تشخیص زودهنگام آن نقش کلیدی در بهبود کیفیت زندگی بیماران و افزایش اثربخشی درمانها دارد. روشهای سنتی تشخیص آلزایمر، مانند ارزیابیهای بالینی و تصویربرداری عصبی، معمولاً پرهزینه و زمانبر هستند. در سالهای اخیر، فناوریهای یادگیری ماشین پتانسیل قابل توجهی برای خودکارسازی و افزایش دقت تشخیص از طریق تحلیل دادههای گسترده مانند تصاویر MRI و نتایج آزمونهای شناختی نشان دادهاند. نوآوری این پژوهش در ادغام دادههای تصویربرداری MRI و آزمونهای شناختی در یک مدل تشخیصی مبتنی بر یادگیری ماشین نهفته است؛ ترکیبی که امکان شناسایی جامعتر و دقیق تر مراحل اولیه آلزایمر را فراهم میسازد، در حالی که روشهای سنتی معمولاً تنها بر یک نوع داده تکیه دارند. در این مطالعه، مدلی ترکیبی توسعه داده شد که با استفاده از الگوریتمهای یادگیری ماشین، دادههای MRI و نتایج آزمونهای شناختی را تحلیل و طبقهبندی می کند. این مدل از طریق اعتبارسنجی متقابل مورد ارزیابی قرار گرفت تا پایداری و دقت آن تضمین شود. نتایج نشان داد که مدل به دقت ۹/۹۱ درصد، دقت پیش بینی ۹/۹۲ درصد قرار گرفت تا پایداری و دقت آن تضمین شود. نتایج نشان داد که مدل به دقت ۹/۹۱ درصد، دقت پیش بینی مشخصه عملکرد حساسیت ۱/۹۱ درصد و نمره F1 برابر با ۹/۹۱ درصد دست یافته است. علاوه بر این، مساحت زیر منحنی مشخصه عملکرد گیرنده (ROC) یا همان AUC برابر با ۹/۴ محاسبه شد که بیانگر توانایی بسیار بالای مدل در تمایز میان موارد آلزایمر و غیرآلزایمر است.

كلمات كليدى: هوش مصنوعي، تشخيص زود هنگام، آلزايمر، هوشمند.

نویسندگان: مصطفی کامل گاطع











كد مقاله: icbme-1451

عنوان مقاله: طبقه بندی بیماران پارکینسون و افراد سالم با بهره گیری از ویژگیهای غیرخطی و الگوریتم های یادگیری ماشین

چکده: بیماری پارکینسون یک اختلال عصبی پیشرونده است که با از دست دادن نورونهای دوپامینرژیک و علائمی مانند لرزش، سفتی عضلات و کندی حرکات مشخص میشود، و تشخیص بالینی آن به دلیل پیچیدگی و دشواری در مراحل اولیه پراش برانگیز است. در این پژوهش، سیگنالهای الکتروانسفالوگرافی از پایگاه داده عمومی PRED+CT پس از پیش پردازش و تقسیم به بخشهای زمانی ۲ ثانیهای، مورد تحلیل قرار گرفتند. ویژگیهای غیرخطی شامل آنتروپی فازی، آنتروپی تجزیه مقدار منفرد (SVD) و تحلیل نوسانات چندفراکتالی بدون روند (MFDFA) استخراج شده و به مدلهای طبقهبندی شامل ماشین بردار پشتیبان (SVM)، کانزدیک همسایه (KNN)، درخت تصمیم، جنگل تصادفی و XGBoost اعمال شدند. نتایج نشان داد که KNN با میانگین صحت /۹۷/۹۷ در تمایز افراد سالم از بیماران پارکینسون بدون مصرف دارو و XVM و KNN با میانگین صحت /۹۷/۹۷ بهترین نتایج را ارائه کردند. همچنین، منحنیهای ROC با سطح زیر منحنی برابر ۲۰۱۱ در تمام سناریوها، دقت کامل مدلها را تأیید میکنند. این یافتهها پتانسیل بالای روش پیشنهادی را به عنوان یک ابزار تشخیص غیرتهاجمی، دقیق و سریع برای تشخیص زودهنگام و نظارت بر اثرات درمانی پارکینسون تأیید میکنند، که میتواند در عمل بالینی به کار گرفته شود.

کلمات کلیدی: آنتروپی تجزیه مقدار منفرد، آنتروپی فازی، الکتروانسفالوگرافی (EEG) بیماری پارکینسون، تحلیل نوسانات چندفراکتالی بدون روند، تشخیص خودکار، طبقه بندی، یادگیری ماشین

نویسندگان: محمد جواد عبدی - پریا شکری - امیرحسین تجرد - تانیا حسین خانی - اصغر زارعی



كد مقاله: icbme-1453

عنوان مقاله: بهبود تخمین ضربان قلب در دستگاههای پوشیدنی تجاری با استفاده از فیلتر کالمن و مدلهای رگرسیون

چکده: تشخیص سریع اختلالات قلبی و پیشگیری از بیماریهای مرتبط نیازمند پایش مداوم و دقیق ضربان قلب (HR) است. در سالهای اخیر، فناوریهای پوشیدنی هوشمند به سبب ویژگیهای غیرتهاجمی و امکان استفادهی مداوم، توجه گستردهای در حوزههای پژوهشی و بالینی جلب کردهاند. با این حال، دقت این ابزارها در مقایسه با الکتروکاردیوگرام مرجع (ECG) همچنان نیازمند بررسی بیشتر است. در این مطالعه، مقادیر HR اندازه گیری شده در حین انجام فعالیتهای مختلف، توسط شش دستگاه انیازمند بررسی بیشتر است. در این مطالعه، مقادیر HB اندازه گیری شده در حین انجام فعالیتهای مختلف، توسط شش دستگاه ویوشیدنی، شامل Apple Watch، Fitbit. Xiaomi Mi Band، Garmin، Empatica E۴ پوشیدنی، شامل ECG، عدال از جمله آرتیفکت حرکتی، فیلتر کالمن بر سیگنالهای خام اعمال شد و خروجی پالایش شده به عنوان ورودی به سه مدل رگرسیونی وارد شد. آموزش و ارزیابی مدلها با استفاده از اعتبار سنجی متقابل انجام شد و عملکرد آنها بر اساس شاخصهای میانگین قدر مطلق خطا (MAE)، ریشه میانگین مربعات خطا (RMSE) و ضریب تعیین (R) ارزیابی شد. نتایج نشان داد که دستگاههای پوشیدنی با فراهم کردن میانگین MAE برابر با ۱۳/۲۰ در حین انفس عمیق میانگین عملکرد مناسبی در تخمین ضربان قلب هستند. در میان ابزارهای بررسی شده، ساعت Apple عملکرد برتری داشت و این یافتهها بر ضرورت استفاده از روشهای پیشرفته پردازش سیگنال و انتخاب دقیق دستگاههای پوشیدنی در کاربردهای بالینی یافتهها بر ضرورت استفاده از روشهای پیشرفته پردازش سیگنال و انتخاب دقیق دستگاههای پوشیدنی در کاربردهای بالینی و پوههشی تأکید می کنند.

کلمات کلیدی: الکتروکاردیوگرام، پایش ضربان قلب، حسگر نوری، دستگاههای پوشیدنی، مدلهای رگرسیونی، نشانگرهای زیستی دیجیتال، یادگیری عمیق.

نویسندگان: میلاد رضایی ارجمند - تانیا حسین خانی - امیرحسین تجرد - علیرضا طالش جفادیده - اصغر زارعی



ICBME
2025